University of Kent at Canterbury
Centre for Materials Research
School of Physical Sciences

Submitted for the grade of
Doctor of Philosophy (PhD) of the University of Kent at Canterbury
Discipline: Polymer Chemistry

Nicholas Agostino Antonio Rossi

# Synthesis and characterisation of poly(methylphenylsilane) block copolymers

# Abstract

Samples of α,ω-dichloropoly(methylphenylsilane) (diClPMPS) were synthesised via the Wurtz-reductive coupling polymerisation. Subsequent bromination of PMPS afforded monomodal polymers with halogenated chain ends, namely α,ω-dihalopoly-(methylphenylsilane) (diXPMPS). Condensation reactions of diXPMPS with alcohols were investigated in order to determine the reactivity of the halide end groups. Condensation reactions involving polymeric alcohols such as poly(ethylene oxide) and poly(ethylene glycol) methyl ether with diXPMPS to form amphiphilic block copolymers were attempted, but proved ultimately unsuccessful.

An alternative route whereby a PMPS macroinitiator was used to form ABA block copolymers via a transformation mechanism is described. ABA block copolymers of methyl methacrylate and methylphenylsilane (PMMA-PMPS-PMMA) were synthesised using a methodology based on atom transfer radical polymerisation (ATRP). The reaction of samples of diXPMPS with 2-hydroxyethyl-2-methyl-2-bromopropanoate gave suitable macroinitiators for the ATRP of methacrylic monomers. Amphiphilic ABA block copolymers were synthesised via the polymerisation of either 2-hydroxyethyl methacrylate (HEMA) or methoxy-capped oligo(ethylene glycol) methacrylate (OEGMA). In addition, an alternative PMPS macroinitiator was synthesised to form block copolymers of styrene and methylphenylsilane via TEMPO-mediated free radical polymerisation. In this case, diXPMPS was endcapped with 2,2,6,6,-tetramethyl-1-(1-phenyl-2-hydroxyethyloxy)-piperidine to form a suitable macroinitiator.

All block copolymers were characterised using $^{1}H$ NMR and $^{13}C$ NMR spectroscopy and size exclusion chromatography. Preliminary evidence of phase separation in samples of PMMA-PMPS-PMMA was observed via differential scanning calorimetry. The amphiphilic block copolymers were also investigated to determine their suitability for applications in three areas of research – drug delivery systems, cell growth, and bioelectronics.

# Acknowledgements

A great deal of thanks to Professor Dick Jones and Dr. Simon Holder for funding, guidance, and support. I would like to thank Dick for giving me the opportunity and belief I needed to do a PhD. A special thanks to Simon, whose knowledge, influence, and friendship has made all the difference. I would also like to thank Dr. Nico Sommerdijk, under whose guidance I managed to learn so much in such a short space of time. A thank you as well to Alison and Stefano for suggestions and proof-reading. PhD. funding was gratefully received from the Japan Chemical Innovation Institute through the Industrial Science and Frontier Program supported by the New Energy and Industrial Technology Development Organisation (NEDO). Research at the Technical University of Eindhoven (TUE) was funded by the European Science Foundation SMARTON. I am also thankful to the School of Physical Sciences at the University of Kent and to Macrogroup UK (D.H. Richards Memorial Bursary) for finance for conferences.

Thanks also to Mark, Alkay, and Vicky for your friendship and for never letting the lab become too dull; to James and Graham for barking out instructions at the beginning; to Meade and Holls for being genuinely funny; to Fiorella, Robert, and everyone else who made me feel so welcome in Eindhoven and who helped make my trip such a successful one; to Simon for amusing us in the pub and throwing good parties; to Stef for cooking great pasta and having a knack for throwing good parties; and to Ali for just being great to me. Thanks to all my friends and family, and to everyone in the lab past and present.

To Mum, Dad, and David

# Contents

## Abbreviations

| | |
|---|---|
| ABCs | amphiphilic block copolymers |
| ATRP | atom transfer radical polymerisation |
| bpy | 2,2′-bipyridine |
| CRP | controlled/"living" free radical polymerisation |
| diClPMPS | α,ω-dichloropoly(methylphenylsilane) |
| diXPMPS | α,ω-dihalopoly(methylphenylsilane) |
| DMSO | dimethylsulphoxide |
| $DP_n$ | degree of polymerisation |
| DSC | differential scanning calorimetry |
| GPC | gel permeation chromatography |
| HEMA | 2-hydroxyethyl methacrylate |
| HO-St-TEMPO | 2,2,6,6,-tetramethyl-1-(1-phenyl-2-hydroxyethyloxy)piperidine |
| IR | infra-red |
| LS | light scattering |
| LFRP | living free radical polymerisation |
| MMA | methylmethacrylate |
| $M_n$ | number average molecular weight |
| mp | melting point |
| $M_p$ | peak molecular weight |
| $M_w$ | weight average molecular weight |
| $M_w/M_n$ | polydispersity |
| *n*-BuLi | *n*-butyl lithium |
| NMR | nuclear magnetic resonance |
| OEGMA | oligo(ethylene glycol) methyl ethyl methacrylate |
| PEO | poly(ethylene oxide) |
| PEGME | poly(ethylene glycol) methyl ether |
| PMMA | poly(methylmethacrylate) |
| PMPS | poly(methylphenylsilane) |
| $PMPS(init)_2$ | α,ω-di(2'-oxyethyl-2-bromomethylpropanoate)poly(methyl-phenylsilane) |

| | |
|---|---|
| $PMPS(TEMPO)_2$ | α,ω-di(oxyethyl-2-phenyl-2-(2,2,6,6-tetramethyl-1-piperidinyl-oxy)poly(methylphenylsilane) |
| ppm | parts per million |
| PS | polystyrene |
| RI | refractive index |
| SEC | size exclusion chromatography |
| SEM | scanning electron microscopy |
| SFRP | stable free radical polymerisation |
| S-MB | (*S*)-(-)-2-methyl-1-butanol |
| St | styrene |
| St-TEMPO | 2,2,6,6,-tetramethyl-1-(1-phenylethyloxy)-piperidine |
| *t*-but | tertiary butanol (2-methyl-2-propanol) |
| TEM | transmission electron microscopy |
| TEMPO | 2,2,6,6-tetramethyl-1-piperidinyloxy |
| THF | tetrahydrofuran |
| $T_g$ | glass transition temperature |
| TMS | trimethylsilyl |
| UV | ultra-violet |

| | |
|---|---|
| $PMPS_n$-$PEO_m$ | poly(methylphenylsilane)-*block*-poly(ethylene oxide) |
| PEGME-PMPS-PEGME | poly(ethylene glycol methyl ether-*block*-methylphenyl-silane-*block*-ethylene glycol methyl ether) |
| PHEMA-PMPS-PHEMA | poly(2-hydroxyethyl methacrylate-*block*-methylphenyl-silane-*block*-2-hydroxyethyl methacrylate) |
| PMBMA-PMPS-PMBMA | Poly((S)-(-)-2-methyl-1-butyl methacrylate-*block*-methylphenylsilane-*block*-(S)-(-)-2-methyl-1-butyl methacrylate) |
| PMMA-PMPS-PMMA | poly(methyl methacrylate-*block*-methylphenylsilane-*block*-methyl methacrylate) |
| POEGMA-PMPS-POEGMA | poly(oligo(ethyleneglycol) methyl ethyl methacrylate-*block*-methylphenylsilane-*block*-oligo(ethylene glycol) methyl ethyl methacrylate) |
| PS-PMPS-PS | poly(styrene-*block*-methylphenylsilane-*block*-styrene) |

## Publications and Presentations

Some of the research presented in this thesis has been published or presented as follows:

(a) in "Synthesis and characterisation of poly(methyl methacrylate)-*block*-poly-(methylphenylsilane)-*block*-poly(methyl methacrylate) using ATRP" Rossi, N.A.A.; Holder, S.J.; Jones, R.G. *J. Polym. Sci. Part A., Polym. Chem.* **2003**, 40, 30.

(b) in "Synthesis of poly(styrene-*block*-methylphenylsilane-*block*-styrene) via TEMPO-mediated 'controlled' free radical polymerisation" Rossi, N.A.A.; Anderson, R.M.; Holder, S.J.; Jones, R.G. *Polym. Int.* (submitted).

(c) in "ABA triblock copolymers: from controlled synthesis to controlled function" Holder, S.J.; Rossi, N.A.A.; Yeoh, C.T.; Durand, G.G.; Boerakker, M.J.; Sommerdijk, N.A.J.M. *J. Mater. Chem.* (submitted).

(d) in "Self-patterning of amphiphilic ABA block copolymers for the oriented growth and electric stimulation of muscle cells" Popescu, D.C.; Lems, R.; Rossi, N.A.A.; Yeoh, C.-T.; Wouters, D.; Leclere, P.; Thune, P.; Bouten, C.V.C.; Holder, S.J.; Sommerdijk, N.A.J.M. *J. Am. Chem. Soc.* (submitted).

(e) at the Young Macromolecular Researchers Conference - University of Strathclyde, April 2001. "Synthesis of ABA polysilane block copolymers using atom transfer radical polymerisation, ATRP" (oral presentation).

(f) at the International Workshop on Silicon Containing Polymers (ISPO) - University of Kent, June 2001. "Synthesis and characterisation of polysilane block copolymers via ATRP" (poster).

(g) at the Polymers in the Third Millennium - Univ. Montpellier II, September 2001. "Synthesis and characterisation of polysilane block copolymers via ATRP" (poster).

## Thesis Outline

Introductions and literature reviews to two subjects – polysilanes and atom transfer radical polymerisation (ATRP) – are reported in chapters **1** and **2** respectively.

The synthesis of polysilanes, and in particular the Wurtz-reductive coupling reaction of poly(methylphenylsilane) (PMPS), is discussed in chapter **3**. The procedure for synthesising monomodal PMPS containing halogenated endgroups (diXPMPS) and their subsequent reactions with alcohols is detailed.

A brief review of block copolymers is reported in chapter **4**.

Chapter **5** summarises the literature dedicated to the synthesis of polysilane copolymers (in particular block copolymers) and follows with a discussion on condensation reactions between diXPMPS and hydrophilic poly(ethylene glycol) derivatives. These reactions were shown to be ultimately unsuccessful.

In Chapter **6** the reaction of samples of diXPMPS with 2-hydroxyethyl-2-methyl-2-bromoproprionate gave suitable macroinitiators for the ATRP of alkyl methacrylate monomers. The synthesis and characterisation of ABA block copolymers of alkyl methacrylate and methylphenylsilane (PMMA-PMPS-PMMA and PMBMA-PMPS-PMBMA) using a methodology based on atom transfer radical polymerisation (ATRP) is discussed.

In chapter **7** diXPMPS was reacted with 2,2,6,6-tetramethyl-1-(1-phenyl-2-hydroxyethyloxy)piperidine to yield suitable macroinitiators for the controlled free radical polymerisation of styrene. Successful synthesis of ABA block copolymers of styrene and methylphenylsilane (PS-PMPS-PS) using a methodology based on TEMPO-mediated controlled free radical polymerisation is discussed.

Chapter **8** describes the synthesis of PMPS amphiphilic ABA block copolymers using a similar methodology to that described in chapter **6**. 2'-Hydroxethyl methacrylate (HEMA) and (oligoethylene glycol) methyl ether methacrylate (OEGMA) were successfully polymerised using a range of PMPS macroinitiators.

In chapter **9** preliminary research into these amphiphilic block copolymers is reported. The main areas of research focused on the aggregation behaviour and thin film properties of the copolymers.

# 1. Introduction to polysilanes

## 1.1. Overview

Polysilanes are linear polymers with a backbone made up entirely of catenated silicon atoms. On each of the silicon atoms are two substituents, most commonly alkyl and aryl groups (fig. **1.1**). Electron delocalisation through the backbone via σ-electron mobility gives polysilanes quite unusual electrochemical and photochemical properties.[1,2]

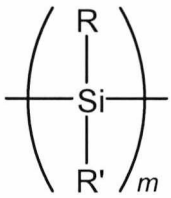


where R, R' = H, Me, *n*-Hex, *c*-Hex, Ph, etc.

**Fig. 1.1.** Polysilanes

Interest in polysilanes primarily stems from the σ-electron delocalisation, giving rise to a number of electronic properties not shared by their saturated carbon analogues. In many ways their behaviour most closely mimics that of the π-conjugated unsaturated carbon polymers; consequently their behaviour as semiconducting,[3] photoconducting,[4] electroluminescent[5] and non-linear optical[6] materials has been investigated. Further research has also centred on the homolytic breaking of the silicon backbone, a property that has been exploited in their application as precursors to β-SiC fibres,[7] photoresist materials for microlithography,[8] and photoinitiators in radical polymerisations.[9]

## 1.2. History

The first substituted polysilane was synthesised by Kipping in the 1920s.[10] Although the condensation reaction of diphenyldichlorosilane with sodium was successful, the resulting polymers were poorly characterised and intractable. The interest in polysilanes was very limited and it was not until some 50 years later in the 1970s

when further attention was paid to polysilanes. Perhaps most significantly, Yajima *et al.*[7] described the preparation of β-silicon carbide from polysilane pre-cursors which helped to spark interest in the field. In 1980, Wesson and Williams[11] described the synthesis of random copolymers containing dimethylsilylene units with either ethylmethylsilylene or methyl-*n*-propylsilylene. The following year, Trujillo and co-workers[12] then managed to synthesise a soluble homopolymer, poly(methylphenylsilane), PMPS, from methylphenyldichlorosilane using sodium in refluxing *n*-dodecane with yields of the crude polymer approaching 60%. The synthesis of this bimodal polymer showed that polysilanes need not be insoluble and intractable materials as previously thought. Along with the unique electronic properties evidenced in the UV spectra of polysilanes, these properties ensured that interest in polysilanes has continued to develop.

## 1.3. Synthesis

Polysilanes can be synthesised via a number of routes. The Wurtz-reductive coupling reaction[10] is the most common route used to synthesise polysilanes and involves the polymerisation of dichlorodiorganosilanes ($Cl_2R_2Si$) using a metal such as sodium. Other methods include disilene/silylene polymerisation, the dehydrogenative coupling of diorganosilanes, and the ring-opening polymerisation of strained cyclosilanes. The mechanisms and kinetics of the synthesis of polysilanes, and in particular the Wurtz reaction, is discussed in detail elsewhere [chapter 3].

## 1.4. Physical properties

The physical properties of polysilanes are dependent on the nature of the substituent organic groups. Symmetrically substituted polysilanes, such as poly(dimethylsilane), are most often semi-crystalline[13] and usually intractable.[14] Crystallinity increases as the substituent alkyl chains become longer (e.g. poly(di-*n*-hexylsilane)), as does solubility in organic solvents. For instance, polysilanes which have one or more alkyl chain longer than *n*-propyl are tractable solids which are rubbery elastomers at room temperature.

### 1.4.1. Thermal properties

The physical properties of a polymer are related to and are determined by the conformation and substitution patterns of the chain.[1,15] A polymer will form semi-crystalline solids, sometimes with higher melting points if the backbone is symmetrically substituted.[16] Above the melting point of polymers such as *n*-alkyl substituted polysilanes, a hexagonal columnar liquid crystalline mesophase (hclq) is adopted.[17] Asymmetrically substituted atactic polysilanes have also shown the same hclq mesophase, although poly(alkylaryl)silanes such as PMPS are usually reported as being amorphous polymers.[18,19]

The glass transition temperatures, $T_g$, of polysilanes range from –76°C (rubbery elastomers) to above 120°C (hard, brittle solids, e.g. PMPS). Some polysilanes such as PMPS have been shown to be thermally stable above 300°C by thermogravimetric analysis.[20] Polysilanes of this nature show interesting phase transitions, as do copolymers which contain units with similar side groups.

Some dialkyl substituted polysilanes can undergo a rod-to-coil transition which can result in an abrupt bathochromic shift when cooled. This is also known as thermochromism and an example of a polysilane showing bathochromic shifts is poly(di-*n*-hexyl)silane. A "red" shift from 315 nm to 370 nm (i.e. left to right on the UV absorption spectrum) occurs on cooling below 42°C.[15] This 55 nm bathochromic shift is associated with a reversible change in conformation from a disordered helix to planar zig-zag (disorder-order) transitions.

The thermal characterisation of PMPS has been carried out using the following techniques: thermogravimetry (TGA), differential scanning calorimetry (DSC), dynamic thermochemical analysis (DMA), and thermomechanical analysis (TMA).[19]

### 1.4.2. Light scattering

Light scattering (LS) has provided some interesting information on the chain structure of polysilanes in solution.[21] Comparisons of the molecular weights of polysilanes determined via gel permeation chromatography (GPC) and LS were found to be in agreement.[22] Studies had previously shown that that polystyrene calibrated GPC was not particularly accurate for polysilane analysis, although useful in a relative sense.[21]

For example, the $M_w$ of PMPS was shown to be twice as high when calculated using LS compared to polystyrene calibrated GPC.

## 1.5. Molecular structure

Oligosilanes have been used in many cases as a model for understanding linear polysilanes.[2] The extrapolation of the properties of short chain fragments can be used to predict the properties of the longer polymer chains. For example, for a typical oligosilane, the bond length is 2.36 Å, while Si-Si-Si bond angles are typically larger than tetrahedral angles and depend on the nature of the substituents. Si-C bond lengths which exist between substituents and the silicon backbone are typically around 1.88 Å. Dihedral angles (ω) are more complicated,[23] since rotation around the single bonds of the backbone does not involve any bond breaking and is quite facile as long as steric hindrance is not too great.

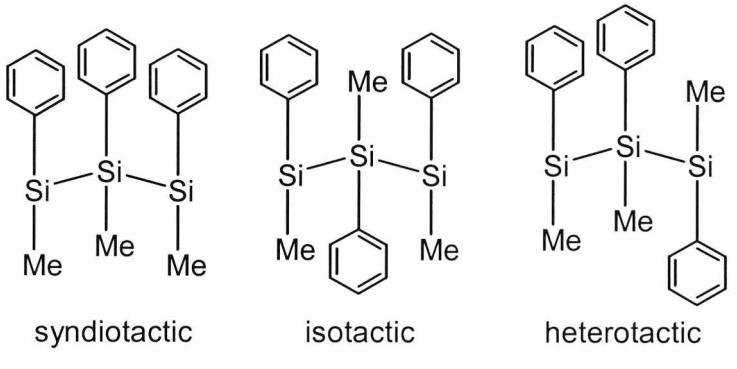


**Scheme 4.2.** Tacticity of PMPS

For unsymmetrically substituted polysilanes there are three possible configurations – syndiotactic, isotactic, and heterotactic (scheme **4.2**).[24]

### 1.5.1. NMR spectroscopy

$^{1}H$, $^{13}C$, and $^{29}Si$ NMR spectroscopy have all been used to characterise polysilanes. The NMR of unsymmetrical alkyl substituted polysilanes synthesised via the Wurtz reaction show broad characteristic peaks indicative of random atactic conformations.[25]

However, for aryl substituted polysilanes, such as PMPS, the $^{29}Si$ NMR spectrum shows several peak intensities within the silicon multiplet, suggesting a non-random collection of stereocentres.[26] Using NMR spectroscopy, PMPS synthesised via the Wurtz reaction has been shown to have a predominantly trans conformation (planar zig-zag).

### 1.5.2. Infra-red spectroscopy

Vibrational spectra are dominated by the substituents in the IR and Raman spectra.[27] The vibrations of the polysilane backbone are quite low, typically between 350 and 400 $cm^{-1}$ for Si-Si stretch, about 600-700 $cm^{-1}$ for the Si-C stretch, and 700-900 $cm^{-1}$ for Si-CH.

## 1.6. Electronic Properties

The $\sigma-\sigma^*$ electron transitions involving the easily ionised electrons in Si-Si bonds account for the polysilane absorptions in electronic spectroscopy. The position of the near UV absorption (between 290 and 410 nm) is dependent on the nature of the substituents present, which have an effect on main chain conformation. In addition, an increase in intensity and a shift to lower energy occurs as chain length increases. UV bands for some polysilanes in both solution[28] and solid films[29] have also been found to be thermochromic.

### 1.6.1. Bonding

The delocalisation of the $\sigma$-electrons of the silicon backbone gives rise to a number of electronic properties that are not shared by saturated carbon chain polymers. The delocalisation leads to a number of properties used increasingly in technological applications, including strong electronic absorption, conductivity, photoconductivity, and photosensitivity. Accordingly, their performance as semiconducting,[3] photoconducting,[4] electroluminescent,[5] and non-linear optical[6] materials has been investigated.

The σ-electrons in Si-Si bonds have much lower ionisation energies and are less tightly bound compared to those found in organic or siloxane polymers. The bonding in polysilanes between silicon atoms involves approximately $sp^3$ hybrid orbitals. The orbitals are located on the Si atoms and point to their neighbours and to substituent orbitals, for example the 1s orbital on a hydrogen or, in the case of a methyl group, $sp^3$ orbitals. The resonance integral, $\beta_{vic}$, is due to two $sp^3$ orbitals located on adjacent silicons and pointing at each other (fig. **1.2**). These orbitals are responsible for the Si-Si σ bond formation. In terms of orbital splitting, each pair of orbitals is split into a strongly bonding $\sigma_{SiSi}$ and a strongly anti-bonding $\sigma^*_{SiSi}$. $\beta_{gem}$ is a less strongly negative resonance integral between two $sp^3$ hybrids located on the same Si atom and is responsible for the interaction between localised orbitals carried by the same Si atom. The extent of electron delocalisation is dependent on the ratio of $\beta_{gem}$ to $\beta_{vic}$. If the ratio tends towards zero, then no delocalisation will occur, whereas if the ratio is 1:1, then delocalisation is considered to be perfect.

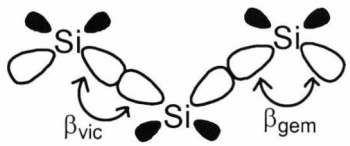


**Fig. 1.2.** Bonding orbitals of polysilanes

The interaction between neighbouring Si orbitals is relatively large, with σ and σ* transitions due to bonding (HOMO) and anti-bonding (LUMO) respectively. As the length of the polysilane increases, transitions between σ HOMO and σ* LUMO decrease, leading to a valence band of filled orbitals and a conduction band of unfilled orbitals. The σ–σ* conduction band in polysilanes causes them to absorb energy from the UV region. Since σ→σ* is permitted, absorptions are relatively intense, with extinction coefficients, ε, of between 5 000 and 10 000 per Si-Si bond.

### 1.6.2. UV spectroscopy

All unsymmetrical alkyl substituted polysilanes have a σ–σ* absorption between 300 and 325nm. Those polysilanes with one or more aryl substituents show absorption

maxima that are strongly red-shifted. For instance, the absorption maximum, $\lambda_{max}$, of PMPS occurs between 330 and 340 nm, depending on chain length as well as chain conformation. These values are substantially higher compared to dialkylsilanes, due in part to the mixing of phenyl π-orbitals, and also because PMPS is predominantly made up of all-trans sequences. These sequences are separated by segments of conformational disorder, known as gauche turns. Hence, PMPS can be described as being a random coil of semi-rigid rods.[30] In addition, the length of the chain will have an effect on the position, absorption, and extinction coefficients observed. Beyond a certain chain length, a limit is reached after which no significant increase in $\lambda_{max}$ is observed. For PMPS this occurs when the degree of polymerisation reaches about 35.[30] Chain-end effects contribute to the observed red shift in the absorption maximum as chain length increases. Furthermore, the conformation of the chain influences the $\sigma$–$\sigma^*$ separation and therefore the value for $\lambda_{max}$. In general, as the occurrence of trans Si-Si-Si-Si conformations increase, $\lambda_{max}$ will also tend to increase. Polysilanes with longer-chain alkyl substituents, such as poly(di-*n*-hexylsilane), PDHS, show more dramatic conformational behaviour depending on temperature.

### 1.6.3. Conductivity

Conductivity in polysilanes occurs from the transfer of electrons from the Si-backbone to oxidising agents, leading to the formation of a polysilane cation radical, or "hole".[31] This hole can be delocalised along the polysilane chains and electrons can "hop" from one chain to another enabling bulk conductivity.[32] Hence, by treating polysilanes with oxidising agents such as $AsF_5$, $SbF_5$, and $H_2SO_4$, they can become electrical conductors. Polysilanes are very good charge transporters in electrophotography because of their high hole drift mobilities of ~ $10^4$ ($cm^2/Vs$) at room temperature.[4,33] Untreated, pure polysilanes are insulators with conductivities of the order of less than $10^{-12}$ $ohm^{-1}cm^{-1}$.

## 1.7. Photochemistry

Polysilanes are radiation-sensitive polymers that undergo chain scission when exposed to light or ionising radiation, resulting in the formation of smaller fragments.

Some recombination and cross-linking through unsaturated pendant groups can occur during polysilane irradiation. In this respect, polysilanes are unique and differ compared to carbon-based polymers. Hence polysilanes possess the prerequisite properties needed in applications of resist materials in microlithography [34] and as photoinitiators in radical polymerisations.[35]

### 1.7.1. Photochemical degradation

The most common form of photochemical reaction that leads to the breaking up of the polysilane backbone is known as chain abridgement.[36] In this case, two adjacent Si-Si bonds are broken, whilst one Si-Si bond is formed. The process can occur quite efficiently even at low temperatures (scheme **1.2**).

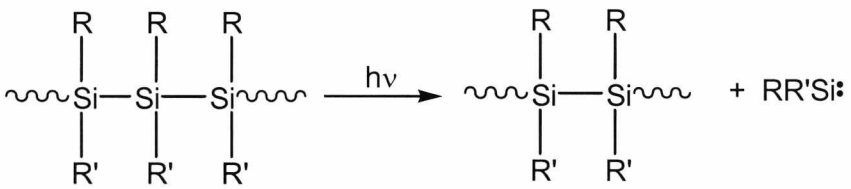


**Scheme 1.2.** Chain abridgement

Another photochemical process is chain cleavage, which occurs via reductive elimination. Here, one Si-C and one Si-Si bond is lost, whilst a new Si-C bond is formed (scheme **1.3**). Alternatively, homolytic bond cleavage leads to the formation of two silyl radicals (scheme **1.4**).

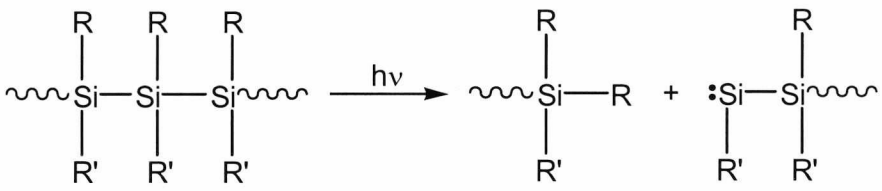


**Scheme 1.3.** Reductive elimination

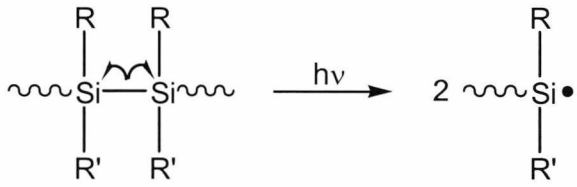


**Scheme 1.4.** Homolytic cleavage

Little is known about the relative or absolute quantum yields or rates for these processes as a function of oligosilane conformation, temperature, photon energy, etc. However, it is known that the first two photochemical reactions proceed very rapidly, while the last process is proposed to occur from the triplet state.

For arylated polysilanes, the photochemical behaviour is more complicated. A silene-forming 1,3-shift is possible and intramolecular charge-transfer states have low energies in polar solvents. It is possible that intersystem crossing is enhanced, leading to the abridgement reaction proceeding in the triplet state in a non-concerted manner.

### 1.7.2. Photooxidation of polysilanes

There have been several studies on the nature and effect of degradation of polysilanes.[37] Photooxidation studies on both linear, e.g. PMPS,[38] and branched polysilanes (polysilynes), e.g. $(SiPh)_m(SiMe_2)_n$,[39] revealed that photooxidation in air leads to some cross-linking in thin films, as opposed to complete degradation. The cross-linking of the polysilane fragments has been shown to lead to the formation of siloxane network solids. The development of these networks has been followed using techniques such as IR spectroscopy, whereby siloxane peaks (Si-O-Si, 1000 to 1100 $cm^{-1}$) and silanol peaks (Si-OH, 3000 to 3750 $cm^{-1}$) are measured as progressive bleaching of the polysilane films continues. For linear polysilanes such as PMPS, lower doses are needed for the saturation of absorbances. This is in part due to the fact that radical recombination may be more likely for branched/network polysilanes, as well as its higher absorptivity at the wavelength at which the polymer was irradiated (337 nm). In summary, both siloxane and silanol derivatives are formed photochemically, whereas it seems that linear PMPS has lower oxygen concentration, possibly due to having a lower density and a lower degree of oxidation compared to branched/network polysilanes.

### 1.7.3. Photopolymerisation

PMPS has been used extensively in the photopolymerisation of monomers[40] such as styrene, ρ-chlorostyrene, methyl methacrylate, and *n*-butyl methacrylate. Photolysis initiates homolytic scission of the PMPS backbone, with the resulting radical species being used to polymerise vinyl monomers. The photolysis of PMPS uses UV light of wavelengths between 300 and 400 nm in order to avoid photopolymerisation of the monomers. This polymerisation has been compared in terms of kinetics and molecular weight characteristics to other initiators such as AIBN, and has been found to produce polymers with higher molecular weights for the most part. In addition, partial photochemical degradation of PMPS to initiate polymerisation of styrenes and (meth)acrylates has been used to form block copolymers [section 5.1.6].

## 1. References


[1] West, R. *J. Organomet. Chem.* **1986**, 300, 327.

[2] Miller, R.D.; Michl, J. *Chem. Rev.* **1989**, 89, 1359.

[3] Shieh Y. T.; Hsu T. M.; Sawan S. P.; *J App Polym Sci* **1996**, 62, 1723.

[4] a) Kepler, R.G.; Zeigler, J.M.; Harrah, L.A.; Kurtz, S.R. *Phys. Rev. B.* **1987**, 35, 2818.

b) Samuel, L.M.; Sanda, P.N.; Miller, R.D. *Chem. Phys. Lett.* **1989**, 159, 227.

[5] a) Hiramoto, M.; Sakata, Y.; Yokoyama, M. *Jpn. J. Appl. Phys. 1* **1996**, 35. 4809.

b) Suzuki, H.; Hoshino, S.; Furukawa, K.; Ebata, K.; Yuan, C.H.; Bleyl, I. *Polym. Adv. Tech.* **2000**, 11, 460.

[6] a) Lovinger, A.J. *Polym. Commun.* **1989**, 30, 356.

b) Kajzar, F.; Messier, J.; Rosilio, C. *J. Appl. Phys.* **1986**, 60, 3040.

c) Hasegawa T.; Iwasa Y.; Koda T.; Kishida H.; Tokura Y.; Wada S.; Tashiro H.; Tachibana H.; Matsumoto M.; Miller R. D. *Synthetic Metals* **1995**, 71, 1679.

d) Kishida, H.; Hasegawa, T.; Iwasa, Y.; Koda, T.; Tokura, Y.; Tachibana, H.; Matsumoto, M.; Wada, S.; Lay, T.T.; Tashiro, H. *Phys. Rev. B* **1994**, 50, 7786.

[7] a) Yajima, S.; Hasegawa, J.; Hayashi, H.; Iimura, H. *J. Mater. Sci.* **1978**, 13, 2569.

b) Yajima, S.; Hayashi, J.; Omori, M. *Chem. Lett.* **1975**, 931.

[8] Yagci Y.; Onen A.; Schnabel W. *Macromolecules* **1991**, 24, 462.

[9] Wolff, A.R.; West, R. *Appl. Organomet. Chem.* **1987**, 1, 7.

[10] Kipping, F. *J. Chem. Soc.* **1921**, 119, 330.

[11] a) Wesson, J.P.; Williams, T.C. *J. Polym. Sci., Polym. Chem.* **1980**, 18, 959.

b) Wesson, J.P.; Williams, T.C. *J. Polym. Sci., Polym. Chem.* **1981**, 19, 65.

[12] Trujillo, R.E. *J. Organomet. Chem.* **1980**, C28, 198.

[13] a) Rabolt, J.F.; Hofer, D.; Miller, R.D.; Fickes, G.N. *Macromolecules* **1986**, 19, 611.

b) Kuzmany, H.; Rabolt, J.F.; Farmer, B.L.; Miller, R.D. *J. Chem. Phys.* **1986**, 85, 7413.

[14] Kipping, F.S. *J. Chem. Soc.* **1924**, 125, 2291.

[15] Miller, R.D.; Hofer, D.; Rabolt, J.F.; Fickes, G.N. *J. Am. Chem. Soc.* **1985**, 107, 2172.

[16] Rabolt, J.F.; Hofer, D.; Miller, R.D.; Fickes, G.N. *Macromolecules* **1986**, 19, 611.

[17] a) Karikari, E.K.; Greso, A.J.; Farmer, B.L.; Miller, R.D.; Rabolt, J.F. *Macromolecules* **1993**, 26, 3937.

b) Karikari, E.K.; Farmer, B.L.; Hoffman,C.L.; Rabolt, J.F. *Macromolecules* **1994**, 27, 7185.

[18] Yuan, C.-H.; West, R. *Macromolecules* **1994**, 27, 629.

[19] For a review of thermal properties and phase behaviour of polysilanes see: Demoustier-Champagne, S.; Devaux, J. In *Silicon-Containing Polymers*; Jones, R.G.; Ando, W.; Chojnowski, J. (Eds.) Kluwer Academic Publishers, Netherlands, **2000**.

[20] Walsh, R. *Acc. Chem. Res.* **1981**, 14, 246.

[21] Cotts, P.M.; Miller, R.D.; Trefonas III, P.; West, R.; Fickes, G.N. *Macromolecules* **1987**, 20, 1047.

[22] Strazielle, C.; de Mahieu, A.-F.; Daoust, D.; Devaux J. *Polymer* **1992**, 33, 4174.

[23] Neumann, F.; Teramae, H.; Downing, J.W.; Michl J. *J. Am. Chem. Soc.* **1998**, 120, 573.

[24] Jones, R.G.; Benfield, R.E.; Evans, P.J.; Holder, S.J.; Locke, J.A.M. *J. Organomet. Chem.* **1996**, 521, 171.

[25] a) Schilling, F.C.; Bovey, F.A.; Ziegler, J.M. *Macromolecules* **1986**, 19, 2309.
b) Wolff, A.R.; Maxka, J.; West, R. *J. Polym. Sci., Polym. Chem. Ed.* **1988**, 26, 713.

[26] Wolff, A.R.; Nozue, I.; Maxka, J.; West, R. *J. Polym. Sci., Polym. Chem. Ed.* **1988**, 26, 701.

[27] Ziegler, J.M.; Harrah, L.A.; Johnson, A.W. *Proc. SPIE* **1985**, 539, 166.

[28] a) Trefonas III, P.; Damewood, J.R.; West, R.; Miller, R.D. *Organometallics* **1985**, 4, 1318.
b) Harrah, L.H.; Ziegler, J.M. *J. Polym. Sci., Polym. Lett. Ed.* **1985**, 23, 209.

[29] Kuzmany, H.; Rabolt, J.F.; Farmer, B.L.; Miller, R.D. *J. Chem. Phys.* **1986**, 85, 7413.

[30] Jones, R.G.; Wong, W.K.C. *Organomet.* **1998**, 17, 59.

[31] Nakayama, Y.; Hirooka, K.; West, R. *Solid State Communications* **1996**, 100, 759.

[32] Abkowitz, M.A.; Rice, M.J.; Stolka, M. *Phil. Mag.* **1991**, B61, 25.

[33] Stolka, M.; Yuh, H.-J.; McGrane, K.; Pai, D.M. *J. Polym. Sci. Polym. Chem.* **1987**, 25, 823.

[34] a) Peinado, C.; Alonso, A.; Catalina, F.; Schnabel, W. *Macromol. Chem. Phys.* **2000**, 201, 1156.
b) Yagci Y.; Schnabel, W. *Makromol. Chem. Symp.* **1992**, 60, 133.

[35] Miller, R. D.; Wallraff, G.; Clecak, N.; Sooriyakumaran, R.; Michl, J.; Karatsu, T.; Mckinley, A. I.; Klingensmith, K. A.; Downing, J. *Polym. Eng. Sci.* **1989**, 29, 882.

[36] a) Ramsey, B.G. *J. Organomet. Chem.* **1974**, 67, C67.
b) Sakurai, H.; Kobayashi, Y.; Nakadaira, Y. *J. Am. Chem. Soc.* **1974**, 96, 2656.
c) Sakurai, H.; *J. Orangomet. Chem.* **1980**, 200, 261.

[37] Watanabe, A.; Miike, H.; Tsutsumi, Y.; Matsuda, M. *Macromolecules* **1993**, 26, 2111.

[38] Kabeta, K.; Shuto, K.; Sugi, S.; Imai, T. *Polymer* **1996**, 37, 4327.

[39] Bianconi, P.A.; Weidman, T.W. *J. Am. Chem. Soc.* **1988**, 110, 2342.

[40] Chen, H.B.; Chang, T.C.; Chiu, Y.S.; Ho, S.Y. *J. Polym. Sci., Polym. Chem.* **1996**, 34, 679.

# 2. Introduction to Atom Transfer Radical Polymerisation

## 2.1. Overview

Over the past decade or so, atom transfer radical polymerisation (ATRP)[1,2] has become one of the most successful controlled synthetic routes available for the polymerisation of styrenes, (meth)acrylates, (meth)acrylamides, etc. ATRP is one of the more versatile controlled radical polymerisations and can produce well-defined polymers which were previously unknown. Also, it can be used to synthesise polymers with low polydispersities and predetermined molecular weights. It has been described as a 'robust' process which can tolerate a range of reaction conditions. Incorporating several components, including the initiator, metal-ligand complex, and solvents or additives, the reaction conditions can be altered in order to optimise polymerisation of a particular monomer. The radical nature of ATRP also means that a wide range of monomers with various functionalities can be polymerised, while the initiator can determine the end group functionality of the resulting polymer.

## 2.2. Living polymerisation

In order to describe a process by which polymerisation occurs, it is necessary to take into consideration all of the reactions involved. For instance, the initiation, propagation, chain breaking/termination, and other side reactions such as exchange and isomerism reactions need to be taken into account. A "living" polymerisation can be described as having no chain breaking or termination steps, and can propagate for an indefinite length of time.[3] Since living polymerisations proceed indefinitely, termination occurs only when the reaction is halted by an external process. Since termination is avoidable, this distinguishes "living" polymerisation from other polymer processes where naturally occurring termination is unavoidable.[3] However, no polymer can grow indefinitely or increase in molecular weight beyond certain limits and, it needs to be fed (in the form of monomers) in order to continue to propagate.

In particular, the field of nanotechnology in materials science is of great interest due to the technological advances associated with making smaller and smaller

components. By improving the synthetic procedures that yield highly regular, monodisperse polymer, the behaviour of polymeric nanocrystals is increasingly being studied.[4] In this respect, "living" polymerisation has achieved the necessary predetermined molecular weight characteristics and architectures of block and graft copolymers required for nanomaterial research. This is important since the size and shape of the polymer can greatly influence the characteristics of a material. As is often the case for electrical conductivity and magnetism, certain properties can be altered quite quickly as the size of a polymer changes, even though the structure or chemistry might remain the same.[5]

## 2.3. Free radical polymerisation

Free radical polymerisation (FRP) is the most extensively used and researched chemical chain reaction.[6] The polymerisation is initiated via the formation of free radical (R•) which reacts with the double bond present in the monomer (M). The types of monomers involved in FRP are either mono-substituted or unsymmetrically di-substituted ethylenes. The polymerisation (propagation) involves the free-radical addition, linking monomers predominantly in a head-to-tail. Termination usually occurs via bimolecular termination or chain transfer reactions (scheme **2.1**).

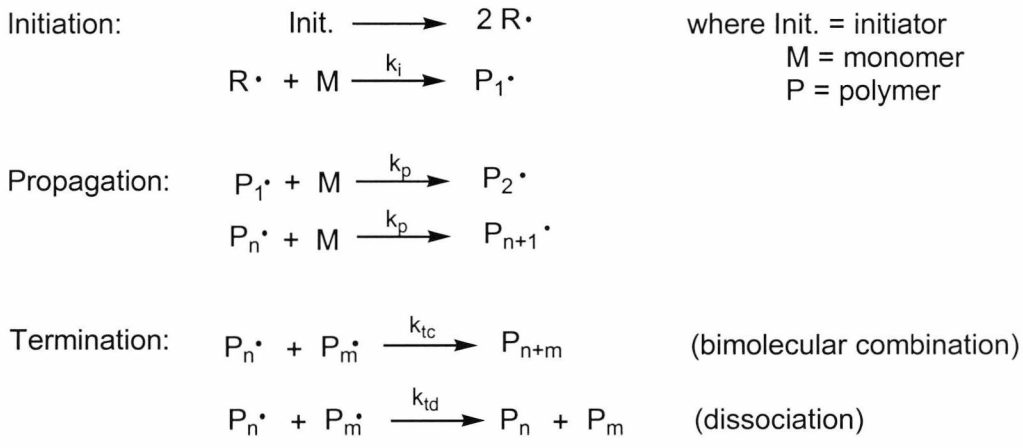


**Scheme 2.1.** Free radical polymerisation

The versatility and simplicity of FRP means a wide range of polymers can be synthesised. Substituents on the monomers influence the reactivities of the propagating radicals, although few restrictions apply to the type of substituents present. The substituents also affect the properties of the resulting polymers.

## 2.4. Controlled/"living" free radical polymerisation

For over 50 years, radical polymerisation has been the most commercially important polymerisation process.[6] However, due to the relative ease with which relevant macromolecular structures can be controlled, most academic research has been carried out on co-ordination,[7] cationic,[8] anionic,[9] and ring-opening polymerisation.[10] Fast and irreversible termination reactions, due to the coupling and disproportionation of the polymer radicals, has made radical polymerisations more difficult to control compared to "living" polymerisations. Recently, controlled radical polymerisation techniques have been developed whereby this termination problem has been suppressed.[11]

In living radical polymerisation it has proved virtually impossible to prevent bimolecular termination completely. Although the probability of termination can be minimised, it cannot be discounted altogether, and therefore there are limits associated with "living" polymerisation. As the polymerisation progresses to yield higher molecular weight polymer, the influence of termination, transfer, and side reactions need to be considered as they become more and more likely.[12]

The polymerisation is described as being "controlled" since the molecular weight parameters and the functionalities can be determined through the preparation of the polymer. Controlled radical polymerisation makes use of radical processes that are more tolerant of functional groups and impurities.[6] A rapid growth in understanding in this field has occurred relatively recently, following the realisation of the involvement of a rapid dynamic equilibrium between a low concentration of radicals and a high concentration of dormant, deactivated species. Since the greatest difficulty for synthesising well-defined polymers is caused by unavoidable bimolecular termination between growing radicals, this obstacle can be overcome by reducing the radical concentration. Equation 2.1 illustrates the kinetics involved in controlled radical polymerisation.

$$R\bullet + R\bullet \rightarrow R\text{-}R \qquad R_t = k_t[R\bullet]^2 \qquad (2.1.1.)$$

$$R\bullet + M \rightarrow R\text{-}M\bullet \qquad R_p = k_p[R\bullet][M] \qquad (2.1.2.)$$

The rate of termination ($R_t$) is second order with respect to the concentration of propagating radicals ([R•]), while the rate of propagation ($R_p$) is first order with respect to [R•] monomer concentration ([M]). Hence, the conditions required for low polydispersity polymers are that the deactivated species needs to be more prominent than the activated species, i.e. the equilibrium lies to the left. In other words, the rate of exchange between the dormant species and growing radicals needs to be greater than the rate of propagation. Finally, the polydispersity of the polymer will be low since the probability that a monomer molecule will be added will be the same for each propagating chain.

### 2.4.1. Synthesis of materials and functionality

Polymers synthesised via living polymerisation are well defined in terms of both molecular weight and architecture. The initiation step is crucial in determining how well the molecular weights can be controlled. As mentioned earlier, if the rate of initiation is at least as fast as the rate of propagation and the exchange between the deactivated and activated species is also fast, the polydispersity ($DP_n$) can be kept low, and the molecular weights of the polymers can be pre-determined simply by adjusting the monomer ($[M]_0$) to initiator ($[I]_0$) molar ratio (Equation 2.2).

$$\overline{DP_n} = [M]_0/[I]_0 \qquad (2.2)$$

The functionality of the polymer can be determined by altering the structure of the initiator and the active end groups. Thus, a range of new materials have been developed using living polymerisation. For example, the topology of polymeric structures can be manipulated to give comb, star, and dendritic polymers. In addition, the composition of copolymers can be altered to include random, graft, and block structures [for further discussion and references, see chapter **4**].

### 2.4.2. Types of controlled/"living" polymerisation

Controlled/"living" radical polymerisation methods can be divided into three main types, namely stable free radical polymerisation (SFRP),[13] atom transfer radical polymerisation (ATRP),[1] and degenerative transfer.[14]

#### 2.4.2.1. Stable free radical polymerisation

The reversible capture of the polymeric radical ($P_n\cdot$) by another species ($X\cdot$) to form a stable molecule serves to limit the rate of polymerisation of the monomer (M) (scheme **2.2**).[15] An example is TEMPO-mediated stable free radical polymerisation.[16] The mechanism of SFRP and the synthesis of block copolymers using this method are discussed in greater detail elsewhere [chapter **7**].

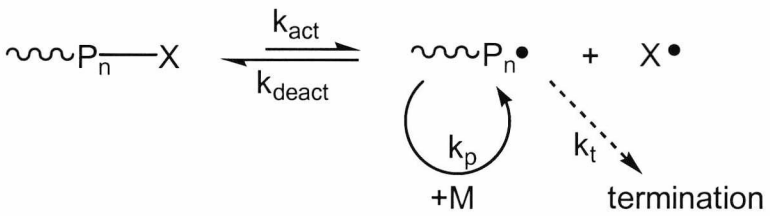


**Scheme 2.2.** Persistent or stable free radical polymerisation

#### 2.4.2.2. Metal-catalysed atom transfer radical polymerisation

The rapid reversible transfer of a functional group (X) between propagating radicals and a transition element co-ordination site results in dormant and active polymer chain ends (scheme **2.3**). An example is atom transfer radical polymerisation.[1]

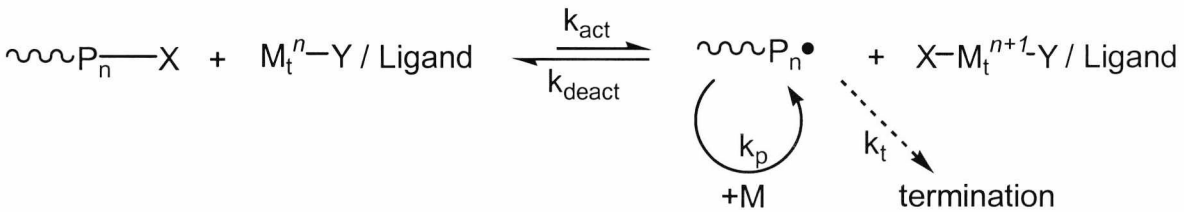


**Scheme 2.3.** Atom Transfer Radical Polymerisation (ATRP) (M = monomer, $M_t$ = transition metal, Y = ligand)

### 2.4.2.3. Degenerative transfer

Degenerative transfer systems require a rapid and reversible exchange of highly active transferable groups and polymer radicals. The transfer process is a thermodynamically neutral exchange between growing radicals, existing at low concentrations, and dormant species (scheme **2.4**).[14] An example of this is reversible addition-fragmentation chain transfer (RAFT), which involves the polymerisation of vinyl monomers using, for example, dithioesters as transfer agents.[17]

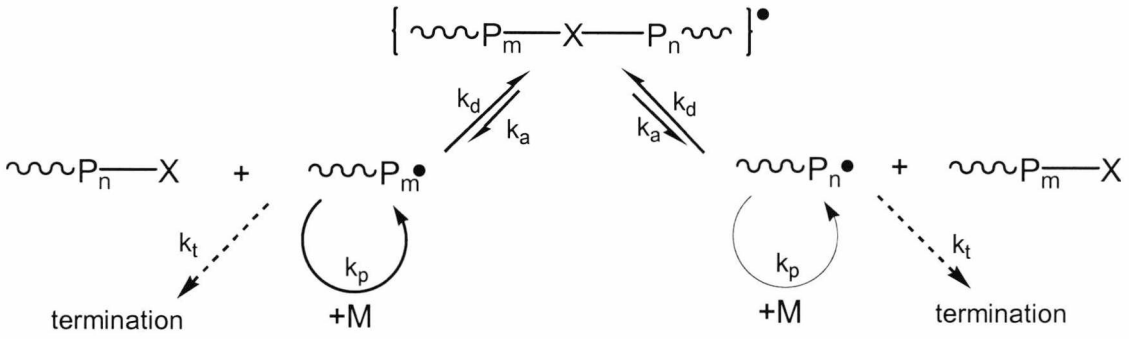


**Scheme 2.4.** Polymerisation via a thermodynamically neutral exchange process

## 2.5. Atom transfer radical addition

The origins of ATRP are found in atom transfer radical addition (ATRA)[18] which is a process involving the formation of C-C bonds. There are two types of ATRA. Firstly, atom abstraction or homolytic substitution occurs when a univalent atom, such as a halogen, is transferred from a neutral molecule, R-X, to form a radical, R• (scheme **2.5.1**). This radical then reacts to form a new σ-bond with another molecule, usually an alkene, forming a new radical (scheme **2.5.2**). Hence, in ATRA an alkyl group, R, will act as both the initiator and as the propagating radical (as is the case for ATRP). Secondly, transition metals are present in catalytic amounts to act as carriers for halogen atoms in the redox process. After the addition reaction, the halogen can be returned to the alkyl radical, and the metal can be regenerated, allowing the sequence to start again (scheme **2.5.3**).

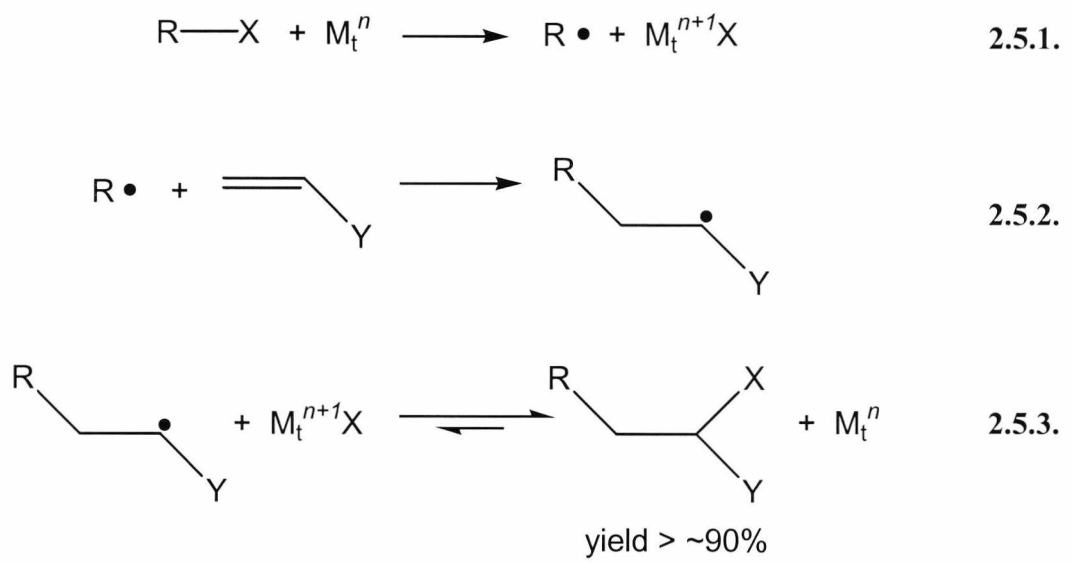


**Scheme 2.5.** Atom transfer radical addition

The yield for this reaction is high, suggesting that the redox reaction of $M_t^n/M_t^{n+1}$ gives a low concentration of free radicals. Several ATRAs will occur if firstly the macromolecular alkyl halides are reactive enough towards the transition metal, and secondly if there is an excess of alkene (monomer) molecules. ATRP involves the extension of several ATRA reactions to yield a polymerisation process which has a degree of "livingness".

## 2.6. Mechanism and kinetics of ATRP

Control over radical polymerisations such as ATRP is based on two principles: fast initiation to form a constant concentration of growing polymer chains, and the existence of most of the growing chains in the dormant state. ATRP achieves these two aims by using a catalytic complex made up of a transition metal and a suitable ligand. This complex is used to set up a reversible equilibrium between the dormant species and the propagating radicals (scheme **2.6**). Equilibrium is determined through the choice of ligand, which is also used to solubilise the catalyst complex. The deactivated species should be favoured in order to keep the concentration of propagating radicals low enough, ensuring termination is minimal. Generally, the

proportion of terminated chains is relatively low (<5%) compared to the proportion of functional chains that result (>95%).[19]

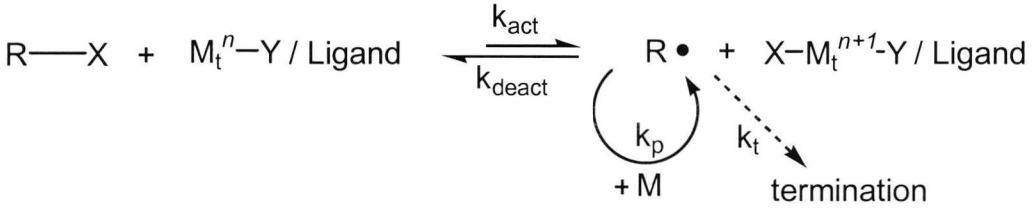


**Scheme 2.6.** Reversible equilibrium reaction of ATRP (M = monomer, $M_t$ = metal)

The elaborated mechanism of ATRP is shown in scheme **2.7** from which the initiation, propagation, and termination steps of the chain reaction are derived. A copper catalyst is used as an example.

Initiation:

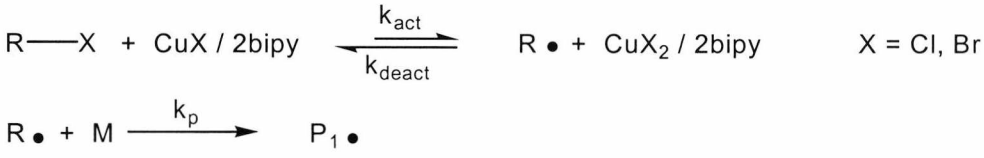


Propagation:

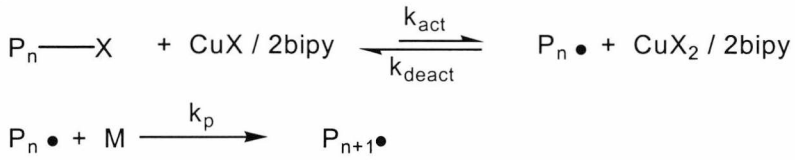


Termination:

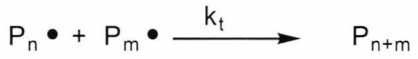


**Scheme 2.7.** Reaction mechanisms of ATRP

Initiation needs to be relatively fast compared to propagation in order to ensure that the chains start to grow at the same time such that a product of low polydispersity is obtained.

Propagation can be viewed as an "insertion" process, proceeding via radical intermediates. Also, although bimolecular termination is negligible, it can still occur either through combination or by disproportionation. Some side-reactions, such as chain-transfer, can also occur and both these effects lead to a broadening of the molecular weight distribution.

The rate law[12] is represented in equation 2.3, where $R_p$ is the rate of polymerisation, and $k_{app}$ is the apparent rate constant for the overall reaction (other notation corresponds to that used in scheme 2.7). It is derived by omitting the termination step since it is generally accepted that, although termination will occur in ATRP, it is in fact insignificant. A fast-equilibrium approximation is used.

$$R_p = k_{app}[M] = k_p[P\cdot][M] = k_p K_{eq}[R\text{-}X]\frac{[Cu(I)]}{[Cu(II)]}[M] \qquad (2.3)$$

$$\text{where } K_{eq} = \frac{k_{act}}{k_{deact}} = \frac{[P\cdot][Cu^{II}X]}{[Cu^{I}][PX]}$$

The control and the molecular weight parameters of the polymeric product depend on the stationary concentration of the growing radicals as well as the relative rates of propagation and deactivation. The growing polymer radical does not have the catalyst bound to it as such, and so ATRP can be described as being similar for both homogeneous and heterogeneous systems. Because ATRP is a catalysed reaction, the choice of catalyst and the amount used will affect the equilibrium of the system. Therefore, the active radical concentration will be affected, and this in turn will determine the rate of polymerisation ($R_p$). $R_p$ is first order with respect to monomer concentration, [M], initiator, R-X, and the transition metal complex, i.e. the catalyst. In accordance with equation 2.2, the reaction is also usually negative first order with respect to the deactivator, e.g. Cu(II)X.[12]

In reality, the kinetic law is more complex for the deactivated species since some is spontaneously formed during the reaction. A persistent radical effect[11] is established as a consequence because at the beginning of the reaction, both the radicals and the deactivator are present in very high concentrations.

## 2.7. Components and reaction conditions of ATRP

### 2.7.1. Overview

Made up of components such as the initiator (R-X), activator, ligands, monomer, deactivator, growing chains, and additives (solvent), ATRP is often referred to as a "multi-component system".[2] Hence, the chemistry, structure, and concentration of the initiator are considered, as well as its relationship to the monomers involved. Also, the type of ligand used is important in terms of solubilising the transition metal and the type of deactivated species that will result. In addition, ATRP reactions can be carried out either in the 'bulk' or in solution, usually in relatively non-polar solvents such as toluene, and at elevated temperatures. Finally, ATRP reactions can take from between a few minutes to several hours to achieve high conversions.

### 2.7.2. Initiators

ATRP is initiated by halogenated alkyl groups (R-X), sometimes described as alkyl(pseudo)halides,[20] that are activated by allyl, aryl, sulfone, or carbonyl substituents (scheme **2.8**).

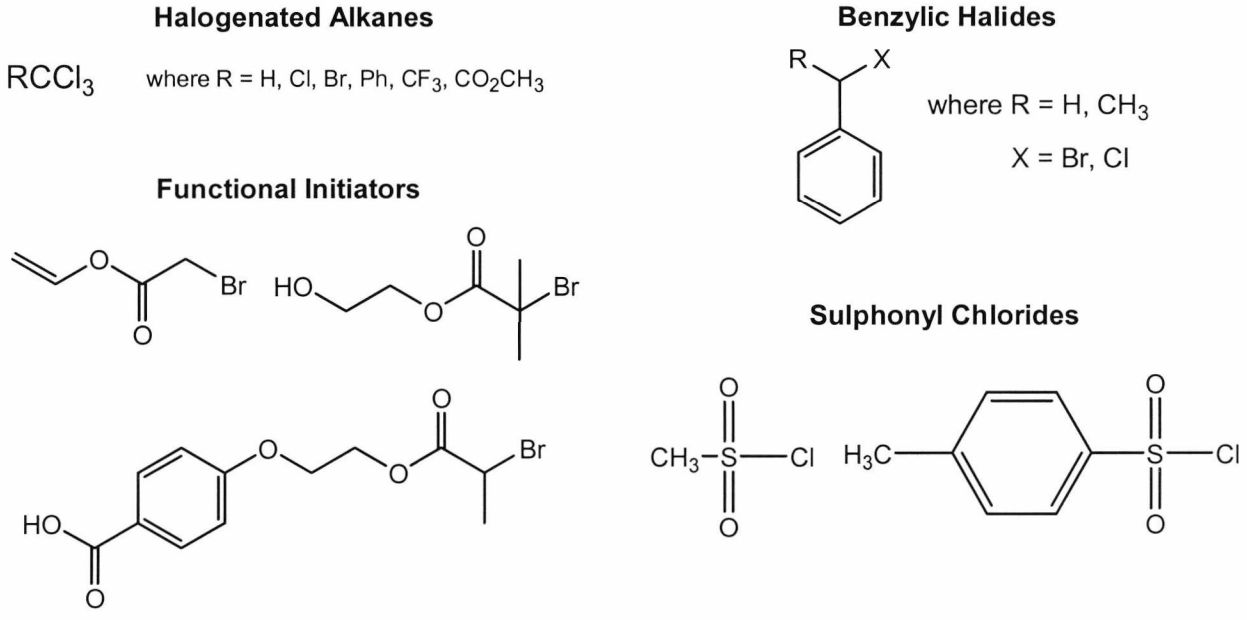


**Scheme 2.8.** Some examples of ATRP initiators

Recent development of controlled/"living" polymerisations has lead to research into the effects of substituents on the initiator. Generally, any R-X group with activating substituents on the α-carbon can be used for ATRP initiation. The substituents on the α-carbon are important because their steric and electronic characteristics affect how well vinyl monomers, such as (meth)acrylates and styrenes, can be polymerised. The concentration of the initiator also determines the number of chains that will be grown during the polymerisation. The monomer to initiator molar ratio, $[M]_o/[I]_o$, shows that the amount of initiator will be inversely proportional to the molecular weight of the resulting polymer chains.

#### 2.7.2.1. The alkyl group

Alkyl halides can be cleaved either homolytically or heterolytically depending on the substituents as well as the environment in which the reaction is taking place. The homolytic dissociation energy of the carbon-halogen bond is of importance because the ease with which radicals are formed is relevant to the kinetics of ATRP. In the case of alkyl halides such as dichloromethane, efficient chlorine atom transfer from R-Cl to Cu(I)Cl in order to form the alkyl radical and the Cu(II)Cl is very difficult because of the strength of the C-Cl bond. Hence, a lower bond dissociation energy is preferred and this is achieved by the inclusion of a stabilising substituent, which will make transfer easier, and thereby increase initiator efficiency and reduce the polydispersity of the product.[2,21] If the alkyl group of the initiator has a similar architecture, this will usually ensure that the rate of initiation will be at least as fast as the rate of re-initiation of the deactivated polymer species. However, this is not always possible and in the cases where the initiators are not similar to the architecture of the propagating chain, it is important to choose initiators that form less reactive radicals compared to the dormant polymer chain ends. There is also an upper limit to the stability of the derived radical. Due to the kinetics discussed previously, if the R• species is too stable, then the concentration of radicals in the system will be too high. In terms of block copolymer synthesis, the R group of the initiator can also be a functionalised polymer. A detailed discussion on ATRP block copolymers is presented in chapter **6**.

### 2.7.2.2. The halogen

Alkyl chlorides or alkyl bromides with substituents that have either inductive or resonance stabilising effects are efficient initiators and lead to polymers with quite narrow molecular weight distributions. The halogens most commonly used have been bromine and chlorine, but iodine[22] has also been used. Fluorine is not used since the C-F bond is too strong to undergo homolytic cleavage. The choice of halogen is important when considering the speed and control with which ATRP is carried out. In most cases, the halide group of the initiator matches that of the metal salt. However, the use of a mixed halide initiating system can lead to a more efficient polymerisation by increasing the relative rate of initiation vs. propagation. This is due to the relative strengths of the R-Cl and R-Br bonds.[23]

The weakness of the C-I bond has limited the use of initiators involving iodine to the synthesis of acrylates and thiocyanates. For example, R-I initiators tend to take part in side reactions when used in the polymerisation of styrene via the heterolytic elimination of HI. As far as fluorine initiators are concerned, fluorine tends to bind too strongly with the α-carbon and therefore the formation of radicals has proved difficult. Pseudohalogens such as thiocyanates have been used for the synthesis of polyacrylates and polystyrenes. Other alkyl halides, such as *t*-butyl chloride, $C_4H_9Cl$, and dichloromethane, $CH_2Cl_2$, are poor initiators and give uncontrolled polymers that have high molecular weights and broad molecular weight distributions.[21] Other types of initiators have been reviewed by Matyjaszewski and Xia[2] and include polyhalogenated compounds, such as $CCl_4$ and $CHCl_3$, and many other compounds containing weak C-X bonds.

### 2.7.3. Metal-ligand complexes

There are many types of metal-ligand complexes that have been the subject of extensive research in ATRP. Copper salts with amino ligands have formed the complexes most commonly used, although transition metal complexes have also been investigated.

### 2.7.3.1. The metal ion

Metal-ligand complexes are required to fulfil certain requirements[12] in order to catalyse ATRP efficiently:

- High selectivity towards the atom transfer process, and relative lability towards the resulting deactivated complexes, $X\text{-}M_t^{n+1}$.
- The metal should undergo a one-electron transfer redox cycle rather than a two-electron cycle, which would result in addition/elimination reactions.
- The metal needs to have a high affinity for the halogen atom, X, and a low affinity for hydrogen atoms and alkyl radicals. If not, organometallic compounds may be formed, and these can interfere with propagation and control.
- Most importantly, ATRP does not involve electron transfer, but atom transfer, so the metal centre must be able to change its coordination in order to accommodate the transferred halogen atom. For example, the copper-2,2′-bipyridine complex is shown in scheme **2.9**. In this case, the complex will need to change from a tetra-coordinate to a penta-coordinate species.

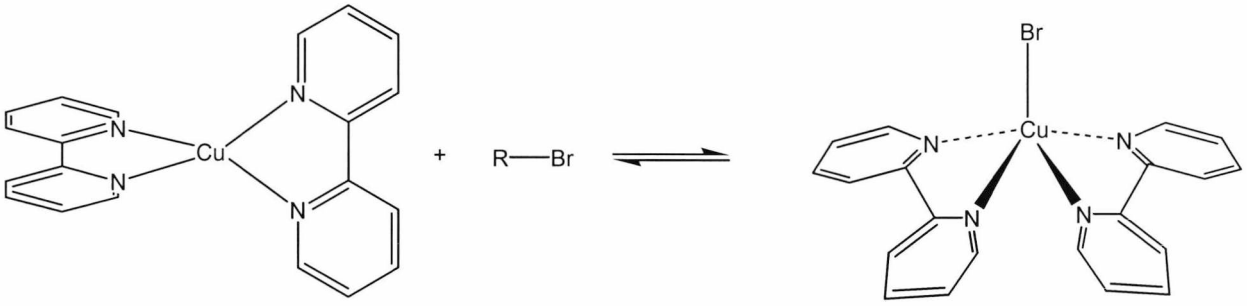


**Scheme 2.14.** Proposed change in structure and coordination number of a metal-ligand complex ($Cu^{I}$2bipy to Br-$Cu^{II}$2bipy).[12]

### 2.5.3.2. The Ligand

Ligands generally have three recognised roles, each of which will be addressed in turn:[24]

- The optimisation of redox properties.
- The control of selectivity via steric/electronic effects.

- Solubilisation of the transition metal

Nitrogen-based ligands have been used extensively in copper and iron-mediated ATRP.[2,25] Phosphine ligands are used in complexes containing metals such as ruthenium, rhodium, iron, nickel, and palladium, but are not used in copper-based catalysts. Sulphur and oxygen co-ordinated ligands are also used but are less effective.

The position of the atom transfer equilibrium is important. The equation is dependent on the nature of both the metal and the ligands. Good electron-donating ligands increase the stability of the high oxidation state of the metal complex, $XM_t^{n+1}L_2$, thereby accelerating polymerisation. Monodentate (e.g. tributylamine) and bidentate (e.g. bipyridine) ligands have been used in iron-mediated ATRA. However, in copper-based reactions, the coordination chemistry of the metal complex is such that it has an important effect on the activity of the catalyst. Unlike in ATRA, monodentate ligands have been shown to be unsuited to ATRP, whilst bidentate and multidentate ligands have been shown to be quite successful.

Also, deactivation needs to be fast or else control of molecular weight will be lost and polydispersity will increase. Therefore a good deactivator will reduce polymerisation rates and polydispersities, but may also take part in side reactions.

The electronic and steric properties of the ligands can lead to a reduction in activity and efficiency of the catalyst. This can result from steric hindrance around the transition metal centre or strong electron-withdrawing groups on the ligands. An extensive review[2,24] has resulted in several general trends being identified, which include the following:

- Activity increases as the number of coordinating sites increases, i.e. $N_4 > N_3 > N_2 >> N_1$.
- Activity decreases as the number of bridging carbon atoms between the nitrogen atoms increases, i.e. $C_2 > C_3 >> C_4$.
- Activity increases when the ligands contain bridged and cyclic groups as opposed to linear segments.

Some catalysts are insoluble in non-polar media (such as in bulk polymerisations of styrene or methyl methacrylate). However, it is possible to solubilise metal complexes in low permittivity media by using ligands, such as N-(n-propyl)-2-pyridylmethanimine,[26] which have suitable functional groups including long alkyl chains or "tails". The ligand structure can be varied to suit the particular monomers and solvent, and this is an area which is currently being researched extensively. Appropriate ligand design is particularly important when ATRP is carried out either in heterogeneous mixtures, water, or ionic liquids. The efficiencies of the ligands are dependent on the partition coefficients involved, as well as the temperature at which the reaction takes place. Hence, a range of ligands derived from amines such as bipyridine are shown in scheme **2.10**. There are many variations of amino ligands which have different groups which are capable of solubilising the complex in different solvents and monomers.

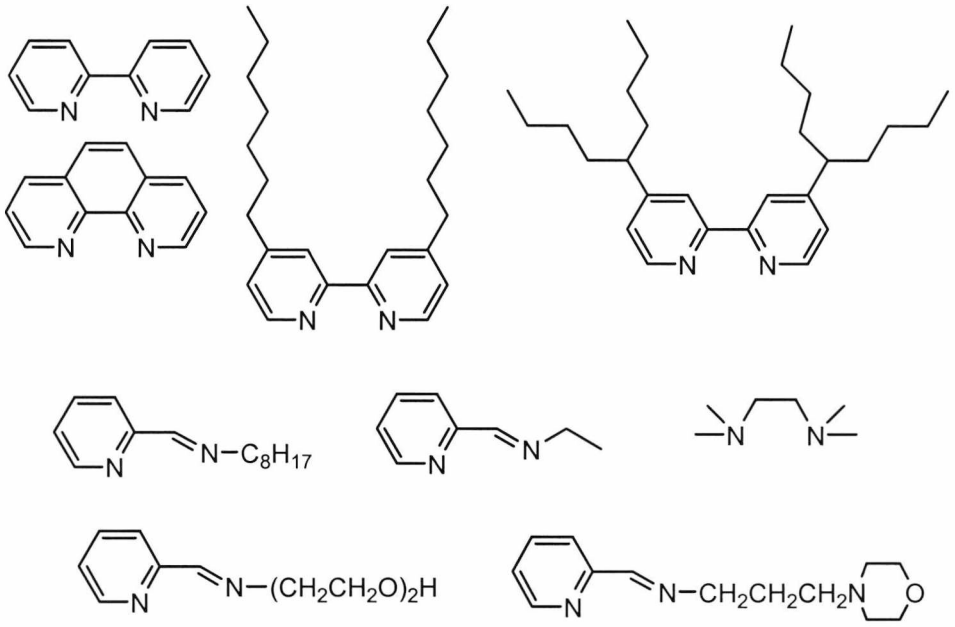


**Scheme 2.10.** Examples of ligands used in ATRP

Thus, the ligand has several purposes with respect to the successful design of the catalyst, including the tuning of the atom transfer equilibrium constants and dynamics. The ligand also determines selectivity, solubility and complex stability when using different monomers, solvents, and temperatures. Finally, it can also influence how

easily the catalyst is removed (and possibly recycled) by how well the catalyst is immobilised.

### 2.7.4. Monomers

ATRP has been used to polymerise a wide variety of vinyl monomers, including (meth)acrylates, styrenes, (meth)acrylamides, and acrylonitrile (scheme **2.15**).

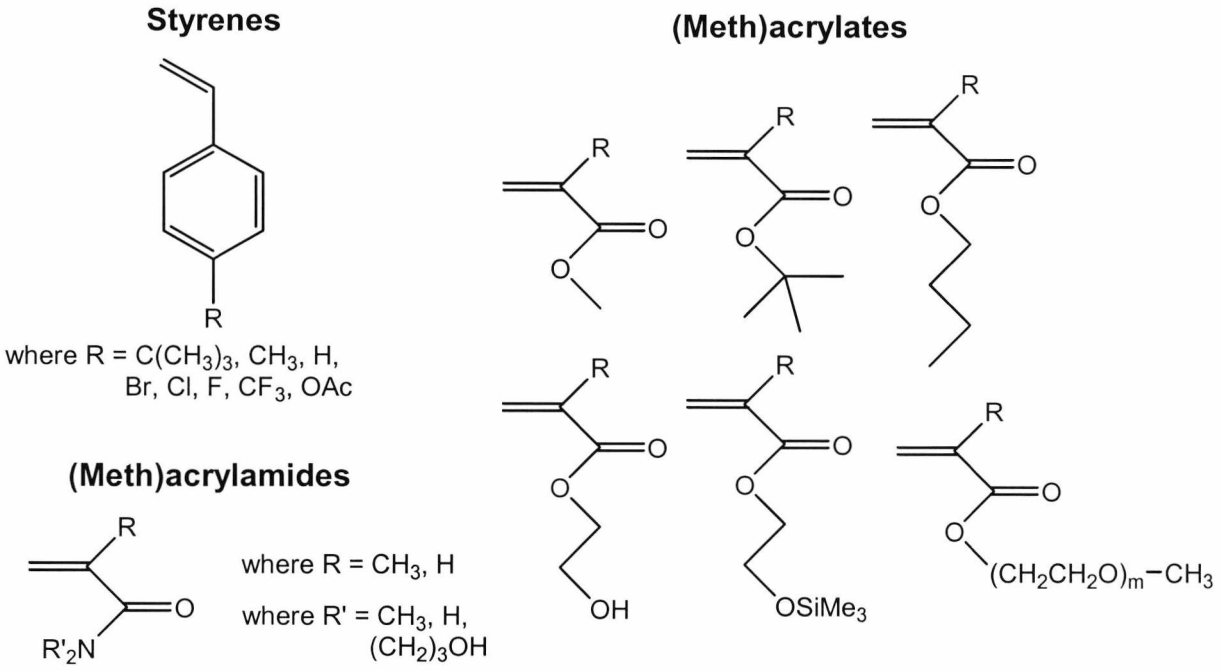


**Scheme 2.11.** Examples of monomers used in ATRP

Like the alkyl halide initiators, these monomers all have substituents capable of stabilising propagating radicals. In experiments where all the reaction conditions except the identity of the monomer have been kept the same, it has been shown that each monomer has its own unique propagation rate based on the equilibrium rate constant ($K_{eq}=k_{act}/k_{deact}$). In order to maintain control over polymerisation of various monomers with differing radical propagation rates, the concentrations of radicals and the rates of deactivation need to be adjusted. Since ATRP is a catalysed reaction, the equilibrium therefore relies not only on the monomer and the deactivated species, but also on the nature of the transition metal catalyst. Functional monomers can also be

polymerised using ATRP and the resulting polymers can then be used to synthesise copolymers via further ATRP reactions or step-growth reactions.[2]

Although ATRP can be used to polymerise a number of different monomers, some less reactive monomers, such as ethylene and vinyl chlorides, which produce unstable reactive radicals are not susceptible. Furthermore, some monomer structures can lead to heterolytic as well as homolytic cleavage of the R-X bond, which is indicated by the involvement of cationic intermediates. Acidic monomers, such as (meth)acrylic acid, cannot be polymerised owing to the formation of carboxylates in the deactivator($Cu^{II}$), making reduction back to the active $Cu^{I}$ complex difficult.[27]

### 2.7.5. Solvents and additives

ATRP can be carried out in either bulk, in solution, or in heterogeneous systems. Although most ATRP reactions have been carried out in bulk, a solvent can be added when a solid monomer is to be polymerised. The rate of an ATRP reaction carried out in solution will be different compared to the corresponding bulk reaction. Since the rate of reaction is proportional to monomer concentration, the use of a solvent will usually mean the rate of polymerisation will decrease. However, in some cases, it has been proposed that the presence of a solvent can change the structure of the catalyst.[28]

In addition, the solvents used are usually non-polar (*o*-xylene, benzene, THF), but recently ATRP has been carried out in polar solvents such as water and methanol (and combination of both).[29] Polar solvents have also led to the enhancement of rates of some monomers.[30]

The choice of solvent depends on a number of factors. Firstly, solvents should not undergo chain transfer too readily. Secondly, possible interactions between the solvent and the catalyst can hinder polymerisation. These may include solvolysis of the ligand or displacement of spectator ligands. Lastly, the polymer endgroups can undergo interaction with the solvent through solvolysis or elimination reactions (of HX) at elevated temperatures. This is particularly true for very polar solvents.[28]

Additives (such as water or phenol) can be added in small concentrations in order to saturate the coordinating sphere of the active Cu(I) complex or by forming Cu(I)X complexes inactive to atom transfer, thereby, accelerating the rate of polymerisation.[30]

Although ATRP is considered to be a robust process, it is important to note that it is quite sensitive to the presence of oxygen. A small amount can be scavenged by the

catalyst, leading to the oxidation of the catalyst. This means that the complex concentration will be reduced, slowing the rate of polymerisation. Too much oxygen inhibits the polymerisation, as is the case for conventional free radical polymerisation.

### 2.7.6. Reaction Temperature

For each monomer that undergoes ATRP, there exists an optimum temperature range which depends not only on the nature of the monomer, but also on the catalyst and required molecular weight of the resulting polymer. The observed rate of polymerisation increases as temperature increases. This is because of the increase in the radical propagation rate constant, and the atom transfer equilibrium constant. Since the activation energy of propagation is higher than that of a radical termination, the $k_p/k_t$ ratio will increase, thereby improving control over the system. The catalyst can also become more soluble at elevated temperatures. However, at higher temperatures chain transfer and other side reactions become more likely. Therefore the optimum temperature for an individual monomer will need to take such possibilities into account.

### 2.7.7. Reaction Time

The length of time for which a reaction is allowed to proceed can have significant effects on polymer architecture and functionality, as well as molecular weight distribution. Importantly, as the reaction nears completion and complete monomer conversion, the rate of propagation is reduced, whereas the rate at which any side reactions take place is maintained. Therefore, continued heating after all the available monomer has been consumed is ill advised if end group functionality, as is the case when carrying out block copolymerisations, is of importance. In such situations, it is usual to end the reaction before conversion exceeds 95%. [2,31]

## 2. References


[1] a) Wang, J-S.; Matjyaszewski, K. *J. Am. Chem. Soc.* **1995**, 117, 5614.

b) Percec, V.; Barbiou, B. *Macromolecules* **1995**, 28, 1721.

c) Kato, M.; Kamigaito, M.; Sawamoto, M.; Higashimura, T. *Macromolecules* **1995**, 28, 1721.

[2] For a comprehensive review of ATRP and references therein, see: Matyjaszewski, K.; Xia, J. *Chem. Rev.* **2001**, 101, 2921.

[3] Szwarc, M. *Nature* **1956**, 178, 1168.

[4] Forster, S.; Antonietti, M. *Adv. Mater.* **1998**, 10, 195.

[5] Reiss, G.; Hurtrez, G.; Bahadur, P. in *Encyclopedia of Polymer Science and Engineering*; Mark, H.F.; Bikales, N.M.; Overberger, C.G.; Menges, G. (Eds.) Wiley, New York, **1990**.

[6] Georges, M.K.; Veregin, R.P.N.; Kazmaier, P.M.; Hamer, G.K. *Trends Polym. Sci.* **1994**, 2, 66.

[7] Price, C.C.; Osgan, M. *J. Am. Chem. Soc.* **1956**, 78, 4787.

[8] a) Miyamoto, M.; Sawamoto, M.; Higashimura, T. *Macromolecules* **1984**, 17, 265.

b) Minoda, M.; Sawamoto, M.; Higashimura, T. *Macromolecules* **1990**, 23, 1897.

[9] Szwarc, M.; Levy, M.; Milkovich, R. *J. Am. Chem. Soc.* **1957**, 78, 2656.

[10] Clay, R.T.; Cohen, R.E. *Supramol. Sci.* **1995**, 2, 183.

[11] Fischer, H. *Macromolecules* **1997**, 30, 5666.

[12] Matyjaszewski, K.; Patten, T.E.; Xia, J. *J. Am. Chem. Soc.* **1997**, 119, 674.

[13] Solomon, D.H.; Rizzardo, E.; Cacioli, P. U.S. Pat 4581429, 1986; *Chem. Abstr.* **1985**, 102, 221335.

[14] Chiefari,J.; Chong, Y.K.; Ercole, F.; Krstina, J.; Jeffery, J.; Le, T.P.T.; Mayadunne, R.T.A.; Meijs, G.F.; Moad, C.L.; Moad, G.; Rizzardo, E.; Thang, S.H. *Macromolecules* **1998**, 31, 5559.

[15] Matyjaszewski, K. *Chem. Eur. J.* **1999**, 5, 3095.

[16] a) Georges, M.; Veregin, R.; Kazmaier, P.; Hamer, G. *Macromolecules* **1993**, 26, 2987.

b) Hawker, C.J. *J. Am. Chem. Soc.* **1994**, 116, 11185.

[17] Chong, Y. K.; Le, T. P. T.; Moad, G.; Rizzardo, E.; Thang, S. H. *Macromolecules* **1999**, 32, 2071.

[18] Curran, D.P. *Synthesis* **1988**, 489.

[19] Coessens, V.; Pintauer, T.; Matyjaszewski, K. *Prog. Polym. Sci.* **2001**, 26, 337.

[20] a) Davis, K.; O'Malley, J.; Paik, H.-J.; Matyjaszewski, K. *Polym. Prepr. (Am. Chem. Soc., Div. Polym. Chem.)* **1997**, 38, 687.

b) Singha, N.K.; Klumperman, B. *Macromol. Rapid. Commun.* **2000**, 21, 1116.

[21] Wang, J.-S.; Matyjaszewski, K. *Macromolecules* **1995**, 28, 7901.

[22] Kotani, Y.; Kamigaito, M.; Sawamoto, M. *Macromolecules* **1999**, 32, 2420.

[23] Matyjaszewski, K.; Shipp, D.A.; Wang, J.-S.; Grimaud, T.; Patten, T.E. *Macromolecules* **1998**, 31, 6836.

[24] Xia, J.; Zhang, X.; Matyjaszewski, K. *ACS Symp. Ser.* **2000**, 760, 207.

[25] Matyjaszewski, K.; Wei, M.; Xia, J.; McDermott, N.E. *Macromolecules* **1997**, 30, 8161.

[26] Haddleton, D.M.; Crossman, M.C.; Dana B.H.; Duncalf, D.J.; Heming, A.M.; Kukulj, D.; Shooter, A.J. *Macromolecules* **2000**, *33*, 6640.

[27] a) Ashford, E.J.; Naldi, V.; O'Dell, R.; Billingham, N.C.; Armes, S.P. *Chem. Commun.* **1999**, 1285.

b) Wang, X.S.; Jackson, R.A.; Armes, S.P. *Macromolecules* **2000**, 33, 25.

[28] Matyjaszewski, K.; Nakagawa, K.; Jasieczek, C.G. *Macromolecules* **1998**, 31, 1535.

[29] Robinson, K.L.; Khan, M.A.; de Paz-Banez, M.V.; Wang, X.S.; Armes, S.P. *Macromolecules* **2001**, 34, 3155.

[30] Fischer, H. *Macromolecules* **1997**, 30, 5666.

[31] Matyjaszewski, K. *ACS Symp. Ser.* **2000**, 768, 2.

# 3. Synthesis and characterisation of poly(methylphenylsilane)

## 3.1. Introduction

### 3.1.1. Wurtz-reductive coupling reaction

#### 3.1.1.1. Background

In contrast to the synthesis of organic polymers, the synthesis of polysilanes is not easily achieved and has been found to be quite difficult to control in terms of molecular weight distributions. Approximately 80 years ago Kipping first synthesised poly(diphenylsilane) via a condensation reaction using an alkali metal.[1] Despite attempts to find alternative methods of synthesising polysilanes, the Wurtz-reductive coupling reaction of dichlorodiorganosilanes ($Cl_2R_2Si$) using a metal such as sodium is still the most popular method by which polysilanes are prepared (scheme **3.1**).

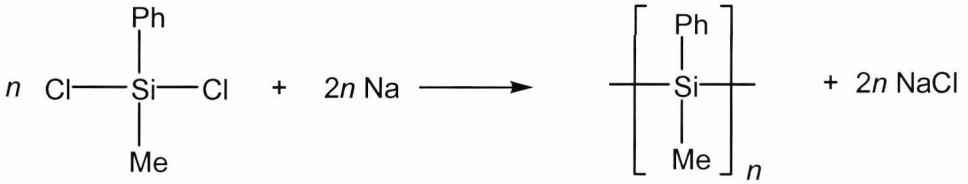


**Scheme 3.1.** Synthesis of poly(methylphenylsilane) via the Wurtz reaction

In most cases, the sodium is present as a dispersion, usually in an inert aromatic solvent such as toluene or xylene. The monomer can be added to the sodium dispersion (normal addition, N), or vice versa (inverse addition, I).[2] The choice of solvent can affect the molecular weight characteristics and the yield of the polymer. For example, the crude polymer will often exhibit a polymodal molecular weight distribution in toluene.

The Wurtz reaction is a very exothermic reaction that takes place in a highly reducing environment. Therefore the substituents that can exist on the silicon backbone are limited. Unless suitably protected, the only substituents that can withstand the conditions are generally alkyl, aryl, and silyl groups.[3] The exothermic nature of the

reaction, the involvement of a boiling solvent such as toluene or THF, and the presence of molten sodium makes the Wurtz reaction potentially hazardous. It is also nearly impossible to synthesise polysilanes with reproducible results as the reaction conditions can be variable and difficult to control. Also, although the Wurtz is known as a condensation reaction, it resembles more closely a chain-growth reaction and therefore polysilanes might be considered to be comparable to homoatomic organic polymers such as polyolefins.[4]

### 3.1.1.2. Poly(methylphenylsilane)

For the polymerisation of poly(methylphenylsilane) (PMPS), the molecular weight distribution has three basic fractions when the Wurtz reaction is carried out in a solvent such as toluene (fig. **3.1**).[5] Firstly, there is a low molecular weight ($M_w$ < 1 000) fraction containing oligomers which are usually made up of five or six-membered cyclic species. These five and six-membered rings are formed during end-biting and back-biting side reactions (scheme **3.2**).

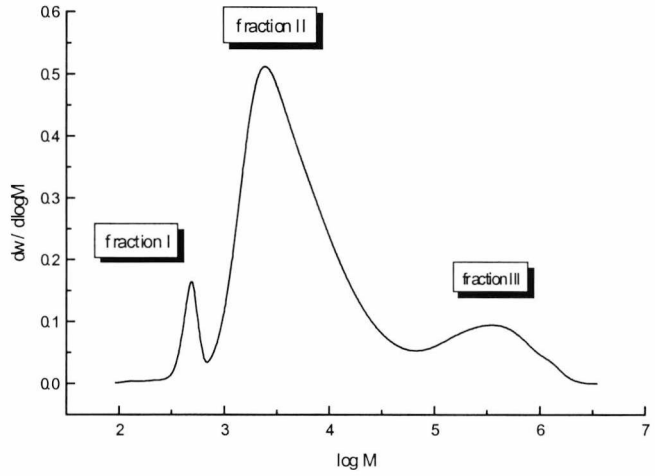


**Fig. 3.1.** Representative molecular weight distribution of a poly(methylphenylsilane) prepared by the Wurtz reaction in refluxing toluene (*Organometallics* 1998, 17, 59)[5]

The bulk of polysilane species formed make up the medium molecular weight fraction ($M_w$ 1 000 – 50 000) and corresponds to an average degree of polymerisation of about 30-40 units. Finally, a high molecular weight fraction ($M_w$ > 50 000) exists that can become insoluble in the reaction medium above a certain molecular weight. The molecular weight distribution and overall yield can be influenced by the reaction

conditions (i.e. alkali metal dispersion, addition procedures, temperature, solvent, reaction time, and the nature of the substituents).[4] In solvents such as THF, the distribution contains almost exclusively low and medium molecular weight fractions, with only a small amount of high molecular weight polymer. The final polymer can also be treated and various fractions isolated to obtain near monodisperse polymer.

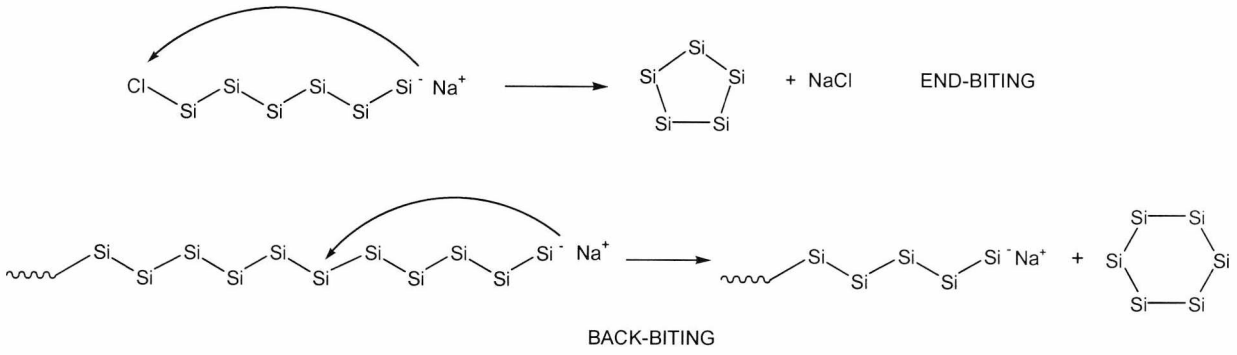


**Scheme 3.2.** Formation of cyclic oligomers during the Wurtz reaction

### 3.1.1.3. Mechanism of the Wurtz reaction

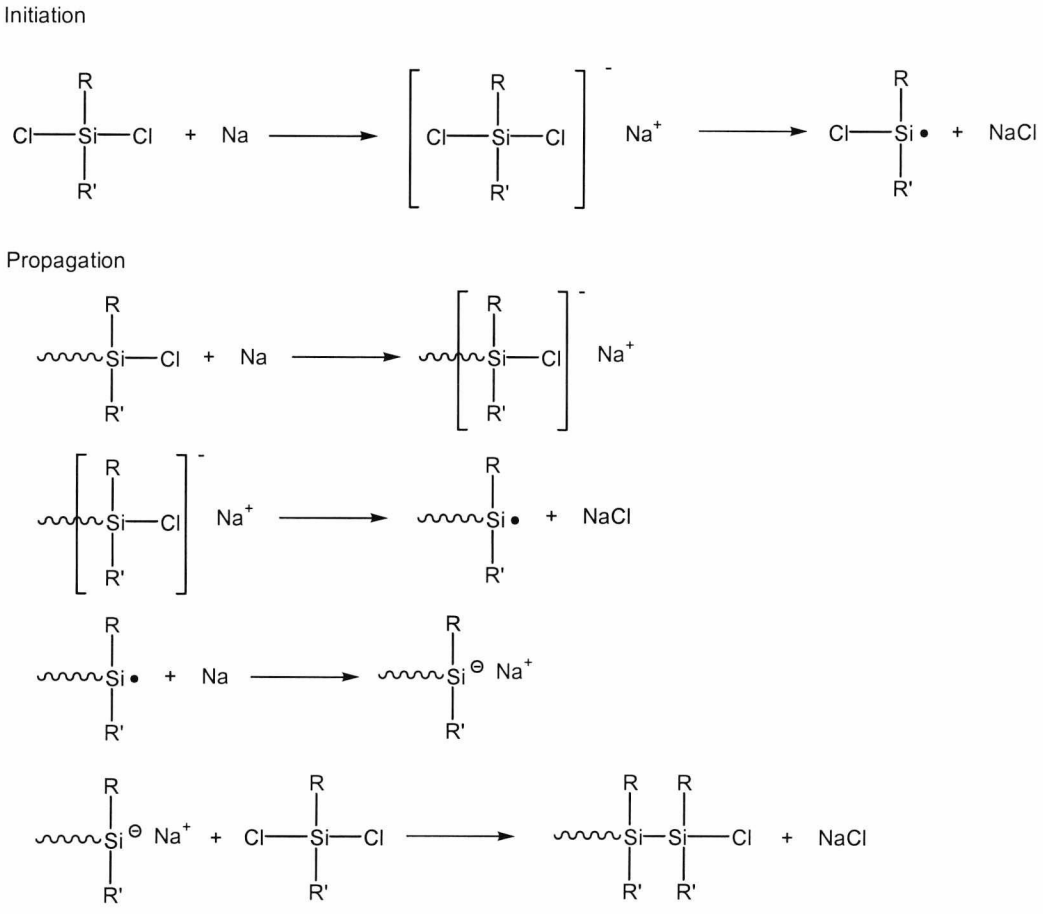


**Scheme 3.3.** Proposed initiation and propagation steps of the Wurtz reaction

The initiation and propagation steps most widely accepted are shown in scheme **3.3**.[6] The termination step involving the radical coupling in the solvent phase is omitted since its affect on the overall mechanism is negligible. Other termination steps involve the formation of cyclic oligomers, such as the end-biting reaction shown in scheme 3.2.

### 3.1.2. Alternative syntheses of polysilanes

One problem which has tended to hinder the development of the chemistry and physics of polysilanes involves the limited methods available for the synthesis of polysilanes. It has proved difficult to determine the structures of polysilanes synthesised via the Wurtz reaction. Moreover, molecular weights and corresponding polydispersities have also been difficult to control.[7] For these reasons, several new and alternative methods have been developed and are described briefly.

#### 3.1.2.1. Anionic polymerisation of disilenes and silylenes

Disilenes contain silicon-silicon double bonds and undergo anionic polymerisation to form polysilanes. However, disilenes are not used as such, since they are not stable enough, and polymerisation occurs too quickly (almost immediately). Instead, cyclics or linear trisilanes have been photolysed to form the disilene species, which are then polymerised (scheme **3.4**).[8] A wide range of substituents is possible since the reaction conditions involved in this particular procedure are less harsh compared to that of the Wurtz reaction.

$$(RR'Si)_n \xrightarrow[77K]{h\nu} [RR'Si:] \xrightarrow{\Delta} RR'Si{=}SiRR' \xrightarrow{\Delta} (RR'Si)_n$$

**Scheme 3.4.** Polymerisation of disilenes[8]

More recently, polysilanes have been prepared using masked disilenes. Masked disilenes contain suitable auxiliary groups, such as a diene, in order to stabilise the disilene temporarily (similar to a Diels-Alder adduct), prior to anionic polymerisation

(scheme **3.5**).[9] This novel method was used successfully to form highly ordered structures.[10]

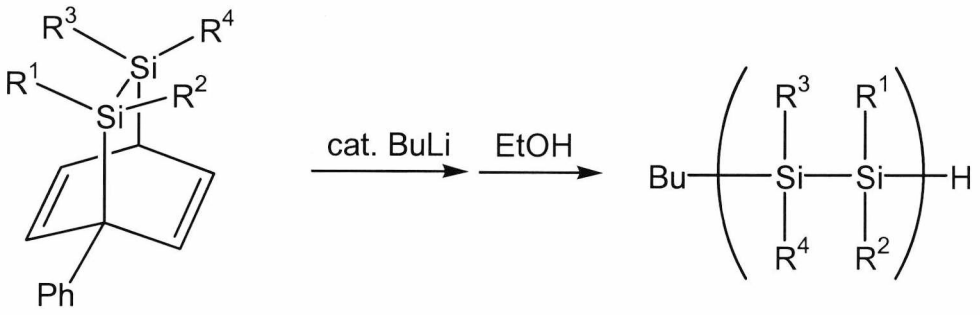


**Scheme 3.5.** Anionic polymerisation of a masked disilene[9]

### 3.1.2.2. Dehydrogenative coupling

The dehydrogenative coupling of diorganosilanes[11] (scheme **3.6**) is more easily controlled compared to the condensation methods, since transition metals can be used as catalysts. The best catalysts found so far included dialkyltitanocenes and zirconocene alkyls and hydrides (e.g. $Cp_2ZrR_2$ or $Cp_2ZrH_2$). However, steric constraints can lead to the formation of dimers instead of polymers. Hence, only primary silanes yield oligomers (of 10-20 Si atoms), while secondary silanes produce dimers.[12]


**Scheme 3.6.** Dehydrogenative coupling[11]

### 3.1.2.3. Catalytic disproportionation of functionalised disilanes

Baney *et al.* have synthesised cyclic polysilanes via the catalytic disproportionation of chloromethyldisilanes.[13] Also, the disproportionation of alkoxydisilanes has been studied to yield cyclic or linear oligosilanes, as well as a network of polysilanes with molecular weights up to 7 000.[14]

### 3.1.2.4. Ring-opening polymerisation of strained cylcosilanes

The ring-opening polymerisation (ROP) of strained cyclotetrasilanes has been studied in depth by Fossum and Matyjaszewski.[15] The ROP of 1,2,3,4-tetramethyl-1,2,3,4-tetraphenylcyclotetrasilane (scheme **3.7**) yielded polymer in high yield, with molecular weights up to 30 000 and polydispersities below 1.5.

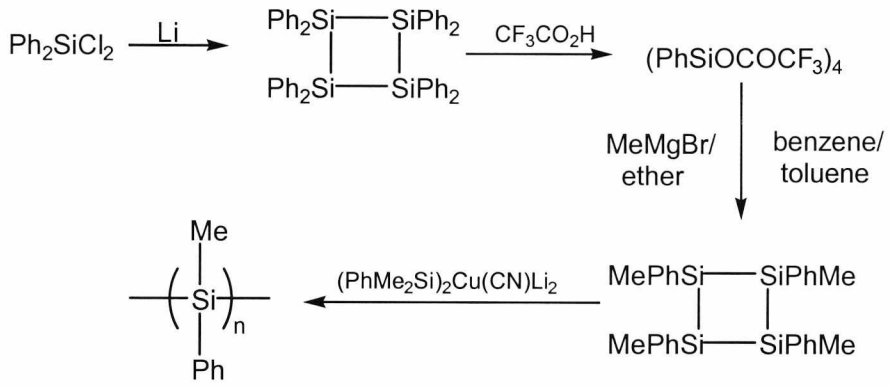


**Scheme 3.7.** ROP of 1,2,3,4-tetramethyl-1,2,3,4-tetraphenylcyclotetrasilane

Other similar polymerisations have been carried with various transition metal catalysts,[16] while poly(ferrocenylsilane) random copolymers have been synthesised using ROP.[17]

### 3.1.3. Chemical modification of polysilanes

### 3.1.3.1. Side group modification

The range of functional groups on the polysilane backbone is limited by the rigorous reaction conditions used when synthesising polysilanes in the presence of sodium. Therefore, a number of methods exist whereby the substituent groups can be modified after polymerisation has been completed. One such method is halogen introduction whereby a Lewis acid catalyst is used to introduce a halogen onto an aromatic substituent (scheme **3.8**).[18] As well as introducing organic and metallic substituents to the polysilane, this method has been used as a means for growing polymers to form graft copolymers [see section 5.1.4].[19]

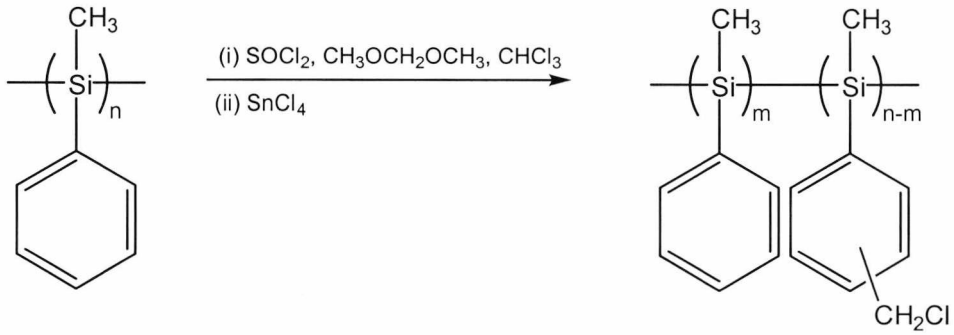


**Scheme 3.8.** Halomethylation of PMPS

The use of functional groups, such as trimethylsiloxanes, on aryl substituents can be converted to hydroxyl groups using methanol.[20] Alternatively, aryl groups can be replaced by Cl under acidic conditions. The resulting Si-Cl bonds are susceptible to nucleophilic displacement, for example *n*-butyl lithium (*n*-BuLi) replaces the Cl with *n*-Bu. Si-H bonds are also quite reactive and may also be used to form, for example, silicon chloride bonds by reaction with $CCl_4$.[21]

Trifluoromethanesulfonic (triflic) acid, $CF_3SO_3H$, has also been used to replace phenyl groups along the backbone.[22] About 50% of the silicon atoms can be dearylated without degradation of the silicon chain. Subsequent conversion of the triflated-substituted groups with nucleophiles has led to a number of polysilane derivatives.[22,23]

### 3.1.3.2. End group modification

Polysilanes which have been synthesised via the Wurtz reaction only contain halogenated chain ends. Hence the chemistry associated with end group modification is somewhat limited with respect to Wurtz-synthesised polysilanes. The Si-Cl end groups are susceptible to nucleophilic attack, and so reactions with alcohols[24] or lithiated compounds[25] are possible. For the most part, end group modification of polysilanes has usually been employed to synthesise block copolymers, although examples are limited. These are discussed in detail elsewhere [section 5.1].

## 3.2. Experimental

### 3.2.1. Materials and Apparatus

*Chemicals*

Diethyl ether was pre-dried with magnesium sulphate and sodium wire, then distilled over sodium. *n*-Hexane was pre-dried over magnesium sulphate and calcium hydride, then distilled over calcium hydride immediately prior to use. Toluene and tetrahydrofuran (THF) were pre-dried over magnesium sulphate and sodium wire, then distilled over sodium wire and benzophenone immediately prior to use.

*o*-Xylene was distilled over sodium and subsequently stored under nitrogen over molecular sieves at –4°C. Methanol (AR grade) and *n*-pentane (AR grade) used as received. Pyridine (anhydrous, 99.8%) was distilled over calcium hydride and stored in a Schlenk under nitrogen over molecular sieves at –4°C.

Dichloromethylphenylsilane (diClMPS) (98%, Aldrich) was distilled under vacuum and stored under nitrogen over magnesium turnings at –4°C. Sodium sticks (99%, in mineral oil, Lancaster) were scraped clean and washed with petroleum ether prior to use. For Wurtz reactions carried out using THF as the solvent, the sodium was made into a fine dispersion by melting in hot, dry toluene and then using a homogeniser (Ultra-Turrax T 8, IKA Labortechnik, Staufen).

2-Methyl-2-propanol (*t*-but) (99+%, Aldrich) was used as received. (*S*)-(-)-2-Methylbutanol (S-2MB) (95%, Fluka) was distilled under vacuum prior to use in order to remove isomeric material and other impurities.

All procedures were performed under a nitrogen atmosphere using freshly dried and distilled solvents and following standard Schlenk line techniques.

*Instrumentation*

$^{1}H$, $^{13}C$ and $^{29}Si$ nuclear magnetic resonance (NMR) spectra were recorded in $CDCl_3$ at 30 °C using a JEOL GX-270 spectrometer. UV-vis. spectroscopic analysis was performed on a UNICAM UV-500 UV-visible spectrometer.

Molecular weights of the polymers were estimated relative to polystyrene standards by gel permeation chromatography (GPC) using equipment supplied by Polymer Laboratories Ltd. All determinations were carried out at room temperature using a 600 mm x 5 mm mixed D PL gel column with THF as eluent at a flow rate of 1 ml $min^{-1}$, and a Knauer variable wavelength detector in series with a refractive index detector.

### 3.2.2. Poly(methylphenylsilane)

#### 3.2.2.1. Wurtz reaction in THF

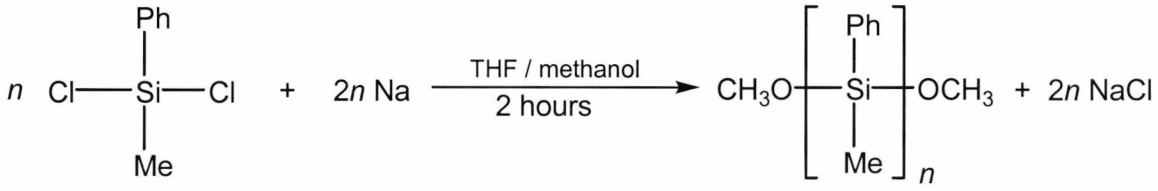


**Scheme 3.9.** The synthesis of α,ω-dimethoxypoly(methylphenyl)silane

The synthesis of α,ω-dimethoxypoly(methylphenyl)silane was based on the method published by Demoutier-Champagne *et al.* (scheme **3.9**)[26]

Sodium (10 g, 0.435 mol) was homogenised in hot toluene in a three-necked round-bottom flask fitted with a condensor and dropping funnel. Toluene was removed prior to the addition of THF (300 ml). Dichloro(methylphenylsilane) (diClMPS) (30 ml, 0.185 mol) was added dropwise to the heterogeneous mixture during the next ten minutes using a dropping funnel. The reaction was refluxed for two hours after the initial appearance of a characteristic dark blue colour of the solution. The reaction was quenched by adding methanol (20 ml) dropwise, after which the mixture was slowly added to methanol in order to fully precipitate out the polymer. The PMPS was reprecipitated and washed with wet methanol in order to remove any remaining sodium derivatives ($M_n$ 5 100, $M_w$ 40 500, $M_w/M_n$ 8.0). The product was then reprecipitated into *n*-hexane from THF and dried under vacuum at 60 °C. ($M_n$ 25 600, $M_w$ 53 000, $M_w/M_n$ 2.07). $^1$H NMR ($CDCl_3$) δ: -1.0 – 0.2 ppm (Si-$CH_3$); 6.0-7.5 ppm

(Si-$C_6H_5$). $^{13}C$ NMR ($CDCl_3$) δ: 127 & 135 ppm (Si-$C_6H_5$); -8 ppm (Si-$CH_3$). UV-vis spectroscopy: 340 nm, $\sigma-\sigma^*_{Si-Si}$, 270 nm $\sigma-\pi^*_{Si-Si}$, 215 nm $\pi-\pi^*_{Si-Si}$.

### 3.2.2.2. α,ω-Dihalopoly(methylphenylsilane)

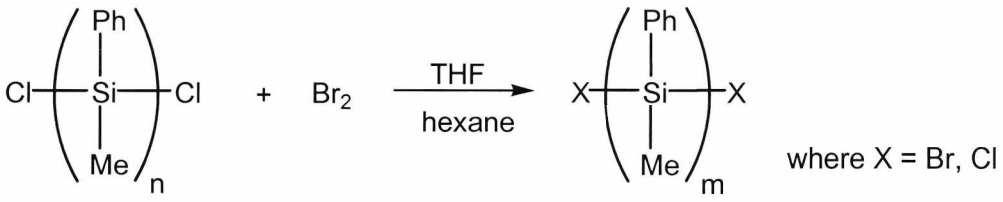


**Scheme 3.10.** Synthesis of diXPMPS

A typical synthesis of α,ω-dihalopoly(methylphenylsilane) (diXPMPS) is described and was based on a procedure described by Hiorns.[27]

PMPS was synthesised using the Wurtz-type reductive coupling of dichloromethylphenylsilane (30 ml, 0.185 mol) using a slight excess of sodium (10 g, 0.435 mol) at room temperature in THF (300ml) according to the literature procedure.[26] After two hours the THF polymer solution was filtered and transferred into a separate Schlenk using a PTFE cannula wire. Much of the solvent was removed under vacuum, leaving 30 ml of a viscous solution prior to the addition of dried hexane (150 ml), whereupon the PMPS was precipitated as a white powder. The solvent was then removed from the Schlenk via cannula filtration, leaving behind the white precipitate. The PMPS was dissolved once more into THF. A few drops of bromine were added to the stirring solution (scheme **3.10**). After twenty minutes of stirring the solution was precipitated via addition of *n*-hexane to form a white solid. Solvent was removed via a cannula wire with a filter attached, after which the product was dried under vacuum. The product was stored in the Schlenk under nitrogen at room temperature ($M_n$ 4 900, $M_w$ 8 500, $M_w/M_n$ 1.74).

A range of diXPMPS samples were synthesised in this manner, with varying relative amounts of bromine being added during the course of the reaction.

$^{29}Si$ NMR ($CDCl_3$) δ: -42 to -38ppm (-Si-Si-); -20.9ppm (Si-O-Si); 6.2 to 6.4 ppm (Si-O-$CH_3$); 14.43 and 14.65 ppm (Si-Br and Si-Cl).

### 3.2.2.3. α,ω–Di(1,1-dimethyl ethoxy)poly(methylphenylsilane)

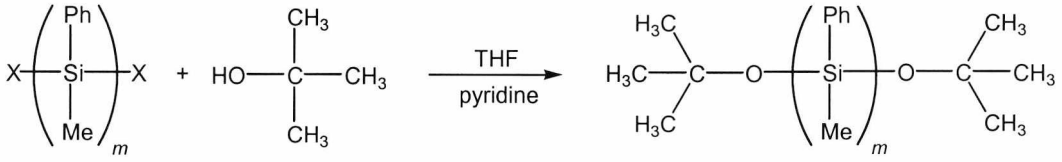


**Scheme 3.11.** Endcapping of PMPS with *t*-butanol

Excess 2-methyl-2-propanol (*t*-but.) (0.2 g, $3.23 \times 10^{-3}$ mol) and pyridine (0.5 ml) were added to diXPMPS (3.0g, $M_n$ 7 000, $4.29 \times 10^{-4}$ mol) in THF and stirred (scheme **3.11**). After one hour, the solution was filtered to give a clear, slightly yellow solution and then precipitated into methanol and isolated before being dried under vacuum at 60 °C to yield a white precipitate. $^1$H NMR ($CDCl_3$) δ: -1.0 – 0.2 ppm (Si-C**H**$_3$); 1.5 ppm (C(C**H**$_3$)$_3$); 6.0 – 7.5 ppm (Si-C$_6$**H**$_5$).

### 3.2.2.4. α,ω-Di(1-methyl propoxy)poly(methylphenylsilane)

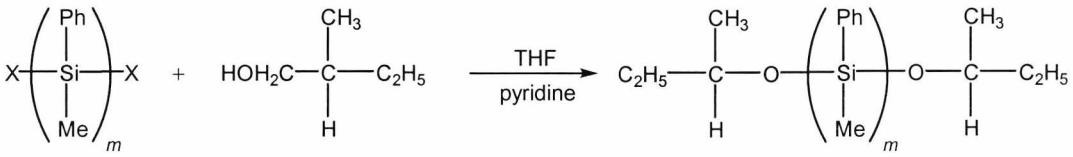


**Scheme 3.12.** Endcapping of PMPS with S-MB

Excess S-MB (0.30 g, 0.0341 mol) was dissolved in THF (1 ml) and added dropwise into a solution of PMPS ($M_n$ 4 700, $M_w/M_n$ 2.3, 6.0 g, $1.28 \times 10^{-3}$ mol) in THF (50 ml) in the presence of pyridine (1.0 ml), until the solution became slightly cloudy (scheme **3.12**). The mixture was filtered to give a clear solution, which was then precipitated into *n*-hexane (200 ml) and isolated. The precipitate was then redissolved in toluene, added to water and shaken vigorously. The organic and aqueous layers were separated during which the aqueous layer, containing any unreacted alcohol, was removed. The remaining toluene layer was reprecipitated in *n*-hexane, vacuum

filtered and dried under vacuum at 60 °C overnight to give a white precipitate. $^{1}H$ NMR ($CDCl_3$) δ: -1.1 – 0.2 ppm (Si-$CH_3$); 0.6 – 0.9 ppm ($OCH_2\mathbf{CH_3}CHCH_2\mathbf{CH_3}$); 1.3 ppm ($OCH_2CH_3\mathbf{CH}CH_2CH_3$); 1.5 ppm ($OCH_2CH_3CH\mathbf{CH_2}CH_3$); 3.0 ppm ($O\mathbf{CH_2}CH_3CHCH_2CH_3$); 6.2 – 7.5 ppm (Si-$C_6H_5$).

## 3.3. Results and Discussion

### 3.3.1. Synthesis and characterisation of PMPS

For all of the reactions discussed here, the same method of synthesising PMPS was employed; i.e. the Wurtz reaction was carried out in THF using a fine sodium sand. THF was chosen as the solvent since the molecular weight distribution involves mainly medium and low molecular weight PMPS. For the purpose of making block copolymers, a monomodal molecular weight distribution of medium molecular weight is ideal.

In each case, the reaction mixture turned a deep blue colour after an initiation period which varied from a few minutes to over an hour.[28] After two hours, the reaction was quenched dropwise with methanol, and any excess sodium removed after precipitation into methanol. SEC analysis of the white polymer revealed characteristic medium and low molecular weight fractions.

#### 3.3.1.1. Molecular weight determination

In general a di- or tri-modal distribution was observed involving medium and low molecular weight fractions, along with a small amount of high molecular weight. Fig. **3.2** shows a typical distribution of PMPS synthesised using THF as the solvent. In this case, low and medium molecular weight fractions are shown, as well as a high molecular weight tail ($M_n$ 1 100, $M_w/M_n$ 19.0).

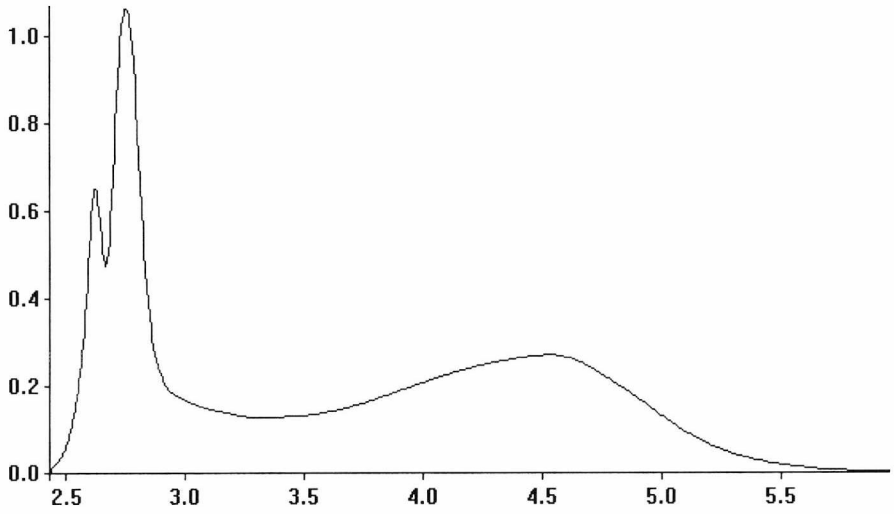


**Fig. 3.2.** GPC plot overlay of PMPS ($M_n$ 1 100, $M_w/M_n$ 19.0)

Reprecipitation into *n*-hexane from THF removed the oligomeric material and PMPS was then re-analysed via GPC revealing a polymer of lower polydispersity ($M_n$ 25 600, $M_w$ 53 000, $M_w/M_n$ 2.07).

### 3.3.1.2. UV analysis

Three peaks corresponding to Si-Si bonds (σ–σ*, 340 nm), aromatic carbon bonds from the phenyl substituents (π–π*, 210 nm), and mixing between the conjugated backbone and aromatic substituents (σ–π*, 270 nm) (fig. **3.3**). UV analysis was carried out in THF, and therefore the aromatic peak associated with the solvent overlaps with the phenyl peak of PMPS.

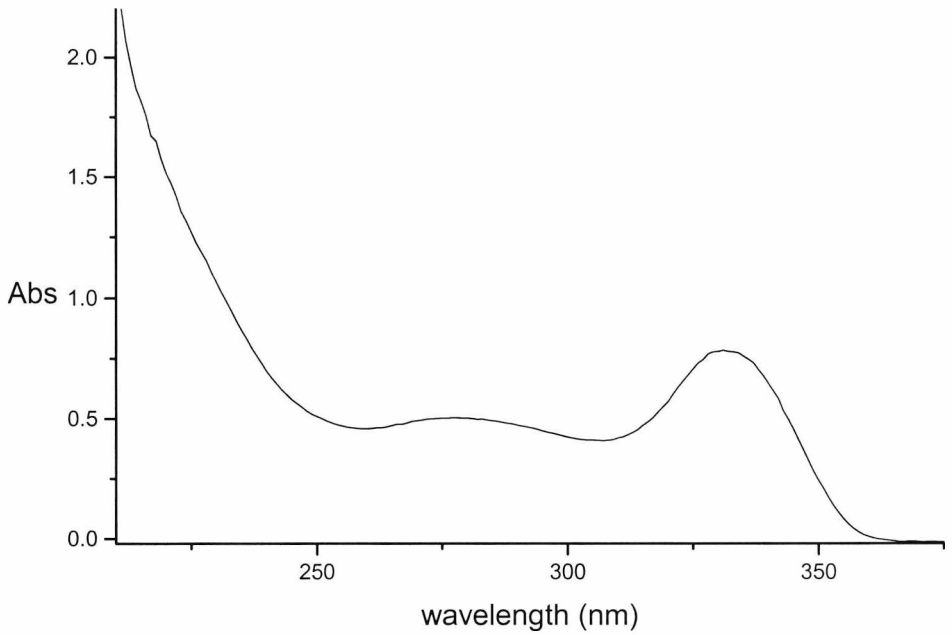


**Fig. 3.3.** UV spectrum of PMPS

### 3.3.1.3.NMR analysis

$^1H$ and $^{13}C$ NMR confirmed the structure of PMPS (fig. **3.4** and fig. **3.5**). The broad peaks are characteristic of polymeric phenyl and methyl pendant groups. Due to the tacticity exhibited by PMPS, the broad peaks seem to made up of overlapping polymeric signals. In the case of the $^1H$ NMR, the methyl groups show three distinct peaks, believed to be due to isotactic, syndiotactic and atactic conformations.[29]

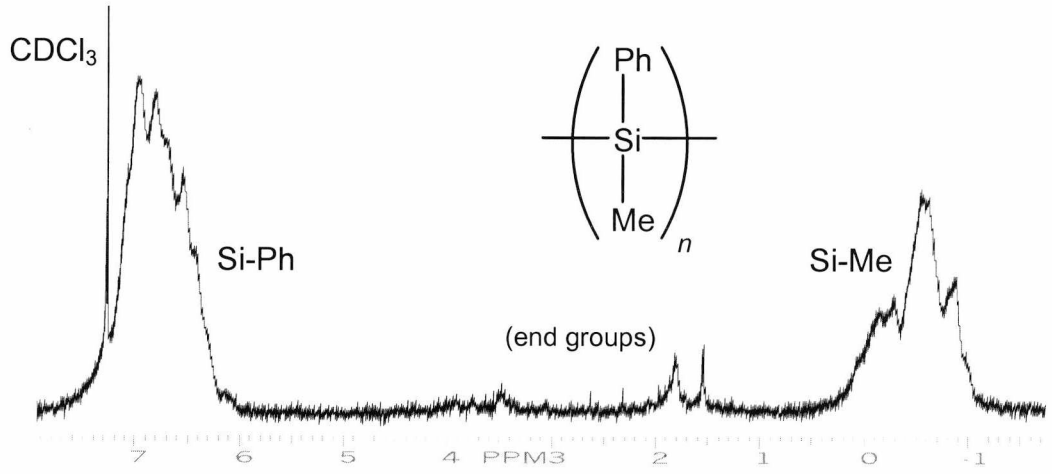


**Fig. 3.4.** $^{1}$H NMR of PMPS

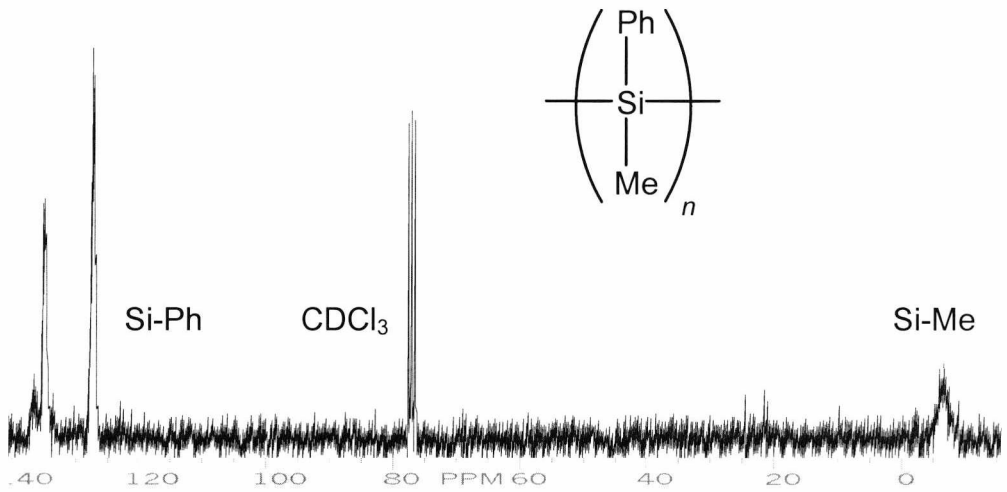


**Fig. 3.5.** $^{13}$C NMR of PMPS

### 3.3.2. α,ω-Dihalopoly(methylphenylsilane)

The synthesis of diXPMPS ($M_n$ 3 800, $M_w/M_n$ 1.63) is discussed here:

Instead of quenching and precipitating the polysilane in methanol, the product was isolated, precipitated into *n*-hexane, and then brominated to form diXPMPS (scheme **3.13**). Because the polymer was not quenched with methanol and was not exposed to any moisture in the air, the halide end groups were maintained.

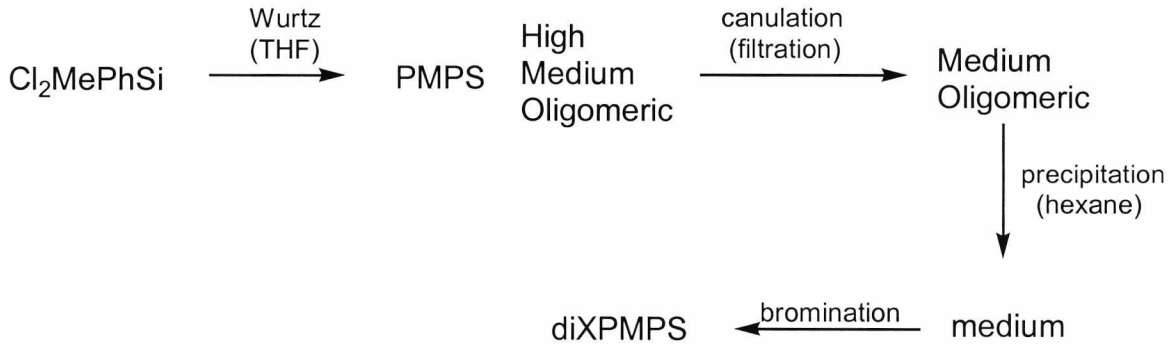


**Scheme 3.13.** Preparation of diXPMPS. The molecular weights present (high, medium, or oligomeric) are shown after each step.

A cannula wire with a filter attached was employed to separate the solution from unreacted sodium, salt, and any high molecular weight polymer that has precipitated from solution. The filtered solution was therefore made up of low and medium molecular weight material, and was a pale golden colour. The disappearance of the characteristic blue colour of the Wurtz reaction is due to the removal of the colloidal sodium species.[28] The precipitation of the solution into *n*-hexane removed the low molecular weight material, yielding monomodal, medium molecular weight polymer ($M_n$ 19 000, $M_w/M_n$ 2.68). The PMPS was reprecipitated twice more from THF into *n*-hexane in order to completely remove the oligomeric fraction, to give a monomodal medium molecular weight fraction. Bromination of PMPS then cleaves the backbone of the PMPS to yield a less polydisperse polymer which includes mainly Si-Br end groups ($M_n$ 3 800, $M_w/M_n$ 1.63) (fig. **3.6**). Bromination not only makes the polymer less polydisperse, but it also decreases the average chain length, meaning that the number of available end groups are more numerous and also more reactive (compared to Si-Cl end groups).

It is important to note that the extent to which the backbone is cleaved, and hence the molecular weight of diXPMPS, depends on the bromine:polymer molar ratio. Since bromine is quite difficult to handle, i.e. it is quite volatile and harmful, the addition of bromine was difficult to measure. Typically, if a certain molecular weight of diXPMPS was required, a few drops of bromine were added, and then the polymer's molecular weight was analysed. If a lower molecular weight was required, a few more drops of bromine were then added to the solution, and so on.

The importance of minimising the amount of moisture through thorough drying procedures and Schlenk line techniques is paramount because of the necessity of maintaining the reactive halogenated polysilane chain-ends.

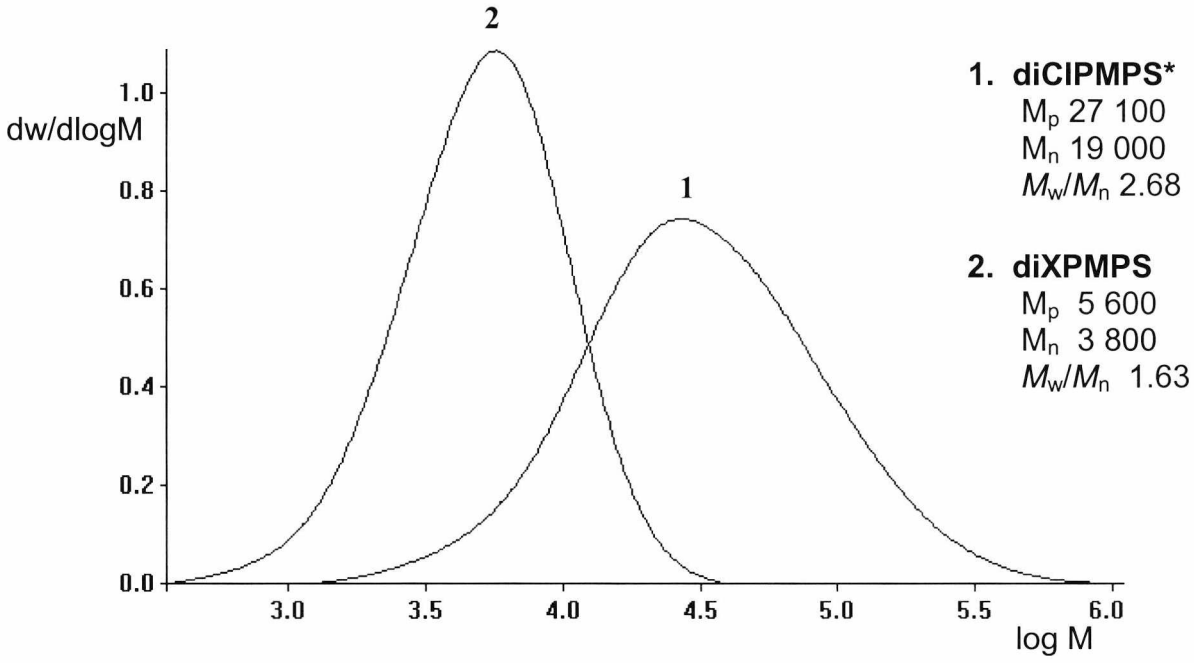


**Fig. 3.6.** dw/dlogM vs. log M plot of PMPS before and after bromination. (*diClPMPS sample has had oligomeric and monomeric fractions removed)

As well as $^{1}H$ and $^{13}C$ NMR, $^{29}Si$ NMR was used to characterise diXPMPS (fig. **3.7**). $^{29}Si$ NMR was used, in particular, to check whether or not the Si-Br and Si-Cl peaks were still intact on the ends of the polysilane chains. The halogenated end groups react readily with any moisture in the sample to form silanol and siloxane groups, which would also be visible using $^{29}Si$ NMR. The peaks were assigned to specific environments, as described in table **3.1**.[30]

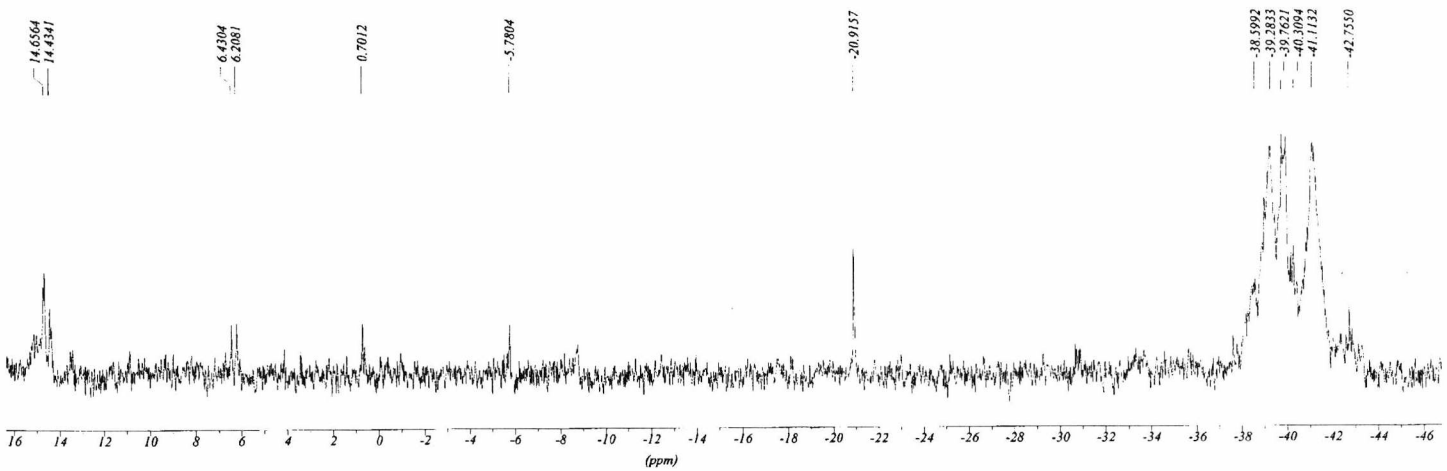


**Fig. 3.7.** $^{29}$Si NMR of diXPMPS

| ppm | Si environment |
|---|---|
| **-42→-38** | MePhSi-SiMePh bonds in backbone - various peaks depending on tacticity (isotactic, syndiotactic, heterotactic) |
| **-20.9** | MePhSi-O-SiMePh due to oxidation of backbone |
| **-5.7** | MePhSi-H group |
| **6.2 & 6.4** | MePhSi-O-Me methoxydation of backbone |
| **14 - 16** | MePhSi-Br and MePhSi-Cl end-groups |

**Table 3.1.** $^{29}$Si NMR of diXPMPS peak assignment

### 3.3.3. Endcapping of diXPMPS with alcohols

#### 3.3.3.1. α,ω–Di(1,1-dimethyl ethoxy)poly(methylphenylsilane)

End group modification of PMPS was investigated by testing the reactivity of the silicon-halide end groups. The extent to which the PMPS could be successfully endcapped with a non-polymeric alcohol would show how reactive the chain-ends

were. The first alcohol chosen to endcap diXPMPS was 2-methyl-2-propanol (tertiary butanol, *t*-but) (scheme **3.13**). The alcohol was reacted with diXPMPS in the presence of a base (pyridine) and then analysed via $^1$H NMR. The presence of any unreacted alcohol had been removed by reprecipitation and drying.

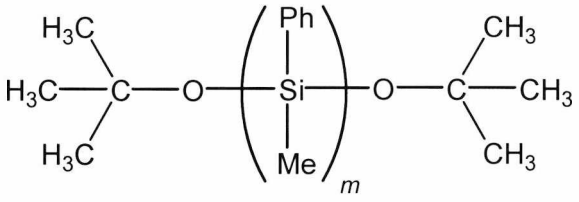


**Scheme 3.14.** α,ω–Di(1,1-dimethylethoxy)poly(methylphenylsilane)

In order to determine how successful *t*-but was in endcapping diXPMPS, the integrals of the characteristic PMPS peaks were compared to the methyl protons of the *t*-but. Using molecular weight data from GPC, the theoretical ratio of integral data from $^1$H NMR data could be determined. This alcohol was chosen because of the fact that the NMR shift would be strong compared to those of PMPS. With nine methyl protons on each end of polysilane chain, the peak due to these endgroups is clearly visible (fig. **3.8**).

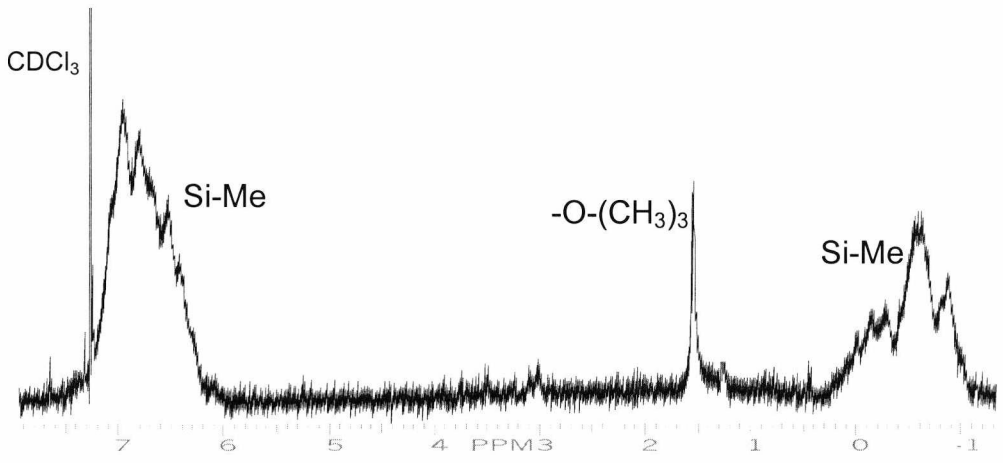


**fig. 3.8.** $^1$H NMR of PMPS-(*t*-but)$_2$

### 3.3.3.2. α,ω-Di(1-methyl propoxy)poly(methylphenylsilane)

A chiral alcohol was attached to the ends of a PMPS chain as part of ongoing studies into inducing chirality into the backbone of PMPS,[31] as well as to determine the Si-X end group reactivity. Previous studies have shown that polysilane chains containing chiral end groups exhibit helical chirality.[32] DiXPMPS was endcapped with (*S*)-(-)-2-methyl-1-butanol (S-MB) (scheme **3.15**) and analysed using $^1$H NMR. The $^1$H NMR of S-MB is shown (fig. **3.9**) and compared with the $^1$H NMR of PMPS endcapped with S-MB (fig. **3.10**). Using cross-correlating data from GPC, it is shown that S-MB was successfully endcapped onto all of the halogenated PMPS chain-ends (table **3.2**).

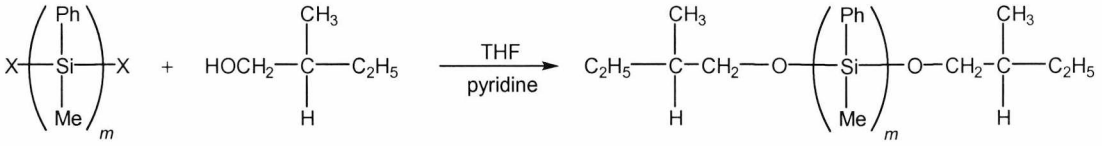


**Scheme 3.15.** Endcapping of PMPS with S-MB

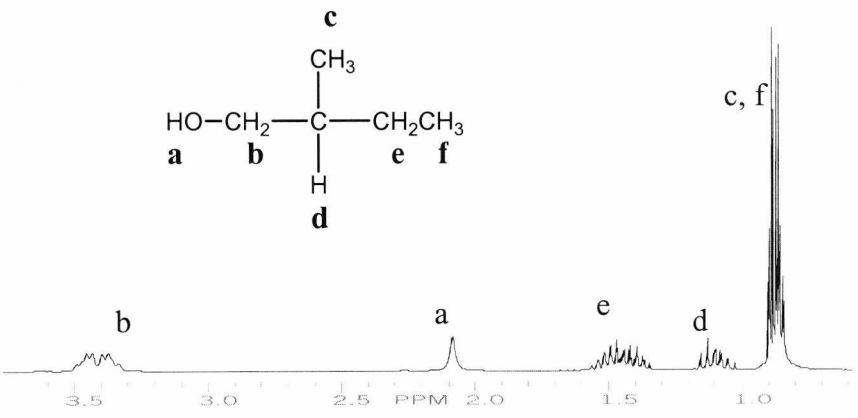


**Fig. 3.9.** $^1$H NMR of (*S*)-(-)-2-methyl-1-butanol (S-MB)

The addition of the chiral alcohol onto the ends of the PMPS chains causes the $CH_2$(b) peak to shift downwards from 3.4 ppm to 3.0 ppm. Also, the OH(a) peak has disappeared completely from the NMR shown in fig. 3.10, indicating the change from

$CH_2$(b)-OH(a) to $CH_2$(b)-O-Si. The shifts of the other peaks associated with the chiral end group remain the same.

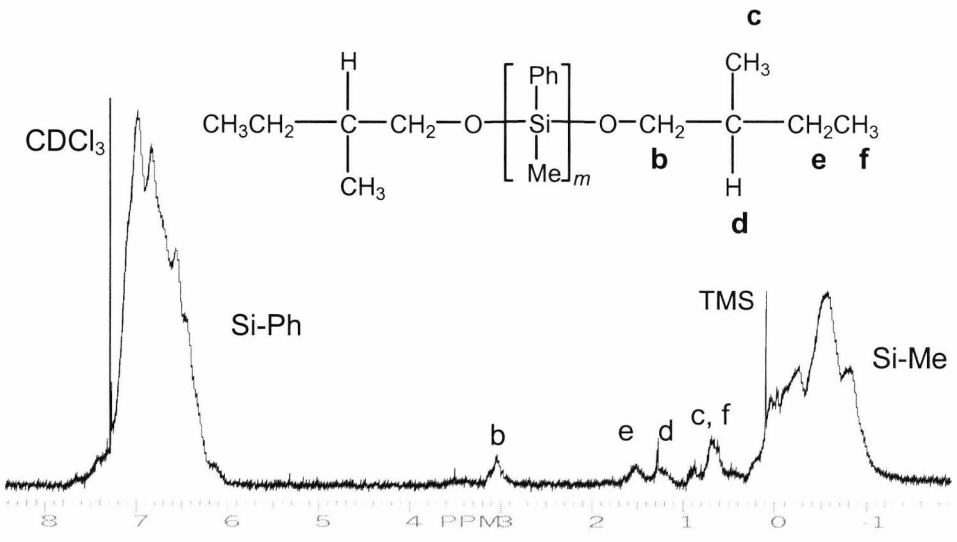


**Fig. 3.10.** $^1$H NMR of PMPS endcapped with S-MB

| Proton environment | Shifts δ | Theoretical ratio of protons | Experimental ratio of protons |
|---|---|---|---|
| Si-**$C_6H_5$** | 6.2 – 7.5 | 196* | 200 |
| Si-**$CH_3$** | -1.2 – 0.2 | 118* | 114 |
| -O**$CH_2$**$CH_3CHCH_2CH_3$ | 3.1 | 4 | 4.0 |
| -$OCH_2$**$CH_3$**$CHCH_2$**$CH_3$** | 0.6 – 0.9 | 12 | 11.5 |
| -$OCH_2CH_3$**CH**$CH_2CH_3$ | 1.3 | 2 | 2.8 |
| -$OCH_2CH_3CH$**$CH_2$**$CH_3$ | 1.5 | 4 | 3.2 |

**Table 3.2.** Integral data of peaks from $^1$H NMR of PMPS endcapped with S-MB compared with theoretical calculated values for 100% conversion. (*values calculated based on PMPS chain containing approx. 39 units ($M_n$ 4 700))

## 3.4. Conclusions

PMPS has been synthesised and characterised using $^{1}H$, $^{13}C$, and $^{29}Si$ NMR. By filtering, precipitating, and brominating PMPS synthesised via the Wurtz reaction in THF, it has been possible to produce a monomodal polymer. Reactions with various alcohols have shown that the halogenated chain ends of the polysilane are reactive, as long as there is little or no moisture present in the reaction vessel. The extent to which the PMPS can be endcapped has been proven using $^{1}H$ NMR. In theory, PMPS block copolymers could be formed by endcapping the PMPS with alcohols such as other polymers or functionalised alcohols such as initiators capable of initiating polymerisation. Hence it was concluded that diXPMPS could be successfully and reproducibly endcapped with alcohols.

## 3. References


[1] a) Kipping, *J. Chem. Soc.* **1921**, 19, 830.

b) Kipping, *J. Chem. Soc.* **1924**, 125, 2291.

[2] Trefonas III, P.; Djurovich, P.I.; Zhang, X.-H.; West, R.; Miller, R.D.; Hofer, D. *J. Poly. Sci. Polym. Lett. Ed.* **1983**, 21, 819.

[3] For a general review of polysilanes, see: Miller, R.D.; Michl, J. *Chem. Rev.*, **1989**, 89, 1359.

[4] Jones, R.G.; Holder, S.J. In *Silicon-Containing Polymers*. Jones, R.G.; Ando, W.; Chojnowski, J., Eds.; Kluwer Academic Publishers: Dordrecht, the Netherlands, **2000**.

[5] Jones, R.G.; Wong, W.K.C.; Holder, S.J. *Organometallics*, **1998**, 17, 59.

[6] Matyjaszewski, K. *Polym. Prepr. (Am. Chem. Soc., Div. Polym. Chem.)* **1987**, 28, 224.

[7] Miller, R.D.; Thompson, D.; Sooriyakumaran, R.; Fickes, G.N. *J. Polym. Sci. Part A, Polym. Chem.* **1991**, 29, 813.

[8] Roark, D.N.; Peddle, G.D. *J. Am. Chem. Soc.* **1972**, 94, 5837.

[9] Sakamoto, K.; Obata, K.; Hirata, H.; Nakajima, M.; Sakurai, H. *J. Am. Chem. Soc.* **1989**, 111, 7641.

[10] Sakamoto, K.; Yoshida, M.; Sakurai, H. *Macromolecules* **1990**, 23, 4494.

[11] a) Aitken, C.T.; Harrod, J.F.; Samuel, E. *J. Organomet. Chem.* **1985**, 279, C11.

b) Aitken, C.T.; Harrod, J.F.; Samuel, E. *J. Am. Chem. Soc.* **1986**, 108, 4059.

[12] For a detailed review see: Gray, G.M.; Corey, J.Y. In *Silicon-Containing Polymers*. Jones, R.G.; Ando, W.; Chojnowski, J., Eds.; Kluwer Academic Publishers: Dordrecht, the Netherlands, **2000**.

[13] Baney, R.H.; Gaul, Jr, J.H.; Hilty, T.K. *Organometallics* **1983**, 2, 859.

[14] a) Watanabe, H.; Higuchi, K.; Kobayashi, M.; Kitahara, T.; Nagai, Y. *J. Chem. Soc., Chem. Comm.* **1997**, 704.

b) Kabeta, K.; Wakamatsu, S.; Imai, T. *Chem. Lett.* **1994**, 835.

c) Kabeta, K.; Wakamatsu, S.; Imai, T. *J. Polym. Sci., Part A: Polym. Chem.* **1996**, 24, 2991.

[15] Fossum, E.; Matyjaszewski, K. *Macromolecules* **1995**, 28, 1618.

[16] Chrusciel, J.; Matijaszewski, K. *J. Polym. Sci., Part A: Polym. Chem.* **1996**, 34, 2243.

[17] Rulkens, R.; Rescendes, R.; Verma, A.; Manners, I.; Murti, K.; Fossum, E.; Miller, P.; Matyjaszewski, K. *Macromolecules* **1997**, 30, 8165.

[18] a) Ban, H.; Sukegawa, K.; Tagawa, S. *Macromolecules* **1987**, 20, 1775.

b) Jones, R.G.; Benfield, R.E.; Holder, S.J.; Swain, A.C. In *Silicon-containing Polymers* Ed. Jones, R.G., Royal Society of Chemistry, Cambridge, **1995**.

c) Jones, R.G.; Benfield, R.E.; Swain, A.C.; Webb, S.J.; Went, M.J. *Polymer* **1995**, 36, 393.

[19] Jones, R.G.; Holder, S.J. *Macromol. Chem. Phys.* **1997**, 198, 3571.

[20] Hayase, S. *Trends Polym. Sci.* **1995**, 3, 304.

[21] Banovetz, J.P.; Hsiaso, Y.L.; Waymouth, R.M. *J. Am. Chem. Soc.* **1993**, 115, 2540.

[22] a) Matyjaszewski, K.; Chen, Y.L.; Kim, H.K. *ACS Symp. Ser.* **1988**, 360, 78.

b) Matyjaszewski, K.; Hrkach, J.; Kim, H.K.; Ruehl, K. *Adv. Chem. Ser.* **1990**, 224, 285.

c) Uhlig, W. *J. Organomet. Chem.* **1996**, 129, 733.

[23] a) Uhlig, W. *J. Organomet. Chem.* **1996**, 516, 147.

b) Lemmer, M.; Bebin, P.; Sepulchre, M.; Marc, N.; Moisan, J.Y. *Polym. Adv. Tech.* **1997**, 9, 125.

[24] Holder, S.J.; Hiorns, R.C.; Sommerdijk, N.A.J.M.; Williams, S.J.; Jones, R.G.; Nolte, R.J.M. *Chem. Commun.* **1998**, 14, 1445.

[25] Lutsen, L.; Jones, R.G. *Polym. Int.* **1998**, 46, 3.

[26] Demoustier-Champagne, S.; Jonas, A.; Devaux, J. *J. Polym. Sci., B., Polym. Phy.*, **1997**, 35, 1727.

[27] Hiorns, R.C. *PhD. Thesis* University of Kent at Canterbury, **2000**.

[28] Benfield, R.E.; Cragg, R.H.; Jones, R.G.; Swain, A.C. *Nature* **1991**, 353, 340.

[29] a) Jones, R.G.; Benfield, R.E.; Evans, P.J.; Holder, S.J.; Locke, J.A.M. *J. Organomet. Chem.* **1996**, 521, 171.

b) Schilling, F.C.; Bovey, F.A.; Ziegler, J.M. *Macromolecules* **1986**, 19, 2309.

c) Wolff, A.R.; Maxka, J.; West, R. *J. Polym. Sci., Polym. Chem. Ed.* **1988**, 26, 713.

[30] Williams, E.A. *Annual reports on NMR spectroscopy* **1983**, 15, 235.

[31] a) Dellaportas, P. *PhD. Thesis* University of Kent at Canterbury, **2003**.

b) Dellaportas, P.; Jones, R.G.; Holder, S.J. *Macromol. Rapid Commun.* **2002**, 23, 99.

[32] Obata, K.; Kabuto, C.; Kira, M. *J. Am. Chem. Soc.* **1997**, 119, 11345.

# 4. Introduction to block copolymers

## 4.1. Introduction

Copolymers are described as having two or more structurally different monomers incorporated into the same polymer chain. Most simply, copolymers can be defined in terms of the relative concentrations of each type of monomer unit present in the copolymer (scheme **4.1**).


**Scheme 4.1.**

The order in which the monomer units exist relative to each other, known as the sequence distribution, describes the composition of the copolymer. The compositions are usually described as being either statistical (random), alternating, block, graft, or as gradient copolymers (fig. **4.1**).

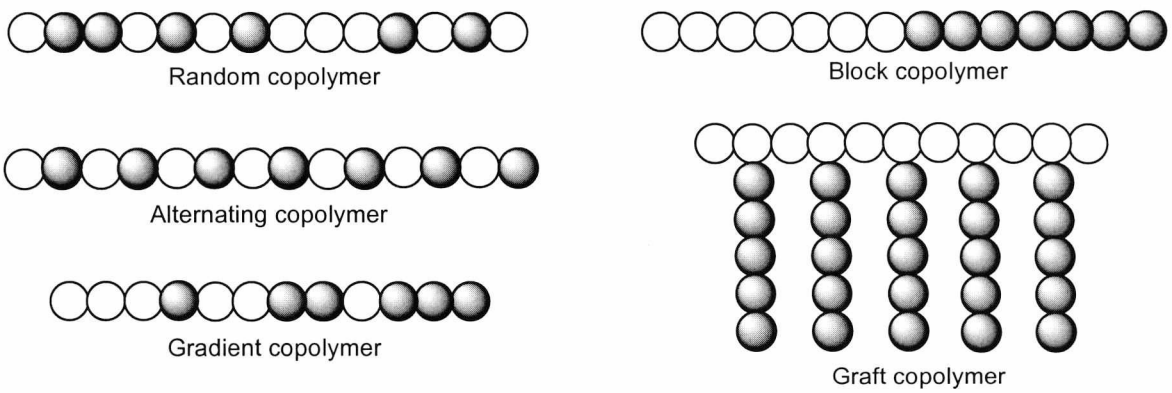


**Fig. 4.1.** Types of copolymer

Finally, the topology of the copolymer describes the linearity of the copolymer. The topology can describe copolymers as being linear, star, network, comb, or hyperbranched. A range of topologies are formed using different functionalised macroinitiators (fig. **4.2**).

A telechelic polymer has end groups that react selectively to form a bond with another molecule. Telechelic polymers are used to form block copolymers by reacting the polymers via functional end groups. Using bi-functional and multi-functional linking reagents they have been used to form polymer networks.[1] In industry, the interest stems from the involvement of telechelic polymers in the preparation of copolymers and the development of thermoplastic elastomers.[2] The number of functional groups on a polymer determines its classification as either mono-, di-, tri-, or polytelechelic. Telechelic polymers that are capable of undergoing further polymerisation to form copolymers such as block, graft, and network are often known as macromolecular monomers, macromonomers, or macroinitiators. While end-functionalised polymers can be used to synthesise block copolymers, polymers functionalised along the backbone can form graft copolymers via a technique known as 'grafting onto'. Graft copolymers can also be prepared using polymers functionalised with polymerisable end groups. This is known as 'grafting from' or 'grafting through'. Also, functionalised dendrimers can initiate polymerisation to form large dendritic copolymers.

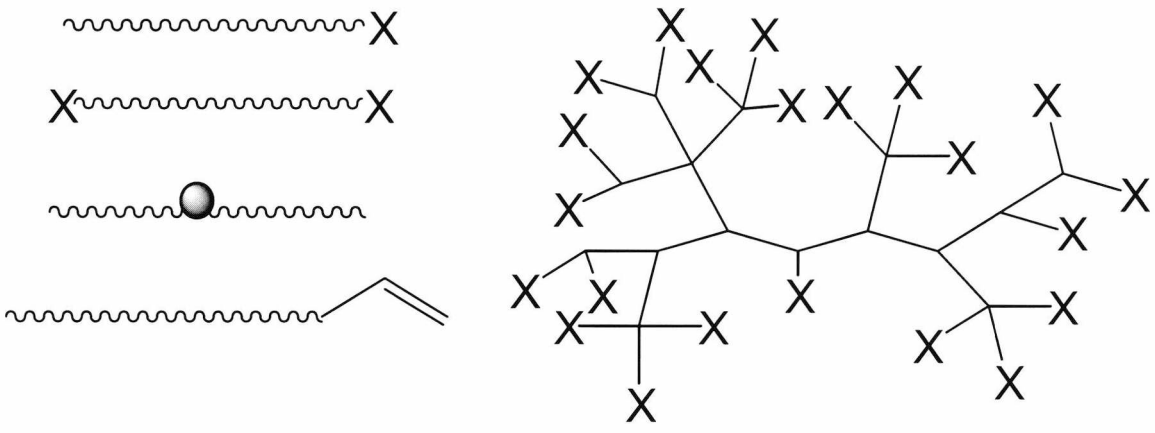

**Fig. 4.2.** Types of functionalised polymers used to synthesise block, graft, and dendritic copolymers (X = initiating sites)

Copolymerisation methods have been used to achieve certain systematic changes in a range of polymer properties, and have been utilised in order to produce novel copolymers for commercial reasons, as well as for studies of structure-property relationships. The combination of two or more polymers in a copolymer system enables the properties of those polymers to be utilised simultaneously.

Copolymerisation can also modify the symmetry of the polymer backbone and can alter the intra- and intermolecular forces, leading to changes in physical properties. These changes are evidenced by alterations in the melting point, glass transition temperature, crystallinity, solubility, elasticity, permeability, and chemical reactivity of the polymer.

## 4.2. Synthesis of block copolymers

Block copolymers are defined as having a linear arrangement of blocks of different monomer compositions, i.e. the segments involved are joined end-to-end. Interest in block copolymers stems primarily from the unique properties they exhibit in solution and in the solid state. Specific examples of polysilane block copolymers are discussed in section 5.1.

There are two general methods used for synthesising block copolymers. The first incorporates an active site on the end of a polymer which is capable of initiating and growing another polymer chain, usually via radical,[3] anionic,[4] or cationic[5] polymerisation. In addition, condensation reactions between different polymer chains can form block copolymers. This is achieved via a chemical reaction between functional endgroups of the polymers involved (scheme **4.1**).

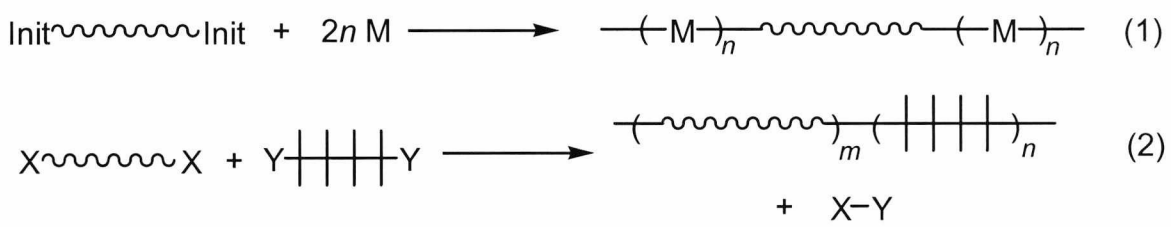


**Scheme 4.1.** Schematic representation of copolymerisation via (1) a macroinitiator and (2) a condensation reaction

Alternatively, polymer blends can be prepared by mixing solutions of the polymers involved, followed by the evaporation of the solvent. This is an uncontrolled, yet relatively simple method, and can be achieved through the use of rollers and extruders. [6]

## 4.3. Amphiphilic block copolymers

### 4.3.1. Properties and applications

Amphiphilic block copolymers (ABCs) are made up of at least two segments, one of which is hydrophilic, while the other is hydrophobic (lypophilic). The term amphiphilic is derived form the terms amphi-, which means "of both kinds", and -philic, which means "having an affinity for". Interest in ABCs is wide-ranging and have found applications as emulsifiers, dispersants, foamers, thickeners, rinse aids, compatibilisers, and drug-delivery systems. However, there are very few well-defined examples of ABCs that are commercially available, e.g. Pluronics (PEO-PPO-PEO block copolymers).[7]

There are several difficulties associated with ABCs involving colloidal solubility, interface activity, and the stabilisation of dispersed particles. Amphiphilic stability has been achieved through choosing appropriate repeat units, copolymerisation procedures, molecular weight characteristics, and polymer architectures. With the recent advances in "living" polymerisations, the choices open to the synthetic chemist are vast and are increasing all the time. In particular, ABCs can be copolymerised more readily and are starting to be used in areas usually dominated by low molecular weight surfactants. For example, ABCs are now being used to solve some heterophase stability problems such as those associated with emulsion polymerisation,[8] the stability of pigments, and the formulation of cosmetics and drugs.[7]

ABCs are able to stabilise colloids through steric and electrostatic properties. The dispersion efficiency can be maintained, even when copolymer solutions are very dilute since the CMC can be quite low. The kinetic stability of the aggregates formed is dependent on both the chemical nature and lengths of the blocks involved. This stability can lead to a lifetime for the aggregate that can last in the regions of a few seconds to several hours (compared to low molecular weight surfactant aggregates which last for only a few milliseconds).

In nature, amphiphiles are used to form aggregates, such as micelles, because segments that are chemically incompatible tend to segregate from one another.

Polymer-like amphiphiles such as proteins and polysaccharides are used to form aggregates, whereas low molecular weight emulsifiers are not. Hence, polymeric amphiphiles that are kinetically stable are very promising as self-organising materials which exist at interfaces or in solution in order to change both interfacial properties and compatibilities. The polymer architecture can also influence the amphiphilic properties that exist in solution, as well as the microdomains which form in the solid state.

### 4.3.2. Synthesis via living polymerisation

Amphiphilic block and graft copolymers can be synthesised using several different types of living polymerisation. Although most block copolymers have been formed via sequential addition, "cross-over" copolymerisations have also been used. Also known as active-centre transformation, the mechanism used to polymerise each segment can be changed in order to suit the monomer.[9] Examples of the types of ABCs synthesised using different types of living polymerisation are briefly discussed in the following subsections.

#### 4.3.2.1. Anionic polymerisation

Anionic polymerisation is used to prepare the well-established polymers such as polystyrene (PS), polyisoprene (PI), poly(methyl methacrylate) (PMMA), poly(ethylene oxide) (PEO), and poly(dimethylsiloxane) (PDMS). PEO is often used in block copolymers containing hydrophobic blocks to form amphiphiles such as PS-PEO[10] because of its capacity to be soluble in a wide range of solvents such as water or toluene.

#### 4.3.2.2. Group transfer polymerisation

Group transfer polymerisation (GTP) involves the repeated addition of a monomer to a propagating chain end that carries a reactive silyl ketene acetal group.[11] GTP is usually used to prepare (meth)acrylates[12] and for preparing block copolymers that stabilise hydrophilic/hydrophobic interfaces and also biological interfaces. One

example of a block copolymer synthesised in this manner is PS-PHEMA, which is capable of forming surfaces that are highly compatible with blood.[13]

#### 4.3.1.3. Ring-opening metathesis polymerisation

Ring-opening metathesis polymerisation (ROMP) has been used to synthesise block copolymers containing functional groups such as amino groups and cyclopentadienes on monomers such as norbornene and methyltetracyclodecene.[14] These groups form stable coordination complexes with a variety of metals.

#### 4.3.1.4. Cationic polymerisation

Cationic polymerisation has been used to form a range of ABCs, particularly via the polymerisation of vinyl ethers.[5] Examples of the synthesis of amphiphilic water-soluble diblocks incorporating methyl tri(ethylene glycol)vinyl ether and isobutyl vinyl ether can be found in publications by Armes and co-workers.[15]

#### 4.3.1.5. Living radical polymerisation

Living radical polymerisation[3] is being used increasingly to prepare block and graft copolymers of styrenes, (meth)acrylates, etc. Block copolymers can be synthesised via sequential addition or by use of a macroinitiator using halogenated end groups [see chapter **6**].

## 4.4. Phase separation

In copolymer systems where two-phase morphologies exist, a number of characteristics determine how a copolymer phase-separates. These include the size and shape of the individual phases, internal structure, the extent to which molecular mixing takes place, adhesion between the two phases, and the average distance between the phase domains. These parameters are influenced primarily by the method used to synthesise the copolymers. Domains will occur if either significant rarifications or densifications are present and if a considerable increase in the free

energy of formation occurs. There are generally three typical morphologies of copolymers – spherical, cylindrical, and lamellar. The shape of the morphology can be influenced by the ratio of the molecular weights of the blocks and this determines the free energy of the system. For the most part, block copolymers form spherical micelles in dilute solutions. However, cylindrical micelles have been observed for a number of block copolymers including poly(ethylene oxide-*block*-polypropylene-*block*-ethylene oxide), PEO-PPO-PEO.[16] Some examples of how copolymers can microphase separate are shown in fig. **4.3**.

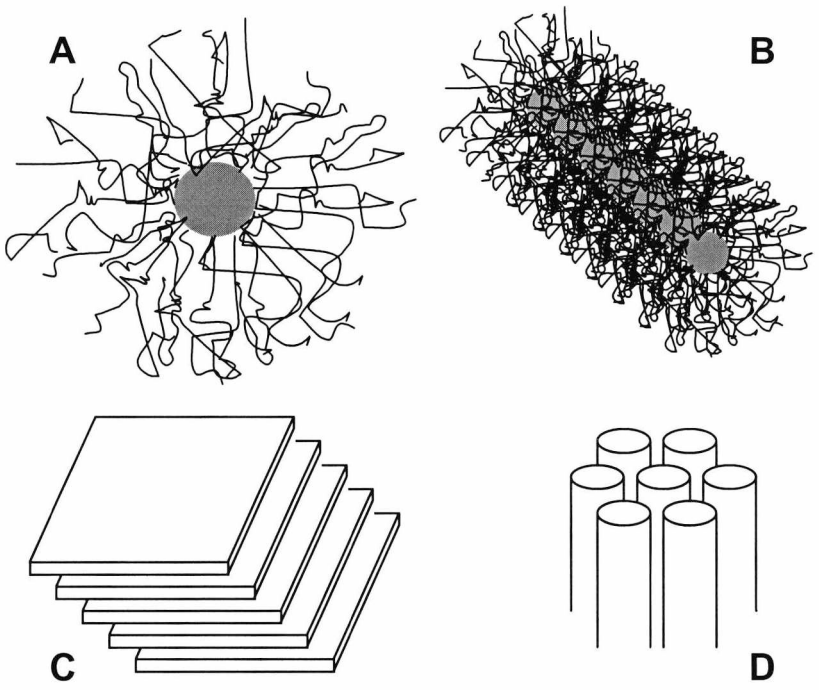


**Fig. 4.3.** Examples of phase separation, including (A) micelle, (B) cylindrical micelle, (C) lamellae, and (D) hexagonal ordered cylinders.

Some copolymers exhibit unique properties because of controlled phase separation which leads to synergistic behaviour. These properties lead to a number of applications including impact-resistant plastics, tires, resilient rugs, knife handles, rubber-soled shoes, and ion exchange resins.

An indication that a system phase-separates includes the appearance of a milky or hazy solution. This is due to the fact that the refractive indices of the two phases can cause intense light scattering. Also, the glass transition, $T_g$, can be used to determine whether or not a material phase-separates, but not if the individual $T_g$s of the corresponding homopolymers are too similar.

### 4.4.1. In solution

Aggregates most commonly formed in solution are micelles and these occur when one of the blocks has been selectively dissolved. Amphiphilic block copolymers can form well-defined micelles containing a central, insoluble core and a soluble outer shell, or corona (scheme **4.2**). More complex aggregates such as cylindrical or spherical micelles and vesicles can also be formed.

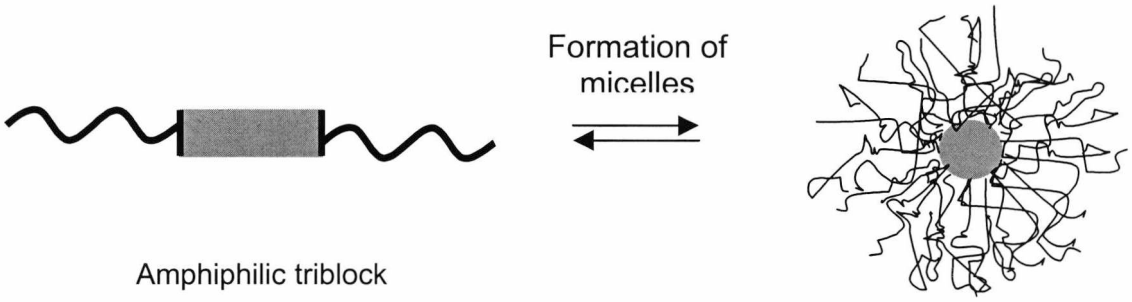


**Scheme 4.2.** Representation of micellar formation

For all micellar applications, it is important to understand the relationship between the number of block copolymers in a micelle (Z), the degree of polymerisation of each segment (N) and the size of the micelle. It has been shown that, in general, equation 4.1 can be used for many diblocks, triblocks, and graft copolymers, as well as for low molecular weight non-ionic, anionic, and cationic surfactants.[17]

$$Z = Z_0 \times N_A^2 \times N_B^{-0.8} \qquad (4.1.)$$

$Z_0$ is related to the interaction parameter $\chi$, the monomer volume, and the packing parameter $v/al$ (equation 4.2):

$$Z_0 = 36\pi N_B^{6E} (v/al)^3 \qquad (4.2)$$

where $v$ = molar vol. of surfactant
$a$ = area per head group
$l$ = contour length of the alkyl chain

The mean size, polydispersity, and colloidal stability of block copolymer micelles can be judged using electron microscopy (TEM, SEM). In accordance with equation 4.2,

Eisenberg and co-workers showed that by increasing the core-block length of an ionic block copolymer, cylindrical and vesicular shapes were obtained.[18, 19]

In addition, the majority of reports on the lyotropic phase behaviour of amphiphiles have focused on PEO-PPO-PEO block copolymers and other weakly segregated systems ("Pluronics").[7,20] In such cases, the phase behaviour depends largely on temperature, for example PEO dehydrates at around 80°C, and PPO between 20°C and 50°C. Also, a decrease in length for the (soluble) block, PEO, can destabilise the cubic and hexagonal phases, leading to lamellar phases being most common. It has been found that these polymeric systems usually form all the types of mesophases observed for conventional surfactants. [21]

### 4.4.2. Solid state

In the solid state block copolymers tend to microphase-separate into different morphologies, depending largely on the lengths, architecture, and interfacial adhesion of the individual blocks. Included in the types of morphologies that can occur are lamellar, hexagonally ordered cylinders, and bicontinuous gyroid structures.[22]

## 4. References


[1] Nuyken, O.; Pask, S. In *Concise Encyclopedia of Polymer Science and Engineering*; Wiley, New York, 1990.

[2] Shipp, D.A.; Wang, J.-L.; Matyjaszewski, K. *Macromolecules* **1998**, 31, 8005.

[3] Georges, M.K.; Veregin, R.P.N.; Kazmaier, P.M.; Hamer, G.K. *Trends Polym. Sci.* **1994**, 2, 66.

[4] Szwarc, M.; Levy, M.; Milkovich, R. *J. Am. Chem. Soc.* **1957**, 78, 2656.

[5] a) Miyamoto, M.; Sawamoto, M.; Higashimura, T. *Macromolecules* **1984**, 17, 265.

b) Minoda, M.; Sawamoto, M.; Higashimura, T. *Macromolecules* **1990**, 23, 1897.

[6] a) Asuke, T.; Chien-Hua, Y.; West, R. *Macromolecules* **1994**, 27, 3023.

b) Demoustier-Champagne, S.; Condier, S.; Devaux, J. *Polymer* **1995**, 36, 1003.

[7] a) Schmolka, I.R.; *J. Am. Oil Chem. Soc.* **1977**, 110.

b) Kabanov, A.V.; Batrakova, E.V.; Alakov, V.Y. *J. Control. Release* **2002**, 82, 189.

[8] Poehlein, G.W. In *Concise Encyclopedia of Polymer Science and Engineering*; Wiley, New York, 1990.

[9] a) Cohen, P.; Abadie, M.J.M.; Schue, F.; Richards, D.H. *Polymer* **1981**, 22, 1316.

b) Cohen, P.; Abadie, M.J.M.; Schue, F.; Richards, D.H. *Polymer* **1982**, 23, 1105.

[10] Hillmyer, M.A.; Bates, F.S. *Macromolecules* **1996**, 29, 6994.

[11] a) Maugh II, T.H. *Science*, **1983**, 222, 39.

b) Webster, O.W.; Hertler, W.R.; Sogah, D.Y.; Farnham, W.B.; Rajanbabu, T.V. *J. Am. Chem. Soc.* **1983**, 105, 5706.

[12] a) Mykytiuk, J.; Armes, S.P., Billingham, N.C. *Polym. Bull.* **1992**, 29, 139.

b) Rannard, S.P.; Billingham, N.C.; Armes, S.P.; Mykytiuk, J. *Eur. Polym J.* **1993**, 29, 407.

c) Baines, F.L.; Armes, S.P.; Billingham, N.C. *Macromolecules* **1996**, 29, 3416.

[13] Okano, T.; Nishiyama, S.; Shinohara, I.; Akaike, T.; Sakurai, Y.; Kataoka, K.; Tsuruta, T. *J. Biomed. Mater. Res.* **1981**, 15, 393.

[14] Clay, R.T.; Cohen, R.E. *Supramol. Sci.* **1995**, 2, 183.

[15] a) Patrickios, C.S.; Forder, C.; Armes, S.P.; Billingham, N.C. *J. Polym. Sci., Part A: Polym. Chem.* **1996**, 34, 1529.

b) Forder, C.; Armes, S.P.; Billingham, N.C. *Polym. Bull.* **1995**, 35, 291.

[16] Schillen, K.; Brown, W.; Johnsen, R.M. *Macromoecules.* **1994**, 27, 4825.

[17] Forster, S.; Zisenis, M.; Wenz, E.; Antonietti, M. *J. Chem. Phys.* **1996**, 104, 9956.

[18] Zhang L.F.; Eisenberg, A. *Science* **1995**, 268, 1728.

[19] Zhang L.F.; Yu, K.; Eisenberg, A. *Science* **1996**, 272, 1777.

[20] Wanka, G.; Hoffman, H.; Ulbricht, W. *Macromolecules.* **1994**, 27, 4145.

[21] Narajan, R. *Colloids Surf. B Bioint.* **1999**, 16, 55.

[22] Forster, S.; Antonietti, M. *Adv. Mater.* **1998**, 10, 195.

# 5. Synthesis of polysilane block copolymers

## 5.1. Review of polysilane block and graft copolymers

### 5.1.1. Introduction

The incorporation of polymers into a copolymer system can lead to increased processability and can also affect the macroscopic ordering of the resulting materials.[1] Copolymerisation reactions involving polysilanes are important because, although polysilanes have many useful properties, mechanically they are relatively poor.[2] This problem can restrict the successful exploitation of polysilanes in research and industry. For example, interest in polysilanes has mostly centred on their unusual spectral properties, as well as their tendency to photodegrade. However, polysilane films are quite brittle and tend to crack quite easily.[2] Therefore, one approach which can be used to overcome this problem is to combine polysilanes with polymers that have good mechanical properties. For the most part, the combination of polysilanes with other polymers has been achieved by blending the polymers together.

To date there are only a handful of examples of polysilane block and graft copolymers. Also, since the majority of polysilanes are synthesised via the Wurtz reaction, it has tended to limit the syntheses of copolymers from polysilanes to condensation reactions of the halide end-groups. Polysilane copolymers have previously been prepared by synthesising random copolymers involving silane monomers containing different substituents. To an extent, the mechanical weaknesses have been overcome by the blending of polysilanes with commodity polymers such as polystyrene via melt mixing and solution casting.[3,4,6] More recently, block and graft copolymers have also been prepared using a variety of methods.[7-20] For example, block copolymers of PMPS have been prepared by polycondensation reactions with polystyryl lithium and polyisopropenyl lithium to form AB and ABA block copolymers.[7] In many cases, the methods of synthesising copolymers have proved to be quite complicated and time-consuming in terms of preparation of the segments of polymers involved as well as being quite difficult with respect to purification. Block copolymers have also been synthesised via a photopolymerisation technique using PMPS as a photoinitiator.[5] However, polysilanes prepared by an alternative means,

i.e. polymerisations of masked disilenes and cyclotetrasilane, have provided a more versatile synthetic pathway in terms of block copolymer synthesis. Most recently, amphiphilic polysilane block copolymers have been prepared, and have been shown to form aggregates such as micelles and vesicles in aqueous solution.

### 5.1.2. Polysilane blends with polystyrene and polypropylene

Molecular composites of poly(dimethylsilylene-*co*-phenylmethylsilylene), also known as polysilastyrene (PSS), were blended with polystyrene (PS) and polypropylene (PP).[3] It has been shown that this leads to improvements in certain properties of the blends which are blended via rotation at 180-200°C. The electronic properties of PSS are of interest since they are quite similar to those of PMPS. Analysis of the blends showed that PSS (up to 5% concentrations) was effectively dispersed in PS, although this was not the case in PP (above 1% the blend became phase separated). A protective effect by the PP or PS matrix against UV degradation of the PSS was evident.

Demoustier-Champagne *et al.*[4] blended PMPS with PS and found a number of interesting properties, which were characterised using thermal, microscopic and x-ray diffraction techniques. Optical microscopy and x-ray diffraction experiments revealed long-range ordering of PMPS, while DSC and other thermal analysis techniques exhibited two thermal transitions. The first transition (~96°C for lower molecular weight PMPS) was assigned to the glass transition, $T_g$, while the second (~200°C) was said to be due to a mesophase order-disorder transition accompanied by the softening of the polymer.

### 5.1.3. PMPS block copolymers

#### 5.1.3.1. Incorporation of poly(methylphenylsilane-*block*-polystyrene (PMPS-*b*-PS) into PMPS and PS blends

The first polysilane block copolymer studied as a model system contained PMPS and PS, and was prepared and characterised by Demoustier-Champagne and co-workers in 1993.[6] The coupling of α,ω-dichloropoly(methylphenylsilane), DiClPMPS, with

polystyryl lithium was described (scheme **5.1**). The formation of di-block and tri-block species were evidenced by increases in molecular weight. However, this was accompanied by broadening of the molecular weight distribution and in some cases to the formation of polymodal distributions. Subsequent SEM studies of PMPS-PS blends have shown that the two homopolymers form a two-phase system. 50%PMPS/50%PS ratios gave coarse dispersions where PMPS exists in a PS matrix. Particle sizes were also relatively large (5-10 μm) and interfacial adhesion was poor. This led to very poor mechanical properties, which were attributed to the high degree of stress concentration at the interfaces. One way of improving adhesion is by incorporating block copolymers, which tend to localise preferentially at the homopolymer-homopolymer interface. For instance, the incorporation of a relatively small amount of PMPS-PS block copolymer (~10 %) in a ternary blend of PMPS and PS led to a marked difference in morphology. This resulted in a finer dispersion of particles of sizes less than 1 μm.

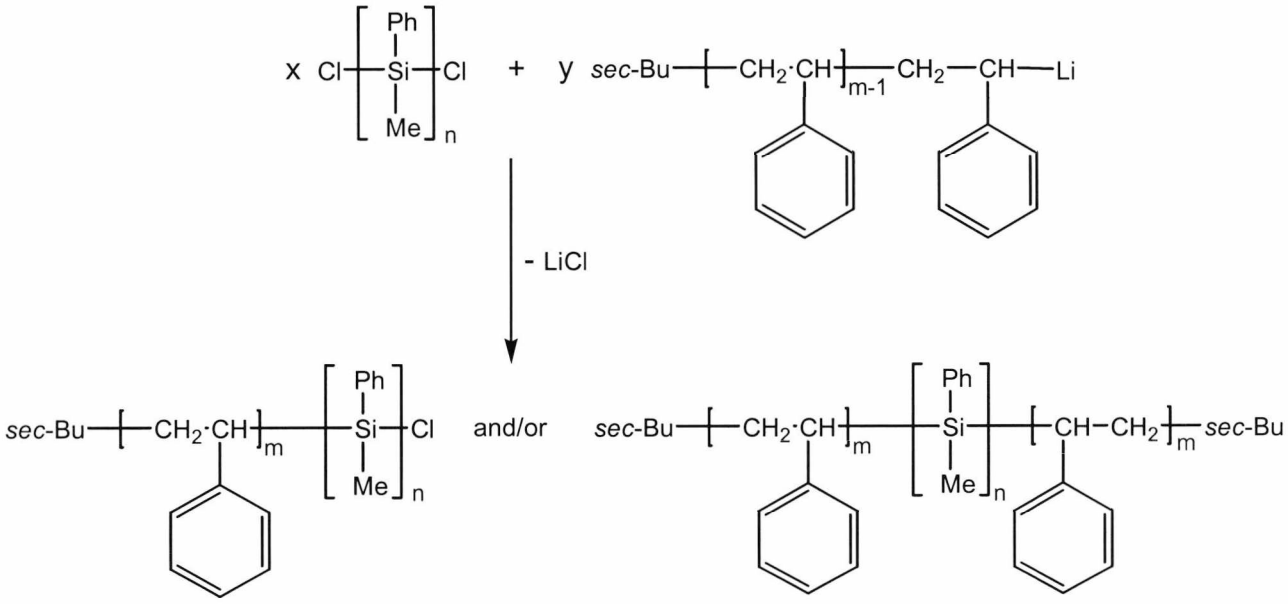


**Scheme 5.1.** Coupling of DiClPMPS with polystyryl lithium

### 5.1.3.2. Formation of polysilane block copolymers incorporating polystyrene and polyisoprene via ring-opening polymerisation

By using alternative means of synthesising PMPS, it has been possible to prepare PMPS-*b*-PS using different methods. Both PMPS-*b*-PS and poly(methylphenylsilane)-*block*-polyisoprene (PMPS-*b*-PI) have been synthesised by polymerising PMPS using ring opening polymerisation (ROP).[7] The block copolymers were prepared using polysilanes synthesised via the addition of a cyclotetrasilane to a solution of either polystyryl lithium, PS-Li (scheme **5.2**), or polyisoproprenyl lithium, PI-Li (scheme **5.3**).[7] A series of block copolymers of varying compositions were prepared and characterised using $^1$H NMR and SEC. Both di- and tri-block copolymers were synthesised in this manner. In this case, the ring opening polymerisation of cyclotetrasilane occurred in the presence of 12-crown-4 in benzene. 12-crown-4 was used since PS-Li and PI-Li are not reactive enough to initiate ring opening polymerisation by themselves.

Thermal analysis of the block copolymers revealed that, although thermal transitions associated with the PMPS were apparently too weak to be observed, the PS and PI segments showed glass transition temperatures which were characteristic of the respective homopolymers (PS $T_g$ = 102°C, PI $T_g$ = -61.5°C). The enthalpies of transition were shown to increase as the weight fraction of each segment increased, although the $T_g$ values remained constant, indicating possible microphase separation in the copolymers.

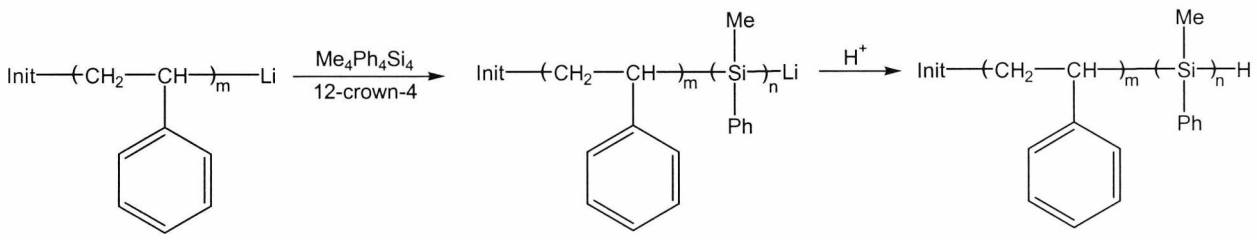


**Scheme 5.2.** Synthesis of PMPS-*b*-PS via the ROP of 1,2,3,4,-tetramethyl-1,2,3,4,-tetraphenylcyclotetrasilane

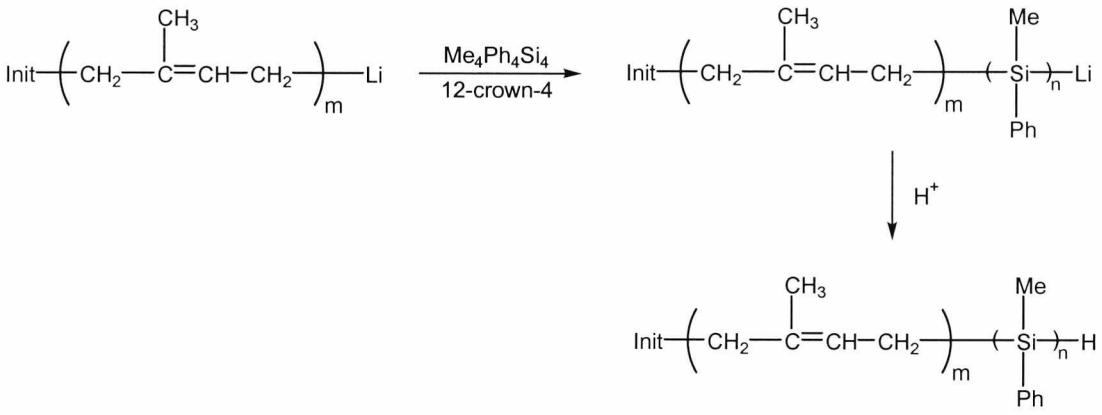


**Scheme 5.3.** Synthesis of PMPS-*b*-PI via the ROP of 1,2,3,4,-tetramethyl-1,2,3,4,-tetraphenylcyclotetrasilane

Subsequent studies of the morphology of PS-*b*-PMPS confirmed the presence of microphase separation.[8] Transmission electron microscopy (TEM) and scanning force microscopy (SFM) experiments on thin films cast from THF have shown cylindrical segments, PMPS, that are surrounded by a polystyrene matrix. Degradation experiments were performed on copolymer films that were exposed to 360 nm UV light. The resulting SFM images showed that the PMPS segments had been degraded, leaving behind a series of "valleys and hills" of uniform size.

### 5.1.3.3. PMPS block copolymers incorporating polystyrene and polyisoprene via condensation reactions

Bromine end-terminated polysilanes have been used by Matyjaszewski and co-workers in a coupling reaction of chain ends to form block copolymers (scheme **5.4**)[7]. In the case of the polystyrene block copolymer, brominated PMPS was added to polystyryl lithium to form either PS-*b*-PMPS or PS-*b*-PMPS-*b*-PS. Bromine end-terminated PMPS is prepared by the reaction of bromine in benzene solution, cleaving the polysilane backbone into smaller fragments. The molecular weight decreases linearly with increased percentage of added bromine. However, since bromination is a random process leading to a statistical distribution, not all chains were functionalised with two bromide end groups. Hence, a mixture of homopolymer, di-blocks and tri-blocks resulted. The molecular weights of the block copolymers were

between the values expected for di- and tri-block copolymers. This was shown by the bimodal GPC traces for the block copolymer.

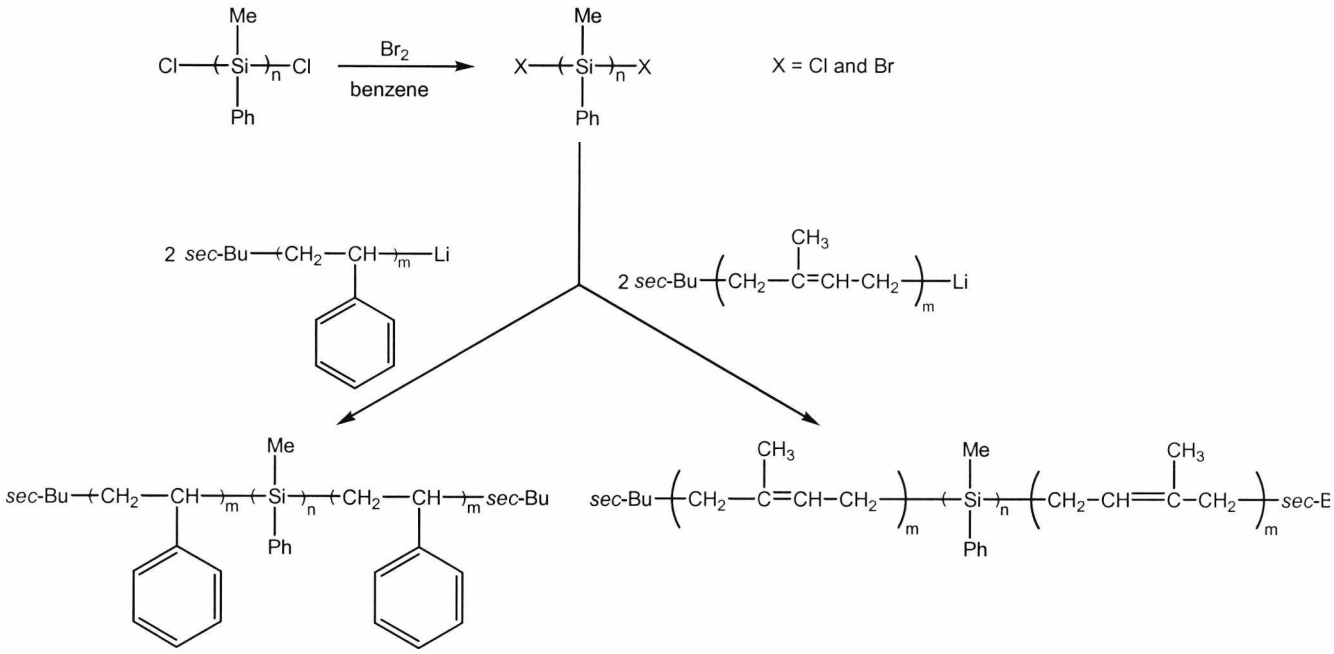


**Scheme 5.4.** Synthesis of PS-*b*-PMPS-*b*-PS and PI-*b*-PMPS-*b*-PI via condensation of diXPMPS with polystyryl lithium and polyisopropyl lithium respectively

In the case of the polyisoprene block copolymer, which is formed in the same manner as that of the polystyrene block copolymer, the synthesis has proved less successful, with a significant amount of uncoupled PMPS chains as well as homopolyisoprene.[7]

### 5.1.3.4. Synthesis of PMPS-*b*-PS using a PMPS macroinitiator for ATRP

Recently, Jones and co-workers have also synthesised PS-*b*-PMPS-*b*-PS block copolymers via functionalised polysilane chains, by adding a functionalised monomer capable of initiating ATRP.[9] The PMPS chains were synthesised via the Wurtz reaction and, after two hours, a solution of monomer, (4-chloromethylphenylethyl)dimethyl-chlorosilylene, CDCS, was directly added to the reaction mixture. The reaction solution was left for a further 30 min., and then the resulting macroinitiator was used for the polymerisation of styrene (scheme **5.5**).

Analysis of the copolymer revealed that a copolymer had indeed formed, although some precursor PMPS remained. Molecular weight data revealed high polydispersities for both the PMPS macroinitiator ($M_n$ = 4,550, $M_w/M_n$ = 5.9) and the resulting copolymer ($M_n$ = 46,550, $M_w/M_n$ = 10.6).

A mixture of AB and ABA block copolymers was prepared, and although the block lengths and molecular weight characteristics were not ideal and not controlled, this procedure was a much more convenient route compared to those involving polymer-polymer reactions. This is due to the fact that ATRP is a more robust technique compared to other more sensitive techniques such as those used in anionic polymerisation.[4,7]

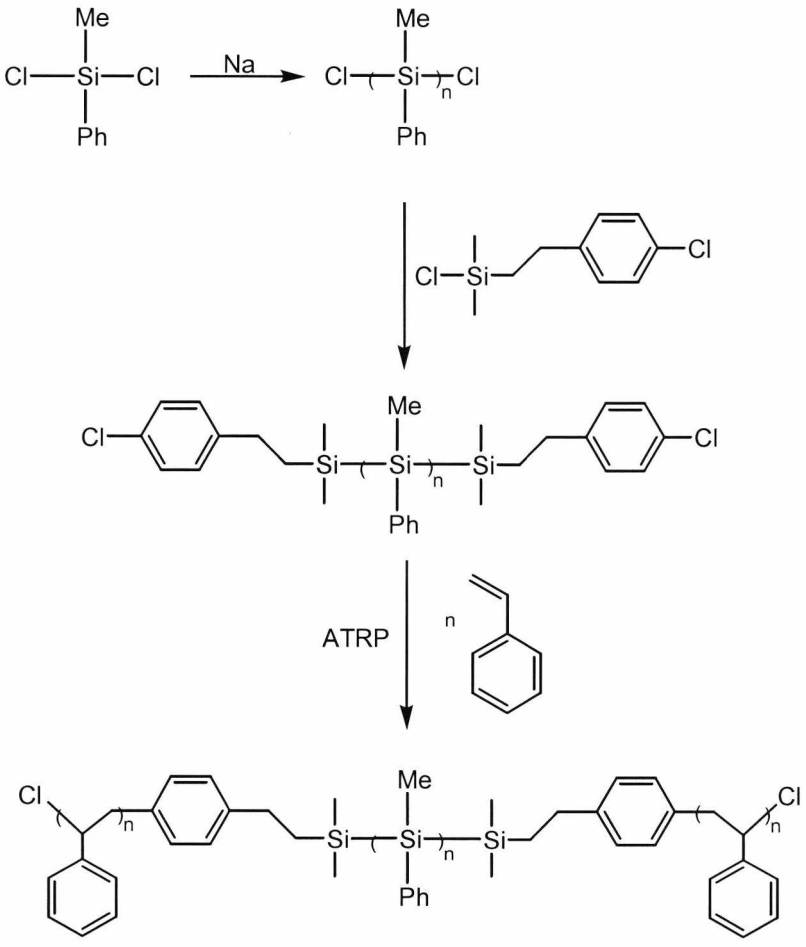


**Scheme 5.5.** Synthesis of PS-*b*-PMPS-*b*-PS

### 5.1.3.5. Poly(methylphenylsilane)-*block*-poly(methyl methacrylate) (PMPS-*b*-PMMA)

PMPS-*b*-PMMA and PMMA-*b*-PMPS-*b*-PMMA have been synthesised by Jones and co-workers via a condensation reaction involving diClPMPS with "living" PMMA chains (scheme **5.6**).[10] Polydispersities for the block copolymers were relatively high (~8), and bimodal peaks were observed in much of the SEC data. This was believed to be due to mixtures of the precursor polymers, along with di- and tri-block copolymers. Some precursor polymer remained, due to deactivated end-groups. This was due to a number of factors, including the dependence of the reaction of two functional groups at the ends of the polymers that are low in concentration and very sensitive to any impurities present.

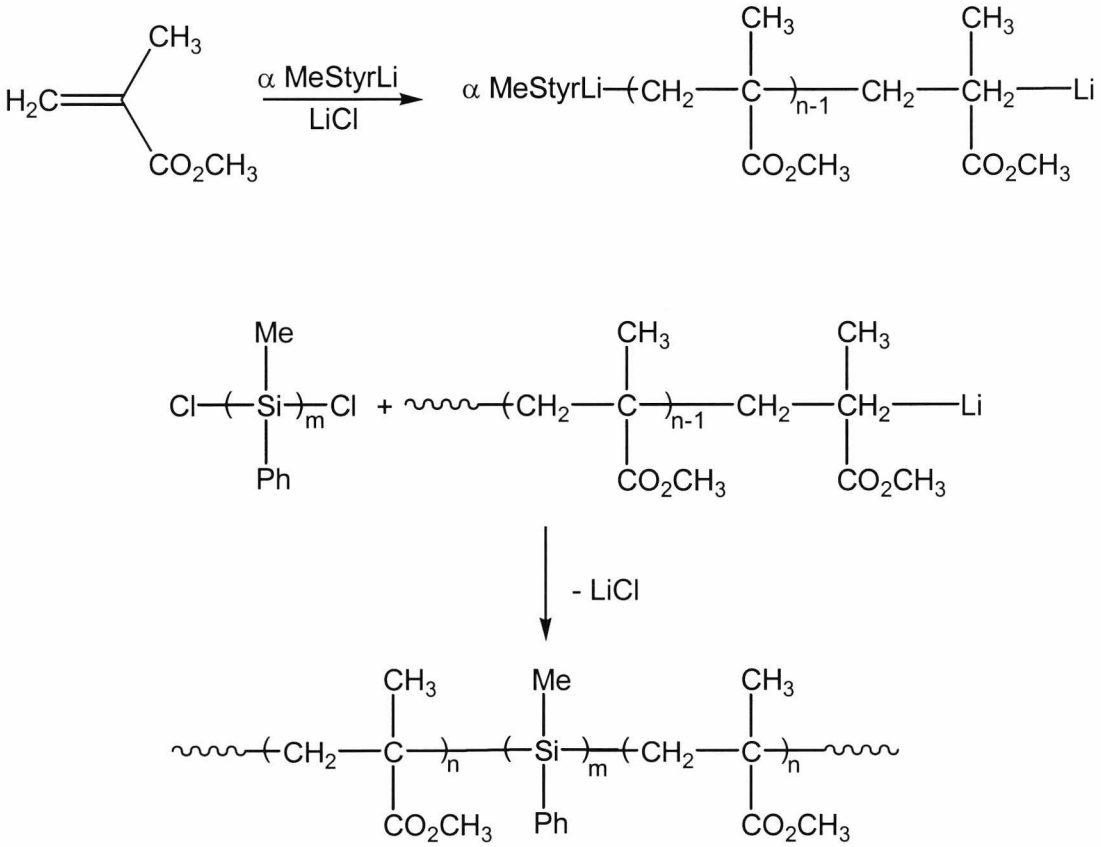


**Scheme 5.6.** Synthesis of PMMA-*b*-PMPS-*b*-PMMA

As is the case with any anionic polymerisations, the purity of the polymers was crucial. Together with a tedious separation procedure, the difficulties associated in the handling of these polymers made it an unattractive method. It is unlikely that a procedure such as this could ever become a standard method whereby polysilanes and commodity polymers could be copolymerised.[10]

### 5.1.4. PMPS graft copolymers

Jones and Holder reported the first convenient synthesis in which a polysilane and a commodity vinyl polymer (polystyrene) were combined in a single copolymer structure.[11] The process involved the synthesis of PMPS containing bromomethyl groups on a number of the substituent phenyl rings. The bromomethyl groups were then used to initiate the ATRP of PS to form the graft copolymer, poly(methylphenylsilane-*graft*-styrene) (PMPS-*graft*-PS) (scheme **5.7**).

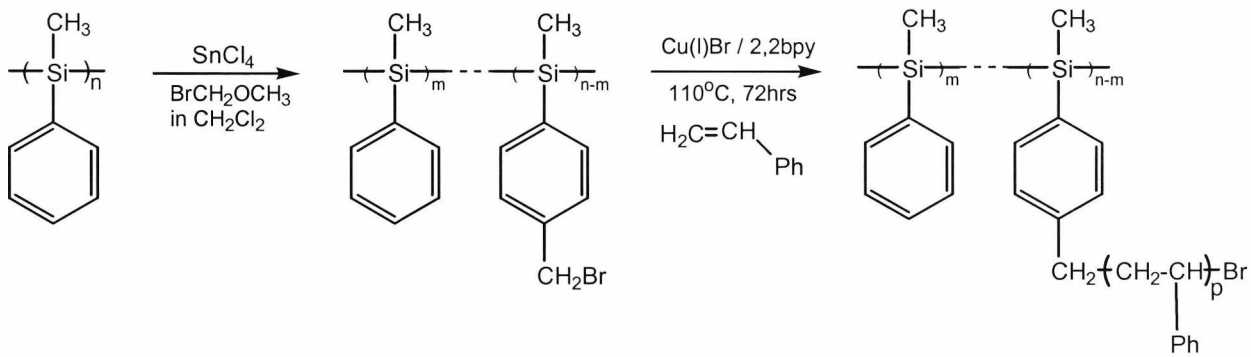


**Scheme 5.7.** Synthesis of PMPS-*graft*-PS ($M_w$ = 87,700, $M_w/M_n$ = 2.5)

UV analysis of the copolymer showed that the characteristic peak of the PMPS segment ($\lambda_{max}$ = 342 nm) remained. Meanwhile, $^1H$ and $^{13}C$ NMR analysis confirmed the structure of the graft copolymer. DSC revealed only one $T_g$ at 80 °C for polystyrene, while no transitions were observed for PMPS. The PMPS transition was believed to be missing since it is too weak compared to that of polystyrene. The $T_g$ at 80 °C is quite low for polystyrene and indicates that a considerable free volume exists and is associated with multiple chain ends.

### 5.1.5. Amphiphilic polysilane block copolymers

#### 5.1.5.1. Poly(methylphenylsilane)-*block*-poly(ethylene oxide) (PMPS-*b*-PEO) amphiphilic block copolymer

A block copolymer of PMPS and poly(ethylene oxide) (PEO) was synthesised via condensation of these two polymers in the presence of pyridine (scheme **5.8**). [12,13] PEO ($M_n$ = 7,000, $M_w/M_n$ = 1.03) was added to a solution of diXPMPS ($M_n$ = 4,400, $M_w/M_n$ = 2.0) in THF and toluene to yield the multi-block copolymer ($M_n$ = 27,000, $M_w/M_n$ = 1.6). The most abundant form of the copolymer was made up of $(PMPS)_3$-$(PEO)_2$, although it is thought that the product was composed of a range of copolymers from simple diblocks up to $(PMPS\text{-}PEO)_{16}$.

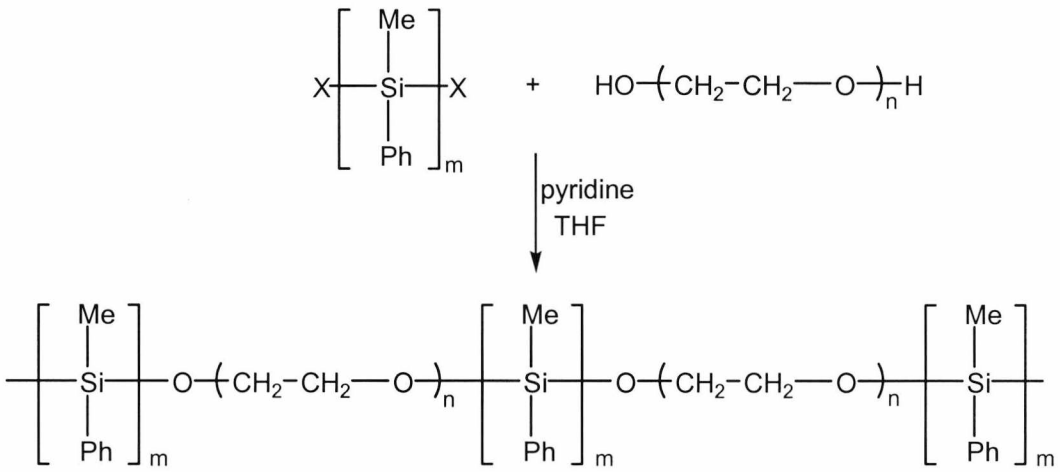


**Scheme 5.8.** Synthesis of PMPS-*b*-PEO (average structure: PMPS-*b*-PEO-*b*-PMPS-*b*-PEO-*b*-PMPS)

It is the first example of an amphiphilic polysilane block copolymer which aggregates in water. It is also the first reported example of a multi-block copolymer which forms vesicles in water. TEM analysis revealed vesicles (fig. **5.1.**) which were prepared either via direct addition of the sample to water via an ultrafiltration/dilution method, or by following a dialysis procedure.[14]

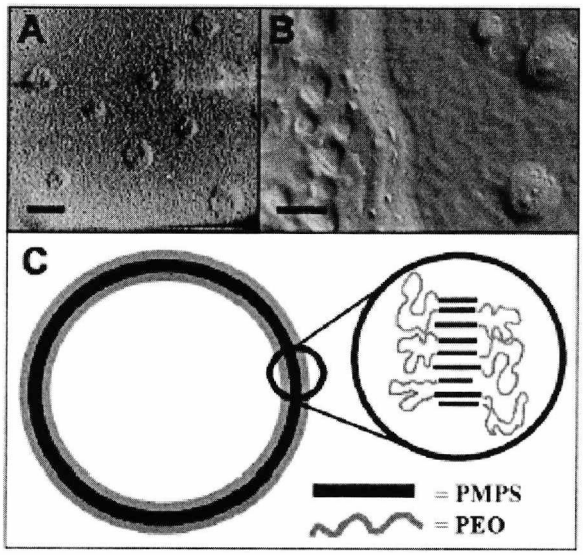


**Fig. 5.1.** (**A**, **B**) TEM analysis of vesicles and (**C**) representation of the possible structure of the vesicles (reprinted from *Macromolecules* 2000, *33*, 8289).

The vesicles were between ca. 100 nm and 180 nm in diameter. In order to prove that the structures seen using electron microscopy were in fact vesicles, an encapsulation experiment was performed using the water-soluble dye, 5-carboxyfluorescein, in a dialysis procedure. After 3 days, the aqueous dispersion was separated using a Sephadex column. It was found that, upon UV analysis of the copolymer aggregates ($\lambda_{max}$ = 355 nm), the dye was also present ($\lambda_{max}$ = 519.5 nm) indicating that closed vesicles had been formed. Other aggregates were observed using electron microscopy, including the formation of micellar rods and also helical aggregates, which formed both left and right-handed helices.[15]

In addition, surface pressure-surface area ($\pi$-A) isotherms were measured during compression of Langmuir monolayers. They revealed that a change in orientation of the PMPS rod occurred. These rods lie flat on the surface of the water and then orientate perpendicularly as the surface pressure is increased, leading to a microphase-separated structure (fig. **5.2**).

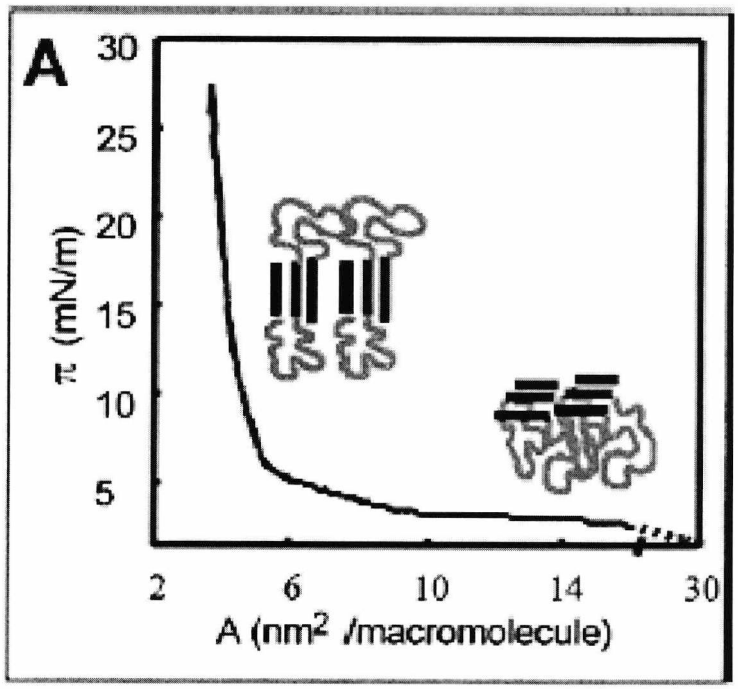


**Fig. 5.2.** Surface area-surface pressure isotherm of a Langmuir monolayer of $PMPS_nPEO_m$, including representations of the proposed macromolecular organisation of the polymer at different states of compression (reprinted from *Macromolecules* 2000, *33*, 8289).

### 5.1.5.2. Poly(1,1-dimethyl-2,2-dihexyldisilene)-*block*-poly(2-hydroxyethyl methacrylate) amphiphilic block copolymers

Sakurai and co-workers[16] have synthesised Poly(1,1-dimethyl-2,2-dihexyldisilene)-*block*-poly(2-hydroxyethyl methacrylate) (PMHS-*b*-PHEMA) copolymers via the anionic polymerisation of masked disilenes, followed by the second-stage polymerisation with 2-(trimethylsilyloxy)ethyl methacrylate.[17] Hydrolysis of the trimethylsilyl protecting groups gave the amphiphilic block copolymer, PMHS-*b*-PHEMA (scheme **5.9**).[16]

Micelles are formed with the PHMS segments making up a hydrophobic core inside a hydrophilic corona containing PHEMA segments. PHMS exhibits abrupt thermochromism in both solution and the solid state, and the electronic properties of the hydrophobic polysilane segments in two different environments (i.e. hydrophilic and hydrophobic) were examined. Two different samples of copolymer were

analysed – one with a longer PHEMA (cop **1**) segment and another with a longer PHMS chain (cop **2**).

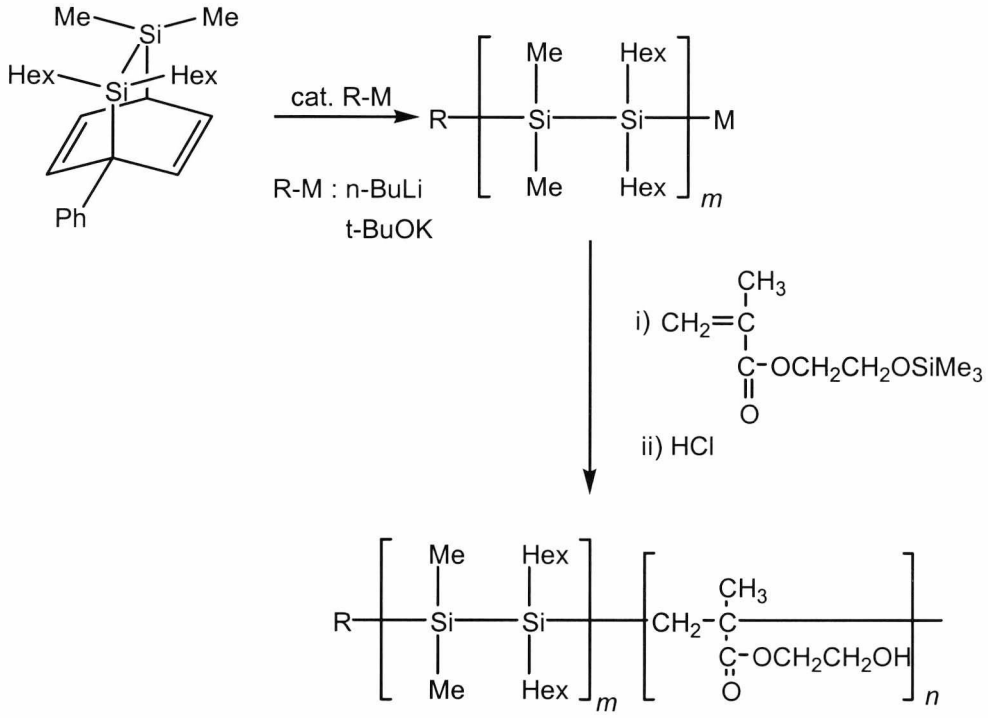


**Scheme 5.9.** Synthesis of PMHS-*b*-PHEMA

UV analysis revealed that for cop **1** the peak at 334 nm in methanol was identical to that of solid state PMHS at room temperature, where PHMS adopts an all-trans conformation. These characteristics show that the PMHS exists in a hydrophobic core as a solid surrounded by hydrophilic PHEMA. Cop **2** showed that, dissolved in toluene, PMHS seemed to exist as the corona, adopting a random conformation. This was reflected in the UV analysis, which shows a $\lambda_{max}$ at 304 nm.

Critical micellisation experiments showed a concentration dependence of UV absorption at 334 nm for cop **1**. As the solution was diluted, the absorption at 334 nm decreased and a new absorption occurred at 280 nm due to the formation of the random coil structure. This can be explained by the conformational changes that occur in the PMHS block as micelles are formed. The micelles were shown to survive down to a certain dilution, after which they dissociated to yield unimers in solution corresponding to the critical micelle concentration, CMC. In addition, the effect of

solvent composition was studied. Methanol and toluene were added in different amounts, which affected the type of micelle that is formed (i.e. whether the corona is hydrophilic or hydrophobic). These changes were followed using UV spectroscopy, while atomic force microscopy (AFM) was used to show ellipsoidal structures of 50-60 nm in size.

### 5.1.5.3. Poly(1,1-dimethyl-2,2-dihexyldisilene)-*block*-poly(methacrylic acid) and the formation of shell cross-linked micelles

Further research into similar copolymers involving PHMS and poly(methacrylic acid) (PMAA) has led to the preparation of nanometer-sized hollow particles, which can be formed by firstly cross-linking the PMAA corona,[18] followed by photochemical degradation of the polysilane core.[19] Poly(1,1-dimethyl-2,2-dihexyldisilene)-*block*-poly(methacrylic acid) (PHMS-*b*-PMAA) is prepared in a similar method used to prepare PHMS-*b*-PHEMA.

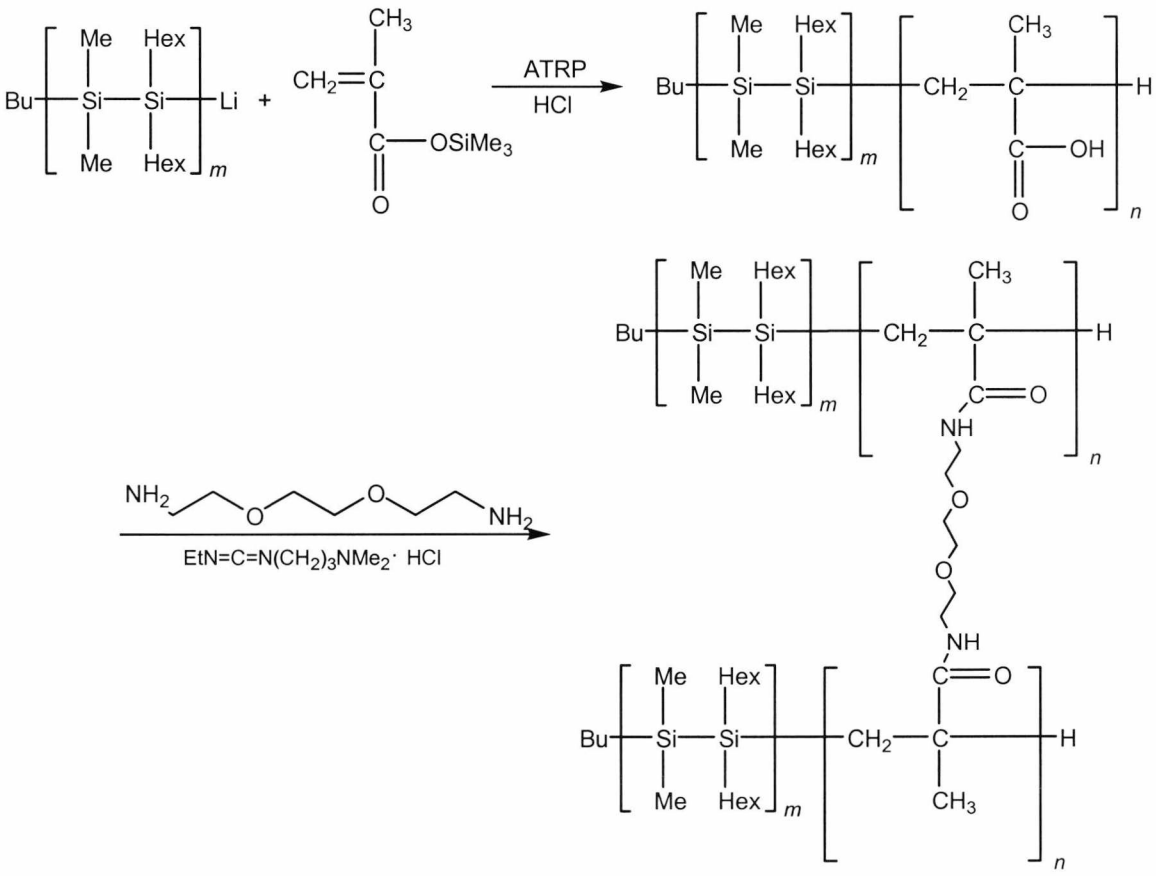


**Scheme 5.10.** Synthesis of PHMS-*b*-PMAA and subsequent shell cross-linking

The critical micelle concentration (CMC) of the copolymer in water was determined, and through the reactive methacrylic groups existing on the corona, the cross-linking reaction was carried out. The shell cross-linking of the carboxylic acid on the PMAA block was achieved by reacting it with 1,10-diaza-4,7-dioxadecane and 1-ethyl-3-(3-dimethylaminopropyl)carbodiimide hydrochloride in solution (scheme **5.10**).

The polysilane core within the shell cross-linked micelle was photodegradated (bleached) by UV irradiation (≥ 280 nm) for a few minutes. The copolymer used had a chemical formula of $(PHMS)_9$-$(PMAA)_{90}$, confirmed using $^1H$ NMR and SEC data. Dialysis against water produced nanometer-sized hollow particles. A schematic representation is shown in fig. **5.3**.

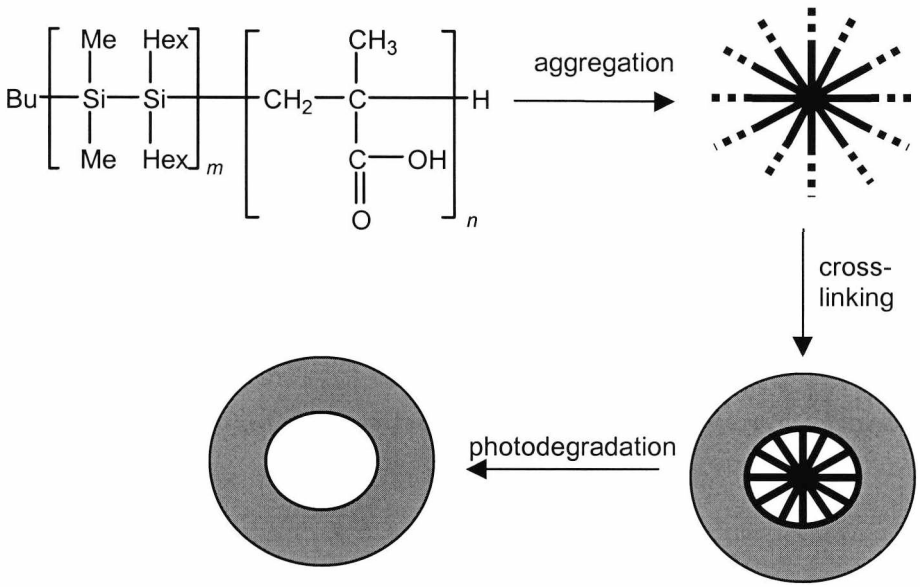


**Fig. 5.3.** Representation of the formation of a hollow particle formed by the cross-linking of micelles, followed by the photochemical degradation of the polysilane core

During photoirradiation, a continuous blue shift was observed in the UV absorption spectra, indicating chain scission of the polysilane. Analysis using dynamic light scattering (DLS) revealed that the hydrodynamic diameter ($D_h$) was much larger (650 nm) compared to that of the template shell cross-linked micelles, SCM (170 nm).

This indicated that expansion occurs in water, and is explained by the swelling of the hydrophilic cross-linked PMAA layer. The most interesting applications for these systems involve the possibility of being able to encapsulate guest molecules.

Therefore, a solution of the hollow SCM's and an excess of 5,6-carboxyfluorescein in water was mixed and then separated by chromatography (GPC). Fluorescence spectra of the SCM was measured and suggested that the dye was localised in an internal aqueous volume, rather than in hydrophobic domains. After dialysis against water for several days, the characteristic absorption (518 nm) gradually disappeared, indicating release of the dye.

### 5.1.6. PMPS block copolymers formed via photopolymerisation

Organic-inorganic hybrids have been developed due to the number of interesting properties they may exhibit, including molecular homogeneity, transparency, rigidness, and optical properties.[20] In particular, the optical properties may have applications in planar waveguides since, in many cases, the refractive index can be controlled by varying copolymer composition. [see photopolymerisation of polysilanes, chapter 1].

PMPS samples have been used as photo-active macroinitiators capable of polymerising monomers such as acrylates and acrylamides in order to form block copolymers. A range of acrylamides such as N,N,-dimethyl acrylamide (DMAA), N,N,-diethyl acrylamide (DEAA), and acryloylmorpholine (ACMO) have been successfully copolymerised with PMPS.[21] Based on a similar method whereby PMPS is photochemically degraded using UV light, the formation of silyl polymer radicals were used to initiate a living polymerisation.[5] The copolymerisation was followed using IR (in order to view characteristic acrylate peaks) and UV (which showed that the characteristic 330 nm peak was still prominent and that the PMPS segment had not been degraded). Some of these acrylic block copolymers have been used as starting materials for sol-gel reactions with tetraethoxy orthosilicate (TEOS), leading to a wide range of polysilane to silicate ratios. The copolymers have shown to form PMPS-silica hybrids via hydrogen bonding between the amide groups and silanol groups on TEOS (scheme **5.11**).

Unusually for copolymers containing hydrophobic PMPS segments, these copolymers show hydrophilic properties, and some have shown good molecular homogeneity and transparency. The resulting copolymers do not tend to phase-separate and the refractive index of the material can be changed over a wide range by altering its composition. Although this method has been used to form PMPS copolymers

containing both acrylate and acrylamide blocks, the results are not completely reproducible. This is because the extent to which the PMPS is degraded, and the resulting shortening of the silane chain lengths, is difficult to control.

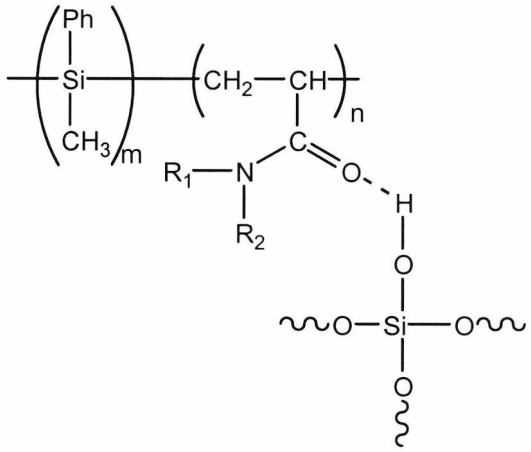


**Scheme 5.11.** Polysilane-acrylamide block copolymer and the hydrogen bonding in the hybrid thin film

### 5.1.7. Summary

Only recently have various examples of polysilane block copolymers been reported. Several interesting properties, including the first example of a vesicle-forming block copolymer in water, have been investigated. However, the number of copolymers which have been reported are limited. In addition, good control over the molecular weights and the compositions of both types of polymer involved has not yet been achieved in most cases.

## 5.2. Experimental - Synthesis of PMPS block copolymers via condensation reactions

### 5.2.1. Materials and Apparatus

THF, toluene, pyridine, methanol were purchased and prepared as described previously [section **3.2.1**]. *n*-Pentane (GPR, 99 %) was purchased from BDH and used as received.

α,ω-Dihalo(methylphenylsilane) (diXPMPS**1** ($M_n$ = 6,500, $M_w/M_n$ = 1.75) and diXPMPS**2** ($M_n$ = 4,500, $M_w/M_n$ = 1.7)), were prepared using the method described previously [section **3.2.2.2**].

Poly(ethylene oxide) (PEO, $M_n$ = ca. 4,000 and $M_n$ = ca. 8,000) was purchased from Aldrich and dried for several days under reduced pressure at 75°C prior to use.

Poly(ethylene glycol methyl ether) (PEGME), $M_n$ = ca. 750 and $M_n$ = ca. 350, were purchased from Aldrich and were degassed and dried under vacuum at 40 °C and 70 °C respectively for 1 hour.

$^1$H nuclear magnetic resonance (NMR) spectra were recorded at 30 °C using a JEOL GX-270 spectrometer from solutions in $CDCl_3$.

Molecular weights of the polymers were estimated relative to polystyrene standards by gel permeation chromatography (GPC) using equipment supplied by Polymer Laboratories Ltd. All determinations were carried out at room temperature using a 600 mm x 5 mm mixed D PLgel column with THF as eluent at a flow rate of 1 ml min$^{-1}$, and a Knauer variable wavelength detector in series with a refractive index detector.

### 5.2.2. Poly(poly(methylphenylsilane)-*block*-poly(ethylene oxide) (PMPS$_n$-PEO$_m$)

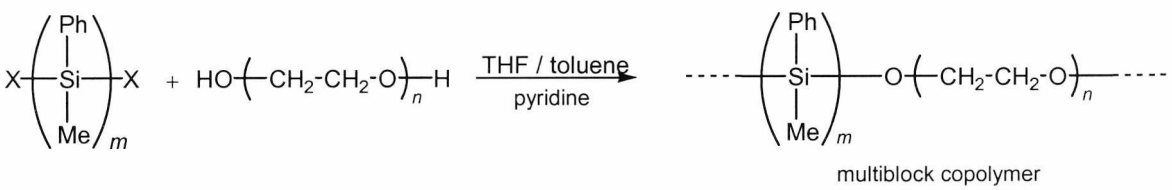


**Scheme 5.12.** Synthesis of PMPS$_n$-PEO$_m$

α,ω-Dihalopoly(methylphenylsilane) (diXPMPS**1**) ($M_n$ = 6,500, $M_p$ 9,000, $M_w/M_n$ = 1.75) was reacted with poly(ethyleneoxide) (PEO) ($M_n$ = 8,000) following the procedure outlined by Jones and co-workers.[13]

Dry PEO (4.92 g, $6.15 \times 10^{-4}$ mol) was dissolved in warm THF (45 °C) and added directly to a THF solution of diXPMPS (2.0 g, $3.08 \times 10^{-4}$ mol). Pyridine (0.050 ml, $6.18 \times 10^{-4}$ mol) was then added to the stirred reaction mixture (scheme **5.12**). After 30 min., an aliquot was removed and analysed via GPC. After 24 hours the reaction was stopped and the mixture was also analysed. The product was precipitated in methanol and *n*-pentane before being filtered at the pump and dried under vacuum at 60°C overnight. The product was analysed using GPC and $^1$H NMR ($M_n$ = 8,900, $M_p$ = 21,000, $M_w/M_n$ = 3.0). $^1$H NMR ($CDCl_3$) δ: -1.1 – 0.2 ppm (Si-C**H**$_3$); 3.55 – 3.75 (-C**H**$_2$C**H**$_2$O-); 6.2 – 7.5 ppm (Si-C$_6$**H**$_5$).

### 5.2.3. Poly{(ethylene glycol)methyl ether-*block*-methylphenylsilane-*block*-(ethylene glycol)methyl ether} (PEGME-*b*-PMPS-*b*-PEGME)

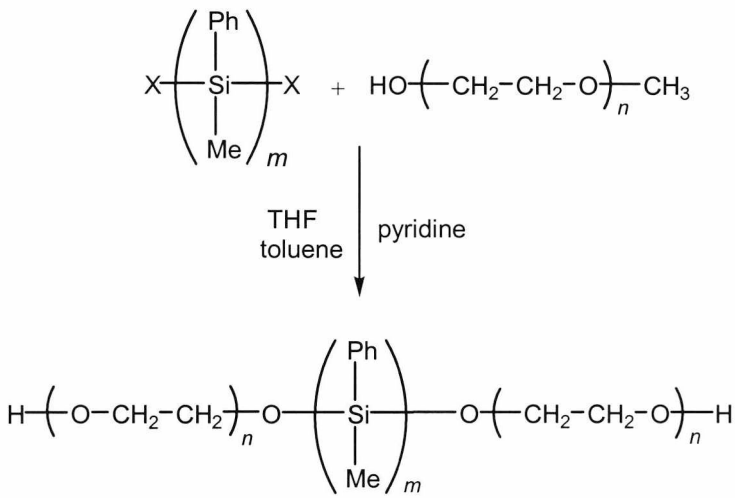


**Scheme 5.13.** Addition of PEGME (n = 5, 10, ~100) to diXPMPS

An excess of PEGME ($M_n$ = 350, 1.8ml, $5.8 \times 10^{-3}$ mol), was added to a 50 ml THF solution of diXPMPS**2** ($M_n$ = 4,500, 4.95 g, $1.10 \times 10^{-3}$ mol), in the presence of pyridine (0.2 ml, $2.74 \times 10^{-3}$ mol) (scheme **5.13**). After 1 hour, the mixture was precipitated into excess methanol, filtered, and then reprecipitated and washed with

methanol and dried overnight under vacuum at 60°C ($M_n$ = 4,500, $M_w/M_n$ = 1.7) (yield 85 %).

$^1$H NMR($CDCl_3$) δ: 6.2 – 7.4 ppm (Si-$C_6\mathbf{H}_5$); 3.6 – 3.8 ppm (-$C\mathbf{H}_2C\mathbf{H}_2O$-); 3.4 ppm (-$OC\mathbf{H}_3$); -1.1 –0.2 ppm (Si-$CH_3$).

A similar reaction was also carried out using PEGME ($M_n$ = 750) and PEGME ($M_n$ = 8,000).

## 5.3. Results and discussion

### 5.3.1. Poly(poly(methylphenylsilane)-*block*-poly(ethylene oxide)) ($PMPS_m$-$PEO_n$)

There were some difficulties encountered when trying to synthesise $PMPS_m$-$PEO_n$. Several attempts revealed that little or no copolymerisation was occurring. The lengths of the PMPS chains were varied from $M_n$ = 3,000 up to $M_n$ = 15,000, while the PEO used varied from $M_n$ = 4,000 and $M_n$ = 8,000. However, almost all the reactions showed no change in molecular weight compared to the original homopolymers. Samples from the reactions were analysed via SEC after 20 min. and also after several days, and still no increase was observed. Certain improvements were carried out in order to improve the reaction conditions, including thorough drying of all solvents and reagents involved. For example, PEO was dried for several days under vacuum, while THF was dried and distilled over sodium and benzophenone twice. Also, since the silicon halide end groups of PMPS were susceptible to attack from any moisture present in the system, reactions were carried out immediately after diXPMPS was synthesised. However, the reactions were still not successful. The synthesis of $PMPS_m$-$PEO_n$ was attempted several times - the most successful attempt is shown here.

#### 5.3.1.1. Molecular weight characterisation

The molecular weights obtained by SEC analysis of the diXPMPS and the copolymer are shown in table **5.1**, the values of which were taken from the plots in fig. **5.4**. From the plots it appears that some copolymerisation has occurred. This is represented by a shift in molecular weight, although homopolymers of both PMPS and PEO remain. After 30 mins. there seems to be a slight shift in molecular weight. After 12 hours a shift from the original molecular weight of the PMPS, $M_p$ = 9,000, to a molecular weight of $M_p$ = 21,000 had occurred. No further growth occurred. The latter peak suggests that some diblock or triblock had formed. The shoulder on the lower molecular weight side of the peak is due to PMPS homopolymer.

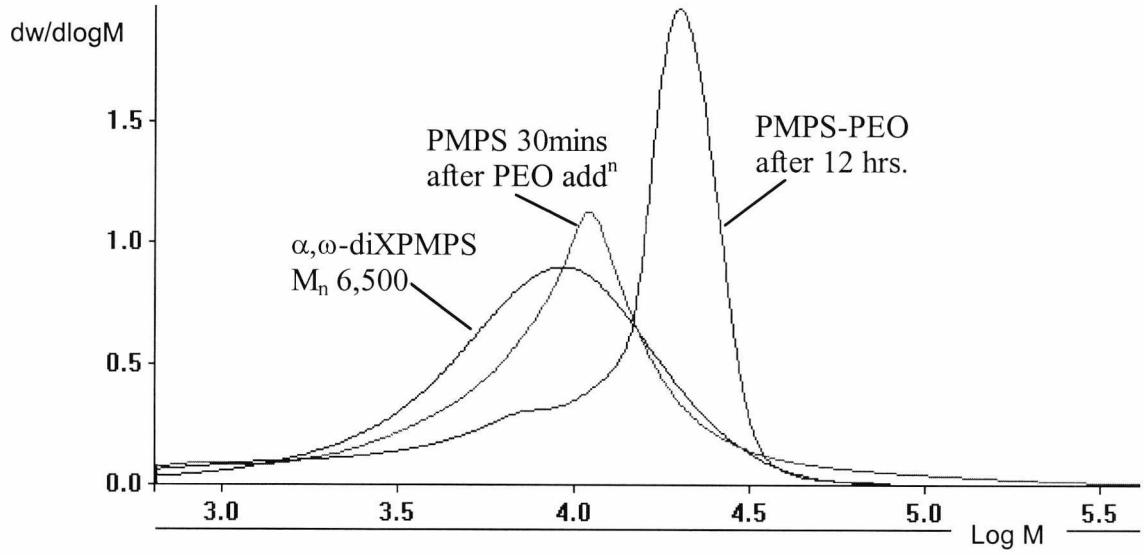


**Fig. 5.4.** Overlay of GPC plots of PMPS (0 min.), $PMPS_m$-$PEO_n$ (30 min.), and $PMPS_m$-$PEO_n$ (12 hrs.)

| | $M_n$ | $M_w$ | $M_p$ | $M_w/M_n$ |
|---|---|---|---|---|
| PMPS | 6 500 | 11 400 | 9 000 | 1.75 |
| PMPS-PEO | 8 900 | 26 600 | 21 000 | 3.00 |

**Table 5.1.** Molecular weight characteristics of PMPS and $PMPS_n$-$PEO_m$

The reaction mixture was precipitated into methanol, at which point the product became cloudy. However, it was not possible to isolate any solid since the product remained as a cloudy suspension in the methanol. Although PMPS is not soluble in methanol, PEO is soluble in this solvent. The appearance of a milky precipitate is often characteristic of amphiphilic materials. The addition of *n*-pentane to aid precipitation was also used. The suspension was less milky, with increased separation of product and solvent. The product was washed several times with methanol/*n*-pentane before being dried in the oven at 70 °C. The difficulty with which the product was precipitated means that some homopolymer remains, and the molecular weight distribution shown in fig. 5.4 remained polydisperse.

### 5.3.1.2. $^1$H NMR analysis

$^1$H NMR was used to characterise the copolymer (fig. **5.5**). The spectrum revealed both the characteristic peaks for each segment of the block copolymer, but it is difficult to tell how much PMPS and PEO homopolymer remains. Due to the difficulty with which the copolymer is precipitated and isolated, along with the evident polymodal nature of the copolymer from the GPC data, it is impossible to extract any other information from the $^1$H NMR.

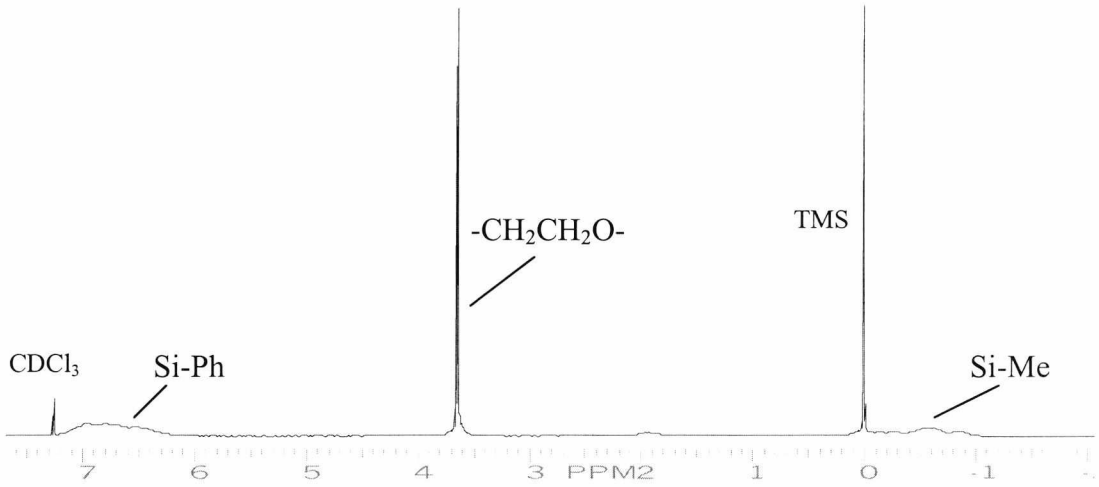


**Fig. 5.5.** $^1$H NMR of $PMPS_nPEO_m$ in chloroform

### 5.3.2. Poly(ethylene glycol)methyl ether-*block*-poly(methylphenyl)silane-*block*-poly(ethylene glycol)methyl ether (PEGME-*b*-PMPS-*b*-PEGME)

A range of poly(ethylene glycol)methyl ether (PEGME) ($M_n$ = 8,000, 750, and 350) samples were used in condensation reactions with a range of diXPMPS. The reaction proved quite difficult to carry out and only very limited success was achieved. Only a small amount of PEGME was successfully reacted with diXPMPS, and only using the lower molecular weight PEGME ($M_n$ = 350).

For PEGME ($M_n$ = 350) a slight shift in molecular weight could not be conclusively revealed by GPC. $^1$H NMR might show that the PEGME had reacted with the diXPMPS endgroups. By reprecipitating and isolating the product, and by the disappearance of the OH peak evidenced in the $^1$H NMR of PEGME (fig. **5.6**) it may be possible to show that PEGME had become attached to the ends of the diXPMPS

chain. On successful addition, the PEGME hydroxyl peak would transform into a Si-O-$CH_2$ peak. However, $^1$H NMR data revealed that not all of the PMPS had reacted with the PEGME. As the product was reprecipitated the $CH_2CH_2O$ peak intensity decreased so that only ~40% of PMPS endgroups contained PEGME.

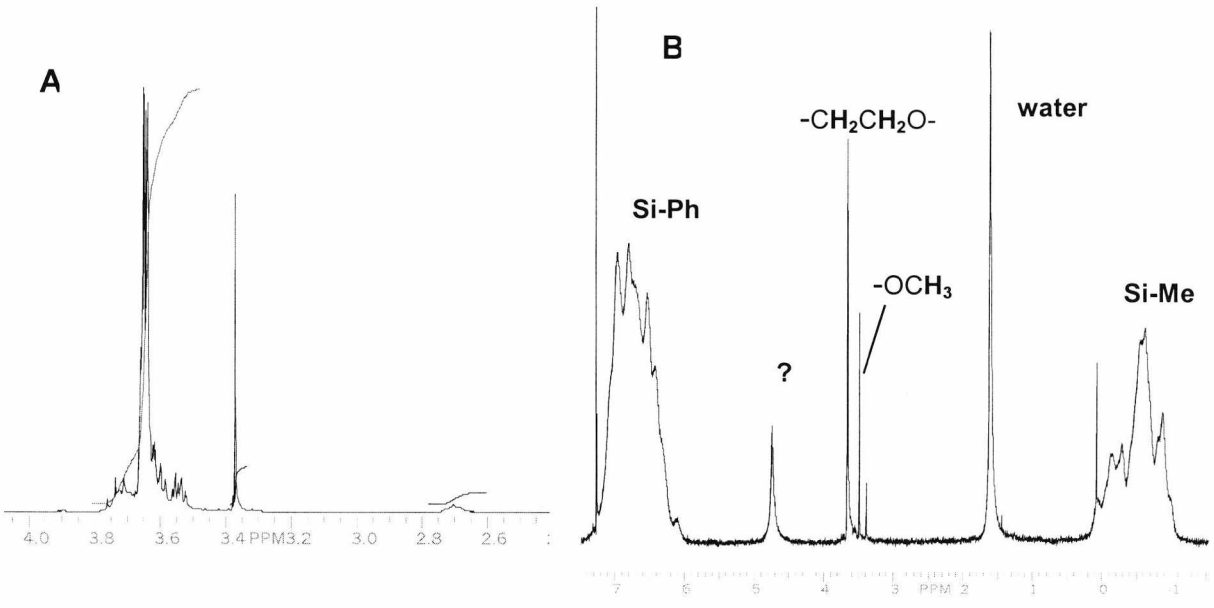


**Fig. 5.6.** $^1$H NMR of (**A**) PEGME ($M_n$ 350) (dried) and of (**B**) PEGME-*b*-PMPS-*b*-PEGME

However, some difficulty remained in the reprecipitation since some water was retained by the product. From the $^1$H NMR data, it was possible to see that some of the PMPS had copolymerised with PEGME.

### 5.3.3. Conclusions

Several experiments were carried out trying to add PEO to diXPMPS. Various molecular weights of PEO and diXPMPS were attempted but were unsuccessful. In order for the reaction to work, the PEO needs to be completely dry as any moisture will destroy the diXPMPS halogenated end groups. Since PEO is very hygroscopic, a substantial amount of water is retained by the polymer. Drying the sample by heating the PEO under vacuum for a week prior to copolymerisation gave little improvement. A higher vacuum as well as other methods of drying the PEO may give better results.

Previously published results[13] have yielded multi-block copolymers with high polydispersity but these experiments could not be reproduced here.

As well as the copolymerisations involving PEO, the reactions involving the endcapping of PEGME onto the ends of the PMPS chains were also unsuccessful. Difficulty remained in trying to react the very water-sensitive halogenated endgroups with the hydrophilic PEGME chains.

Since copolymerisation using the condensation of two polymers had not worked, a more robust method which could be carried out in the presence of impurities was required.

## 5. References


[1] Sakamoto, K.; Obata, K.; Hirata, H.; Nakajima, M.; Sakurai, H. *J. Am. Chem. Soc.* **1989**, 111, 7641.

[2] Demoustier-Champagne, S.; de Mahieu, A.-F.; Devaux, J.; Fayt, R.; Teyssie, Ph. *J. Polym. Sci., Part A: Polym. Chem.* **1993**, 31, 2009.

[3] Asuke, T.; Chien-Hua, Y.; West, R. *Macromolecules* **1994**, 27, 3023.

[4] Demoustier-Champagne, S.; Condier, S.; Devaux, J. *Polymer* **1995**, 36, 1003.

[5] Matsuura, Y.; Matsukawa, K.; Inoue, H. *Chem. Lett.* **2001**, 244.

[6] Demoustier-Champagne, S.; de Mahieu, A.-F.; Devaux, J.; Fayt, R.; Teyssie, Ph. *J. Polym. Sci., Part A: Polym. Chem.* **1993**, 31, 2009.

[7] Fossum, E.; Love, J.A.; Matyjaszewski, K. *J. Organomet. Chem.* **1995**, 499, 253.

[8] Fossum, E.; Matjyaszewski, K.; Sheiko, S.S.; Moller, M. *Macromolecules* **1997**, 30, 1765.

[9] Lutsen, L.; Cordina,G.P.-G.; Jones, R.G.; Schue, F. *Eur. Polym J.* **1998**, 34, 1829.

[10] Lutsen, L.; Jones, R.G. *Polym. Int.* **1998**, 46, 3.

[11] Jones, R.G.; Holder, S.J. *Macromol. Chem. Phys.* **1997**, 198, 3571.

[12] Holder, S.J.; Hiorns, R.C.; Sommerdijk, N.A.J.M.; Williams, S.J.; Jones, R.G.; Nolte, R.J.M. *Chem. Commun.* **1998**, 14, 1445.

[13] Hiorns, R.C.; Holder, S.J.; Schue, F.; Jones, R.G. *Polym. Int.* **2001**, 50(9), 1016.

[14] Zhang, L.; Eisenberg, A. *J. Am. Chem. Soc.* **1996**, 118, 3168.

[15] Sommerdijk, N. A. J. M.; Holder S. J.; Hiorns, R. C.; Jones, R. G.; Nolte R. J. M. *Macromolecules* **2000**, *33*, 8289.

[16] Sanji, T.; Kitayama, F.; Sakurai, H. *Macromolecules* **1999**, 32, 5718.

[17] Hirao, A.; Kato, H.; Yamaguchi, K.; Nakahama, S. *Macromolecules* **1986**, 19, 1294.

[18] Sanji, T.; Nakatsura, Y.; Kitayama, F.; Sakurai, H. *Chem. Comm.* **1999**, 2201.

[19] Sanji, T.; Nakatsura, Y.; Ohnishi, S.; Sakurai, H. *Macromolecules* **2000**, 33, 8524.

[20] Loy, D.A.; Shea, K.J. *Chem. Rev.* **1995**, 95, 1431.

[21] Matsuura, Y.; Matsukawa, K.; Kawabata, R.; Higashi, N.; Niwa, M.; Inoue, H. *Polymer* **2002**, 43, 1549.

# 6. Synthesis of PMPS block copolymers using ATRP

## 6.1. Introduction

### 6.1.1. Background

Conventional free radical polymerisation[1] has been used for many years to synthesise a variety of random and statistical copolymers. It has, however, proved to be very difficult to synthesise block copolymers due to the short lifetime of the growing chain and the continuously occurring initiation process.[2] Atom transfer radical polymerisation (ATRP), along with other controlled radical polymerisation (CRP) methods, can extend the lifetime of radicals to several hours and initiation is very fast. Hence, a range of well-defined block and graft copolymers have been synthesised over the past few years. In addition, since most chains (over 95%)[3] survive from the beginning of an ATRP reaction until the very end, variations in the monomer feed during the course of the reaction are "recorded" along the chain length. Not only has this lead to the formation of block copolymers by sequential addition,[4] but has also led to the synthesis of a new class of copolymers known as gradient copolymers.[5]

### 6.1.2. ATRP block copolymer synthesis

There are several ways in which ATRP can be used to synthesise copolymers. The sequential addition of monomers,[4,5] the formation of end-functionalised polymers,[6] macroinitiators,[7] and the use of multifunctional initiators[8,9,10] and monomers (inimers)[11] have all been used in ATRP copolymerisations. The control over functionality, the simplicity of the process (e.g. "one-pot" syntheses), and the wide range of monomers available makes ATRP an attractive route for synthesis of copolymers. Recently, there have been a number of materials prepared using ATRP which have either only previously been prepared using multi-step synthesis with quite harsh reaction conditions, or have never been synthesised at all.[2]

Block copolymers, usually in the form of di- or tri-block copolymers, can be synthesised either via the sequential addition of monomers or by using a

macroinitiator. Depending on whether the (macro)initiator is mono or difunctional, AB and ABA block copolymers can be synthesised, respectively.

#### 6.1.2.1. Sequential addition

The first example of a block copolymer synthesised entirely by ATRP (via sequential addition) is poly(methyl acrylate)-*block*-polystyrene (PMA-*b*-PS and PS-*b*-PMA).[12,13] Analysis of this block copolymer synthesis included GPC studies, which displayed shifts in the molecular weight curves, and $^{1}$H NMR spectroscopic analysis which demonstrated that the majority of active bromine end groups remained after polymerisation of the first block. ABA block copolymers of this type are known as thermoplastic elastomers, and have a central "soft block" made of methyl acrylate and outer "hard blocks" made up of either polystyrene or methyl methacrylate (MMA). The rates of propagation for different monomers involved in random/statistical copolymerisations need to be of the same magnitude in order for cross-propagation to occur.[14] This is also the case for ATRP block copolymers of, for example, PMMA and PMA.[14] Initiation of the second block will occur if the apparent rate constant of cross-propagation is at least as fast as that of the subsequent propagation. If cross-propagation (initiation of the second block) is slower than propagation, a very polydisperse or bimodal polymer will result. The rate of cross-propagation is a function of macroinitiator composition, end group, and complex composition.[14] Control over molecular weight is particularly important for thermoplastic elastomers since the morphological and rheological properties can be influenced by the polydispersity of the "hard" segment.[15]

#### 6.1.2.2. End group functionality

The incorporation of functional groups at the termini of copolymers of various types can be achieved by either incorporating a functional initiator at the beginning of polymerisation, or by transforming the end group of a polymer. The use of functional initiators such as α-haloesters and benzyl halides in ATRP leads to formation of polymers which have a functional group at one terminal and a halide group at the

other. These functional initiators contain functional groups such as hydroxy,[16] amino, ester, and amide groups.[2]

Difunctional initiators have been used to synthesise AB block copolymers, where one of the functional groups remains unreactive during the ATRP reaction. Subsequently, it can be employed to initiate a further polymerisation. An example is shown in scheme **6.1**, and involves the use of a nitroxy-functional ATRP initiator which is used to polymerise a methacrylic monomer via ATRP. The nitroxy-functionalised polymer is then used to polymerise styrene via living free radical polymerisation.[10]

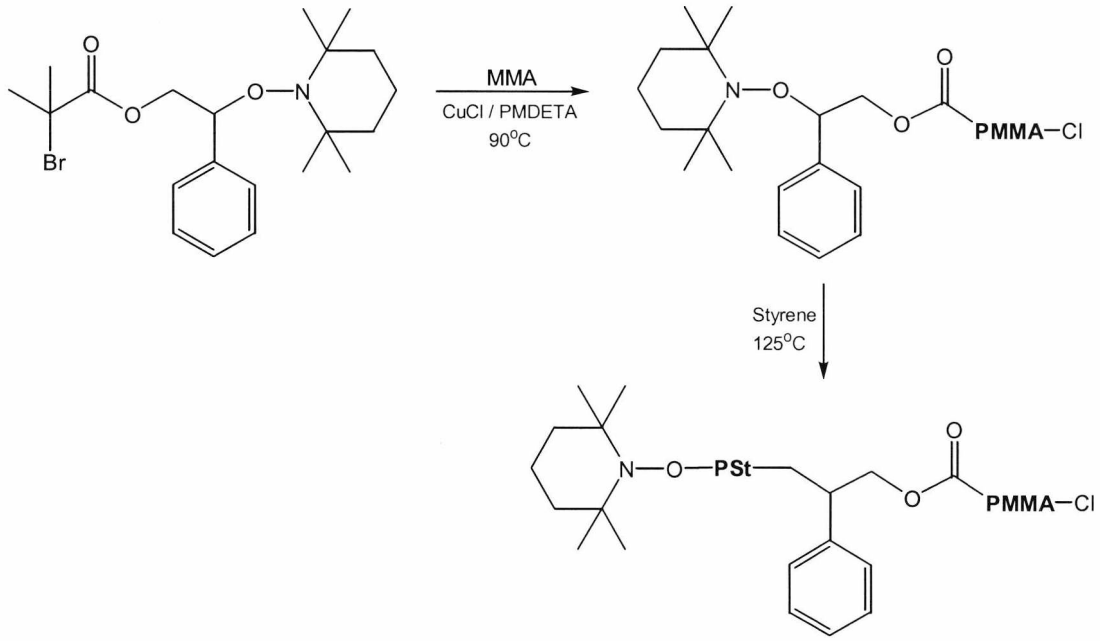


**Scheme 6.1.** Synthesis of poly(methyl methacrylate)-*block*-polystyrene

Alternatively, a polymer synthesised using techniques other than ATRP has been used to initiate copolymerisation by "crossing-over" to ATRP. This has been carried out by altering the end group functionality of the polymer in order to make it a suitable initiator for ATRP. This type of synthesis has been achieved from cationic,[17] step-growth,[18] inorganic polymers,[7,19] dendrimers,[9,20] and ring-opening metathesis polymerisation (ROMP). [21,22] Some examples are shown in scheme **6.2**.

Of all the different polymerisation techniques used in tandem with ATRP to form copolymers, cationic polymerisation is considered the simplest "cross-over" mechanism since the counter anion of the active species is most often a halogen. For

example, the cationic polymerisation of styrene, followed by ATRP of MA or MMA has been shown to form diblocks quite easily.[23]

The inorganic/organic hybrids are another class of block copolymers which have been successfully synthesised by utilising ATRP. One example is poly(styrene-*block*-methylphenylsilane-*block*-styrene), synthesised by Jones and co-workers[7]. In this case, the poly(methylphenylsilane) (PMPS) polymer containing benzyl chloride end-groups was synthesised via the Wurtz reaction and used to initiate the ATRP of styrene [see section 5.1.3.4]. Other examples involve poly(dimethylsiloxane) (PDMS) macroinitiators, which have been used to initiate ATRP of MMA and styrene.[24]

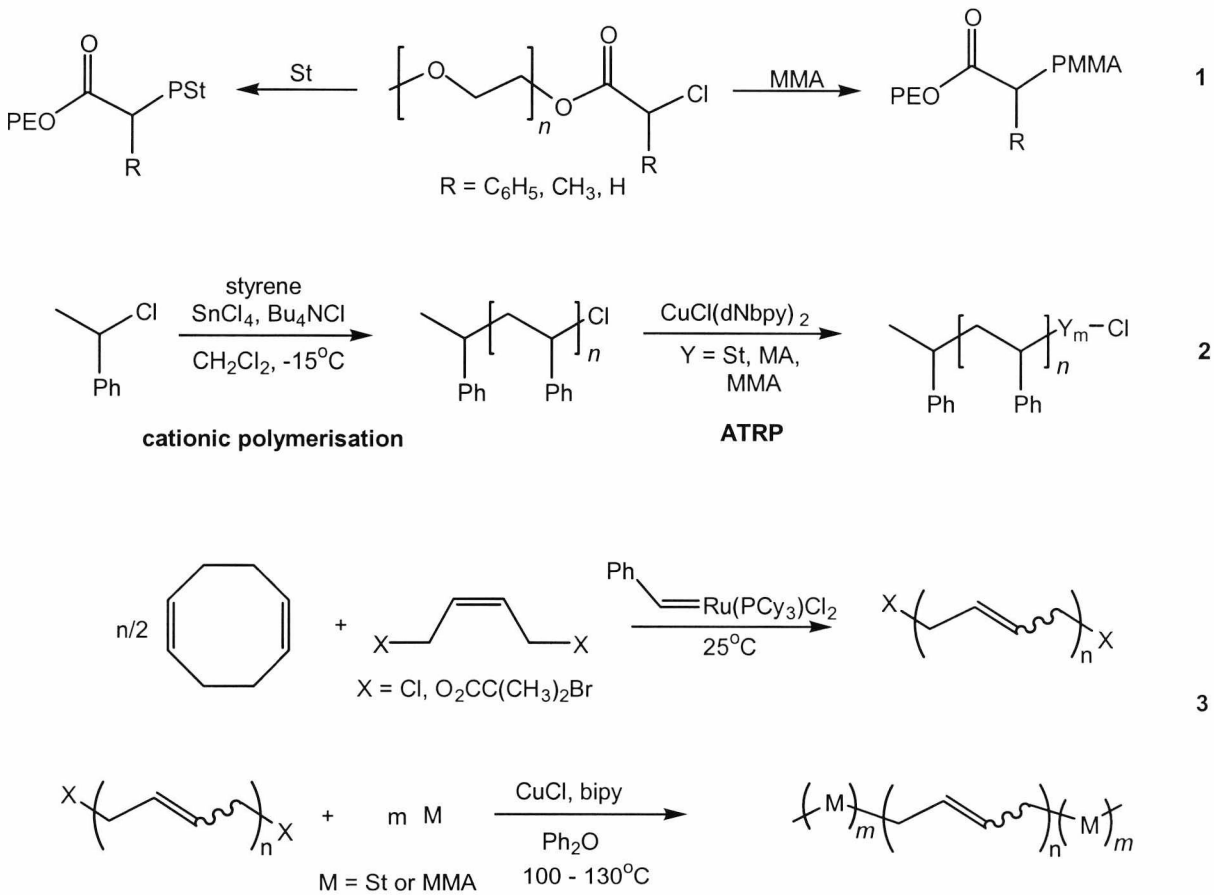


**Scheme 6.2.** 1) ATRP of St or MMA using a PEO macroinitiator.[25]

2) Carbocationic polymerisation of styrene followed by ATRP of St, MA, or MMA.[23]

3) ROMP of 1,5-cyclooctadiene followed by ATRP of St or MMA.[21]

### 6.1.3. Other copolymers formed via ATRP

In conventional radical copolymerisations, the compositions of the various chains within a single sample can vary substantially from chain to chain. Due to chain termination, the compositions of chains formed early on in the polymerisation reaction will differ compared to those formed later on. However, since ATRP has less termination reactions, the control over composition is considerable. Random and gradient copolymers can be synthesised simply by altering the monomer feed, as shown by copolymerisations involving methyl methacrylate and styrene. Being able to control the statistics of the compositions of copolymers is of interest because of the way in which the physical properties vary with composition. Simply, the properties can depend on the local dynamics within the copolymer. In gradient copolymers, a large number of local compositions exist, leading to a range of relaxation times of segmental motions.

Other copolymers formed include graft and comb polymers, as well as branched materials. One method of preparing two and three-dimensional polymers is to use monomers with functional groups capable of initiating ATRP. For example, the synthesis of PMPS-*graft*-PS was carried out by grafting PS onto the polysilane backbone via a functional group [section 5.1.4],[26] and is known as a 'grafting from' process. Another approach is to modify the substituents along the backbone of a polymer with initiators prior to ATRP in order to produce graft copolymers. An example of this is the hydrosilation of poly(methylvinylsiloxane) side groups with silane benzyl chloride groups.[27] Alternatively, macromonomers can be prepared and then copolymerised with a low molecular weight comonomer to form graft copolymers. This technique is known as a 'grafting through' process.

### 6.1.4. Summary

To summarise, ATRP has been used to form several different and new copolymer structures. The simplicity of the system, the variety of monomers that can be used, the control over molecular weight, and the possibility of incorporating polymers synthesised by other means, such as polysilanes, makes it an attractive route. Also, only a few examples of copolymers incorporating both polysilane blocks and segments synthesised via ATRP exist [see chapter 5].[7,28]

## 6.2. Experimental

### 6.2.1. Materials, Apparatus and Analysis

All ATRP reactions and the synthesis of PMPS macroinitiators were carried out under nitrogen using Schlenk line techniques.

*Chemicals*

*o*-Xylene was distilled over sodium and subsequently stored under nitrogen over molecular sieves at –4°C.

Hexane and THF prepared as described in section **3.2.1**. Ethyl acetate (AR grade) was purchased from Fischer and used as received.

Methyl methacrylate (99%, Aldrich) was distilled under vacuum immediately prior to use.

Methacryloyl chloride (80%), 1,8-Diazabicyclo[5.4.0]undec-7-ene (DBU) (98%), 2-bromoisobutyryl bromide (98%), 2-bromoproprionyl bromide (97%), triethylamine (99%), diethyl ether, dichloromethane, 2,2-bipyridine (99+%), methanol (AR), Cu(I)Cl (98+%), and Cu(I)Br (98%) were purchased from Aldrich and used as received. Ethylene glycol (anhydrous, 99.8%, Aldrich) was distilled under vacuum immediately prior to use. Ethyl-2-bromoisobutyrate (98%, Aldrich) and ethyl-2-bromoproprionate (99%, Aldrich) used as received.

*Apparatus*

$^{1}H$ and $^{13}C$ nuclear magnetic resonance (NMR) spectra were recorded at 30 °C using a JEOL GX-270 spectrometer from solutions in $CDCl_3$. F.T. Infrared spectroscopy analysis was carried out using an ATI Mattson Genesis Series FT-IR spectrometer. Elemental analysis was carried out using a Carlo Erba 1106 Elemental Analyzer. Molecular weights of the polymers were estimated relative to polystyrene and, in some cases, poly(methyl methacrylate) standards by gel permeation chromatography (GPC) using equipment supplied by Polymer Laboratories Ltd. All determinations were carried out at room temperature using a 600 mm x 5 mm mixed D PLgel column with THF as eluent at a flow rate of 1 ml $min^{-1}$, and a Knauer variable wavelength UV detector in series with a refractive index detector.

Glass transition temperatures were determined using a Perkin Elmer Differential Scanning Calorimeter (PE DSC 7).

*Kinetic Analysis*

For a number of PMMA-PMPS-PMMA reactions, small aliquots were removed at regular timed intervals. The aliquots were removed from the reaction vessel via syringe and immediately filtered through short (~4 cm) alumina columns using deuterated chloroform ($CDCl_3$) as the eluent. The samples were then analysed directly by $^1H$ NMR spectroscopy. The integrations of relevant peaks were used to follow the progress of the reaction. ($^1H$ NMR ($CDCl_3$) $\delta$: 5.64 & 6.20 ppm ($C\mathbf{H}_2$=C($CH_3$) monomeric vinylic protons); 0.9 – 1.2 ppm ($CH_2$-C($C\mathbf{H}_3$) polymeric PMMA methyl protons); -1.0 – 0.2 ppm (Si-$C\mathbf{H}_3$, PMPS).

A number of similar copolymerisations were also followed via GPC. Aliquots were removed at timed intervals and filtered through alumina using THF as the eluent, and then analysed using GPC.

*Thermal Analysis*

All samples were weighed and pressed into aluminium lids. Samples were then annealed under vacuum at 165 °C for 24 hours prior to DSC analysis being performed. In each case three runs were performed whereby the sample was heated, cooled, and then heated once more. Glass transition temperatures ($T_g$) and enthalpies (J/g) quoted are taken from the cooling run and the second heat run. Indium (m.p. 156.1 °C, J/g 28.5) was used to calibrate the DSC. Baselines were taken for both heating and cooling runs for temperatures between 50 °C and 200 °C.

### 6.2.2. Functionalised ATRP initiators

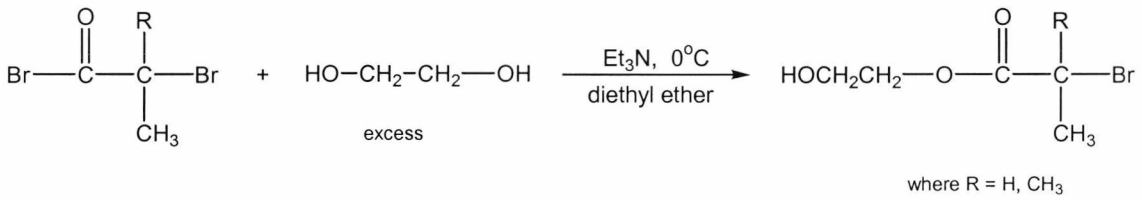


**Scheme 6.1.** Synthesis of a hydroxy-functionalised initiator

### 6.2.2.1. 2'-hydroxyethyl-2-bromo-2-methylpropranoate (initiator 1)

The following reaction was based on the literary procedure for the synthesis of bis(bromoproprionyloxy)ethane)[29].

2-Methyl-2-bromoproprionyl bromide (0.180 mol, 22.2 ml) was added dropwise to a stirred solution of excess ethylene glycol (0.538 mol, 30 ml) and triethylamine (0.180 mol, 25 ml) in diethyl ether (70 ml) (scheme **6.1**). The reaction was kept at a low temperature using an ice bath and was connected to a drying tube containing $CaCl_2$. After the reaction had subsided, the reaction was stirred for 2 hours. The ether and any remaining triethylamine were removed in vacuo before the product was redissolved in diethyl ether (50 ml). The solution was washed several times with a saturated sodium bicarbonate solution (50 ml x 3) and then with water (50 ml x 3). The product was purified via flash chromatography, using a column packed with aluminium oxide (eluent: 50/50 v/v mixture of *n*-hexane and ethyl acetate). Two separate fractions were eluted, the second being identified as the desired product. The solvent was removed under reduced pressure and the final product was obtained as a colourless liquid.

$^1$H NMR ($CDCl_3$) δ: 1.8 ppm (d, 3H, C(Br)(C**H**$_3$)$_2$), 3.02 ppm (s, 1H, O**H**), 3.75 ppm (t, 2H, -$CO_2$-$CH_2$-C**H**$_2$), 4.2 ppm (t, 2H, -$CO_2$-C**H**$_2$-$CH_2$). $^{13}$C NMR ($CDCl_3$) δ: 31 ppm (C(Br)(**C**H$_3$)$_2$), 56 ppm (**C**(Br)(CH$_3$)$_2$), 61 ppm (HO**C**H$_2$CH$_2$O-), 67 ppm (HOCH$_2$**C**H$_2$O-), 172 ppm (**C**=O).

Elemental analysis: % experimental (% theoretical): C 34.29 (33.67); H 5.24 (5.23).

FTIR (KBr, thin film, cm$^{-1}$) 3300 (broad, $\nu_{O-H.}$) 2970 ($\nu_{C-H.}$), 1735 ($\nu_{C=O.}$).

### 6.2.2.2. 2-hydroxyethyl-2-bromopropanoate (initiator 2)

A similar procedure to the one described for the synthesis of initiator **1** was followed in order to synthesise initiator (2-hydroxyethyl-2-bromoproprionate) (initiator **2**) and was based on the published procedure for the synthesis of bis(bromoproprionyloxy)-ethane (scheme 6.1).[29] 2-Bromoproprionyl bromide (19 ml, 0.1792 mol) was added dropwise to a stirring solution of ethylene glycol (30 ml, 0.538mol) and triethylamine (25 ml, 0.1792 mol) in diethyl ether (70 ml). The reaction was kept cool using an ice-bath.

The product was washed before being separated via flash chromatography, using a column packed with aluminium oxide (eluent: 50/50 v/v mixture of *n*-hexane and ethyl acetate). The second fraction eluted was recovered and the solvents removed under reduced pressure. $^{1}$H NMR ($CDCl_3$) δ: 1.8 ppm (d, 3H, C(Br)(H)(**$CH_3$**)), 2.38 ppm (s, 1H, OH), 3.81 ppm (t, 2H, -$CO_2CH_2$**$CH_2$**), 4.26 ppm (m, 2H, -$CO_2$**$CH_2$**$CH_2$), 4.4 ppm (quartet, 1H, C(Br)(**H**)($CH_3$)), 1.2, 1.4, 2, 2.6, 3.58, 3.7, 4.1 ppm (impurities). $^{13}$C NMR($CDCl_3$) δ: 171 ppm (-**$CO_2CH_2CH_2$**-), 67 ppm (-$CO_2$**$CH_2$**$CH_2$-), 61 ppm (-$CO_2CH_2$**$CH_2$**-), 40 ppm (-**C**H**Br**$CH_3$), 22 ppm (-CHBr**C**$H_3$).

Elemental analysis: % experimental (% theoretical): C 30.47 (30.06); H 4.56 (4.57).

### 6.2.3. α,ω-Di(2'-oxyethyl-2-bromo-2-methylpropanoate)poly(methylphenyl-silane)

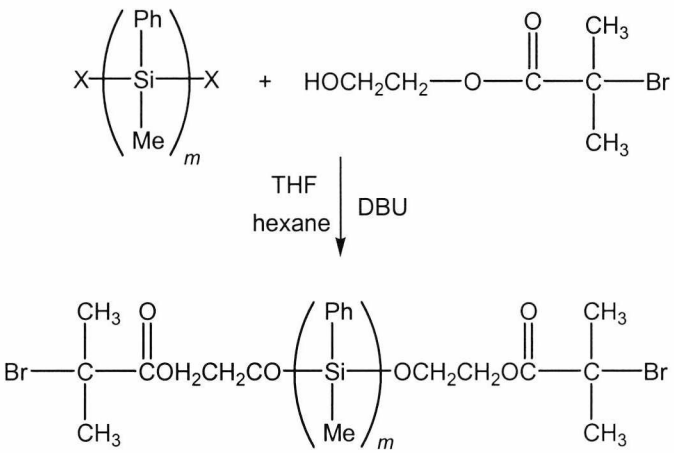




**Scheme 6.2.** Endcapping of diXPMPS with 2'-hydroxyethyl-2-bromo-2-methylpropanoate

A typical ATRP macroinitiator was prepared as follows: diXPMPS (4.00 g, $8.16 \times 10^{-4}$ mol) was added to 2'-hydroxyethyl-2-bromo-2-methylpropanoate (0.350 g, $1.66 \times 10^{-3}$ mol) and 1,8-diazabicylo[5.4.0]undec-7-ene (DBU) (0.252 g, $1.66 \times 10^{-3}$ mol) in THF (30 ml) and stirred for 1 hour at room temperature (scheme **6.2**). After three reprecipitations into hexane the macroinitiator (3.45 g, $6.63 \times 10^{-4}$ mol, 81 % yield) was isolated and dried under vacuum ($M_n$ = 5,200; $M_w/M_n$ = 1.74).

$^{1}$H NMR ($CDCl_3$) δ: -1.0-0.2 ppm (Si-**$CH_3$**), 1.8-2.0 ppm (C(**$CH_3$**)$_2$Br), 3.5-4.1 ppm (–O**$CH_2CH_2$**O–), 6.3-7.3 ppm (Si-$C_6$**$H_5$**). $^{13}$C NMR ($CDCl_3$) δ: -8—5 ppm (Si-**$CH_3$**),

31 ppm (C(**CH$_3$**)$_2$Br), 55.5 ppm (**C**(CH$_3$)$_2$Br), 61 ppm (**CH$_2$**O–CO), 67 ppm (**CH$_2$**O–Si), 127 & 135 ppm (Si-C$_6$**H$_5$**), 171 (**C**=O).

### 6.2.4. Poly(methyl methacrylate-*block*-methylphenylsilane-*block*-methyl methacrylate) (PMMA-PMPS-PMMA)

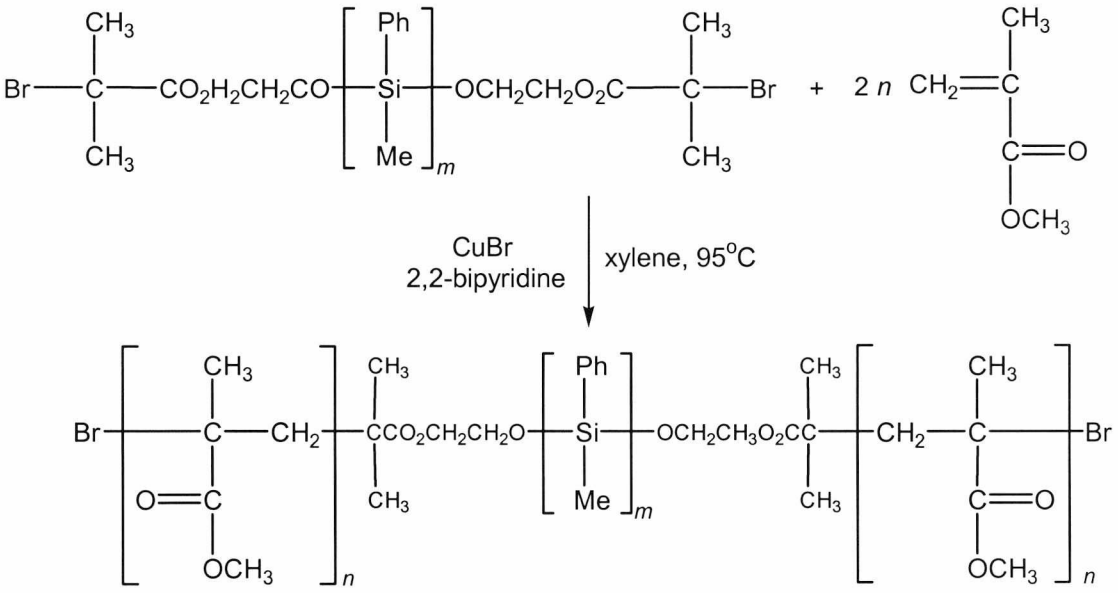


**Scheme 6.3.** Synthesis of PMMA-PMPS-PMMA

A typical procedure is given for the synthesis of PMMA-PMPS-PMMA with DP = 100 units of PMMA on each end of the PMPS macroinitiator:

Cu(I)Br ($1.92 \times 10^{-4}$ mol, $2.76 \times 10^{-2}$ g), 2,2-bipyridine ($3.84 \times 10^{-4}$ mol, $6.01 \times 10^{-2}$ g), and methyl methacrylate (MMA) ($1.92 \times 10^{-2}$ mol, 1.92g) were added to a solution of PMPS(init)$_2$ **1** ($M_n$ = 5,200, $M_w/M_n$ = 1.74, $9.62 \times 10^{-5}$ mol, 0.500 g) in *o*-xylene (2.0 ml). The solution was degassed by three freeze-thaw cycles. The mixture was stirred at 95 °C using an oil bath and left for several hours (scheme **6.3**). The polymerisation was monitored by taking samples for GPC at regular intervals. After the polymerisation was complete (i.e. after the molecular weight of the copolymer ceased to increase), the product was passed through alumina gel using THF as the eluent and precipitated into methanol. The product was filtered at the pump after reprecipitation from THF into methanol once more. A white precipitate (PMMA-PMPS-PMMA **1**) was isolated, dried overnight at 60 °C under vacuum ($M_n$ = 24,700, $M_w/M_n$ = 1.67,

78 % yield). Analysis using $^{1}H$ and $^{13}C$ NMR was used to confirm the structure of the block copolymer.

| copolymer | PMPS(init)$_2$ | | DP of PMMA blocks |
|---|---|---|---|
| | $M_n$ | w/v in xylene | |
| **1** | 3 500 | 0.225g : 2ml | 70 |
| **2** | 5 200 | 0.5g : 2ml | 40 |
| **3** | 5 200 | 0.2g : 2ml | 60 |
| **4** | 5 200 | 0.5g : 2ml | 80 |
| **5** | 5 200 | 0.2g : 2ml | 200 |
| **6** | 9 100 | 0.5g : 1.2ml | 80 |
| **7** | 9 500 | 0.2g : 2ml | 40 |
| **8** | 9 500 | 0.2g : 2ml | 200 |
| **9** | 9 800 | 1.55g : 4ml | 400 |
| **10** | 10 500 | 0.2g : 2ml | 100 |

**Table 6.1.** Reaction conditions for syntheses of PMMA-PMPS-PMMA. (* PMPS(init)$_2$ synthesised as described, except bromination step was omitted, i.e. all diXPMPS chain-ends are Si-Cl groups).

The synthesis was repeated several times (table **6.1**). Variation in initial MMA concentration afforded a range of PMMA block lengths attached to the ends of the PMPS chains. By using PMPS chains of different lengths, copolymers with varied PMPS block lengths, as well differing PMMA blocks, were synthesised. The spectral data for PMMA-PMPS-PMMA **1** is given below and is representative of all samples. $^{1}H$ NMR ($CDCl_3$, ppm) δ: -1.0 – 0.0 (Si-**$CH_3$**), 0.7 – 1.3 ($CH_2C$-**$CH_3$**) 1.5 – 2.1 (**$CH_2$**C-$CH_3$), 3.5 – 3.8 (-O**$CH_3$**), 6.3 – 7.3 (-**Ph**). $^{13}C$ NMR ($CDCl_3$, ppm) δ: -8 – -5. (Si-**$CH_3$**), 16 ($CH_2C$-**$CH_3$**), 18 (1 (**$CH_2$**C-$CH_3$), 45 ($CH_2$-**C**-$CH_3$), 53 (–O**$CH_3$**), , 127, 135 (**Ph**), 178 (**C**=O).

### 6.2.5. Poly((*S*)-(-)-2-methyl-1-butyl methacrylate)-*block*-methylphenylsilane-*block*-(*S*)-(-)-2-methyl-1-butyl methacrylate) (PMBMA-PMPS-PMBMA)

#### 6.2.5.1. (*S*)-(-)-2-methyl-1-butyl methacrylate

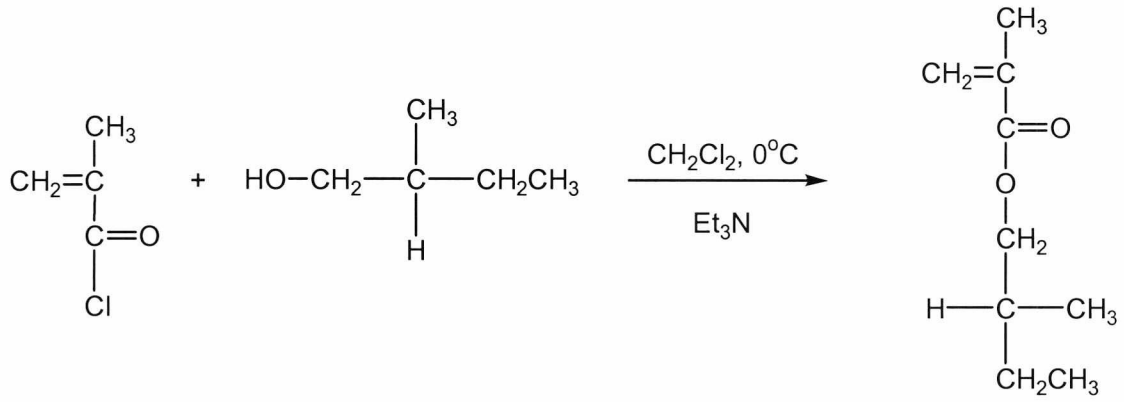


**Scheme 6.4.** Synthesis of (S)-(-)-2-methyl-1-butyl methacrylate

Methacryloyl chloride (0.0478 mol, 5.00 g) was dissolved into dichloromethane (15 ml) at below 4°C. A mixture of triethylamine (0.0478 mol, 4.84 g) and (S)-(-)-2-methyl-1-butanol (0.0478 mol, 4.22 g) was added dropwise over 20 min. with stirring (scheme **6.4**). The reaction was noticeably exothermic and the solution was stirred for an hour at below 4°C. A large amount of yellowish precipitate formed during the reaction. Dichloromethane (40 ml) was added to the solution, which became brick red. The solution was filtered and the dichloromethane was removed using a rotary evaporator to leave a golden orange oil. Any remaining triethylamine and residual alcohol were distilled off under vacuum. The product was recovered and analysed via $^{1}H$ and $^{13}C$ NMR (traces of reactants are evident) (yield = 55%).

$^{1}H$ NMR ($CDCl_3$) δ: 5.50 & 6.05 ppm (d, 2H, $C\mathbf{H_2}$=C($CH_3$); 3.85 – 4.05 ppm (d, 2H, -O$C\mathbf{H_2}$-); 1.9 ppm (s, 3H, $CH_2$=C($C\mathbf{H_3}$); 1.8 – 1.9 (m, 1H, $CH_3C\mathbf{H}CH_2CH_3$); 1.1 – 1.5 ppm (m, 2H, $CH_3CHC\mathbf{H_2}CH_3$); 0.8 – 1.0 ppm (d, 3H, $C\mathbf{H_3}CHCH_2CH_3$); 0.8 – 1.0 ppm (t, 3H, $CH_3CHCH_2C\mathbf{H_3}$).

$^{13}C$ NMR ($CDCl_3$) δ: 167 ppm (**C**=O); 137 ppm ($CH_2$=**C**($CH_3$)); 125 ppm (**C**$H_2$=C($CH_3$)); 69 ppm (-O**C**$H_2$-); 34 ppm ($CH_3$**C**H$CH_2CH_3$); 26 ppm ($CH_3CH$**C**$H_2CH_3$); 18 ppm (**C**$H_3CHCH_2CH_3$); 16 ppm ($CH_2$=C(**C**$H_3$)); 12 ppm ($CH_3CHCH_2$**C**$H_3$).

### 6.2.5.2. Poly((*S*)-(-)-2-methyl-1-butyl methacrylate)-*block*-methylphenylsilane-*block*-(*S*)-(-)-2-methyl-1-butyl methacrylate) (PMBMA-PMPS-PMBMA)

Typically, PMBMA-PMPS-PMBMA was synthesised by following a similar procedure to that outlined for the synthesis of the PMMA-PMPS-PMMA block copolymers (scheme **6.5**). Samples from the reaction were taken and analysed at regular intervals. The reaction conditions of four different polymerisations are shown in table **6.2**.

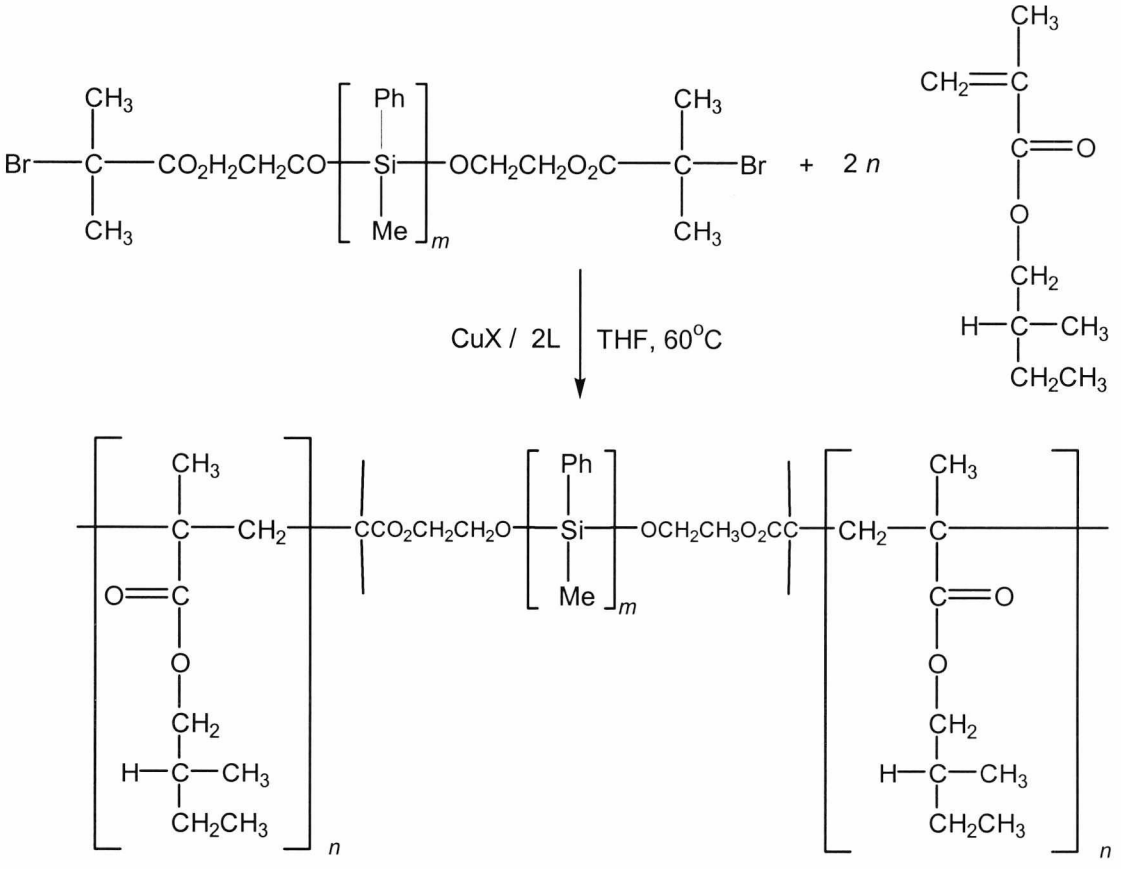


**Scheme 6.5.** Synthesis of PMBMA-PMPS-PMBMA (CuX = CuBr, CuCl)
(L = 2,2-bipyridine or N-(n-propyl)-2-pyridylmethanimine)

| Copolymer | Reaction conditions* | PMPS(init)$_2$ | | MMA:PMPS | [MMA] mol dm$^{-3}$ |
|---|---|---|---|---|---|
| | | $M_n$ | w/v in xylene | | |
| **12** | CuBr/N-ppm | 5 700 | 0.5g : 2.5ml | 60 | 2.31 |
| **13** | CuBr/bpy | 5 700 | 0.2g : 2ml | 100 | 1.93 |
| **14** | CuBr/N-ppm | 5 700 | 0.5g : 2.5ml | 200 | 7.68 |
| **15** | CuCl/bpy | 8 400 | 0.5g : 2ml | 100 | 2.98 |

**Table 6.2.** Reaction details for synthesis of PMBMA-PMPS-PMBMA block copolymers (*N-ppm= N-(n-propyl)-2-pyridylmethanimine, bpy = 2,2-bipyridine)

The block copolymers were characterised via GPC (($M_n$ 14 600, $M_w/M_n$ 1.70) and NMR spectroscopy. The $^1$H and $^{13}$C NMR spectra for PMBMA-PMPS-PMBMA **12** are given below as typical spectra.

$^1$H NMR ($CDCl_3$) δ: 6.2 – 7.4 ppm (Si-$C_6\mathbf{H_5}$); 3.6 – 4.0 ppm (-O$\mathbf{CH_2}$-); 1.9 ppm ($CH_3\mathbf{C}HCH_2CH_3$); 1.6 – 1.9 ppm (-$\mathbf{CH_2}$-$C(CH_3)$-); 1.4 ppm ($CH_3CHCH_2\mathbf{C}H_3$); 0.8 – 1.3 ppm ($\mathbf{CH_3}CHCH_2\mathbf{CH_3}$ & -$CH_2$-$C(\mathbf{CH_3})$-) ; -1.1 – 0.2 ppm (Si-$\mathbf{CH_3}$).

$^{13}$C NMR ($CDCl_3$) δ: 177 ppm (**C**=O); 127 & 135 ppm (Si-$\mathbf{C_6}H_5$); 70 ppm (-O$\mathbf{C}H_2$-); 55 ppm (-$CH_2$-$\mathbf{C}(CH_3)$-); 45 ppm (-$\mathbf{C}H_2$-$C(CH_3)$-); 34 ppm ($CH_3\mathbf{C}HCH_2CH_3$); 27 ppm ($CH_3CH\mathbf{C}H_2CH_3$); 17 ppm ($\mathbf{C}H_3CHCH_2CH_3$); 16 ppm (-$CH_2$-$C(\mathbf{C}H_3)$-); 12 ppm ($CH_3CHCH_2\mathbf{C}H_3$); -7 ppm (Si-$\mathbf{C}H_3$).

## 6.3. Results and discussion

### 6.3.1. PMPS macroinitiator

#### 6.3.1.1. Background

The use of macroinitiators in ATRP to form block copolymers is well known.[7,17-23] Matyjaszewski and co-workers have synthesised polysiloxane macroinitiators that are capable of initiating ATRP reactions of styrenes[30] and methacrylates.[31] In order to initiate the ATRP of styrene, the hydrosilation of poly(dimethyl)siloxane (PDMS) was used to transform the hydrosilyl- or vinylsily-terminal groups into benzyl chloride end groups (scheme **6.6.A**). In the case of methacrylate polymerisation, a more effective PDMS macroinitiator containing α-bromoesters has been synthesised (scheme **6.6.B**). Both macroinitiators have been used to form well-defined, controlled-structure ABA block copolymers. Other PDMS macroinitiators have lead to the formation of AB,[32] ABA, and ABC[31] block copolymers.

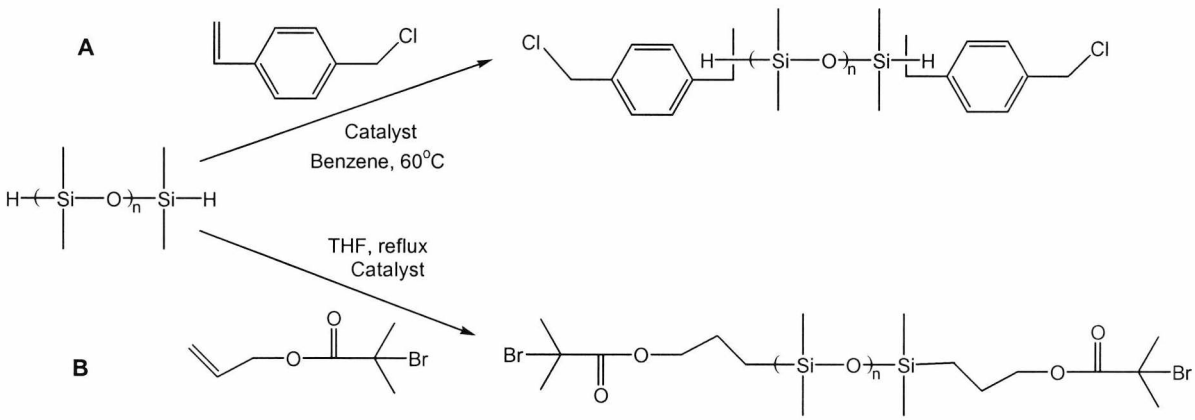


**Scheme 6.6.** Synthesis of di-functional PDMS macroinitiators

A number of polysilane macroinitiators have been used to form polysilane block copolymers, and have been discussed previously [section 5.1]. In particular, PMPS macroinitiators have previously been synthesised by Jones and co-workers [section 5.1.3.4].[7] A functional group was added to the ends of the PMPS polymer directly after it had been synthesised via the Wurtz reaction. However, since the PMPS was

untreated after the Wurtz reaction, the PMPS macroinitiator had a high polydispersity (~5.9) as did the resulting copolymer (~10.6).

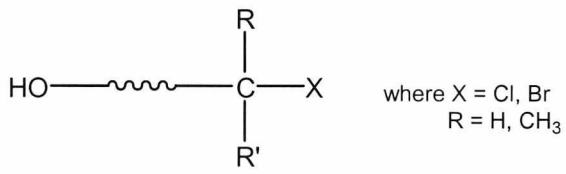


**Scheme 6.7.** Functional initiator for ATRP

As has been illustrated previously [section 3.3.3], the highly reactive Si-halide termini make it possible to successfully endcap PMPS with alcohols. Hence, an initiator which also contains a hydroxy group can be used to form a difunctional PMPS macroinitiator, similar to the PDMS macroinitiators depicted in Scheme **6.6**. Therefore, a difunctional initiator capable of initiating the polymerisation of methacrylates requires an alkyl halide group as well as a hydroxy group (scheme **6.7**). Hence an alcohol was reacted with an acyl bromide to form a suitable initiator.

### 6.3.1.2. 2-Hydroxyethyl-2-methylbromopropanoate

2-Hydroxyethyl-2-methylbromopropanoate (initiator **1**) was synthesised by reacting 2-bromoisobutyryl bromide with excess ethylene glycol, according to a published procedure.[29] Reactions between acid halides and alcohols are rapid and irreversible. A base acts as a catalyst, but is also used in these reactions to neutralise any HX that might be present. Triethylamine was used as the base in order to aid reaction and also avoid reaction of the bromide situated next to the carbonyl group to form the macroinitiator. The use of a less selective base (such as a secondary amine) could cause a reaction with either of the bromide groups present in the 2-bromoisobutyryl (scheme **6.8**). Excess ethylene glycol was used in the reaction so that most of the product formed would contain mono-substituted ethylene glycol.

$^1$H NMR confirmed the structure of the initiator (fig. **6.1**) and elemental analysis confirmed its purity. Infrared analysis was used to distinguish between the two fractions, which were obtained after being separated using column chromatography. The first fraction was unreacted 2-bromoisobutyryl bromide and showed no hydroxyl group stretches at ~ 3 300 cm$^{-1}$, while the second eluted fraction did, indicating that an

OH group was present alongside the characteristic IR peaks of the initiator (fig. **6.2**). The characteristic C-$CH_3$ stretches can be seen at ~2900 $cm^{-1}$, while the carbonyl peak from an ester is seen at 1735 $cm^{-1}$.

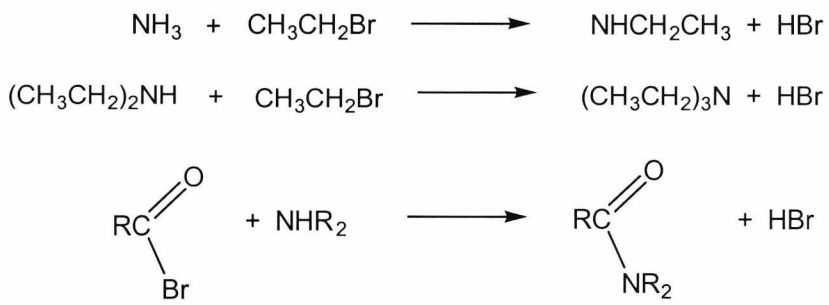


**Scheme 6.8.** Reactions of alkyl/acid bromides with primary and secondary amines

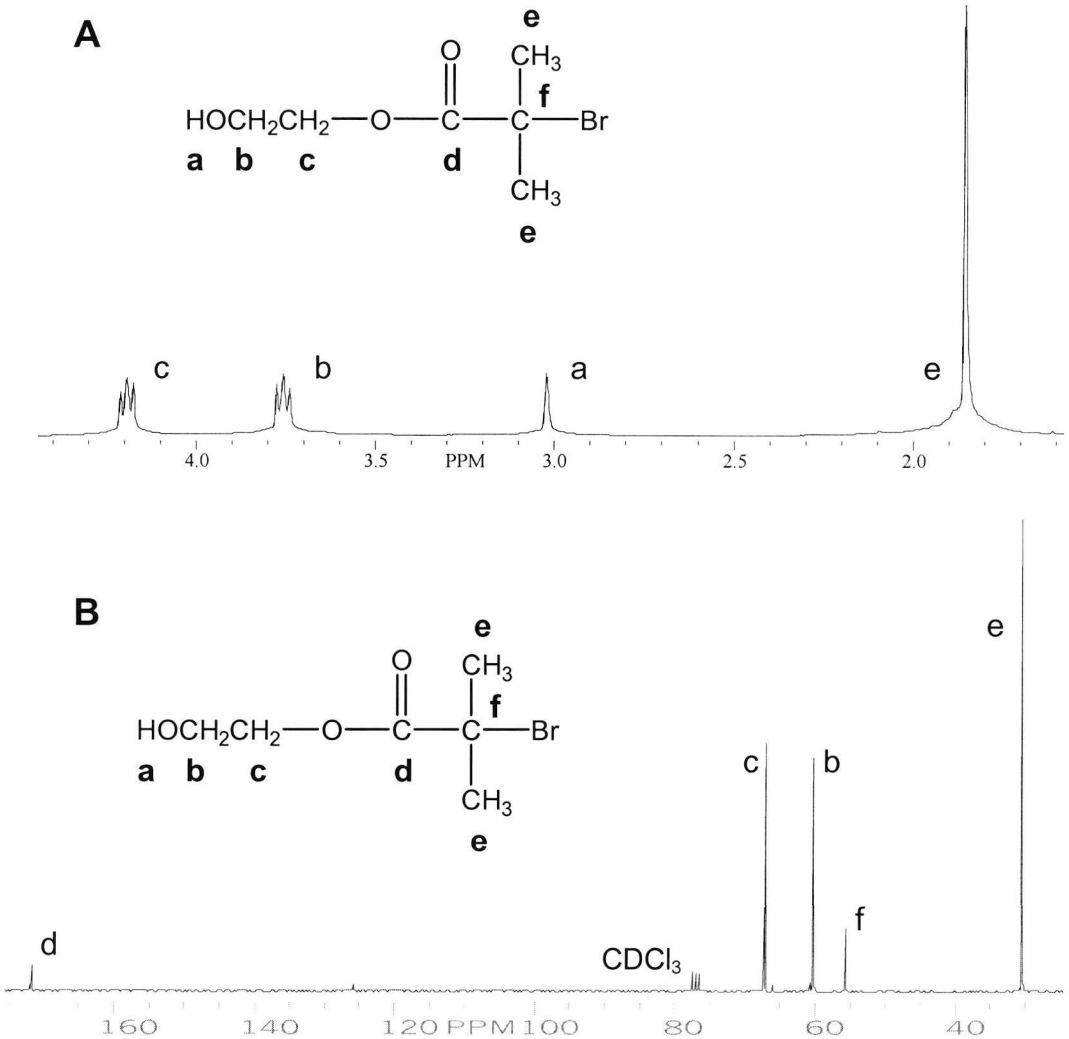


**Fig. 6.1.** $^{1}H$ NMR (**A**) and $^{13}C$ NMR (**B**) spectra of 2-hydroxyethyl-2-methylbromopropanoate (initiator **1**)

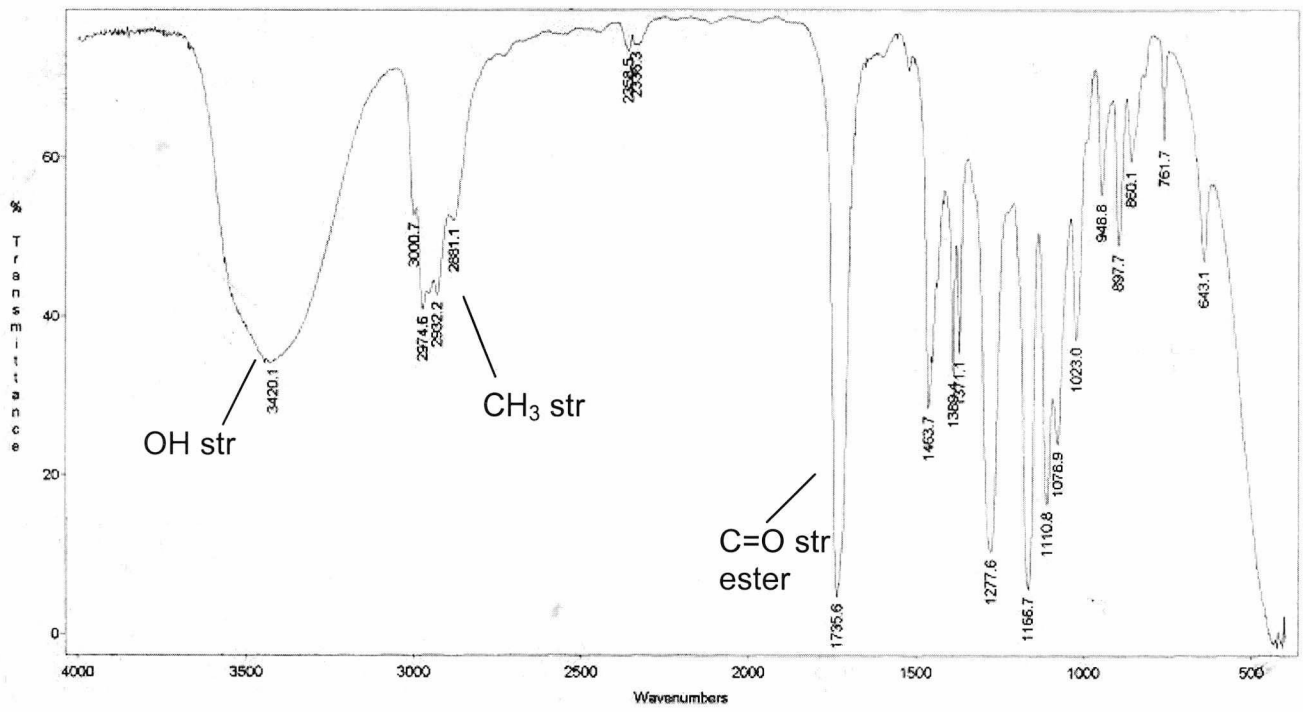


**Fig. 6.2.** IR of 2-hydroxyethyl-2-methylbromopropanoate (initiator **1**)

### 6.3.1.3. Synthesis and characterisation of 2-hydroxyethyl-2-bromopropanoate

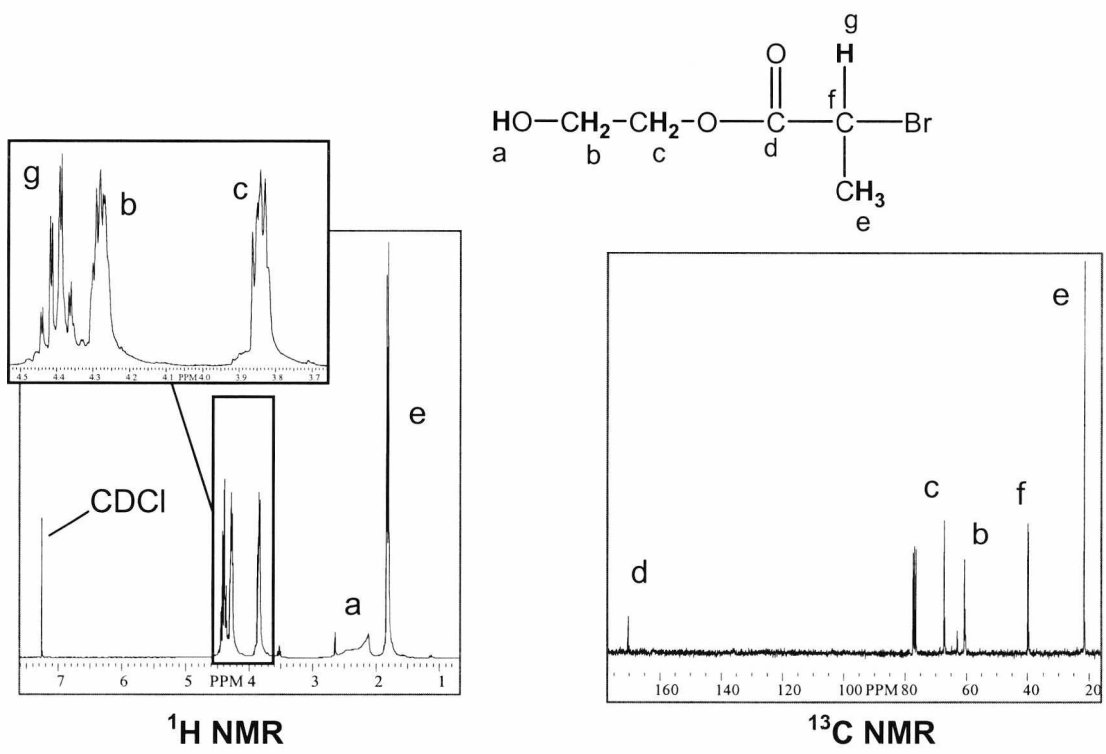


**Fig. 6.3.** $^{1}$H NMR and $^{13}$C NMR spectra of 2-hydroxyethyl-2-bromopropanoate

2-Hydroxyethyl-2-bromopropanoate (initiator **2**) was synthesised following a similar procedure used for the synthesis of initiator **1**. $^1$H NMR was used to characterise the initiator (fig. **6.3**). Although the same purification procedure was employed to purify the product, some small impurities may have remained (as revealed in the NMR spectra). However, elemental analysis showed good agreement between the theoretical and experimental abundance of C and H in the product. Since it proved difficult to obtain a pure sample of initiator **2**, initiator **1** was used to synthesise PMPS macroinitiators instead. However, in theory, initiator **2** could also be used to synthesise macroinitiators.

### 6.3.1.4. PMPS macroinitiator

DiXPMPS was endcapped with 2-hydroxethyl-2-methylbromopropanoate (initiator **1**) to form a PMPS macroinitiator (PMPS(init)$_2$). A solution of diXPMPS had been prepared immediately prior to the addition of initiator **1**, in order to ensure that the Si-X end groups remained intact. 1,8-Diazabicylo[5.4.0]undec-7ene (DBU), a sterically hindered base, used to aid the reaction and quench any HX which was formed. DBU was also was used in order to avoid reaction of the C-Br group on the initiator. That diXPMPS was endcapped with initiator **1** to form PMPS-init$_2$ was confirmed by $^1$H NMR spectroscopic analysis (fig. **6.4**). Compared to the $^1$H NMR spectrum of the initiator shown in fig. 6.2, the characteristic $CH_2$ and $CH_3$ groups remained, while the OH peak disappeared. The extent to which the ends of the PMPS chains were endcapped was difficult to demonstrate conclusively since the polymeric peaks from the PMPS tended to dwarf those peaks associated with the end groups. Nevertheless, $^1$H NMR is still the best method available whereby the presence of end groups can be shown. Using integration data together with GPC data, it is possible to show that conversion from diXPMPS to PMPS macroinitiator is close to 100 % (table **6.3**).

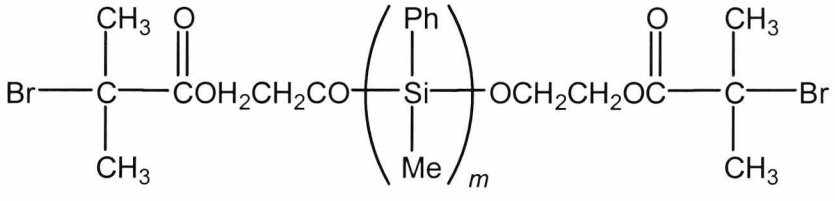


**Scheme 6.7.** PMPS(init)$_2$

An example of how the integrals were used to calculate the percentage of Si-X chain ends that had reacted is shown in table **6.3**. In this case, diXPMPS ($M_n$ = 5,700) has about 43 repeat units according to the GPC data. Theoretically, the average polymer will therefore have 220 Si-Ph protons (43 units x 5 Ph protons) and 130 Si-$CH_3$ protons (43 x 3). Therefore, if each polymer is difunctionalised with initiator **1** then the ratios of the protons can be determined. For example, the theoretical number of methyl protons on the initiator end groups is twelve. Percentage conversion is based on the ratio of theoretically derived integrals vs. the experimentally determined integrals from the proton NMR in fig. **6.4** for each of the individual environments. Some error will occur since the GPC determined molecular weight of the polymer might not be accurate (since it is calibrated using PS standards).

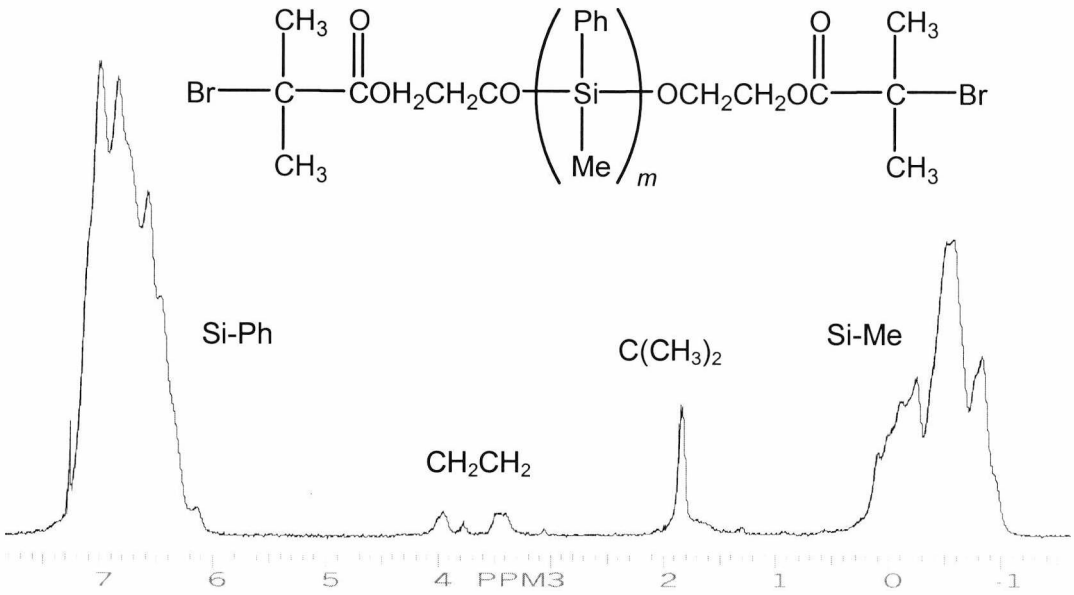


**Fig. 6.4.** $^1$H NMR of the PMPS macroinitiator ($M_n$ 5 200)

A range of block copolymers were synthesised using PMPS macroinitiators to polymerise methyl methacrylate (MMA) (table **6.4**). The PMPS block lengths were varied by changing the amount of bromine added to the untreated PMPS. If the amount of bromine added to a solution of PMPS is increased, the extent of cleavage of the polysilane backbone also increased, leading to shorter PMPS chains. This also leads to a larger number of reactive sites at the ends of the chains available for reactions with alcohols. Each macroinitiator shown in table 6.4 was analysed in the same manner, as illustrated by table 6.3. In each case, the integration data from the

$^1$H NMR spectra showed that the PMPS chains had been endcapped successfully. The percentage of endcapped chain-ends are also shown, and were derived by comparing the -$OCH_2$-$CH_2O$- and the $C(CH_3)_2$ integrals of the initiator with the Si-$CH_3$ integral of the PMPS chain.

| Proton environment | Theoretical integral[a] | Experimental integral[b] | Percentage endcapped |
|---|---|---|---|
| Si-**$CH_3$** | 130 | 130 | - |
| Si-**$C_6H_5$** | 217 | 220 | - |
| **$OCH_2CH_2O_2C(CH_3)_2Br$** | 8.0 | 7.7 | 96 % |
| $OCH_2CH_2O_2C$(**$CH_3$**)$_2Br$ | 12.0 | 12.2 | 102 % |

**Table 6.3.** Percentage of PMPS **2** ($M_n$ 5 200) chain-ends that are endcapped according to data calculated via (a) GPC molecular weight characteristics and (b) $^1$H NMR spectroscopy

| **PMPS macroinitiator** | **$M_n$** | **$M_w/M_n$** | **% endcapping*** |
|---|---|---|---|
| PMPS **1** | 3 500 | 1.70 | - |
| PMPS **2** | 5 200 | 1.74 | 99% |
| PMPS **3** | 9 100 | 1.63 | 106% |
| PMPS **4** | 9 500 | 2.13 | - |
| PMPS **5** | 9 800 | 1.65 | - |
| PMPS **6** | 10 500 | 3.30 | 110% |
| *PMPS **7** | 15 300 | 3.1 | 105% |

**Table 6.4.** PMPS macroinitiators. Percentage of endcapped chain-ends is determined by 1H NMR integrals. The value is an average taken from the different proton environments of the initiator. (* PMPS **7** was not treated with bromine).

#### 6.3.1.5. Summary

A di-functionalised ATRP initiator capable of endcapping diXPMPS to form a macroinitiator was successfully synthesised, purified, and characterised. The extent to which the PMPS chains were endcapped was determined by correlating molecular weight data (GPC) with the end group analysis from the $^{1}H$ NMR spectra. The advantage of this method compared to other PMPS macroinitiators discussed previously is that the polymer is near-monodisperse and molecular weights can be determined before endcapping.

### 6.3.2. Poly(methyl methacrylate-*block*-methylphenylsilane-*block*-methyl methacrylate (PMMA-PMPS-PMMA)

#### 6.3.2.1. Synthesis

An important aspect of any ATRP reaction is the homogeneity of the reaction mixture. By increasing the homogeneity, i.e. the solubility of the various components (monomer, initiator, metal complex), the reaction proceeds at a faster rate, while polydispersity can be kept low.[33] For most of the copolymerisations involving PMPS and MMA, the complex used was CuBr and bipyridine (bpy). Bpy was chosen because of its availability and since it is the simplest, most commonly used ligand in ATRP reactions. Although some problems with solubility may exist, preliminary copolymerisations involving the complex were shown to be quite successful. Since PMPS is not soluble in MMA, bulk polymerisations could not be carried out, and therefore a solvent was required. Because the reaction was to be carried out at a relatively high temperature (in order to increase the rate of reaction), a high boiling solvent, i.e. xylene, was used. The colour of the reaction mixture was usually a brownish colour with a green tint.

In most cases, an increase in viscosity of the reaction mixture was observed as polymerisation progressed. In only one case, involving the growth of PMMA blocks of ~200 units (COP9), did the reaction mixture become hard and glassy. Reactions were usually stopped when the molecular weights of the copolymers ceased to increase (according to GPC data). The copolymers were subsequently purified by diluting the reaction mixture in THF, allowing the solution to be passed through

alumina in order to remove the copper complex. Successive precipitations in methanol removed any remaining monomer to produce a pure white copolymer. The samples were dried at elevated temperature under vacuum in order to remove any remaining solvents from the copolymers, and were stored in the dark, away from any source of UV light.

A number of PMMA-PMPS-PMMA copolymers were synthesised by varying the length of the PMPS macroinitiator and by altering the length of the PMMA blocks. As is the case for any ATRP reaction, the degree of polymerisation is determined by the molar ratio of monomer to initiator.

### 6.3.2.2. Molecular weight analysis

A range of copolymers were synthesised and analysed using GPC (table **6.5**). In each case, the GPC data revealed a monomodal increase in molecular weight, with little or no trace of PMPS homopolymer. Yields were typically about 80% due to fractionation, and also since complete conversion was not achieved, as revealed by the $^1$H NMR spectra [see table 6.6, section 6.3.2.3]. There is also no PMMA homopolymer present due to the fact that MMA can only be initiated by the PMPS macroinitiator. Simultaneous analysis using refractive index (RI) and UV detectors (at both 254 nm and 334 nm) confirmed that the product was a block copolymer. An example of a typical GPC plot is shown in fig. **6.5**. For each copolymer, the length of the PMMA chains could be determined from the macroinitiator to monomer ratio.

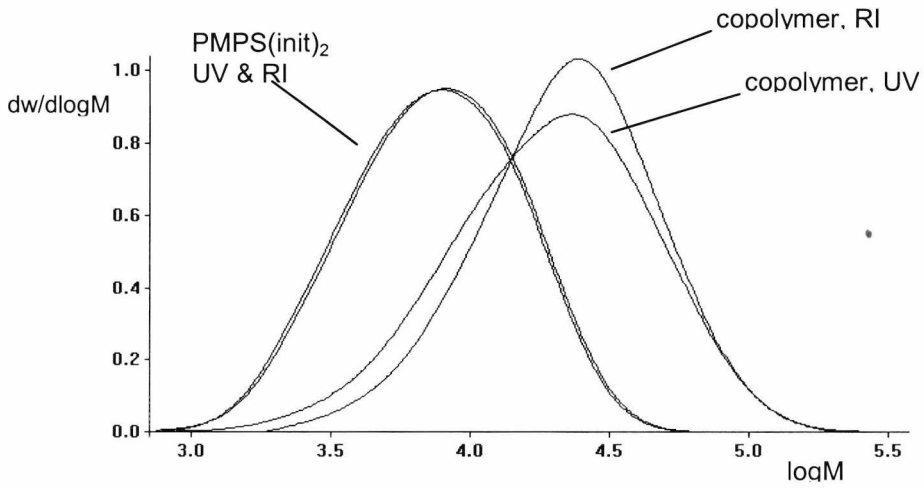


**Fig. 6.5.** Overlay of GPC plots of a PMPS2 ($M_n$ = 5,200) and PMMA-PMPS-PMMA, COP5 ($M_n$ = 24,700), using RI and UV ($\lambda$ 334 nm) detectors.

Using the molecular weight characteristics of the copolymer from the GPC data, it was possible to calculate the lengths and the polydispersities of the individual PMMA blocks. Since PMMA synthesised via ATRP usually has a polydispersity of between 1.1 and 1.3,[34] the copolymer should become less polydisperse. The values given are calculated by assuming all PMPS macroiniators have initiating groups both at ends of the polymer, and that both PMMA blocks on a tri-block are of the same length. In general, the polydispersities for the MMA blocks are higher than expected. This could be due to the fact that some of the PMPS chains have not been successfully endcapped with initiators. This means that some AB block copolymers may be formed and PMPS homopolymer may remain.

The GPC was calibrated using both polystyrene (PS) and PMMA standards. Values quoted here are derived from a polystyrene calibration curve, although some polymers were characterised via GPC according to PMMA standards, which usually resulted in molecular weight values being approximately 10% higher. This is due to the intrinsic viscosity ($\eta$) of PMMA being lower compared to that of PS.[35] If a PMMA and a PS sample have the same molecular weight, [M], the hydrodynamic volume of PMMA will be smaller (equation **6.1**). Therefore, PMMA polymer samples will appear to be lower in terms of molecular weight when analysed using a PS calibration curve.

$$\text{Hydrodynamic volume} = [\eta]\,[M] \qquad \textbf{(6.1)}$$

The polydispersities of most of the copolymers synthesised here were less than the only other example of a PMMA-PMPS-PMMA block copolymer synthesised previously showed bimodal molecular weight distributions ($M_w/M_n \sim 8$).[36] In the present work, poydispersities were relatively low (<2) and control over the copolymer composition could be achieved accurately by adjusting the macroinitiator : monomer ratio. However, since monodisperse ($M_w/M_n \sim 1.1$) PMMA homopolymers have been synthesised using ATRP, the PMMA segments synthesised here seem to be relatively high. By using different complexes, the molecular weight characteristics of the PMMA segments might also be altered.

| Copolymer (COP) | Initiator | PMMA-PMPS-PMMA | | | PMMA block | | | % yield[a] |
|---|---|---|---|---|---|---|---|---|
| | | $M_n$ Calc.* | $M_n$ GPC | $M_w/M_n$ GPC | $M_w/M_n$ GPC | DP Calc.* | DP GPC | |
| **1** | PMPS1 | 10 500 | 11 000 | 1.60 | 1.55 | 35 | 37.5 | - |
| **2** | PMPS2 | 9 200 | 10 000 | 1.85 | 1.96 | 20 | 24 | 78 |
| **3** | PMPS2 | 11 200 | 10 300 | 1.74 | 1.74 | 30 | 25.5 | - |
| **4** | PMPS2 | 13 200 | 14 500 | 1.80 | 1.83 | 40 | 46.5 | 70 |
| **5** | PMPS2 | 25 200 | 24 700 | 1.67 | 1.65 | 100 | 97.5 | - |
| **6** | PMPS3 | 17 100 | 19 500 | 1.64 | 1.65 | 40 | 52 | 70 |
| **7** | PMPS4 | 13 500 | 14 200 | 1.85 | 1.29 | 20 | 13.5 | 70 |
| **8** | PMPS4 | 29 500 | 29 000 | 2.05 | 2.01 | 100 | 97.5 | 86 |
| **9** | PMPS5 | 49 800 | 47 200 | 1.97 | 2.06 | 200 | 187 | 75 |
| **10** | PMPS6 | 20 500 | 21 600 | 2.70 | 2.13 | 50 | 55.5 | 80 |

**Table 6.5.** Molecular weight characteristics (GPC) of copolymers. (*calc. using monomer : macroinitiator ratios, i.e. 2xDP = [MMA]/[PMPS]) ([a]yields determined gravimetrically.)

### 6.3.2.3. NMR analysis

$^1$H NMR and $^{13}$C NMR were used to characterise the copolymers and confirm their structures. An example is shown in fig. **6.6**. $^1$H NMR was also used to determine the relative abundance of each block involved in the block copolymers. By correlating the GPC data with the integrals of the Si-Me and Si-Ph $^1$H NMR peaks, the lengths of the PMMA chains could be estimated. Comparisons between the lengths of the PMMA chains estimated using GPC data and NMR data are shown in table **6.6**.

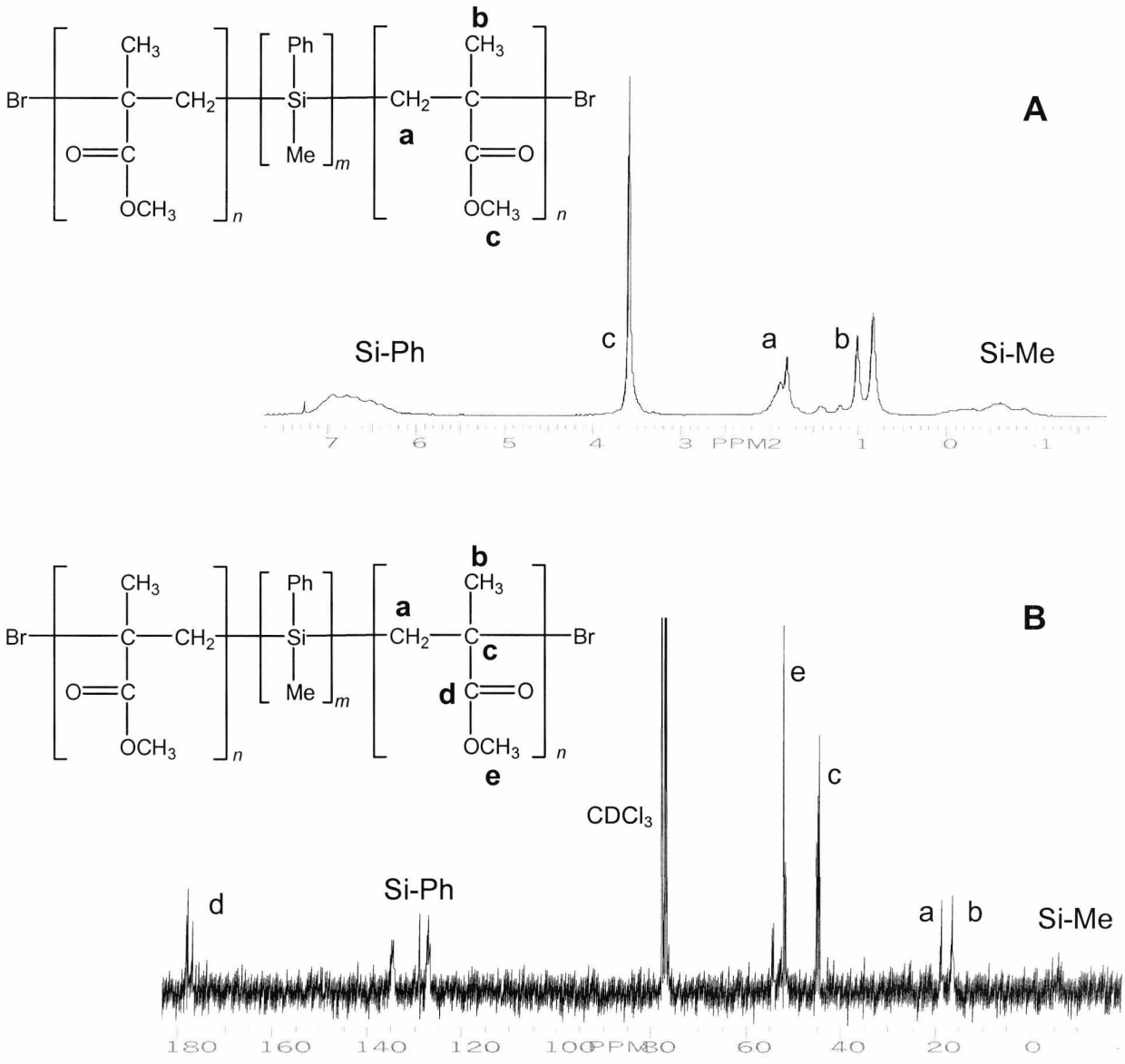


**Fig. 6.6.** $^{1}H$ (**A**) and $^{13}C$ (**B**) NMR of PMMA-PMPS-PMMA **1**

The block lengths determined by NMR are consistently shorter than the values determined by GPC. This may be due to the fact that the GPC is calibrated against polystyrene standards, and that PMMA-PMPS-PMMA block copolymers behave differently in solution.

Percentage conversions were also determined by comparison of the integrals of vinyl peaks with PMMA peaks at the ends of the reactions. In order to obtain percentage conversion, the copolymers were passed through alumina with $CDCl_3$ and were not

precipitated in methanol. This ensured the remaining monomer was not removed. Percentage conversions for most copolymerisations were around 80%.

| Copolymer (COP) | $M_n$ PMMA block Theory | $M_n$ PMMA block GPC | $M_n$ PMMA block NMR* | DP PMMA block GPC | DP PMMA block NMR* | P'age conv.$^+$ |
|---|---|---|---|---|---|---|
| **1** | 3 500 | 3 750 | 3 400 | 37.5 | 34 | 85% |
| **3** | 3 000 | 2 550 | 2 300 | 25.5 | 23 | 81% |
| **4** | 4 000 | 4 650 | 4 000 | 46.5 | 40 | - |
| **5** | 10 000 | 9 750 | 8 600 | 97.5 | 86 | 87% |
| **9** | 20 000 | 18 700 | 17 700 | 187 | 177 | - |

**Table 6.6.** Comparison of GPC and $^1$H NMR spectroscopy data for various copolymers. (*calculated from integrals of PMMA peaks compared to integral of Si-$CH_3$ (PMPS) peak) ($^+$conversion calculated by comparison of PMMA peaks (C-$CH_3$)with vinyl MMA ($CH_2$=C) peaks)

### 6.3.2.4. Kinetic Analysis

#### 6.3.2.4.1. Comparison of $^1$H NMR peaks

Aliquots of the reaction mixture were taken at timed intervals and were analysed using GPC and $^1$H NMR. Samples were passed through alumina using $CDCl_3$ as the eluent in order to remove the catalyst and halt the reaction. The reaction solvent was not removed since it was thought the concentration of MMA may decrease. However, the characteristic vinyl peaks were still evident at 5.64 and 6.21 ppm, while the $CH_3$ peak characteristic of polymeric PMMA was observed at 0.9 to 1.2 ppm. The progress of these reactions was followed by comparing the integrals of monomeric MMA peaks with the integrals of the polymeric PMMA. The intensity of the monomeric

peak decreases as monomer is used up while the polymeric methyl peak increases as the reaction progresses. Fig. **6.7** shows how the reactions were followed for two copolymerisations, i.e. for COP 3 and COP 5 (table 6.4).

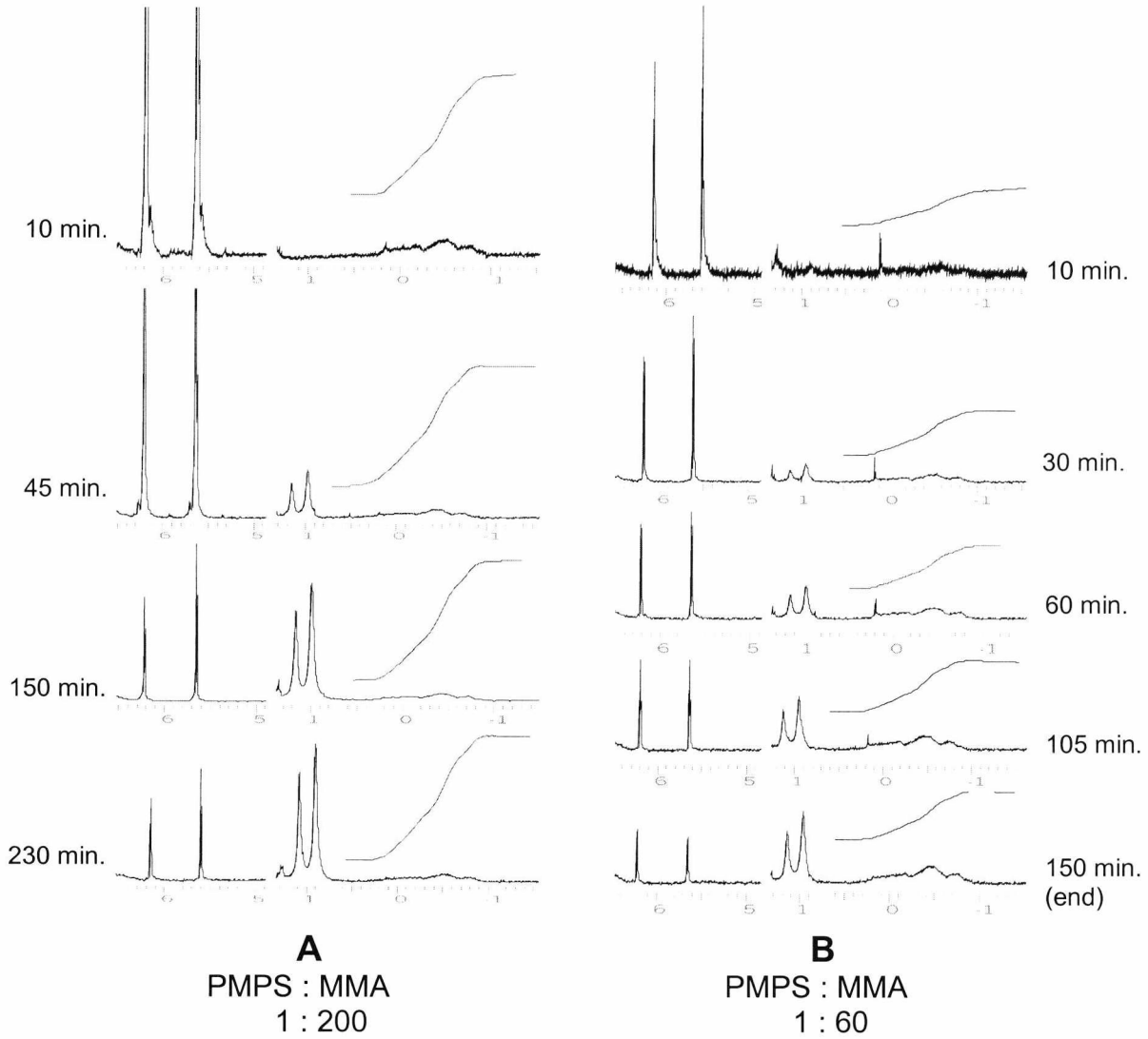


**Fig. 6.7.** $^{1}$H NMR spectra as two polymerisation reactions occur to form (**A**) COP 5 and (**B**) COP 3. The times at which the samples were removed from the reaction mixture are shown. In each case, the intensity of the Si-$CH_3$ (δ: -1.0 – 0.2 ppm) peak is used as a reference.

### 6.3.2.4.2. Kinetic Plots

The percentage conversion is calculated using equation 6.2. At the start of the reaction (0 min.) the relative fractional concentration of polymer, [PMMA], is equal to zero, while the initial relative monomer concentration, $[M]_0$, is equal to unity. In

each of the $^1$H NMR spectra, the integrals of the vinyl peaks were set to 0.5 (total = 1.0). Therefore [M] in each NMR spectrum was equal to unity (equation 6.3). Theoretically, at 0 % conversion, $[M]_t = 1$, while at 100 % conversion, $[M]_t = 0$. Since [M] always equals unity, the percentage conversion (fig. **6.8**) can be calculated from equation 6.4.

$$\% \text{ conversion} = \ln[M]_0/[M]_t \quad \text{where } [M]_t = [M]/([M]+[PMMA]) \tag{6.2}$$

$$[M]_t = 1/(1 + [PMMA]) \tag{6.3}$$

$$\% \text{ conv.} = (1 - [M]_t) \times 100\% \tag{6.4}$$

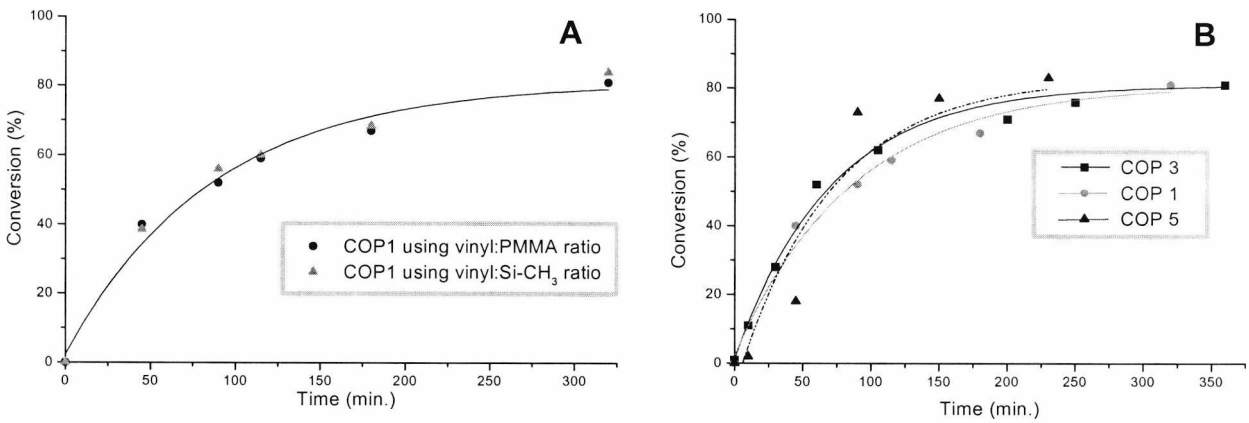


**Fig. 6.8.** Percentage conversion plots for (**A**) COP 1 according to $^1$H NMR data of ratios between the integrals of vinyl peaks vs. PMMA (C-$CH_3$) and PMPS (Si-$CH_3$) peaks, and (**B**) copolymers **1**, **3**, and **5** (determined from vinyl:PMMA peak ratios)

Another method involves the use of a standard (usually a small amount of high boiling solvent) that can act as a reference peak in $^1$H NMR. Although a standard was not used, since the amount of PMPS remains constant throughout the reaction, the Si-$CH_3$ peak was used as a reference. The intensities of the monomeric MMA $CH_2$ peaks were compared to the intensity of the Si-$CH_3$ peak and the percentage conversion was determined using equation 6.5. Admittedly, this method is not as accurate, although good agreement is observed for COP 1 in fig. 6.8.A.

$$\%\text{conv.} = \{1-([M]_t/[M]_0)\} \times 100 \tag{6.5}$$

The corresponding plots of $\ln[M]_0/[M]$ vs. time for copolymers 1, 3, and 5 revealed that the polymerisation of MMA was first order with respect to monomer concentration (fig. **6.9**). In ATRP, the rates of polymerisation decrease as the solubility of the complexes increase. Hence, the change in rate is most probably due to a slight loss of control early on in the reaction. For ATRP reactions in general, the rate of polymerisation is 1st order with respect to the monomer concentration [M] the initiator (R-X), and the transition metal complex.[37] Hence a straight line is expected for plots of $\ln[M]_0/[M]$. For copolymers 1 and 3, a rate change is seen after approximately 50 minutes.

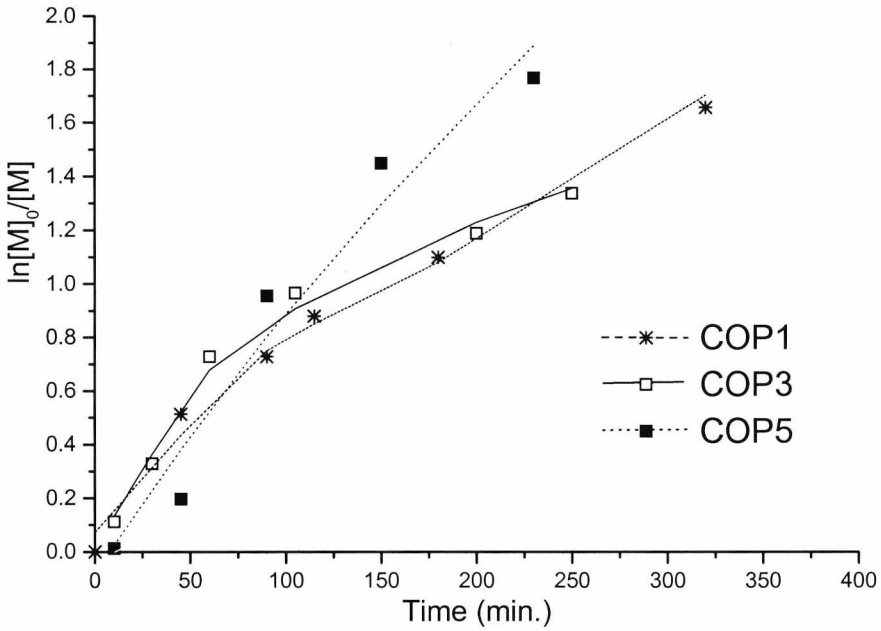


**Fig. 6.9.** Kinetic plots of copolymers **1**, **3**, **5**, and **11**

### 6.3.2.4.3. GPC Analysis

The changes in the molecular weight characteristics were also followed using GPC (fig. **6.9**). From the overlays, it is possible to see that the monomodal nature of the block copolymer is maintained throughout the reaction. In the example shown, no further growth occurred after 150 min., while polydispersity has not changed significantly. A decrease in polydispersity would be expected, as the PMMA segments are grown off the ends of the PMPS macroinitiator. However, as Fig. 6.9

illustrates, a tailing off on the lower molecular weight end of the distribution can be seen. The tail is due to the presence of PMPS homopolymer or AB block copolymer, due to the possibility that not all PMPS chain ends were successfully endcapped.

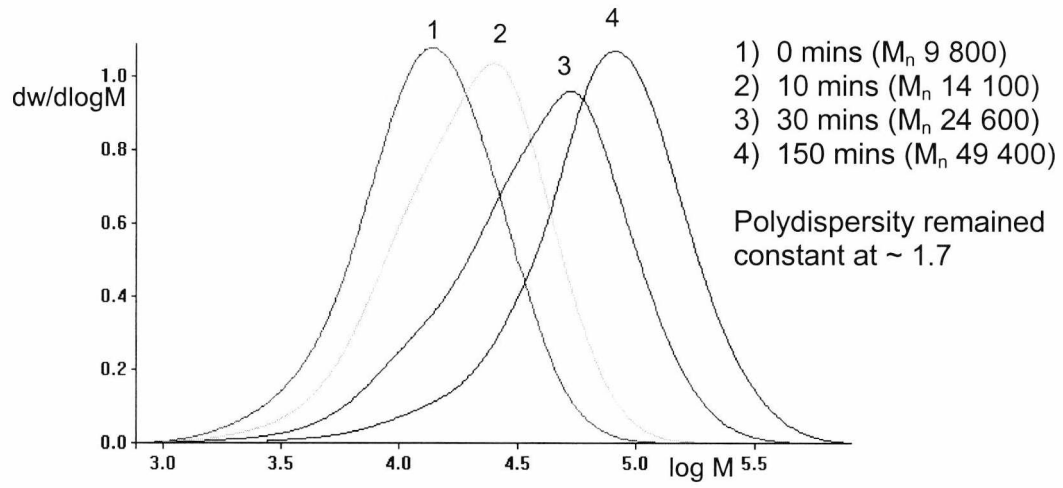


**Fig. 6.10.** Overlay of dw/dlogM vs. log M plots at timed intervals for COP9

### 6.3.2.5. Thermal analysis - differential scanning calorimetry (DSC)

Thermal analysis of selected polymer samples was performed using differential scanning calorimetry (DSC). The glass transition temperatures, $T_g$, were measured for a range of block copolymers (Table **6.6**). The PMPS block length was kept constant, while the molecular weights of the PMMA chains were altered. As with most lower molecular weight polymers, the $T_g$ of PMMA increases as molecular weight increases. The thermal data for homopolymers of PMPS and PMMA were measured in order to ascertain whether or not the PMPS and PMMA blocks would behave similarly in the copolymer environment compared to that of the homopolymer. The PMMA homopolymers were chosen because of the proximity of molecular weights compared to those of the blocks that exist in the copolymers. The PMPS sample is shown as a comparison.

| (Co)polymer [composition] | PMMA block | | | | PMPS block$^{+}$ | | | |
|---|---|---|---|---|---|---|---|---|
| | Heat | | Cool | | Heat | | Cool | |
| | $T_g$ | J/g | $T_g$ | J/g | $T_g$ | J/g | $T_g$ | J/g |
| **2** [PMPS $(MMA_{20})_2$] | 83 | 0.12 | 76 | 0.050 | 127 | - | 125 | - |
| **4** [PMPS$(MMA_{40})_2$] | 98 | 0.33 | 99 | 0.037 | 130 | 0.12 | 124 | - |
| **5** PMPS$(MMA_{100})_2$] | 100 | 0.52 | 103 | 0.30 | 132 | 0.40 | 135 | - |
| **PMPS 5** ($M_n$ 9 500) | | | | | 126 | - | 122 | - |
| **PMMA** ($M_n$ 10 300) | 103 | - | 100 | - | | | | |
| **PMMA** ($M_n$ 3 800) | 81 | - | 73 | - | | | | |
| **PMMA** ($M_n$ 2 400) | 70 | - | 66 | - | | | | |

**Table 6.6.** Glass transition temperatures, $T_g$, for a range of block copolymers and homopolymers. *Compositions measured using GPC and NMR (table 6.1). $^{+}$Certain enthalpy measurements were too small to determine

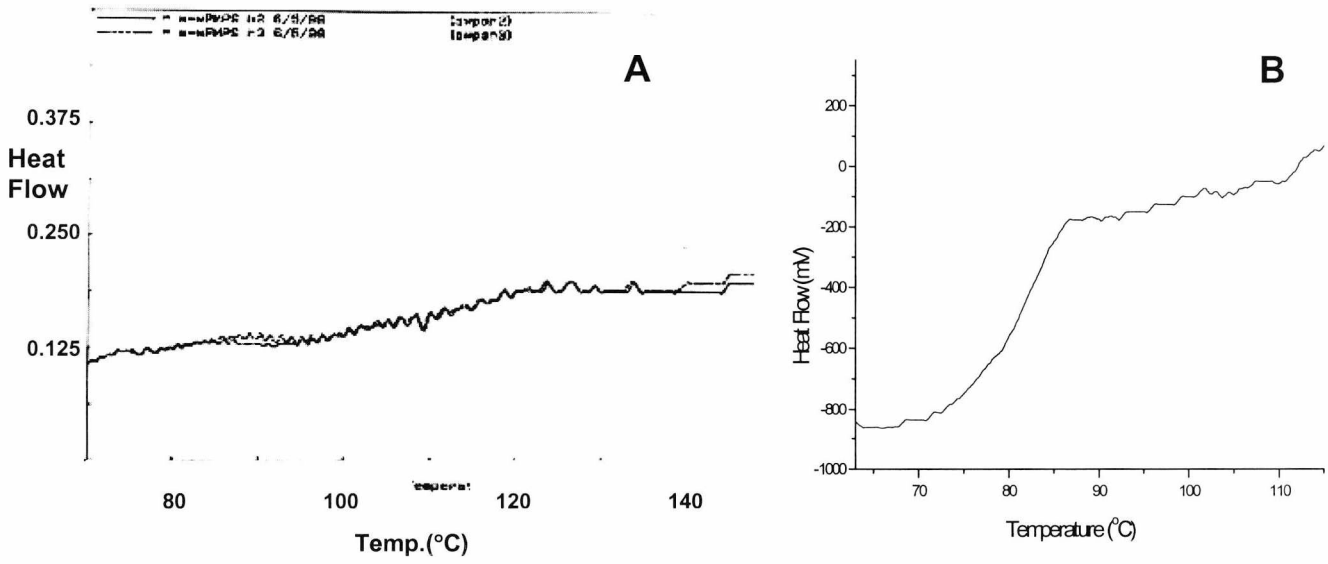


**Fig. 6.11.** (**A**) DSC plot of PMPS ($M_n$ ~ 4 000, $T_g$ 110°C). Two separate heat runs are shown. (**B**) PMMA ($M_n$ 3 800) as sample is heated.

An example of the DSC plot for a PMMA sample ($M_n$ = 3,800) and diXPMPS ($M_n$ ~ 4 000) is shown in fig. **6.13**. Ziegler and co-workers first reported the $T_g$ of PMPS to be 122°C.[38] It has since been shown that PMPS generally has two thermal transitions, the first of which has a midpoint occurring between 90°C and 120°C depending on molecular weight. The second transition temperature midpoint occurs between 185°C and 225°C.[39] Since PMPS is generally regarded as being an amorphous solid, no melting point, $T_m$, is seen.[40] For crystalline materials, the $T_m$ is the temperature at or above which a substance exhibits translational movement or flow. The $T_g$ for an amorphous material occurs over a temperature range, even though it is often reported as a single value. Differences in $T_g$ values can occur due to a number of reasons, including the method by which a polymer is synthesised, the thermal history of the polymer, and the molecular weight characteristics.

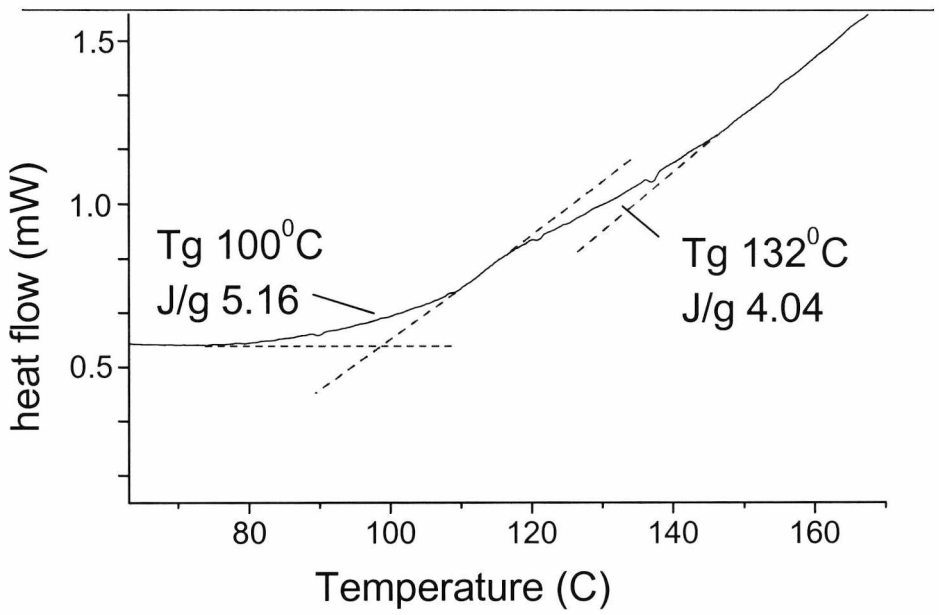


**Fig. 6.13.** DSC plot as COP8 ($M_n$ 29 000) is heated (central PMPS block has an $M_n$ ~ 9 500).

For each block copolymer, two $T_g$'s can be seen, suggesting that some molecular ordering and phase separation occurs. An example of a typical DSC plot is shown in fig. **6.13**. It is important to note that, since the $T_g$ of PMPS is not as intense as the $T_g$ of PMMA, it was often difficult to detect. Therefore some values were difficult to determine and a degree of error may exist because of this. The $T_g$ is represented by a change in slope as the temperature increases. The midpoint between the change is

taken as the $T_g$ value. An overlay of three DSC plots, which show the transitions as the samples are heated, is shown in fig. **6.14**. It is observed that, while the change that occurs due to the PMPS glass transition remains constant, the $T_g$ of the PMMA blocks increases as the block length increases.

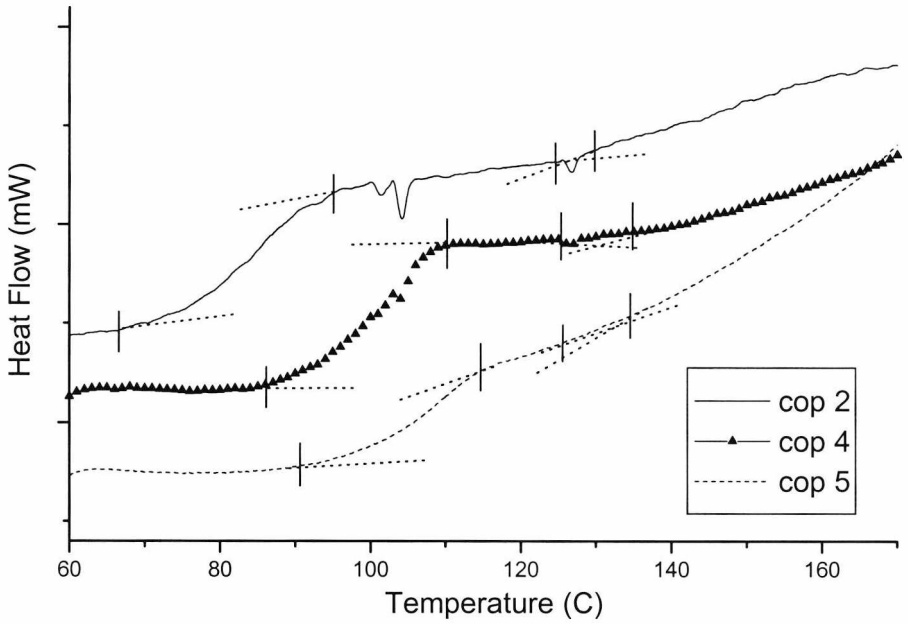


**Fig. 6.14.** DSC plots of copolymers 2, 4, and 5 as samples are heated. $T_g$ for PMMA blocks increases with number of MMA units (24, 47, and 98 units respectively).

### 6.3.2.6. Conclusions and future work

A well-defined PMPS macroinitiator was synthesised and characterised successfully. A range of macroinitiators, varying in molecular weight, were synthesised and used to initiate the ATRP of MMA to form different PMMA-PMPS-PMMA block copolymers. It was possible to grow the PMMA blocks to a predetermined length with a high degree of accuracy by altering the relative concentrations of macroinitiator and monomer. Previously, PMPS block copolymers containing PMMA segments had been synthesised without much control over molecular weight. The resulting block copolymers also had high polydispersities ($M_w/M_n \sim 8$). Control over the lengths of the individual blocks has been achieved and the living nature of the polymerisation has been characterised. Kinetic analysis of the reactions involved

revealed that the rate of polymerisation was first order with respect to monomer concentration, as is expected for a controlled ATRP reaction. However, a number of reactions seemed to involve an initial period of approximately 45-60 minutes during which the rate of polymerisation was faster, indicating that some uncontrolled growth was occurring. Thermal analysis revealed two $T_g$ values, indicative of phase separation occurring in block copolymers.

Although characterised using NMR spectroscopy, the most effective way to show that the PMPS has been endcapped is to carry out block copolymerisation. If only some of the chain ends have been endcapped, this could result in the presence of polysilane homopolymer and AB block copolymers. This would result in the broadening of the corresponding GPC plot and perhaps even a polymodal distribution.

Future research might involve the synthesis of PMPS macroinitiators containing different initiating groups at the chain ends, such as benzylic halides. A different macroinitiator, as well as the alteration of reaction conditions (temperature, catalyst complex, medium, etc.) may yield less polydisperse PMMA segments.

### 6.3.3. Poly((*S*)-(-)-2-methyl-1-butyl methacrylate)-*block*-methylphenylsilane-*block*-(*S*)-(-)-2-methyl-1-butyl methacrylate) (PMBMA-PMPS-PMBMA)

#### 6.3.3.1. (*S*)-(-)-2-methyl-1-butyl methacrylate

(*S*)-(-)-2-methyl-1-butyl methacrylate (MBMA) was synthesised in order to form a monomer containing a chiral side group. MBMA was synthesised via a condensation reaction involving methacryloyl chloride and (*S*)-(-)-2-methyl-1-butanol. The temperature was kept low (below 4°C) because the reaction was quite exothermic. Triethylamine was used in order to aid the reaction. The structure and purity of the monomer was determined using $^{1}H$ NMR (fig. **6.14**) and $^{13}C$ NMR (fig. **6.15**).

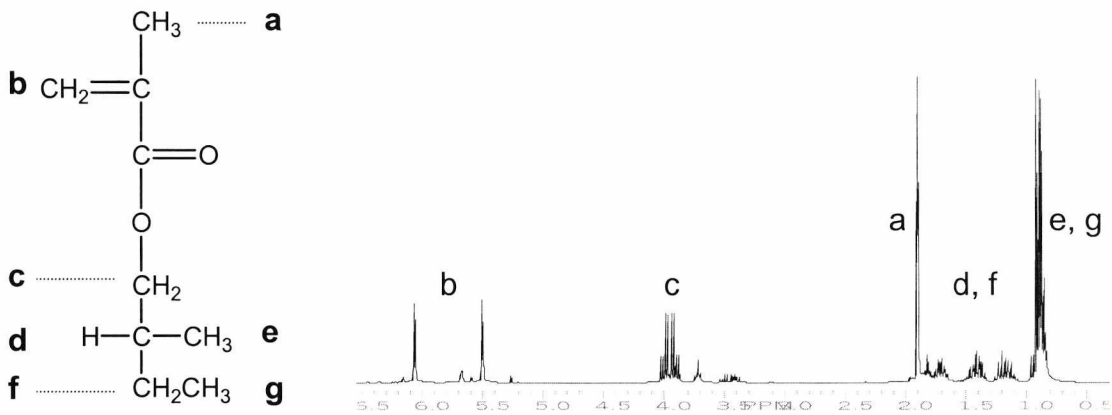


**Fig. 6.14.** $^{1}H$ NMR of (*S*)-(-)-2-methyl-1-butyl methacrylate (MBMA)

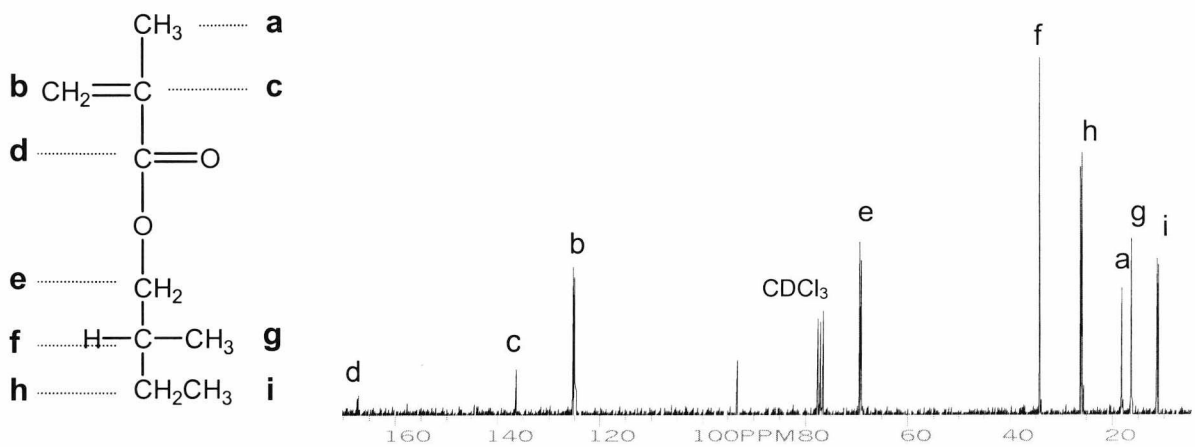


**Fig. 6.15.** $^{13}C$ NMR of (*S*)-(-)-2-methyl-1-butyl methacrylate (MBMA)

### 6.3.3.2. Synthesis

Previous research has revealed how chiral substituents have induced chirality into polymer backbones.[41] Part of the research undertaken by our group has shown how the chirality of helices of polysilane chains can be influenced by the choice of solvent.[42,43] Here, the synthesis of a PMPS block copolymer containing methacrylic segments with chiral side groups is described.

The polymerisation of MBMA using a PMPS macroinitiator was very similar to the procedure described for the synthesis of PMMA-PMPS-PMMA [section 6.3.2.1]. A number of different complexes were used in the ATRP reaction in order to ascertain which combinations of CuX and ligand would lead to more successful reactions (i.e. higher yields, more controlled reactions). On each occasion, after a few minutes, the reaction became a strong aqua-green colour.

### 6.3.3.3. Molecular weight analysis

Molecular weight analysis revealed a characteristic shift in molecular weight (fig. **6.16**). Simultaneous analysis using RI and UV (λ 334 nm) detectors were used. The UV detector was set at a wavelength of 334 nm in order to show that the copolymer contained a polysilane segment.

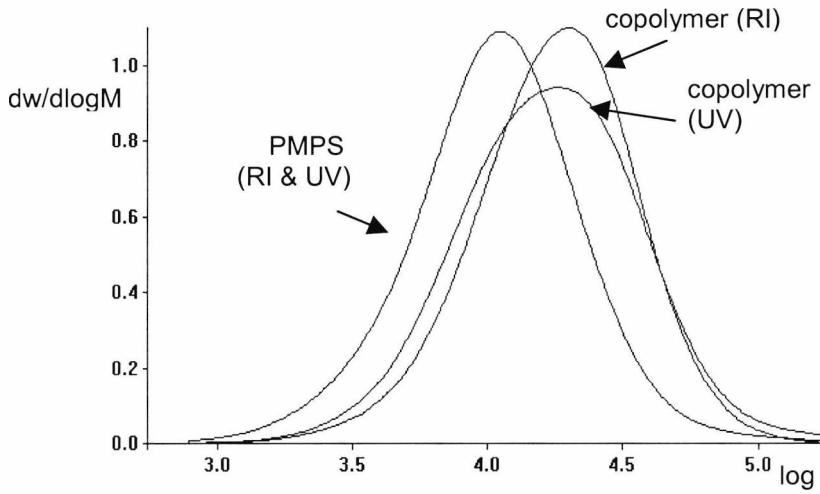


**Fig. 6.16.** GPC overlay of PMPS ($M_n$ 5 700, $M_w/M_n$ 1.76) and COP 12 ($M_n$ 14 100, $M_w/M_n$ 1.72). Analysis carried out using both RI and UV (λ 334 nm) detectors.

The molecular weight characteristics of the copolymerisation reactions that were carried out are shown in table **6.7**. The conditions for a number of reactions were varied, including the macroinitiator:monomer ratios, as well as the type of ligand used. For the copolymers shown in table 6.7, COP 12 and COP 14 were synthesisied using a CuBr/N-(n-propyl)-2-pyridyl(methanimine) (CuBr/PPMA), while COP 13 was synthesised using a CuBr/bipyridine (CuBr/bpy) complex. COP 15 was polymerised using CuCl/bpy as the complex.

After 3 hours, GPC analysis of COP 13 showed some increase in molecular weight of the polymer ($M_n$ 12 000, $M_w/M_n$ 1.9). After 24 hours GPC analysis revealed an increase in molecular weight ($M_n$ 14 600, $M_w/M_n$ 1.7). After several days, no further increase in molecular weight was observed. $^1$H NMR was used to characterise the copolymers as well as to estimate the lengths of the PMBMA chains.

| | **PMPS(init)$_2$** | | **DP$_n$*** | **PMBMA-PMPS-PMBMA** | | | **% yield** |
|---|---|---|---|---|---|---|---|
| | $M_n$ | $M_w/M_n$ | | $M_n$ | $M_w/M_n$ | DP$_n$$^+$ | |
| Cop **12** | 5 700 | 1.76 | 30 | 14 100 | 1.72 | 27 | 79 |
| Cop **13** | 5 700 | 1.76 | 50 | 14 600 | 1.70 | 29 | - |
| Cop **14** | 5 700 | 1.76 | 100 | 22 500 | 2.58 | 54 | 65 |
| Cop **15** | 8 400 | 1.95 | 50 | 12 400 | 1.65 | 13 | <50 |

**Table 6.7.** GPC data for PMBMA-PMPS-PMBMA copolymers. (*theoretical degree of polymerisation (DP$_n$), $^+$ DP$_n$ determined from GPC data per PMBMA block)

### 6.3.3.4. NMR analysis

The structure and relative block lengths were determined using $^1$H (fig. **6.17**) and $^{13}$C NMR (fig. **6.18**) and were compared with the data obtained via GPC (table **6.8**). Data is based on the assumption that both PMBMA chains in an ABA block copolymer are

the same length. Conversion was not measured, as the polymers were precipitated to remove unreacted monomer prior to $^1$H NMR measurements.

| Copolymer | GPC data | | | $^1$H NMR data | |
|---|---|---|---|---|---|
| | $M_n$ | $M_w/M_n$ | $DP_n$ | $M_n$ | $DP_n$ |
| **12** | 4 200 | 1.68 | 27 | 5 150 | 33 |
| **13** | 4 450 | 1.66 | 29 | 5 300 | 34 |
| **14** | 8 400 | 2.86 | 54 | 12 300 | 79 |
| **15** | 2 050 | 1.03 | 13 | - | - |

**Table 6.8.** Comparison of PMBMA block lengths determined by GPC and $^1$H NMR data.

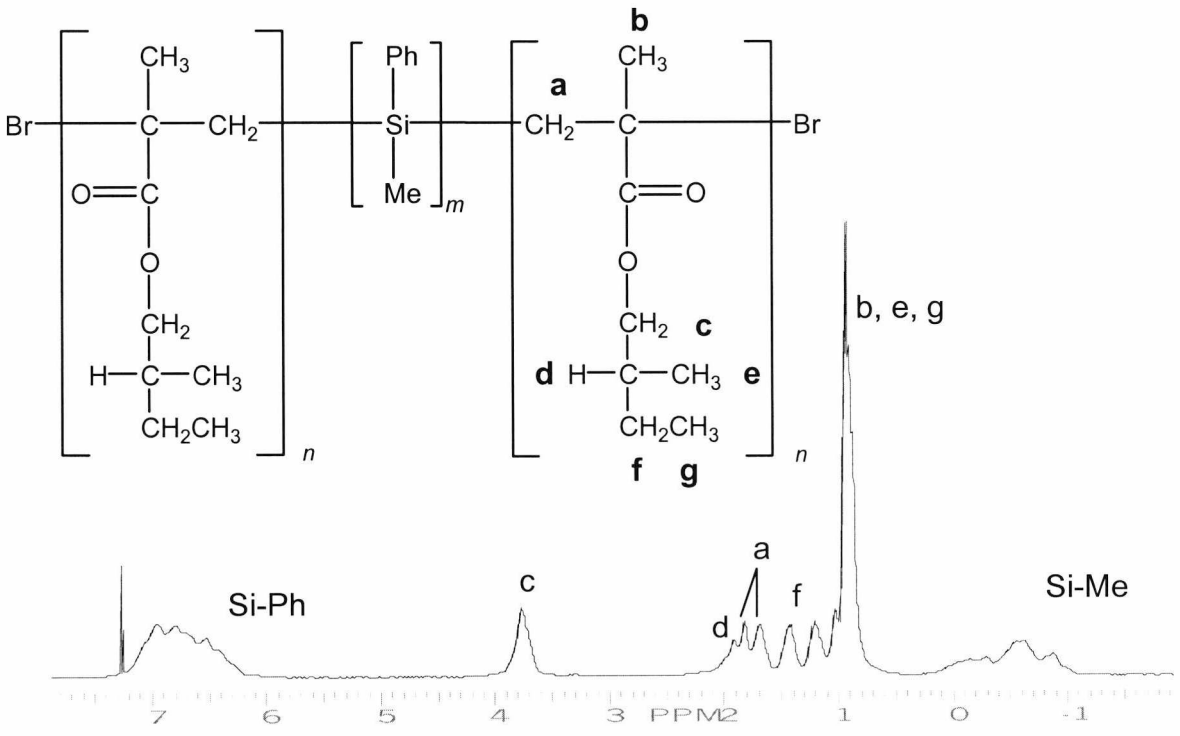


**Fig. 6.17.** $^1$H NMR of PBMA-PMPS-PMBMA (COP 14)

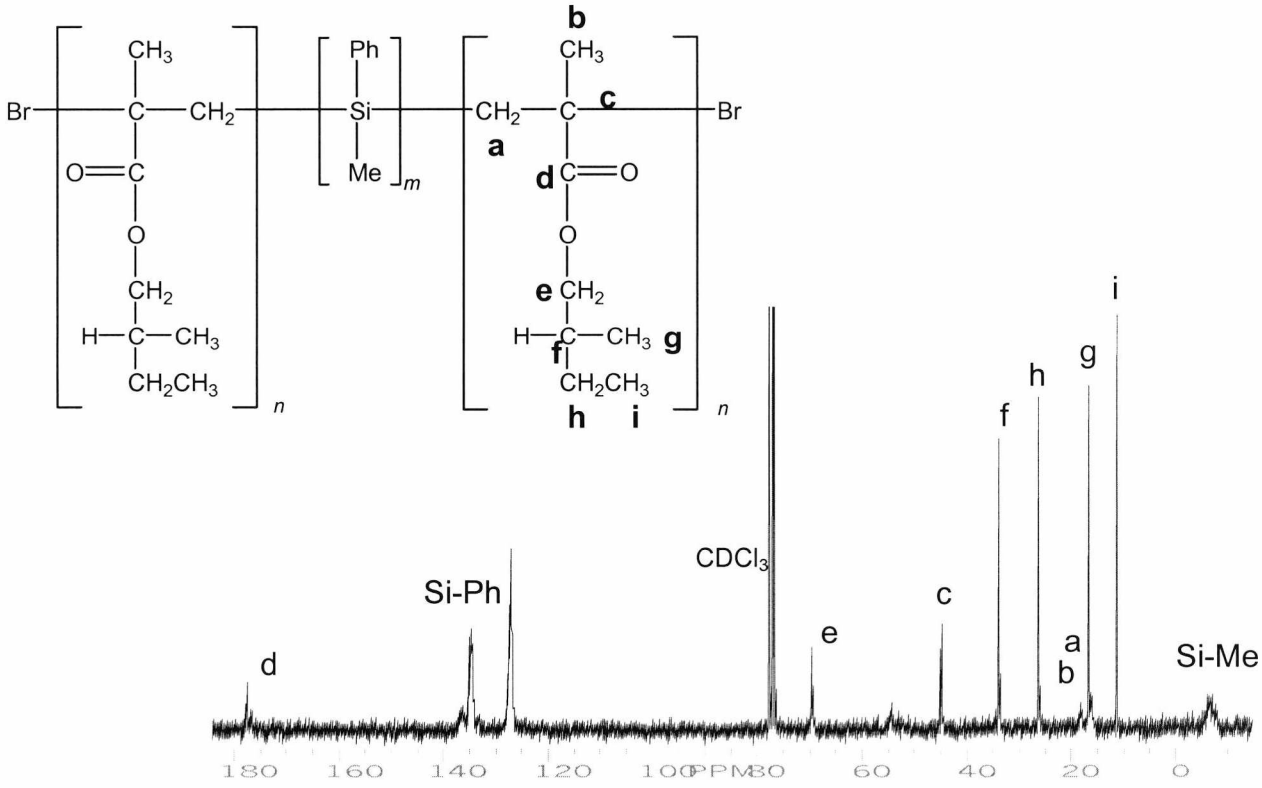


**Fig. 6.18.** $^{13}C$ NMR of PMBMA-PMPS-PMBMA (COP 14)

The degree of polymerisation determined using $^{1}H$ NMR was higher than the GPC data had suggested. This may be due to the fact that the PMBMA chains are not strictly linear and have quite long side chains. Hence, their behaviour in THF will differ compared to that of PS, which was used to calibrate the GPC.

### 6.3.3.5. Conclusions and future work

A monomer with a chiral side group was successfully synthesised and characterised via NMR. Following such a procedure, it should be possible to synthesise other monomers with functional groups for copolymerisation reactions with PMPS. A number of PMBMA-PMPS-PMBMA block copolymers were successfully synthesised and characterised. Further analysis of the copolymers in solution may show how a chiral side-group on the methacrylate segment may induce chirality into the backbone of the polysilane segment.

## 6. References


[1] Georges, M.K.; Veregin, R.P.N.; Kazmaier, P.M.; Hamer, G.K. *Trends Polym. Sci.* **1994**, 2, 66.

[2] Matyjaszewski, K.; Xia, J. *Chem. Rev.* **2001**, 101, 2921.

[3] Coessens, V.; Pintauer, T.; Matyjaszewski, K. *Prog. Polym. Sci.* **2001**, 26, 337.

[4] a) Wang, J.S.; Matyjaszewski, K. *J. Am. Chem. Soc.* **1995**, 117, 5614.

b) Kotani, Y.; Kato, M.; Kamigaito, M.; Sawamoto, M. *Macromolecules* **1996**, 29,6979.

c) Granel, C.; Dubois, P.; Jerome, R.; Teyssie, P. *Macromolecules* **1996**, 29, 8576.

d) Shipp, D.A.; Wang, J.-L.; Matyjaszewski, K. *Macromolecules* **1998**, 31, 8005.

[5] a) Matyjaszewski, K.; Ziegler, M.J.; Arehart, S.V.; Greszta, D.; Pakula, T. *J. Phys. Org. Chem.* **2000**, 13, 775.

b) Greszta, D.; Matyjaszewski, K. *Polym. Prepr. (Am.Chem. Soc., Div. Polym. Chem.)* **1996**, 37, 569.

c) Wang, J.-S.; Greszta, D.; Matyjaszewski, K. *Polym. Mater. Sci. Eng.* **1995**, 72,416.

[6] Coessens, V.; Pintauer, T.; Matyjaszewski, K. *Prog. Polym. Sci.* **2001**, 26, 337.

[7] Lutsen, L.; Cordina,G.P.-G.; Jones, R.G.; Schue, F. *Eur. Polym J.* **1998**, 34, 1829.

[8] Haddleton, D.M.; Waterson, C.; Derrick, P.J.; Jasieczek, C.B.; Shooter A.J. *Chem. Commun.* **1997**, 683.

[9] Hendrick, J.L.; Trollsas, M.; Hawker, C.J.; Anthoff, B.; Claesson, H.; Heise, A.; Miller, R.D.; Mecerreyes, D.; Jerome, R.; Dubois, Ph. *Macromolecules* **1998**, 31, 8691.

[10] Tunca, U.; Karliga, B.; Ertekin, S.; Ugur, A.L.; Sirkecioglu, O.; Hizal, G. *Polymer* **2001**, 42, 8489.

[11] a) Grimaud, T.; Matyjaszewski, K. *Macromolecules* **1997**, 30, 2216.

b) Haddleton, D.M.; Jasieczek, C.B.; Hannon, M.J.; Shooter, A.J. *Macromolecules* **1997**, 30, 2190.

c) Gaynor, S.; Balchardani, P.; Kulfan, A.; Podwika, M.; Matyjaszewski, K. *Polym. Prepr. (Am. Chem. Soc., Div. Polym. Chem.)* **1997**, 38, 496.

d) Grubbs, R.B.; Hawker, C.J.; Dao, J.; Frechet, M.J. *Angew. Chem. Int. Ed. Engl.* **1997**, 36, 270.

[12] Wang, ; Matyjaszewski, K. *J. Am. Chem. Soc.* **1995**, 117, 5614.

[13] Wang *Polym. Mater. Sci. Eng.* **1995**, 73, 416.

[14] Shipp, D.A.; Wang, J.-L.; Matyjaszewski, K. *Macromolecules* **1998**, 31, 8005.

[15] Tong, J.D.; Moineau, G.; Leclere, P.; Bredas, J.L.; Lazzaroni, R.; Herome, R. *Macromolecules* **2000**, 33, 470.

[16] Haddleton, D.M.; Waterson, C.; Derrick, P.J. *Chem. Commun.* **1997**, 683.

[17] a) Coca, S.; Matyjaszewski, K. Macromolecules **1997**, 30, 2808.

b) Coca, S.; Matyjaszewski, K. *J. Polym. Sci., Polym. Chem. Ed.* **1997**, 35, 3595.

c) Higashimura, T.; Ishihama, Y.; Sawamoto, M. *Macromolecules* **1993**, 26, 744.

[18] Gaynor, S.G.; Matyjaszewski, K. *Macromolecules* **1997**, 30, 4241.

[19] a) Brown, D.A.; Price, G.J. *Polymer* **2001**, 42, 4767.

b) Nakagawa, Y.; Miller, P.J.; Matyjaszewski, K. *Polymer* **1998**, 39, 5163.

c) Miller, P.J.; Matyjaszewski, K. *Macromolecules* **1999**, 32, 8760.

[20] Leduc, M.R.; Hawker, C.J.; Dao, J.; Frechet, J.M.J. *J. Am. Chem. Soc.* **1996**, 118, 11 111.

[21] Bielawski, C.W.; Takeharu, M.; Grubbs, R.H. *Macromolecules* **2000**, 33, 678.

[22] Coca, S.; Paik, H.J.; Matyjaszewski, K. *Macromolecules* **1997**, 30, 6513.

[23] Matyjaszewski, K. *Macromolecules*. **1998**, 31, 1527.

[24] Nakagawa, Y.; Miller, P.J.; Matyjaszewski, K. *Polymer* **1998**, 39, 5163.

[25] Reinig, B.; Keul, H.; Hocker, H. *Polymer* **1999**, 3555.

[26] Jones, R.G.; Holder, S.J. *Macromol. Chem. Phys*. **1997**, 198, 3571.

[27] Nakagawa, Y.; Miller, P.J.; Matyjaszewski, K. *Polymer* **1998**, 39, 5163.

[28] Jones, R.G.; Holder, S.J. *Macromol. Chem. Phys*. **1997**, 198, 3571.

[29] Coca, S; Davis, K; Miller, P; Matyjaszewski, K. *Polym. Prepr. Div. Polym. Chem.* **1997**, 38, 689.

[30] Nakagawa, Y.; Miller, P.J.; Matyjaszewski, K. *Polymer* **1998**, 39, 5164.

[31] Miller, P.J.; Matyjaszewski, K. *Macromolecules* **1999**, 32, 8760.

[32] Matyjaszewski, K.; Miller, P.J.; Kickelbick, G.; Nakagawa, Y.; Diamanti, S.; Pacis, C. In *Silicones and Silicone-Modified Materials*; ACS Symposium Series; Clarson, S.; Mark, J. E.; Smith, S., Eds.; American Chemical Society: Washington, DC, 1999.

[33] Matyjaszewski, K.; Nakagawa, Y.; Jasieczek, C.B. *Macromolecules* **1998**, 31, 1535.

[34] Grimaud, T.; Matyjaszewski, K. *Macromolecules* **1997**, 30, 2216.

[35] Kurata, M.; Tsunashima, Y. In *Polymer Handbook*; 3rd edition; Brandrup, J.; Immergut, E.H., Eds.; John Wiley & Sons: USA, 1989.

[36] Lutsen, L.; Jones, R.G. *Polym. Int.* **1998**, 46, 3.

[37] Matyjaszewski, K.; Patten, T.E.; Xia, J. *J. Am. Chem. Soc.* **1997**, 119, 674.

[38] a) Zeigler, J. M.; Harrah, L.A.; Johnson, A. W. *SPIE Adv. Resist. Technol.* **1985**, 539, 166.
b) Zeigler, J. M. *Mol. Cryst. Liq. Cryst.* **1990**, 190, 265.

[39] a) Demoustier-Champagne, S.; Devaux, J. In *Silicon-Containing Polymers*. Jones, R.G.; Ando, W.; Chojnowski, J., Eds.; Kluwer Academic Publishers: Dordrecht, the Netherlands, **2000**.
b) Demoustier-Champagne, S.; Cordier, S.; Devaux, J. *Polymer* **1995**, 36, 1003.

[40] Yuan, C.-H.; West, R. *Macromolecules* **1994**, 27, 649.

[41] Obata, K.; Kabuto, C.; Kira, M. *J. Am. Chem. Soc.* **1997**, 119, 11345.

[42] Dellaportas, P. *PhD. dissertation*

[43] Dellaportas, P.; Jones, R.G.; Holder, S.J. *Macromol. Rapid Comm.* **2002**, 23, 99.

# 7. Synthesis of PMPS block copolymers using TEMPO-mediated controlled free radical polymerisation

## 7.1. Introduction

### 7.1.1. Background

The use of reversible termination of propagating polymer chains in free radical polymerisation gives rise to a "pseudoliving" polymer capable of stepwise chain growth. Otsu *et al.* have shown that certain radicals, referred to as iniferters, are capable of not only initiating polymerisation, but also reversibly reacting with the growing polymer chain.[1] Disulphide iniferters (*Ini*tiator - trans*fer* agent - chain *ter*minator) such as diphenyl sulphide and dithiuram disulphide involve the photochemical dissociation of the C-S bond. The alkyl radical formed is used to initiate polymerisation, while the sulphur radical is used in the termination of the primary radical.

Until recently, difficulties concerning the molecular weight control of the polymers and termination reactions have limited the scope of radical polymerisation with regard to block copolymer synthesis. One approach to improve control of radical polymerisation has been the use of controlled/"living" radical polymerisation (CRP). CRP is based on the reversible formation of growing radicals from a variety of different dormant species. One such species involves nitroxyl and alkoxyamine derivatives, such as the stable free radical, 2,2,6,6-tetramethyl-1-piperidinyloxy (TEMPO). [2] Alkoxyamines that incorporate compounds such as TEMPO are known as thermal iniferters, since an alkyl radical and a stable nitroxide are formed on heating.

Nitroxyl radicals and alkoxyamines were first used in radical polymerisation by Rizzardo and co-workers[2] when low molecular weight polymers and oligomers were synthesised. Both Georges et al.[3] and Hawker[4] managed to polymerise styrene with TEMPO-mediated stable free radical (SFR) polymerisation in order to form well-defined polymers with relatively low polydispersities (ca. 1.1-1.3). Several well-defined block copolymers have also been formed using TEMPO functionalised polymers.[5]

The main disadvantage for TEMPO and initiators like it is that they have mostly been limited to styrenic monomers and have not, until recently, been used to polymerise other vinyl monomers such as (meth)acrylates. This is because styrene self-initiates,[6] whereas polar monomers such as (meth)acrylates are not capable of self-initiation.[7,8,9] Self-initiation is necessary in order to achieve reasonable polymerisation rates in the presence of TEMPO, due to the very low value of the equilibrium constant. In other systems such as ATRP, rates are much higher, and the proportion of chains formed by self-initiation is low, meaning molecular weights and polydispersities are not significantly affected.[7]

### 7.1.2. Mechanisms and kinetics

Although TEMPO has been used as a moderator in the polymerisation of styrene for some time, it has been quite difficult to examine the exact mechanisms and reasons why well-defined polymers are synthesised in this manner. The mechanisms involved[10] are quite comparable to the ATRP whereby a reversible process involving the transfer of a halogen atom takes place. As with ATRP, the rate of polymerisation of styrene is first order with respect to the monomer and independent of the concentration of TEMPO. The molecular weight will also increase linearly up to a certain molecular weight (~30,000), while polydispersity tends to decrease with conversion. Since the rate of polymerisation is similar to that of self-initiated styrene polymerisation, it follows that self-initiation is responsible for providing of radicals needed to maintain reasonable rates.[10]

In the case of 2,2,6,6,-tetramethyl-1-(1-phenylethyloxy)piperidine (St-TEMPO) mediated SFRP of styrene, polymerisation is initiated (e.g. by AIBN) via the formation of the 1-phenylethyl radical and corresponding TEMPO counter radical. This is achieved via the homolytic cleaving of the St-TEMPO adduct (scheme **7.1**). Reversible homolytic cleavage can occur via thermal, photochemical, or catalytic activation. The activation rate constant, $k_a$, for the 1-phenylethyl radical is less than the deactivation process, $k_d$, which leads to the reformation of the deactivated species (St-TEMPO). Therefore, during the course of a reaction, the instantaneous concentration of radicals is significantly less than the 'dormant' TEMPO capped chains.

Propagation occurs via the addition of a styrene monomer (scheme **7.2**). The rate constant for propagation is $k_p$ and in order to simplify the reaction and rates associated with propagation, it is assumed that $k_{p1} = k_{p2} = k_{pn}$.

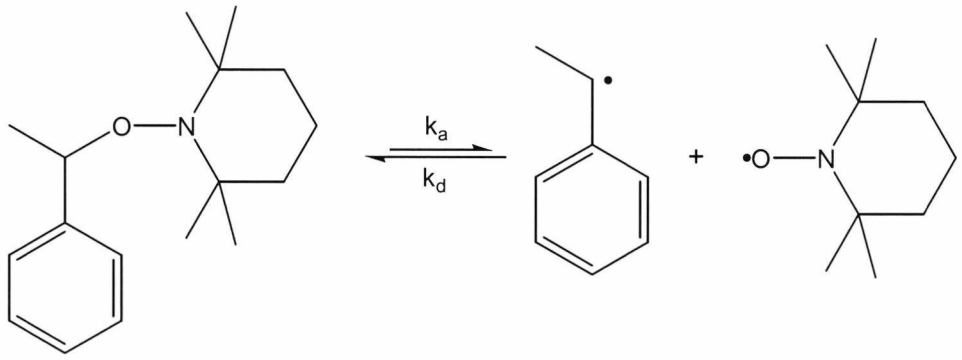


**Scheme 7.1.** Reversible homolytic cleavage of St-TEMPO

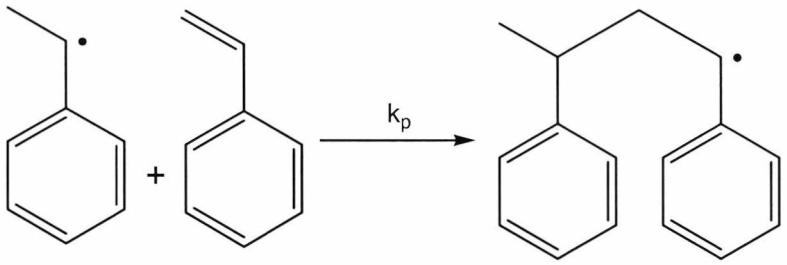


**Scheme 7.2.** Propagation of styrene

The propagating radicals also react reversibly with TEMPO to form stable species (scheme **7.3**). The rate constants are the same as those associated with the homolytic cleavage of TEMPO from scheme **1** and therefore $k_d > k_a$.

In TEMPO-mediated polymerisations, most of the chains have alkoxyamine end groups (due to $k_d > k_a$), and they will exchange with growing radicals existing at very low concentrations. The rate of exchange is similar to that of propagation, but as the polymers grow longer, side reactions become more significant, leading to an increase in polydispersity in some cases. In the polymerisation there is a large excess of counter-radicals in comparison to radicals. A persistent radical effect exists due to a continuously occurring bimolecular termination process, meaning the concentration of

the radicals will never be of the same order of magnitude as the concentration of TEMPO.

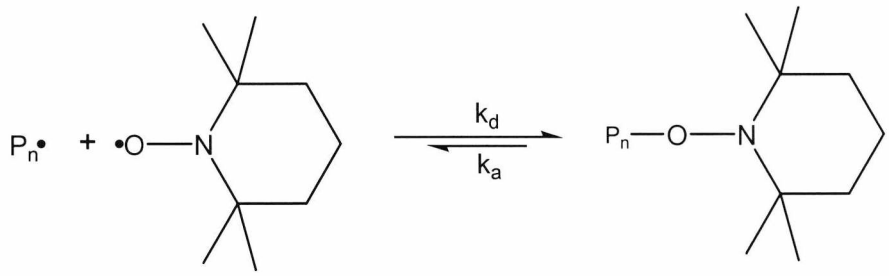


**Scheme 7.3.** Equilibrium between activated and deactivated species

Also, termination can occur mostly via bimolecular coupling of either the 1-phenylethyl radical and the propagating radical (scheme **7.4**). The degree of termination is proportional to the viscosity of the system, chain length, and temperature, therefore termination and self-initiation is more prevalent in bulk polymerisations at temperatures above 100°C.

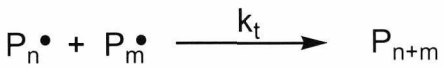


**Scheme 7.4.** Bimolecular coupling of propagating radicals

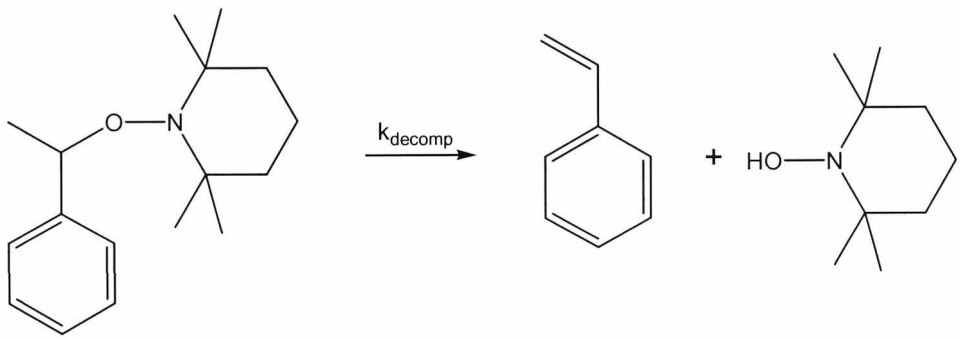


**Scheme 7.5.** Thermal decomposition of St-TEMPO

Other side reactions involving the formation of unsaturated styrene dimers also occur and can contribute to initiation and propagation, as well as termination.[6]

Finally, it is important to note that it has been reported that St-TEMPO can thermally decompose in DMSO at 110°C to give styrene and a hydroxyl derivative of TEMPO (scheme **7.5**).[11]

### 7.1.3. TEMPO-mediated block copolymerisations

#### 7.1.3.1. Sequential addition

A high level of control over the functionality of the polymers synthesised using TEMPO is achieved since one molecule of TEMPO is used to initiate a single chain. As termination is minimal, this leads to the formation of chains with one end containing the TEMPO initiator, while the other end contains the TEMPO counter radical.[4] TEMPO has been successfully employed to copolymerise styrene with a number of different monomers, including methyl, ethyl, butyl, and octyl methacrylates,[12,13] styrenes and styrenic derivatives,[8,9,14] and acrylonitrile.[8] These copolymerisations have yielded mainly random copolymers with narrow polydispersities.

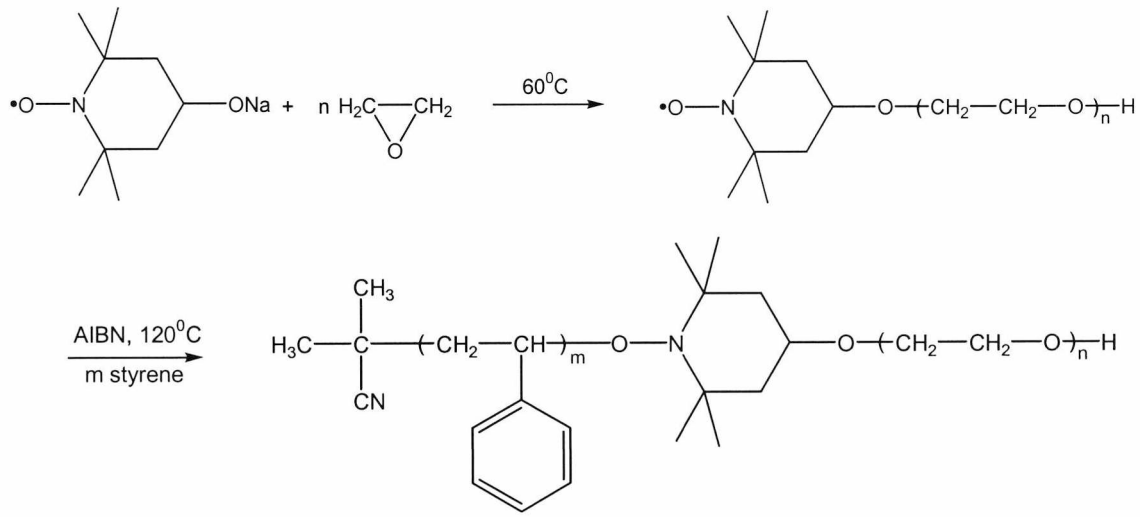


**Scheme 7.6.** Synthesis of PS-*b*-PEO via the formation of a PEO macroinitiator[15]

Quite recently, copolymerisation involving the TEMPO-mediated free radical polymerisation of styrene has yielded a range of well-defined block copolymers, such

as poly(ethylene oxide-*block*-styrene) (PEO-*b*-PS), which can be synthesised via a two-step approach.[15] Firstly, the anionic living polymerisation of the ethylene oxide with sodium 4-oxy-TEMPO (TEMPONa) as an initiator yields a PEO chain end-functionalised with TEMPO. A PEO macroinitiator (e.g. $M_n$ 3 420, $M_w/M_n$ 1.10) is then used to polymerise styrene in a SFRP reaction (scheme **7.6**) to form PEO-PS ($M_n$ 16 900, $M_w/M_n$ 1.38).

### 7.1.3.2. Functionalisation of (macro)molecules

Similarly, well-defined block copolymers incorporating ATRP and then TEMPO-mediated SFRP have been synthesised in either a two-step or one-pot method, without the need to transform or protect the initiating species. An example of such a block copolymer is PS-b-PMMA, whereby a difunctional initiator, 2-phenyl-2-[(2,2,6,6,-tetratmethyl piperidino)oxy] ethyl 2-bromo-2-methyl propanoate, is synthesised and then used to initiate ATRP of MMA.[16] The resulting PMMA macroinitiator is then used to initiate the polymerisation of styrene (scheme **7.7**).

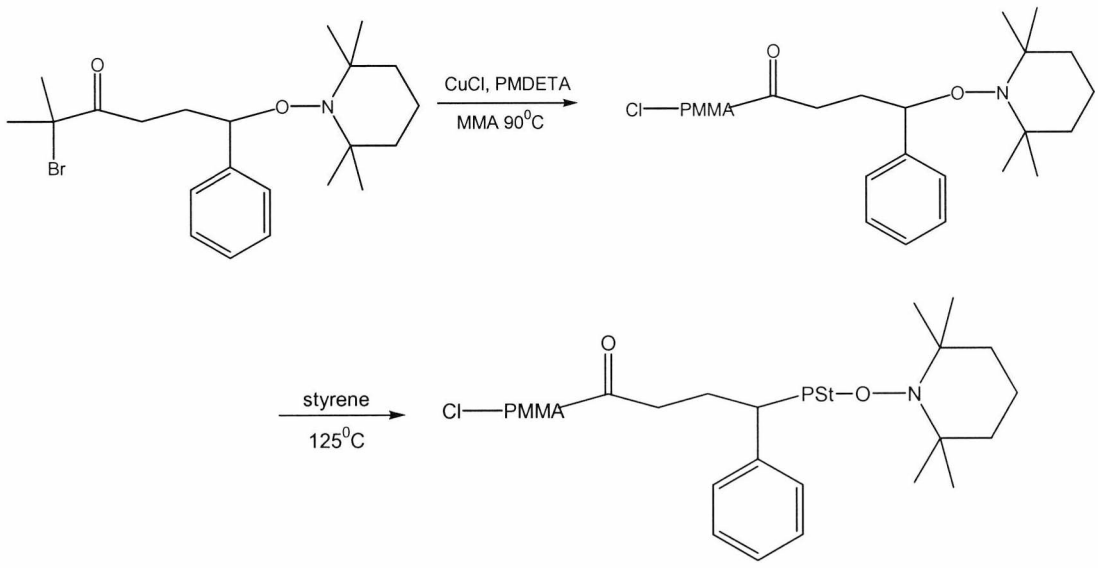


**Scheme 7.7.** Synthesis of PSt-*b*-PMMA via the formation of a PMMA macroinitiator

There are many other examples whereby polystyrene-based diblocks have been synthesised and characterised in ways similar to the previous examples. These

include polystyrene block copolymers incorporating poly(ethylene glycol),[17] poly(butyl acrylate),[18] and metal-containing blocks such as ferrocenylmethyl acrylate.[19]

## 7.2. Experimental

### 7.2.1. Materials and Apparatus

*Materials*

THF and hexane were purchased and dried as described previously [section **3.2.1**]. Methanol (AR grade) was purchased from Fischer and used as received. Mesitylene and xylene were distilled under vacuum and stored over molecular sieves at –4°C. α,ω-Dihalo-(methylphenylsilane) (diXPMPS **1** ($M_n$ 8 500, $M_w/M_n$ 1.7) and diXPMPS **2** ($M_n$ 13 000, $M_w$ 27 300, $M_w/M_n$ 2.1), were prepared using the method described previously [section **3.2.2.2**]. 1,8 Diazabicyclo(5.4.0)undec-7-ene (DBU) (98%) was purchased from Aldrich and used as received. Styrene (99%) was purchased from Aldrich and distilled under vacuum prior to use.

*Apparatus*

$^1$H nuclear magnetic resonance (NMR) spectra were recorded at 30 °C using a JEOL GX-270 spectrometer from solutions in $CDCl_3$. Molecular weights of the polymers were estimated relative to polystyrene standards by gel permeation chromatography (GPC) using equipment supplied by Polymer Laboratories Ltd. All determinations were carried out at room temperature using a 600 mm x 5 mm mixed D PLgel column with THF as eluent at a flow rate of 1 ml min$^{-1}$, and a Knauer variable wavelength detector in series with a refractive index detector.

### 7.2.2. 2,2,6,6-tetramethyl-1-(1-phenyl-2-hydroxyethyloxy)piperidine

The synthesis of 2,2,6,6,-tetramethyl-1-(1-phenyl-2-hydroxyethyloxy)-piperidine (HO-St-TEMPO) (scheme **7.8**) was carried out by R. Anderson at Polymer Laboratories according to a procedure published by Hawker[4]. $^1$H NMR ($CDCl_3$) δ: 7.25-7.40 ppm (C-$C_6$**H**$_5$); 5.85 ppm ($CH_2$-O**H**); 5.27-5.34 ppm (C**H**-O-N); 4.18-4.28 ppm (C**H**$_2$a-OH); 3.66-3.8 ppm (C**H**$_2$b-OH); 1.1-1.7 ppm (C**H**$_3$(TEMPO)). $^{13}$C NMR ($CDCl_3$) δ: 138 & 126-128 ppm (CH-**C**$_6$H$_5$); 83 ppm (**C**H-$C_6$H$_5$); 69 ppm (-$CH_2$OH); 39.5 ppm (**C**$(CH_3)_2CH_2CH_2$-); 32 ppm ($C(CH_3)_2CH_2$**C**$H_2$-); 20 ppm ($C$(**C**$H_3)_2CH_2CH_2$-); 16.5 ppm ($C(CH_3)_2CH_2$**C**$H_2$-).

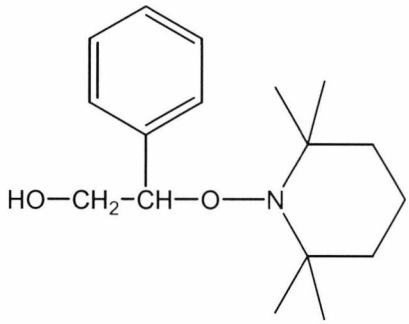

**Scheme 7.8.** HO-St-TEMPO

### 7.2.3. α,ω-Di(St-TEMPO)poly(methylphenyl)silane (PMPS-(TEMPO)$_2$)

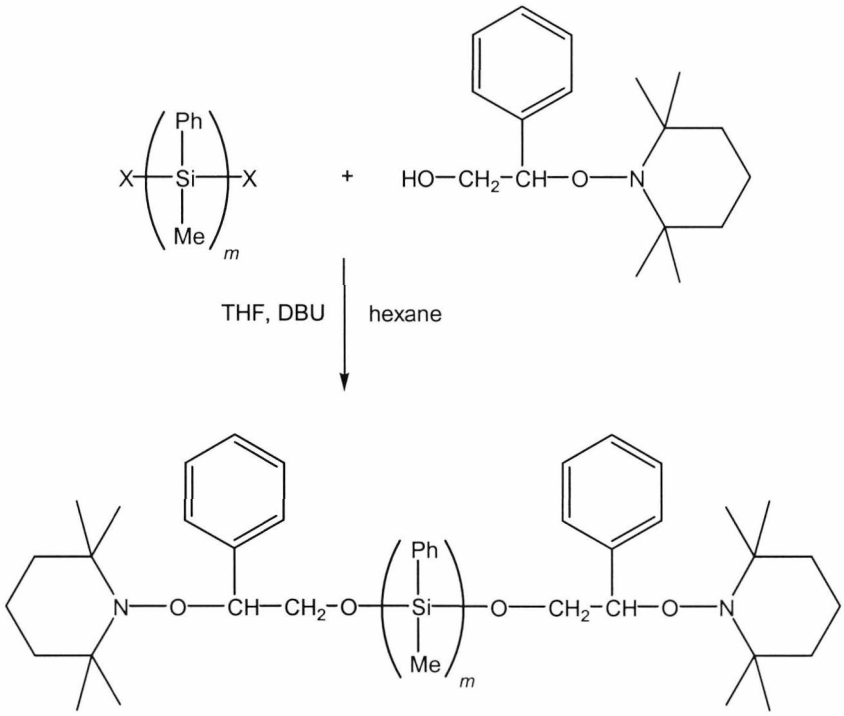


**Scheme 7.9.** Endcapping of diXPMPS with HO-St-TEMPO

α,ω-Dihalopoly(methylphenyl)silane (diXPMPS **1**) ($M_n$ = 8,500, $M_w/M_n$ = 1.7, 1.94 x $10^{-4}$ mol, 2.50 g) was placed into a flame-dried Schlenk and dissolved in dry THF (20 ml) under inert atmosphere. A slight excess of HO-St-TEMPO (0.114 g, 4.5x$10^{-4}$ mol) was added to the diXPMPS and stirred. 1,8 Diazabicyclo(5.4.0)undec-7-ene (DBU)

(0.0684 g, $4.5x10^{-4}$ mol) was added dropwise to the stirred solution (scheme **7.9**). After a few minutes a precipitate (the HCl salt of DBU) began to form. The solution was stirred for an hour and was then filtered to give a clear solution, before being precipitated into excess *n*-hexane. The endcapped PMPS was then redissolved in THF, filtered to remove any remaining salt, and reprecipitated once more into *n*-hexane in order to remove any unreacted HO-St-TEMPO. The product was dried under vacuum at 60 $^0$C overnight. A second diXPMPS sample ($M_n$ = 13,000, $M_w$ = 27,300, $M_w/M_n$ = 2.10) was also successfully endcapped. $^1$H NMR ($CDCl_3$) δ: 6.0-7.5 ppm (Si-$C_6$**H$_5$**(PMPS) & C-$C_6$**H$_5$**(St)), 3.45 - 4.1 (C**H$_2$**-O), 3.0-3.1 (C**H**-O-N), 0.9-1.9 ppm ($CH_3$(**TEMPO**)), -1.0 – 0.2 ppm (Si-Me).

### 7.2.4. Poly(styrene-*block*-methylphenylsilane-*block*-styrene) (PS-PMPS-PS)

#### 7.2.4.1. Without solvent

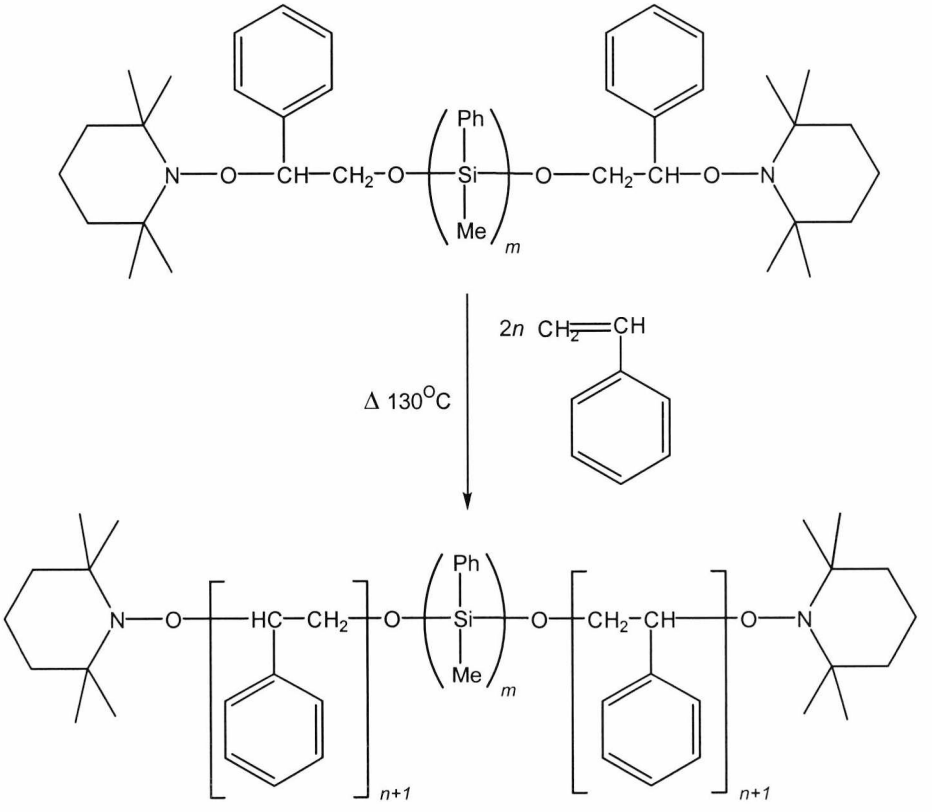


**Scheme 7.10.** Synthesis of PS-PMPS-PS

PMPS-(TEMPO)$_2$ ($M_n$ = 13,000, $M_w/M_n$ = 2.10) was used in a bulk polymerisation reaction of styrene. A sample of PMPS-(TEMPO)$_2$ (0.572 g, 4.24x10$^{-5}$ mol) was dissolved in styrene (0.750 g, 7.20 x 10$^{-3}$ mol) in a dried Schlenk under inert atmosphere (scheme **7.10**). The Schlenk was heated in an oil bath at 130 °C and left for 24 h. The hard, glassy brown solid was dissolved in THF (7 ml) to give a brown solution. The solution was precipitated into methanol (40 ml). After further reprecipitations from THF into methanol, a white precipitate was isolated and dried under vacuum at 60 °C (COP **1**, Yield 51%). ($M_n$ = 21,000, $M_w$ = 61,000, $M_w/M_n$ = 2.90). $^1$H NMR($CDCl_3$) δ: 7.3 – 6.0 ppm (Si-**C$_6$**H$_5$ (PMPS) & CH-**C$_6$**H$_5$ (PS)); 3.5 ppm (C-H (PS)); 1.2 – 2.1 ppm ($CH_2$ (PS)); -1.0 – 0.2 ppm Si-$CH_3$ (PMPS)).
The shorter PMPS-(TEMPO)$_2$ ($M_n$ = 8,500, $M_w/M_n$ = 1.7) macroinitiator was also used to polymerise styrene in bulk. Following the same procedure as before, but with an initiator/monomer ratio of 100. (COP **2**, Yield 50 %) ($M_n$ = 10,400, $M_w/M_n$ = 2.4).

### 7.2.4.2. "Bulk" synthesis of PS-PMPS-PS using a large excess of styrene

PMPS(TEMPO)$_2$ (0.075 g, $M_n$ = 8,500, 9.15 x 10$^{-6}$ mol) was dissolved into polystyrene (0.476 g, 4.57 x 10$^{-3}$ mol) in a Schlenk. The macroinitiator/monomer molar ratio was 1:500. The Schlenk was placed in an oil bath at 135 °C and left for 48 h. After 48 h, the glassy product was dissolved in THF (2 ml) and precipitated (twice) into methanol (20 ml). (COP **3**, Yield 35 %). ($M_n$ = 20,800, $M_w$ = 73,000, $M_w/M_n$ = 3.5). $^1$H NMR ($CDCl_3$) δ: 6.0-8.0 Si-Ph(PMPS) & C-Ph(PS), 1.0-2.0 CH & $CH_2$ (PS), -1.0-0.1 Si-Me (PMPS). $^{13}$C NMR($CDCl_3$) δ: 127-129 & 146 ppm (CH-**C$_6$**H$_5$ (PS)); 126 & 134 ppm (Si-**C$_6$**H$_5$ (PMPS)); 40-45 ppm (-**C**H$_2$-**C**H- (PS)); -6 ppm (Si-**C**H$_3$ (PMPS)).

### 7.2.4.3. Synthesis of PS-PMPS-PS using a solvent

The same reaction described previously [section **7.2.4.1**] was carried out in the presence of mesitylene (2 ml) and also *o*-xylene (2 ml). GPC analysis revealed no increase in molecular weight.

## 7.3. Results and discussion

### 7.3.1. 2,2,6,6,-Tetramethyl-1-(1-phenyl-2-hydroxyethyloxy)-piperidine

2,2,6,6,-Tetramethyl-1-(1-phenyl-2-hydroxyethyloxy)piperidine (HO-St-TEMPO) was synthesised in order to endcap PMPS by reacting the hydroxy groups with the halide end groups of PMPS. The corresponding PMPS chain ends would therefore contain a group capable of initiating and moderating a living free radical polymerisation to form a PS-PMPS-PS block copolymer.

HO-St-TEMPO was first prepared as a difunctional initiator by Hawker and co-workers.[5] Control of chain ends was demonstrated when HO-St-TEMPO was used to form hydroxy-terminated polystyrene. The type of functional group was also altered by reacting the hydroxy group prior to styrene polymerisation. Other similar functional initiators involving TEMPO have also been investigated in order to form end-functionalised polymers.[4,20]

Difunctional initiators such as HO-St-TEMPO have been used to form block copolymers. Recently, HO-St-TEMPO has been used as a double-headed initiator in order to synthesise block copolymers containing polycaprolactone and polystyrene segments.[21] This was achieved by first carrying out the TEMPO-mediated polymerisation of styrene, followed by the ring-opening polymerisation of ∈-caprolactone, and vice-versa. Alternatively, the hydroxy group of HO-St-TEMPO can be used to attach the initiator to the end group of a polymer in order to form a macroinitiator.[22] Recently, poly(dimethylsiloxane) (PDMS) was end-functionalised with a styryl-TEMPO group. The PDMS macroinitiator was then used to polymerise styrene to form PDMS-*b*-PS.[23]

$^{1}H$ NMR and $^{13}C$ NMR spectroscopy were used to confirm the structure of the initiator (fig. **7.1**). The $^{13}C$ NMR shows a small amount of impurity at ~60 ppm, probably due to the fact that the $^{13}C$ NMR of the sample was recorded some time after it was received and used in the relevant experiments. The reason for the degradation may be because the HO-St-TEMPO was stored at room temperature in the dark, and not in a freezer. Over time, the TEMPO could have decomposed to form the hydroxyl derivative of TEMPO.

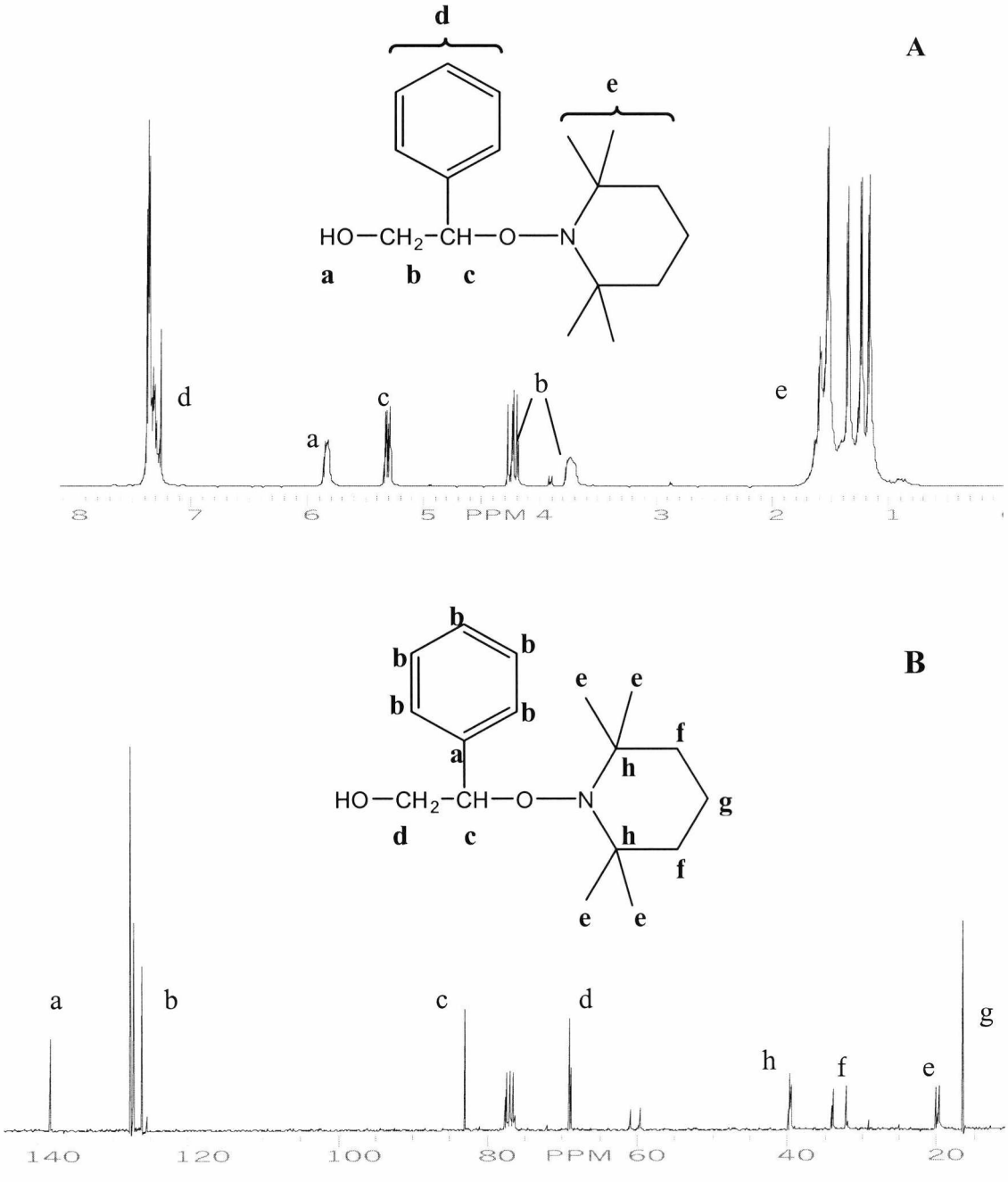


**Fig. 7.1.** $^{1}H$ NMR (**A**) and $^{13}C$ NMR (**B**) of HO-St-TEMPO

### 7.3.2. Preparation of TEMPO end-functionalised poly(methylphenylsilane)

HO-St-TEMPO was added to the halogenated endgroups of diXPMPS in the presence of 1,8 diazabicyclo(5.4.0)undec-7-ene (DBU) in order to aid the reaction and remove excess HX species. The resulting macroinitiator was characterised by $^{1}H$ NMR (fig. **7.2**).

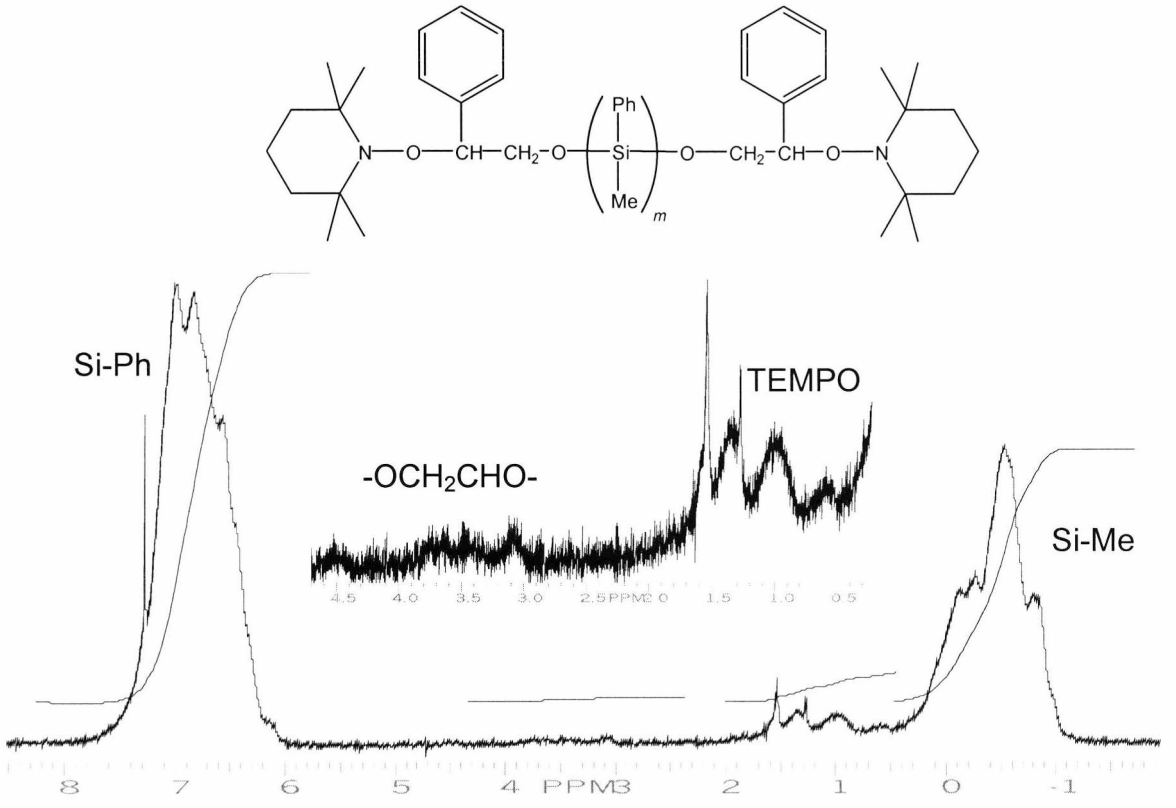


**Fig. 7.2.** $^1$H NMR of PMPS(TEMPO)$_2$ ($M_n$ 13 500)

| Proton environment | δ ppm | Integrals* | | Percentage conversion |
|---|---|---|---|---|
| | | theory | expt'l | |
| TEMPO | 0.5 – 2.0 | 36 | 38.5 | 107 |
| -$OCH_2CHO$- | 3.0 – 4.6 | 6 | 6.7 | 112 |
| Si-$CH_3$ | -1.2 – 0.4 | 330 | 330 | - |
| Si-$C_6H_5$ | 6.1 – 7.7 | 550 | 570$^+$ | 104 |

**Table 7.1.** $^1$H NMR integration data for PMPS(TEMPO)$_2$ ($M_n$ 13 500). (*Data according to Si-$CH_3$ protons) ($^+$includes $CDCl_3$ peak, therefore higher than expected).

The extent with which the diXPMPS was endcapped could be determined by comparison of the integrals of the characteristic HO-St-TEMPO peaks with the characteristic PMPS peaks. The molecular weight data obtained via GPC was used to

calculate the number of repeat units present, and hence the number of protons, present in the diXPMPS polymer. The percentage conversions are given in table **7.1**, and show how the percentage conversion from diXPMPS to macroinitiator (PMPS-$(TEMPO)_2$) was determined. Since there is quite a lot of noise apparent in the NMR spectrum, and because of the relatively large intensities of the polymeric peaks vs. the end group peaks, there is some error associated with the data. However, from the NMR peak data a good conversion is shown and, although some error may exist, it is the only method available whereby the end groups can be accounted for.

### 7.3.3. Poly(styrene-*block*-methylphenylsilane-*block*-styrene) (PS-PMPS-PS)

#### 7.3.3.1. In bulk

The monomer/macroinitiator molar ratio was 170 and therefore blocks of styrene 85 units in length were aimed for. GPC analysis showed a characteristic increase in molecular weight associated with the formation of a block copolymer. Simultaneous analysis using both a RI and a UV detector (set at 334 nm) confirmed that a block copolymer had been synthesised (fig. **7.3**). Since polystyrene absorbs in the UV region at 254 nm, and not at 334 nm, it follows that the molecular weight distribution observed must contain a segment of PMPS. A broadening effect ($M_w/M_n$ 2.9) may be due to the presence of PMPS homopolymer, as evidenced by a lower molecular weight 'tail'. Equally, the formation of AB block copolymer would lead to a broader molecular weight distribution.

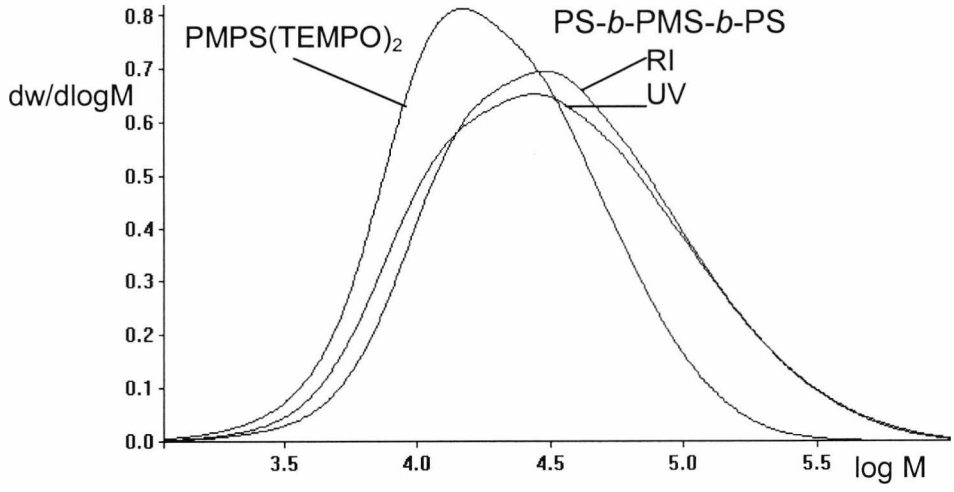


**Fig. 7.3.** GPC overlay of $PMPS(TEMPO)_2$ and PS-PMPS-PS (cop **1**)

At the beginning of the reaction in bulk, the homogeneous mixture of PMPS in styrene was very viscous. The reaction did not seem to go to completion (as evidenced by a low yield and a lower than expected $M_n$) before the reaction mixture became a hard glassy light brown solid. This was probably due to the fact that the PMPS chains were no longer soluble in the styrene monomer. However, after dissolving the product into THF and reprecipitating into methanol, a white powder was isolated quite easily.

$^1$H NMR analysis showed the presence of characteristic polystyrene peaks alongside the PMPS peaks, although the aromatic peaks of both blocks overlap at 6.0 to 7.3 ppm (fig. **7.4**). In Table **7.2** the integration data from the $^1$H NMR peaks and the shifts in molecular weights shown by the GPC plots are compared for cop **1**. By comparing the data with the theoretical block length (based on the assumption that two PS blocks would be grown per macroinitiator, and that all styrene monomer would be consumed), it was observed that the block lengths were shorter than expected. The yield was of the copolymer was 51%. A different macroinitiator ($M_n$ 8 500) was used to carry out a less successful copolymerisation, yielding cop **2** ($M_n$ 10 400) (yield was low and not recorded). Also shown in table 7.2 is cop **3**, which is discussed elsewhere [section 7.3.3.2.]

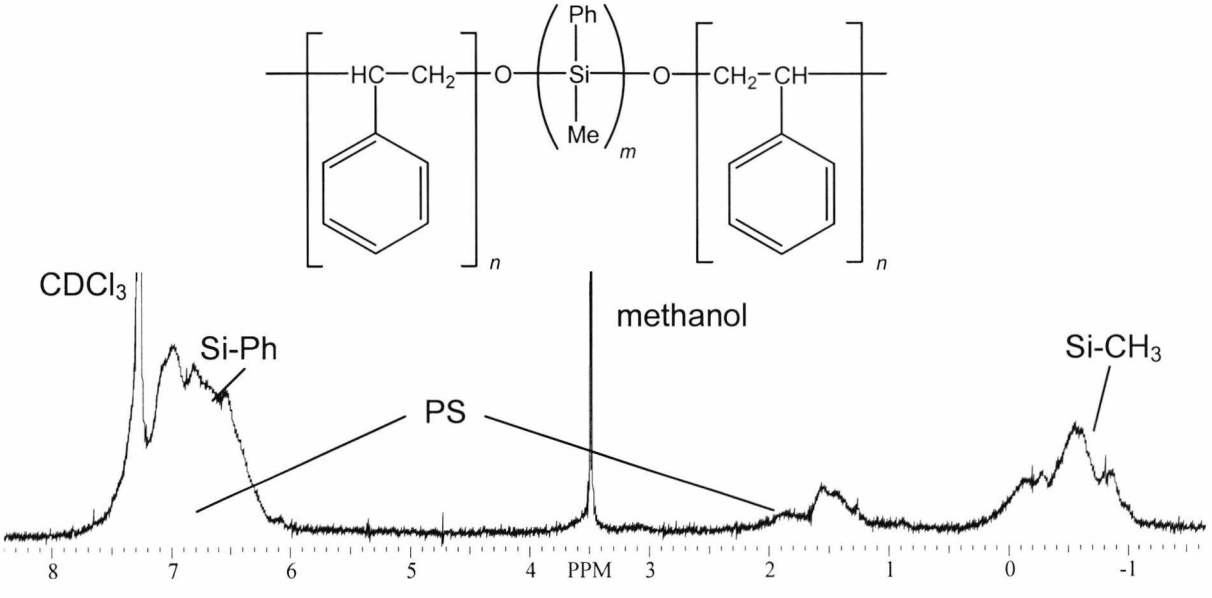


**Fig. 7.4.** $^1$H NMR of PS-PMPS-PS (cop **1**)

| Cop | PMPS-(TEMPO)$_2$ | | PS block | PS-PMPS-PS | | | | | |
|---|---|---|---|---|---|---|---|---|---|
| | $M_n$ | $M_w/M_n$ | (theoetical) | $M_n$ | $M_w/M_n$ | $M_n$ | $DP_n$ | $DP_n$[(a)] | Yield |
| **1** | 13 000 | 2.1 | 85 | 21 000 | 2.9 | 4 000 | 38 | 29 | 51% |
| **2** | 8 500 | 1.7 | 50 | 10 400 | 2.0 | 950 | 9 | - | 50% |
| **3** | 8 500 | 2.1 | 250 | 20 800 | 3.5 | 6 150 | 59 | 70 | 35% |

**Table 7.2.** Molecular weights of PS-PMPS-PS copolymers **1**, **2**, and **3** (Values quoted according to GPC data (UV detector, λ 334 nm) and [(a)]$^1$H NMR spectroscopy).

### 7.3.3.2. In bulk using a large excess of styrene (COP 3)

Using the high boiling solvents, mesitylene and xylene, for the copolymerisation reaction of PMPS(TEMPO)$_2$ with styrene did not work. The reasons for this remain unclear. However, without a solvent present, the reaction mixture seemed to solidify before the completion of the reaction could occur. A large excess of styrene was then used as both a monomer and to dissolve the copolymer that was forming. After 18 hours, the reaction mixture seemed very viscous, although it did not solidify as previous reactions had. After more than 24 hours a solid gel formed, and after 48 hours the reaction mixture had become solid. Analysis via GPC revealed an increase in molecular weight, although polydispersity had increased considerably (table 7.2).

$^1$H and $^{13}$C NMR confirmed the presence of PS and PMPS segments in the copolymer (fig. **7.4**). In this case the Si-$C_6H_5$ peak of PMPS was dwarfed by the two peaks associated with the phenyl ring of PS. The integrals of the aliphatic PS peaks (-$CH_2$-CH-) were compared with the Si-$CH_3$ peak in order to determine the composition of the block copolymer, which was only slightly higher than the values obtained via SEC (table 7.2).

The molecular weight and NMR data for three copolymerisations are compared in table 7.2. The average lengths of the PS blocks attached to either end of the PMPS according to SEC data is about 59 units whereas, according to the $^1$H NMR data, the average number of units is about 70. An increase in polydispersity ($M_w/M_n$ = 3.5) may be due to the presence of diblocks and homopolymer, i.e. PMPS macroinitiators

which failed to polymerise styrene. This may have occurred because a significant number of the PMPS chains may not have been endcapped. Some polystyrene homopolymer may also have formed via self-initiation reactions.[6]

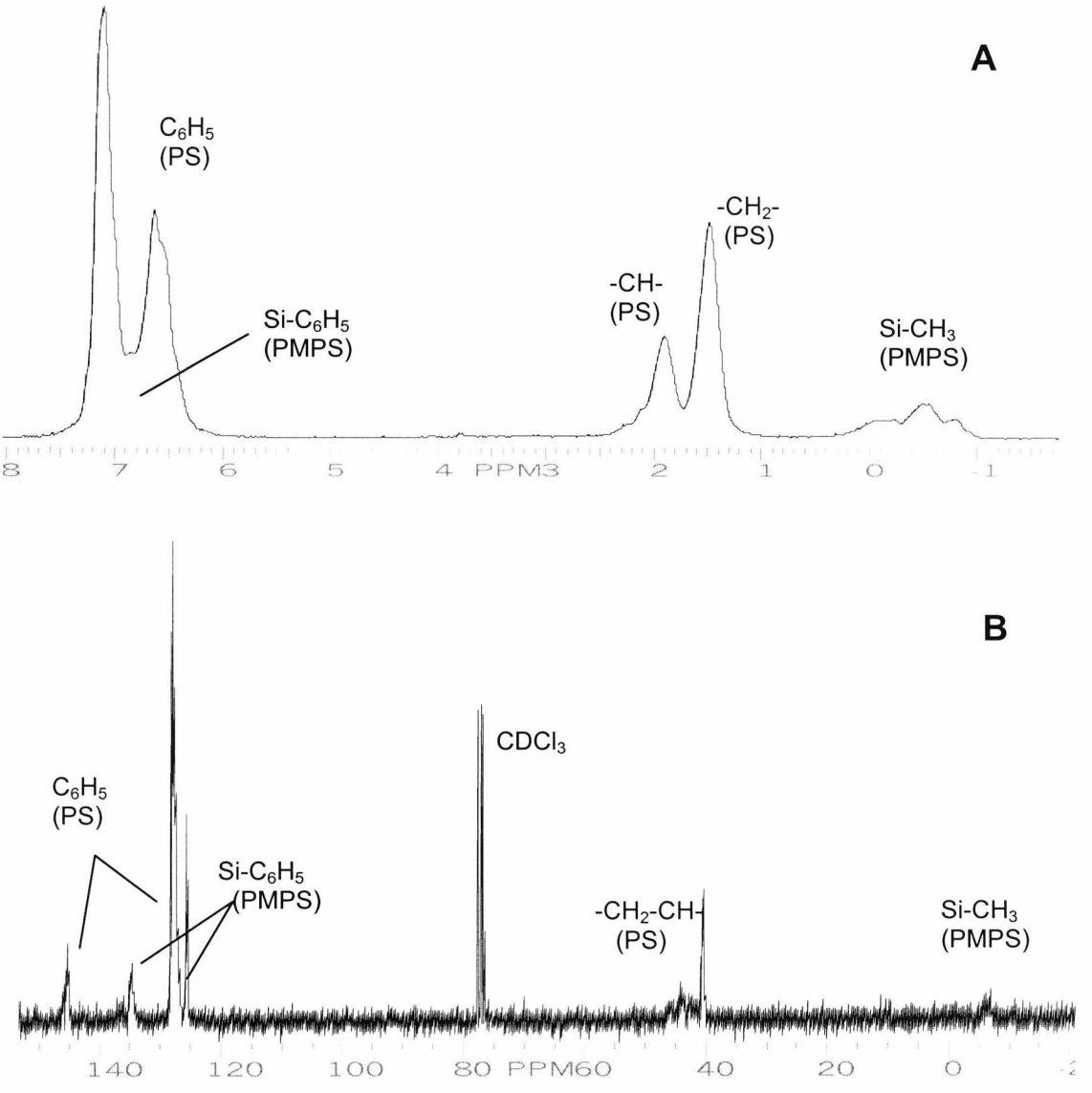


**Fig. 7.4.** $^{1}H$ NMR (**A**) and $^{13}C$ NMR (**B**) spectra of PS-PMPS-PS (COP **3**)

### 7.3.3.2. In solution

The copolymerisation had worked to an extent in bulk, but the gel point had seemingly been reached after only a couple of hours. Therefore a high boiling solvent such as mesitylene was evaluated as a solvent for the copolymerisation to increase the

degree of conversion reached prior to gelation. Several attempts involving mesitylene and xylene were carried out using macroinitiators **1** and **2**. However, no increase in molecular weight was seen at all, and other attempts using xylene as a solvent also proved unsuccessful. No change in the viscosity of the reaction mixture occurred and an increase in molecular weight was not observed, even after 48 hours (fig. **7.5**). Further research into the effects of solvent is needed.

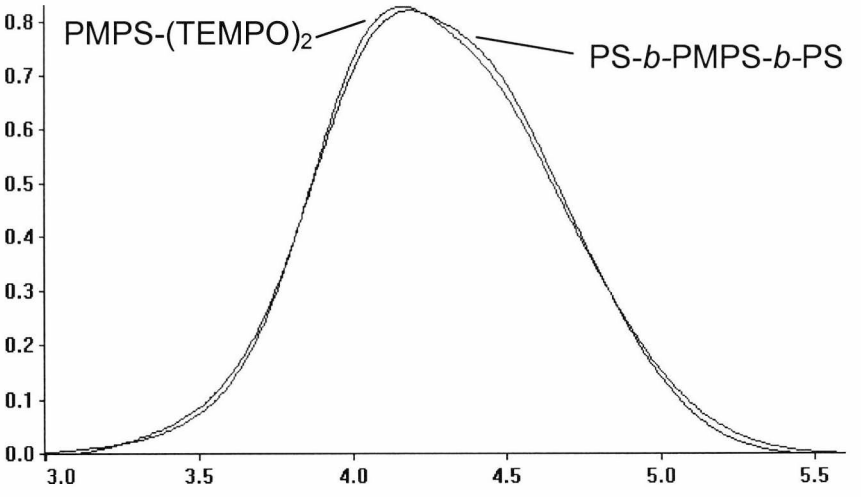


**Fig. 7.5.** GPC plot of PMPS(TEMPO)$_2$ ($M_n$ 13 000) and plot taken after two days of copolymerisation with styrene in mesitylene at 130°C (PS-PMPS-PS).

### 7.3.4. Conclusions and future work

The first example of a TEMPO-mediated SFRP polymerisation involving a polysilane macroinitiator has been described. In previous block copolymerisations involving polysilanes and polystyrene, the methods proved to be long-winded in terms of preparation of polymers involved, while the purification of the product has been difficult. The use of a PMPS macroinitiator has enabled a more controlled synthesis of a PS-PMPS-PS block copolymer.

The copolymerisation worked in bulk, but the gel point was apparently reached after only a couple of hours. Therefore a high boiling solvent such as mesitylene was evaluated as a possible medium for copolymerisation to go closer to completion.

However, no increase in molecular weight was observed, and other attempts using xylene also proved unsuccessful.

Subsequent research might involve the use of various high boiling solvents such as toluene which are able to both dissolve the copolymer effectively and enable controlled polymerisation. Characterisation of the thermal properties of the copolymers would also be of interest. Also, a block copolymer of PMPS and PS could be synthesised using a PMPS macroinitiator such as the one described elsewhere [section 6.3.2]. Equally, a PMPS macroinitiator containing a benzyl halide-initiating group might be used for the ATRP of PS. Comparisons between these three different macroinitiators, in terms of conversion, rate, and control, would be of interest. Finally, it should be possible to synthesise similar block copolymers by polymerising different styryl monomers.

## 7. References


[1] a) Otsu, T.; Yoshida, M. *Makromol. Chem., Rapid Commun.* **1982**, 3, 127.

b) Otsu, T.; Yoshida, M.; Tazaki, T. *Makromol. Chem., Rapid Commun.* **1982**, 3, 133.

c) Otsu, T.; Yoshida, M.; Kuriyama, A. *Polym. Bull.* **1982**, 7, 45.

d) Otsu, T.; Kuriyama, A. *Polym. Bull.* **1984**, 11, 135.

e) Otsu, T.; Kuriyama, A. *Polym. J.* **1985**, 17, 97.

f) Otsu, T. *J. Polym. Sci. Part A. Polym. Chem.* **2000**, 38, 2121.

[2] Solomon, D.H.; Rizzardo, E.; Cacioli, P. U.S. Pat 4581429, 1986; *Chem. Abstr.* **1985**, 102, 221335.

[3] a) Georges, M.; Veregin, R.; Kazmaier, P.; Hamer, G. *Macromolecules* **1993**, 26, 2987.

b) Georges, M.; Veregin, R.; Kazmaier, P.; Hamer, G. *Polym. Mater. Sci. Eng.* **1993**, 68, 6.

c) Georges, M.; Veregin, R.; Kazmaier, P.; Hamer, G. *Trends Polym. Sci.* **1994**, 2, 66.

[4] Hawker, C.J. *J. Am. Chem. Soc.* **1994**, 116, 11185.

[5] a) Hawker, C.J.; Hedrick, J.L. *Macromolecules* **1995**, 28, 2993.

b) Hawker, C.J. *Angew. Chem., Int. Ed. Engl.* **1995**, 34, 1456.

[6] a) Mayo, F.R. *J. Am. Chem. Soc.* **1953**, 75, 6133.

b) Mayo, F.R. *J. Am. Chem. Soc.* **1968**, 90,1289.

[7] Greszta, D.; Matyjaszewski, K. *Macromolecules* **1996**, 29, 7661.

[8] Fukuda, T.; Terauchi, T.; Goto, A.; Tsujii, Y.; Miyamoto, T. *Macromolecules* **1996**, 29, 3050.

[9] Hawker, C.J.; Elce, E.; Dao, J.; Volksen, W.; Russel, J.P.; Barclay, G.G. *Macromolecules* **1996**, 29, 2686.

[10] Greszta, D.; Matyjaszewski, K. *Macromolecules* **1996**, 29, 7661.

[11] Li, I.; Howell, B.A.; Matyjaszewski, K.; Shigemoto, T.; Smith, P.B.; Priddy, D.B. *Macromolecules* **1995**, 28, 6692.

[12] Yoshida, E.; Ishizone, T.; Hirao, A.; Nakahama, S.; Takata, T.; Endo, T. *Macromolecules* **1994**, 27, 3119.

[13] Yousi, Z.; Jian, L.; Rongchuan, Z.; Jianliang, Y.; Lizong, D.; Lansun, Z. *Macromolecules* **2000**, 33, 4745.

[14] Butz, S.; Baethge, H.; Schmidt-Naake, G. *Macromol. Rapid Commun.* **1997**, 18, 1049.

[15] Hua, F.J.; Yang, Y.L. *Polymer* **2001**, 42, 1361.

[16] Tunca, U.; Karliga, B.; Ugur, A.L.; Sirkecioglu, O.; Hizal, G. *Polymer* **2001**, 42, 8489.

[17] Chen, X.; Gao, B.; Kops, J.; Batsberg, W. *Polymer* **1997**, 39, 911.

[18] Tortosa, K.; Smith, J.-A.; Cunningham, M.F. *Macromol. Rapid. Commun.* **2001**, 22, 957.

[19] Baumert, M.; Frohlich, J.; Stieger, M.; Frey, H.; Mulhaupt, R.; Plenio, H. *Macromol. Rapid. Commun.* **1999**, 20, 203.

[20] a) Hawker, C.J. *Acc. Chem. Res.* **1997**, 30, 373.

b) Malmstrom, E.E.; Hawker, C.J. *Macromol. Chem. Phys.* **1998**, 199, 923.

[21] Hawker, C.J.; Hedrick, J.L.; Malmstrom, E.E.; Trollsas, M.; Mecerreyes, D.; Moineau, G.; Dubois, Ph.; Jerome, R. *Macromolecules* **1998**, 31, 213.

[22] a) Kobatake, S.; Harwood, H.J.; Quirk, R.P. *Macromolecules* **1997**, 30, 4238.

b) Kobatake, S.; Harwood, H.J.; Quirk, R.P. *Macromolecules* **1998**, 31, 3735.

[23] Morgan, A.M.; Pollack, S.K.; Beshah, K. *Macromolecules* **2002**, 35, 4238.

# 8. Synthesis of amphiphilic block copolymers via ATRP

## 8.1. Introduction

A range of amphiphilic block copolymers (ABCs) including triblocks and pentablocks can be prepared using ATRP. ABCs have been synthesised using similar methods to those involved in the formation of other block copolymers using ATRP [section 6.1]. Since hydrophilic and hydrophobic monomers are usually immiscible, some difficulties can occur in terms of the homogeneity of the reaction mixture. The choice of ligand and solvent is important when trying to achieve homogeneity. Alternatively, a typical route for synthesising ABCs involves the chemical modification of segments after the copolymer has been synthesised. One such example involves the copolymerisation of *n*-butyl acrylate (*n*-BA) with 2-trimethylsiloxyethyl (TMS) protected 2-hydroxyethyl acrylate (HEA-TMS).[1] The PHEA-TMS block is then deprotected in acid conditions (HCl in THF) to form the amphiphilic block copolymer, poly(*n*-butyl acrylate-*block*-2-hydroxyethyl acrylate) P(*n*-BA)-*b*-PHEA (scheme **8.1**).

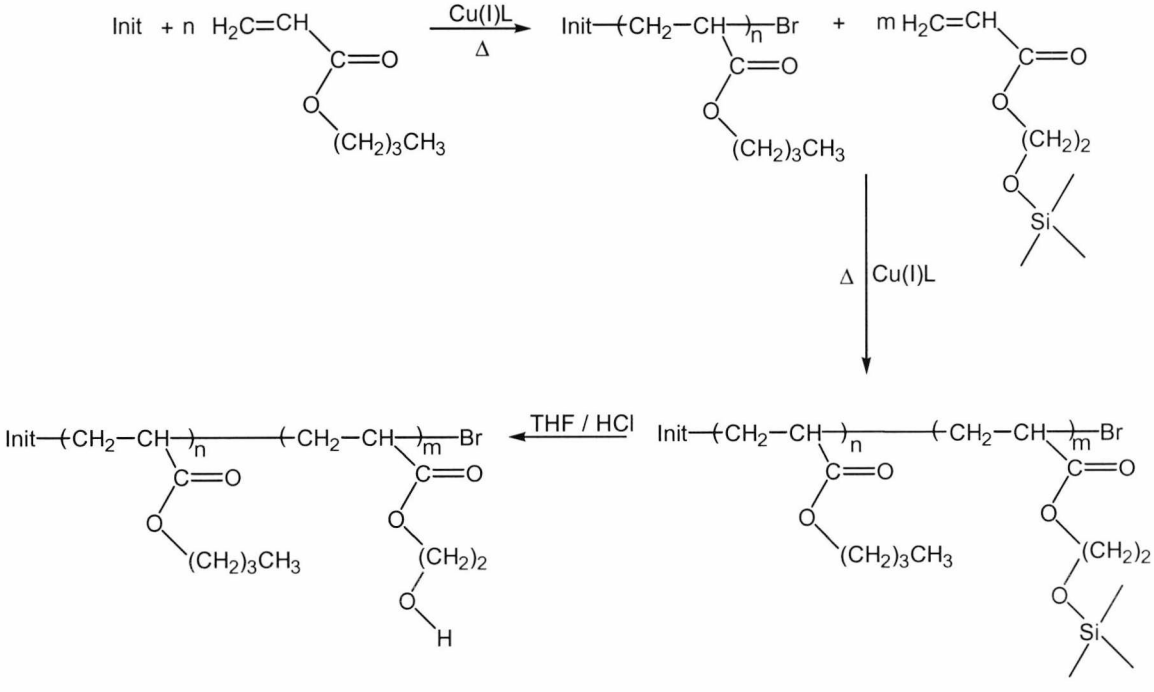


**Scheme 8.1.** Synthesis of P(*n*-BA)-*b*-PHEA[1]

Aggregates of highly asymmetric polystyrene-*block*-poly(acrylic acid) (PS-*b*-PAA) in which the polystyrene (PS) blocks are much longer compared to the PAA blocks have been described as being "crew-cut" aggregates.[2] As the PAA block decreases in length, the morphology of the aggregate changes from spherical to rodlike, then to lamellar or vesicular, and finally to large compound micelles.

Another example is poly(styrene-*block*-ethylene oxide) (PS-*b*-PEO), which can also aggregate to produce different morphologies depending on the relative block lengths.[3] Morphological changes can also occur via the addition of ions in micromolar ($CaCl_2$, HCl) and millimolar (NaCl) concentrations. These effects are due to changes in repulsion (steric and electrostatic) of the hydrophilic blocks, e.g. protonation of PAA (HCl) or ion binding/bridging by $Ca^{2+}$.[4]

## 8.2. Experimental

### 8.2.1. Materials and apparatus

*Materials*

PMPS macroinitiators (PMPS(init)$_2$) were prepared using the same methods described previously [section **6.2.1**]. 2-Hydroxyethyl methacrylate (99+%) (HEMA) was purchased from Aldrich and distilled under vacuum prior to use. Poly(ethylene glycol) methyl ether methacrylate ($M_n$ ca. 300, Aldrich) (OEGMA) was used as received. *o*-Xylene was distilled under vacuum and stored over molecular sieves at -4°C and THF was purchased and prepared as described previously [section **3.2.1**]. *n*-Hexane and propanol (AR grade, Fischer) were used as received. 2,2,-Bipyridine, Cu(I)Cl (98+%), and Cu(I)Br (98%) were purchased from Aldrich and used as received. N-(n-propyl)-2-pyridyl(methanimine) was synthesised by J. Parker at the University of Kent. 3-morpholino-4-propyl-2-pyridylmethanimine[5] and 2-(2-pyridyl methanimine) aminoethoxyethanol were synthesised by C. T. Yeoh at the University of Kent. Aluminum oxide (activated, neutral) was purchased from Acros Organics.

*Apparatus*

$^1$H nuclear magnetic resonance (NMR) spectra were recorded at 30°C using a JEOL GX-270 spectrometer from solutions in $CDCl_3$. In some cases a mixture of DMSO and $CDCl_3$ was used to dissolve the copolymer. Molecular weights of the polymers were estimated relative to polystyrene and, in some cases, poly(methyl methacrylate) standards by gel permeation chromatography (GPC) using equipment supplied by Polymer Laboratories Ltd. All determinations were carried out at room temperature using a 600 mm x 5 mm mixed D PLgel column with THF as eluent at a flow rate of 1 ml min$^{-1}$, and a Knauer variable wavelength detector in series with a refractive index detector.

### 8.2.2. Poly(2-hydroxyethyl methacrylate-*block*-methylphenylsilane-*block*-2-hydroxyethyl methacrylate) (PHEMA-PMPS-PHEMA)

A range of amphiphilic block copolymers, PHEMA-PMPS-PHEMA, were synthesised using different copper complexes and ligands (scheme **8.2**). A typical ATRP reaction is reported using a PMPS macroinitiator ($M_n$ = 8,400, $M_w/M_n$ = 1.95) to polymerise 2-hydroxethyl methacrylate (HEMA). The monomer to macroinitiator ratio was 100.

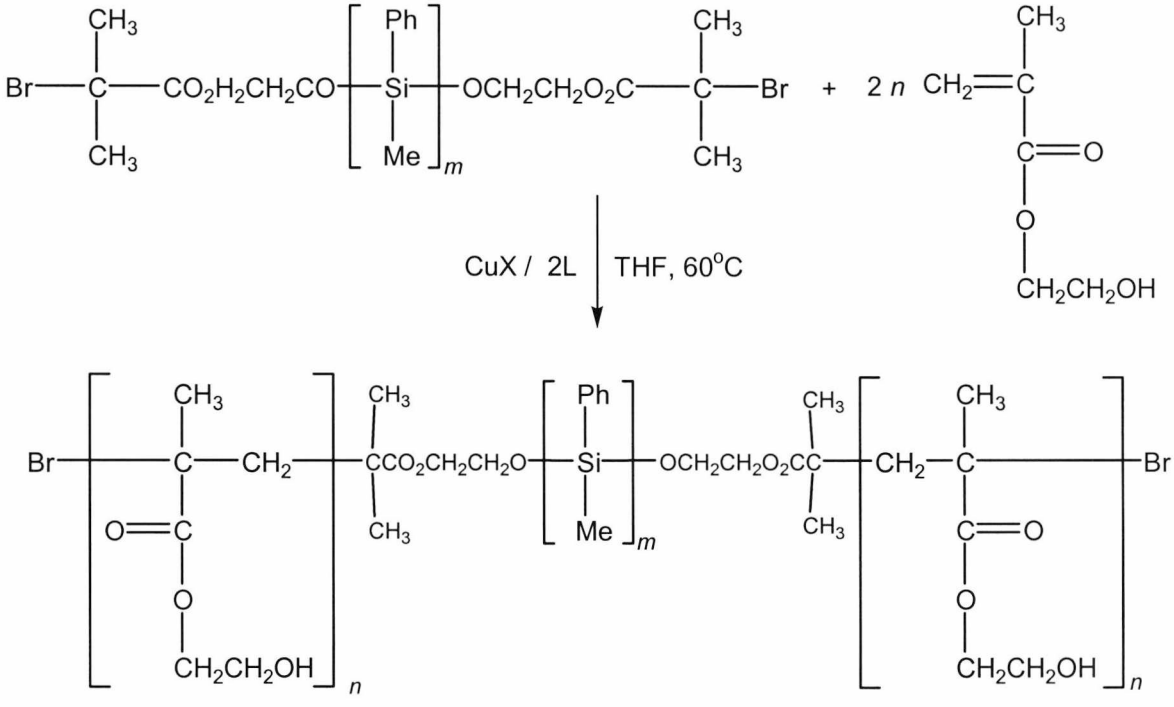


**Scheme 8.2.** Synthesis of PHEMA-PMPS-PHEMA (CuX = CuBr or CuCl) (L = 2,2,-bipyridine, *N*-(n-propyl)-2-pyridyl(methanimine), 3-morpholino-4-propyl-2-pyridylmethanimine, or 2-(2-pyridyl methanimine) aminoethoxyethanol)

CuCl (0.0133 g, 5.68 x $10^{-5}$ mol), bipyridine (0.0355 g, 2.27 x $10^{-4}$ mol), and HEMA (0.739 g, 5.68 x $10^{-3}$ mol) were added to a solution PMPS(init)$_2$ (0.477 g, 5.68 x $10^{-5}$ mol) in THF (2 ml). The solution was degassed by three freeze-thaw cycles. The mixture was stirred at 65 °C using an oil bath, and progress of the reaction was monitored using SEC. After 24 h, the reaction mixture was cooled, diluted with THF (3 ml) and filtered through alumina using THF as the eluent. The product was

precipitated into a 50/50 v/v mixture of *n*-hexane and propanol. The product was filtered and recovered as a slightly brown solid, which was dried under vacuum at 65°C ($M_n$ = 10,300, $M_w/M_n$ = 1.9). $^1$H NMR ($CDCl_3$) δ: 6.2 – 7.2 ppm (Si-$C_6$**H**$_5$); 4.6 – 4.8 ppm ($OCH_2CH_2$**OH**); 3.8 – 4.1 ppm ($OCH_2$**C**$\mathbf{H_2}$OH); 3.1 – 3.55 ppm (O**C**$\mathbf{H_2}CH_2OH$); 1.7 – 1.9 ppm (-**C**$\mathbf{H_2}$C($CH_3$)-); 0.85 – 1.3 ppm (-$CH_2$C(**C**$\mathbf{H_3}$)-); -1.1 – 0.1 ppm (Si-**C**$\mathbf{H_3}$). $^{13}$C NMR ($CDCl_3$) δ: 177 ppm (**C**=O); 126, 134 ppm (Si-**C**$_6$H$_5$); 65 ppm (O**C**$H_2CH_2OH$); 58 ppm ($OCH_2$**C**$H_2$OH); 44 ppm (-$CH_2$**C**($CH_3$)-); 22 ppm (-**C**$H_2$C($CH_3$)-); 16 ppm (-$CH_2$C(**C**$H_3$)-); -8 ppm (Si-**C**$H_3$).

Other similar reactions were carried out using alternative solvents (*o*-xylene at 95°C), ligands (*N*-(n-propyl)-2-pyridyl(methanimine), 3-morpholyl-4-propyl-2-pyridylmethanimine, or 2-(2-pyridyl methanimine) aminoethoxyethanol), copper halides (CuBr), and monomer to macroinitiator ratios (see table **8.1** [section 8.3.2])

### 8.2.3. Poly(oligo(ethylene glycol) methyl ethyl methacrylate-*block*-methylphenylsilane-*block*-oligo(ethylene glycol) methyl ethyl methacrylate) (POEGMA-PMPS-POEGMA)

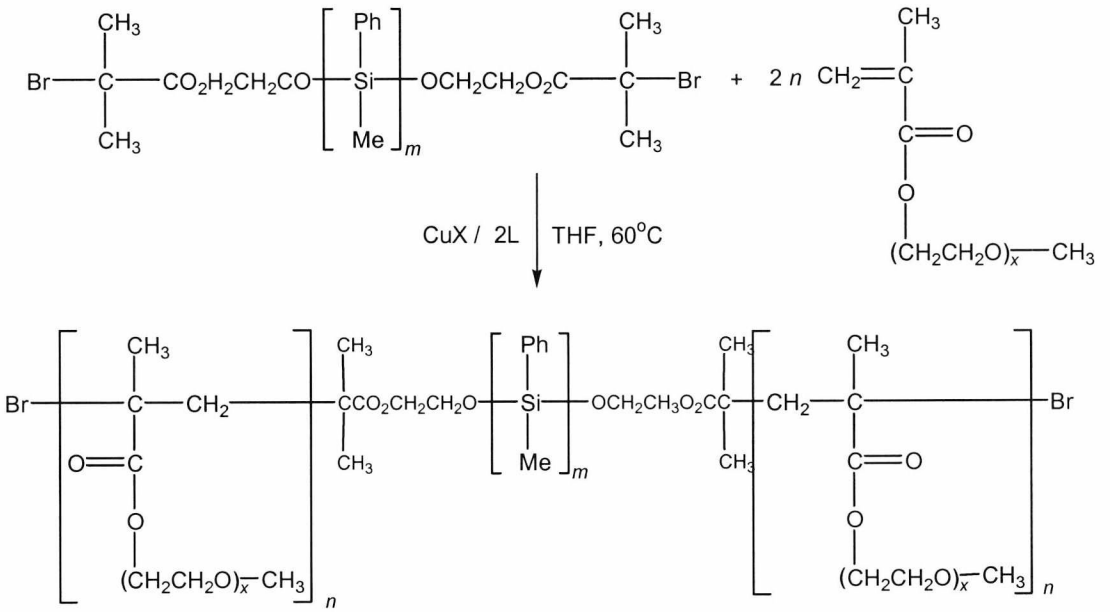


**Scheme 8.3.** Synthesis of POEGMA-PMPS-POEGMA (CuX = CuBr, CuCl) (L = 2,2,-bipyridine, 2-(2-pyridyl methanimine) aminoethoxyethanol)

A range of POEGMA-PMPS-POEGMA copolymers were synthesised using different reaction conditions. A typical procedure is shown using PMPS(init)$_2$ ($M_n$ = 8,400, $M_w/M_n$ = 1.95) and 60 equivalent units of OEGMA ($M_n$ = 300).

CuCl (0.0113 g, 5.68 x $10^{-5}$ mol), 2-(2-pyridyl methanimine) aminoethoxyethanol (0.0441g, 2.27 x $10^{-4}$), and 60 equivalent units of OEGMA (1.02 g, 3.41 x $10^{-3}$ mol) were added to a solution of PMPS(init)$_2$ (0.477 g, 5.68 x $10^{-5}$ mol) in THF (2 ml) (scheme **8.3**). The reaction mixture was degassed and heated to 65°C using an oil bath. After 24 hours, the reaction was allowed to cool and was then diluted with THF (3 ml). The mixture was then passed through alumina using THF as the eluent and precipitated into a 50/50 v/v mixture of propanol and *n*-hexane. The product was isolated and dried overnight under vacuum at 60 °C ($M_n$ = 21,000, $M_w/M_n$ = 2.1). $^1$H NMR ($CDCl_3$) δ: 6.2 – 7.2 ppm (Si-$C_6\mathbf{H_5}$); 4.1 ppm ($CO_2C\mathbf{H_2}CH_2O$-); 3.5 – 3.8 ppm (-$OC\mathbf{H_2}C\mathbf{H_2}$-); 3.35 ppm (-$OC\mathbf{H_3}$); 1.65 – 2.1 ppm (-$C\mathbf{H_2}C(CH_3)$-); 0.8 – 1.3 ppm (-$CH_2C(C\mathbf{H_3})$-); 0.1 – 1.1 ppm (Si-$C\mathbf{H_3}$). $^{13}$C NMR ($CDCl_3$) δ: 177 ppm (**C**=O); 127, 134 ppm (Si-$\mathbf{C_6}H_5$); 60 – 72 ppm (-$OCH_2\mathbf{C}H_2$-); 54 ppm (-$OCH_3$); 45 ppm (-$CH_2\mathbf{C}(CH_3)$-); 25 ppm (-$\mathbf{C}H_2C(CH_3)$-); 16 ppm (-$CH_2C(\mathbf{C}H_3)$-); -8 ppm (Si-$\mathbf{C}H_3$).

Several other reactions were carried out using similar procedures, and are summerised in table **8.2** [section 8.3.3].

## 8.3. Results and discussion

The synthesis of the ABA block copolymer involving PEO and PMPS via a condensation reaction had proved unsuccessful [chapter 5]. However, it was possible to synthesise a PMMA-PMPS-PMMA ABA block copolymer via ATRP [chapter 6]. Therefore, various PMPS macroinitiators were used to grow hydrophilic monomers, i.e. 2-hydroxyethyl methacrylate (HEMA) and oligo(ethylene glycol methyl ethyl methacrylate) (OEGMA), in order to form amphiphilic block copolymers. Different ligands were chosen in order to increase the solubility of the catalyst in the organic solvent (THF or xylene).

### 8.3.1. PMPS macroinitiators

A range of macroinitiators were synthesised and used in various experiments involving the polymerisation of hydrophilic monomers (table **8.1**). These macroinitiators were used in the copolymerisation reactions involving HEMA and OEGMA. The macroinitiators were synthesised and characterised in the same manner as described previously in chapter 6 [section **6.2.3**. (synthesis); section **6.3.1.4**. (characterisation)].

| **Macroinitiator** | **PMPS block** | | |
|---|---|---|---|
| | $\mathbf{M_n}$ | $\mathbf{M_w/M_n}$ | $\mathbf{DP_n}$ |
| PMPS **8** | 3 800 | 1.6 | 32 |
| PMPS **9** | 7 000 | 1.9 | 58 |
| PMPS **10** | 8 400 | 1.95 | 70 |

**Table 8.1.** Molecular weight characteristics for PMPS macroinitiators used in the block copolymerisation of HEMA and OEGMA

### 8.3.2. Poly(2-hydroxyethyl methacrylate-*block*-methylphenylsilane-*block*-2-hydroxyethyl methacrylate) (PHEMA-PMPS-PHEMA)

#### 8.3.2.1. Synthesis

A number of PHEMA-PMPS-PHEMA block copolymers were synthesised using different macroinitiator to monomer ratios, copper complexes, ligands, and solvents (table **8.2**). THF was used as the solvent in order to dissolve the PMPS macroinitiator, which was insoluble in HEMA. The PHEMA-PMPS-PHEMA copolymers were synthesised using a combination of either CuBr or CuCl with *N*-(n-propyl)-2-pyridyl(methanimine), 3-morpholyl-4-propyl-2-pyridylmethanimine, or 2-(2-pyridyl methanimine)aminoethoxyethanol ligands (scheme **8.3**).

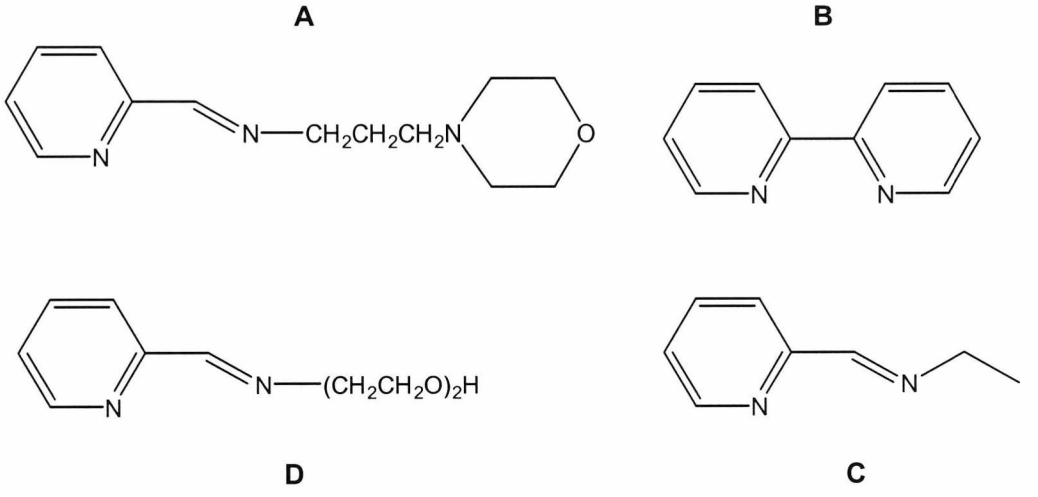


**Scheme 8.3.** (**A**) 3-morpholino-4-propyl-2-pyridylmethanimine, (**B**) 2,2-dipyridine, (**C**) N-(n-propyl)-2-pyridyl(methanimine), (**D**) and 2-(2-pyridyl methanimine)aminoethoxyethanol

Initial experiments involving CuBr and bipyridine were quite successful (e.g. PHEMA-PMPS-PHEMA **1**). However, in several reactions involving PMPS macroinitiators of higher molecular weight (i.e. above $M_n$ = 3,800), no change in molecular weight was observed and the reaction mixture seemed to be quite heterogeneous. Subsequently, an ATRP system involving CuCl and bipyridine was also attempted. The functional ligands, 3-morpholino-4-propyl-2-pyridylmethanimine and 2-(2-pyridyl methanimine)aminoethoxyethanol were used in order to aid the reaction by solubilising the copper catalyst in the organic media and creating a more

homogeneous reaction mixture. The ligand containing an organic alkyl chain, *N*-(n-propyl)-2-pyridyl(methanimine), was not successful at dissolving the copper catalyst. It has been shown previously that the polymerisation of HEMA using a CuBr and N-(n-propyl)-2-pyridyl(methanimine) complex is a more controlled and slower reaction compared to CuBr and 2,2-bipyridine mediated ATRP.[6]

Purification of the block copolymers proved very difficult, as the copper complex was not easily removed, especially in the case of copolymers formed using ligands with hydrophilic functional groups. Precipitation of samples containing relatively long PHEMA chains (i.e. COP **3**) was not possible at all, and so some monomeric material also remained.

In addition, ATRP of HEMA in methanol/water mixtures has previously afforded near-monodisperse polymers in high yields.[7] However, such a choice of solvent was not possible since the PMPS macroinitiator would be completely insoluble.

### 8.3.2.2. Molecular weight analysis

The copolymers were analysed using GPC, and on each occasion a shift in molecular weight is seen (fig. **8.3**). However, the increase in molecular weight never increased by more than an equivalent of about 20 HEMA units. Simultaneous GPC analysis using an RI detector as well as a UV detector (λ 334 nm) confirmed the presence of the copolymer. No PHEMA homopolymer was observed.

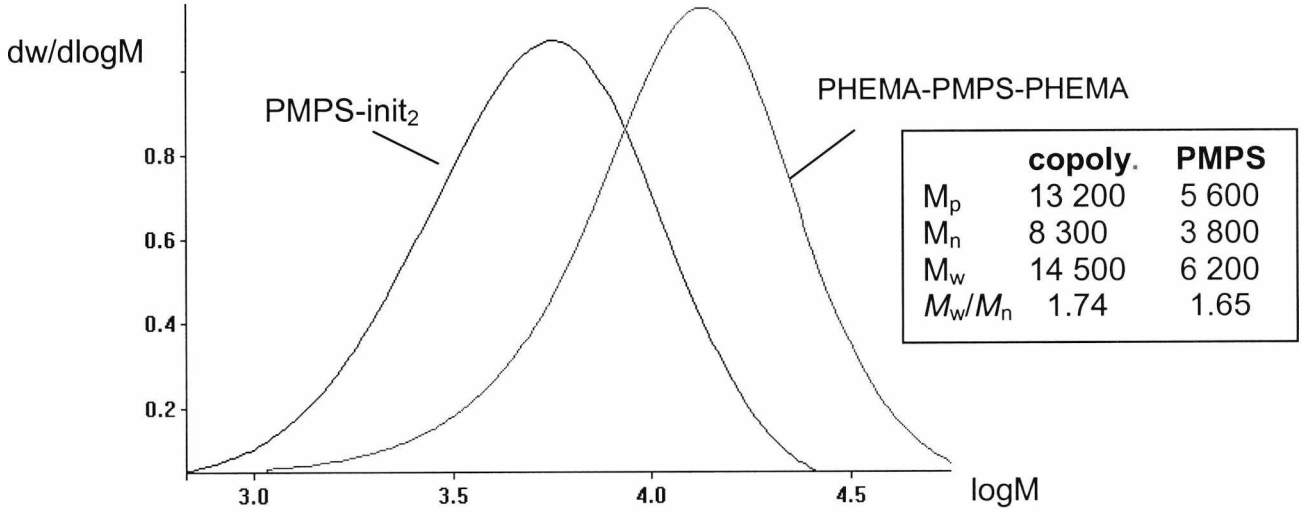


**Fig. 8.3.** dw/dlogM vs. logM plots of PMPS **8** and PHEMA-PMPS-PHEMA **1**. It is possible to conclude that the PHEMA blocks are an average of ~17 units in length ($M_n$ = 2,250).

| COP | Macroinit. | Conditions | | | Copolymer | | |
|---|---|---|---|---|---|---|---|
| | | $DP_n$* | CuX | ligand | $M_n$ | $M_w/M_n$ | $DP_n$+ |
| **1** | PMPS **8** | 40 | CuBr | bpy | 8 300 | 1.74 | 17 |
| **2** | PMPS **8** | 50 | CuCl | bpy | 6 600 | 1.5 | 11 |
| **3** | PMPS **8** | 40 | CuCl | morph | 9 600 | 1.5 | 22 |
| **4** | PMPS **8** | 20 | CuCl | bpy | 6 000 | 1.5 | 8 |
| **5** | PMPS **10** | 50 | CuCl | bpy | 10 300 | 1.9 | 7 |
| **6** | PMPS **10** | 30 | CuCl | ethoxy | 12 500 | 1.55 | 16 |

**Table 8.2.** Conditions for synthesis of PHEMA-PMPS-PHEMA (*theoretically and +experimentally determined using SEC data) (bpy = 2,2-bipyridine, morph = 3 morpholino-4-propyl-2-pyridylmethanimine, ethoxy = 2-(2-pyridyl methanimine)aminoethoxyethanol)

### 8.3.2.3. NMR Analysis

$^1H$ and $^{13}C$ NMR spectroscopy were used to confirm the structure of the PHEMA-PMPS-PHEMA copolymers. The $^1H$ NMR and $^{13}C$ NMR spectra of COP **6** is shown in fig. **8.4**. In this case, the COP **6** was precipitated quite easily in *n*-hexane to yield a copolymer, due to the relatively long PMPS chain. The monomer was successfully removed by this protocol, as evidenced in the NMR spectra. However, a green tint remained due to the copper, which could not be removed by passing through alumina.

| Copolymer | Hydrophilic block (GPC) | | | | Block ($^1H$ NMR) | |
|---|---|---|---|---|---|---|
| | $M_n$ | $M_w/M_n$ | $DP_n$ | %Yield | $M_n$ | $DP_n$ |
| COP **2** | 1 400 | 1.3 | 11 | 50% | 950 | 7 |
| COP **3** | 2 900 | 1.4 | 22 | 66% | 3 650 | 28 |
| COP **4** | 1 100 | 1.2 | 8 | 40% | | - |
| COP **5** | 950 | 1.7 | 7 | 35% | 650 | 10 |
| COP **6** | 2 050 | - | 16 | 50% | 2 250 | 17 |

**Table 8.3.** Comparison of molecular weight data derived from GPC and $^1H$ NMR studies of the PHEMA blocks.

The integral data taken from the $^{1}H$ NMR spectra were used to determine the relative block lengths of the segments involved and were compared to the GPC data (table **8.3**). In order for the amphiphilic copolymer to be dissolved for NMR analysis, a mixture of $CDCl_3$ and DMSO (80/20 v/v) was used.

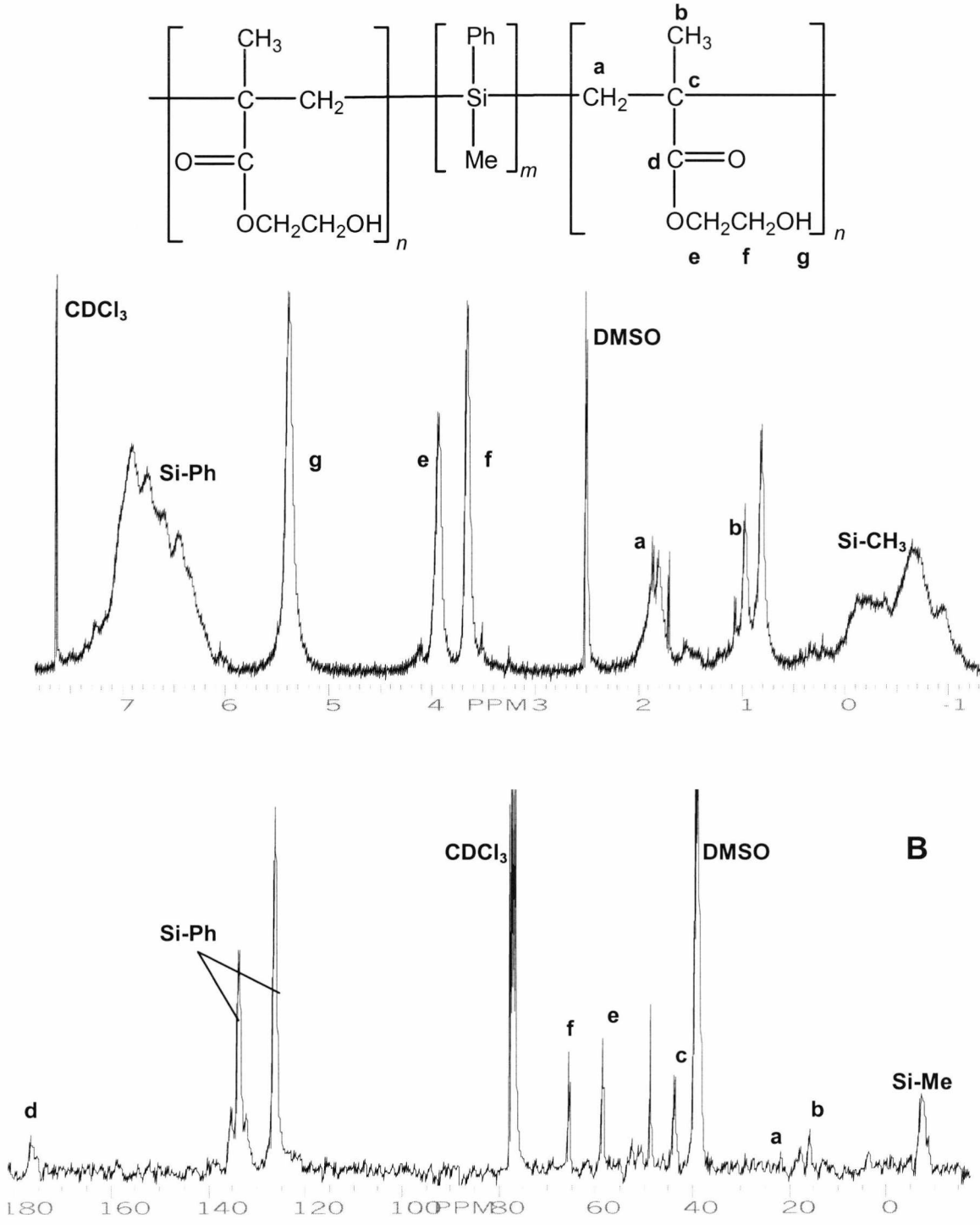


**Fig. 8.4.** $^{1}H$ NMR and $^{13}C$ NMR of PHEMA-PMPS-PHEMA **6**

In cases where the PHEMA chains were long compared to the PMPS segments (e.g. COP **3**), precipitation was not possible, and the product was recovered as a brown gel, while the remaining monomer was not removed. This is shown by the impurities in the $^1$H NMR of COP **3** (fig. **8.5**)

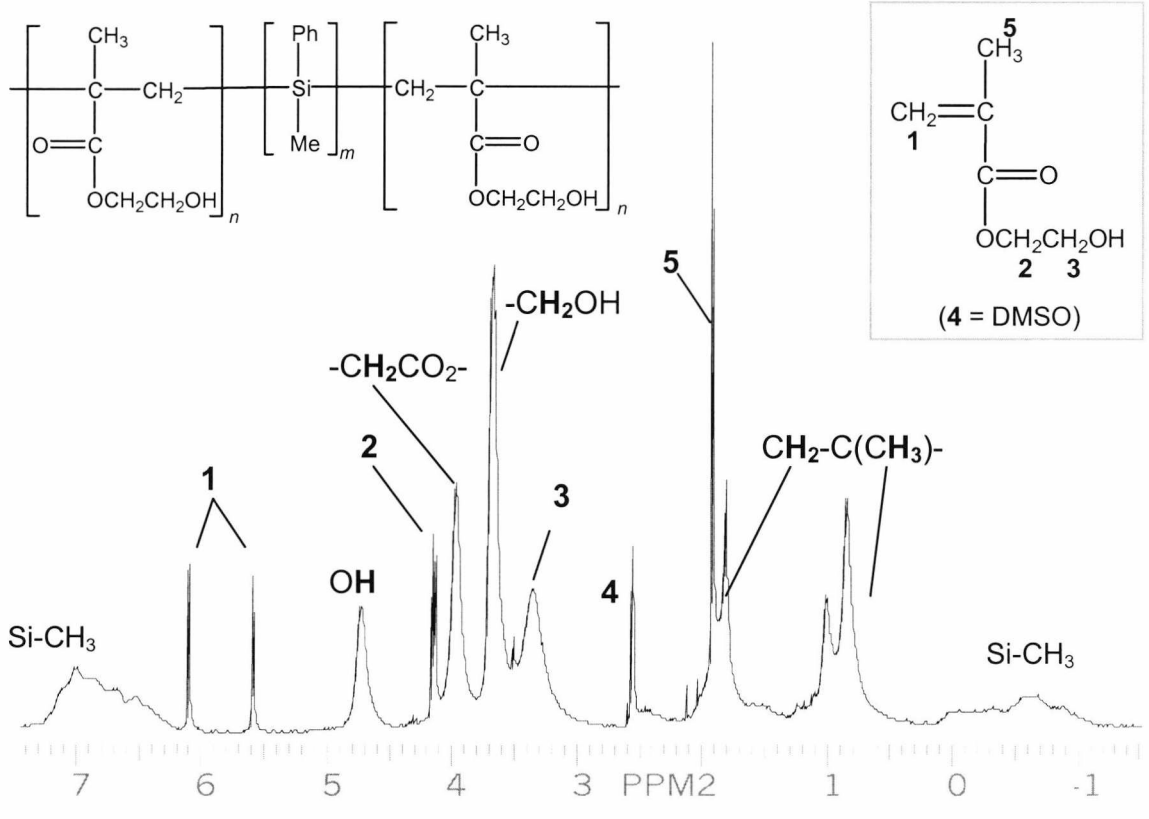


**Fig. 8.5.** $^1$H NMR of PHEMA-PMPS-PHEMA **3** mixture of $CDCl_3$ and DMSO (80/20 v/v).

### 8.3.2.4. Conclusions and Future Work

An amphiphilic block copolymer containing a polysilane block was synthesised using ATRP for the first time. A range of PHEMA-PMPS-PHEMA block copolymers were synthesised by ATRP using different copper catalyst complexes. Molecular weights were varied by using different PMPS macroinitiators. Although PHEMA blocks were successfully grown, control over molecular weights of the hydrophilic segments was not achieved as the monomer conversion was quite low in some cases. The most successful reactions which yielded the longest PHEMA chain lengths involved the use of the 3-morpholino-4-propyl-2-pyridylmethanimine and the 2-(2-pyridyl

methanimine)aminoethoxyethanol) ligands. Difficulties in the purification (via filtration and precipitation) remain, as evidenced by the colour of the sample, as well as the NMR spectra.

Future work should include attempts to purify these block copolymers further, as well as investigations into their thermal properties. It is possible that micelles form in THF once the HEMA segments reach a certain length, and this may cause the chains to stop growing. Aggregation behaviour is discussed elsewhere [chapter 9]. Also, further reactions of the PHEMA blocks via the functional hydroxy groups might be of interest with respect to grafting reactions since it has been shown that the hydroxyl groups attached to the substituents of polymers have been transformed into initiating sites for further polymerisation.[2] Furthermore, an alternative route for the synthesis of PHEMA-PMPS-PHEMA could involve the polymerisation of 2-trimethylsiloxyethyl-protected HEMA, followed by the deprotection of the functional groups. However, the PMPS chain would have to be able to withstand any deprotection reaction, which usually involves harsh acidic reaction conditions.

Further investigations into the effects of $CDCl_3$ and DMSO on the NMR spectra of the block copolymers would also be of interest.

### 8.3.3. Synthesis and characterisation of poly(oligoethylene glycol methyl ether methacrylate)-*block*-poly(methylphenylsilane)-*block*-poly(oligoethylene glycol methyl ether methacrylate) (POEGMA-PMPS-POEGMA)

#### 8.3.3.1. Synthesis

Several ATRP polymerisations were carried out using various PMPS macroinitiators (table **8.1** resulting in a range of POEGMA-PMPS-POEGMA block copolymers (table **8.5**). The OEGMA monomer ($M_n$ 300) contains hydrophilic side chains of an average of 4-5 repeat units in length.

In most of the reactions, CuCl and bipyridine were used. In each case, the reaction mixture was a brownish green colour. Purification of the copoolymer was achieved by filtering throuh alumina columns followed by precipitations into hexane. In all cases, a gel-like precipitate was recovered and dried. A green tint, due to the copper species, remained in most cases. It is believed the hydrophilic segments are responsible for partially solubilising the copper complex, and therefore are not completely removed by passing the polymer solution through alumina.

A different ligand, 2-(2-pyridyl methanimine)aminoethoxyethanol was also used, to observe how homogeneity of the system affected yield and conversion.

#### 8.3.3.1. Molecular weight analysis

The copolymers were analysed using GPC, an example of which is shown in fig. **8.6**. On each occasion a shift in molecular weight is observed, resulting in a monomodal distribution.

The same reaction was repeated several times, each time varying the length of the macroinitiator, the macroinitiator to monomer ratio, the copper complex (CuBr or CuCl), and the type of ligands (*N*-(n-propyl)-2-pyridyl(methanimine), 2,2-dipyridine, 3-morpholino-4-propyl-2-pyridylmethanimine, and 2-(2-pyridyl methanimine)amino-ethoxyethanol).

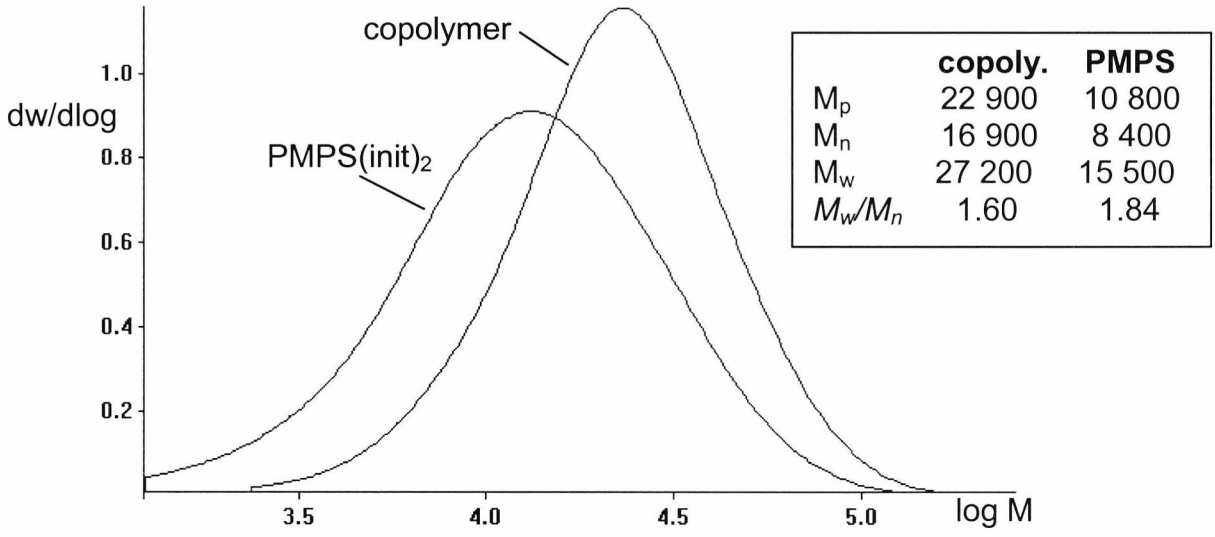


**Fig. 8.6.** dw/dlogM vs. logM overlays of PMPS **10** and POEGMA-PMPS-POEGMA **11**. From the GPC data it can be deduced that POEGMA segments are ~14 units ($M_n$ 4 250) long

| Cop | Macroinit. | Conditions | | | Copolymer | | |
|---|---|---|---|---|---|---|---|
| | | $DP_n$* | CuX | ligand | $M_n$ | $M_w/M_n$ | $DP_n^+$ |
| **7** | PMPS **8** | 30 | CuCl | bpy | 11 100 | 1.85 | 12 |
| **8** | PMPS **8** | 20 | CuCl | bpy | 12 600 | 1.8 | 15 |
| **9** | PMPS **8** | 10 | CuCl | bpy | 10 900 | 1.5 | 12 |
| **10** | PMPS **9** | 25 | CuCl | bpy | 18 700 | 1.75 | 19 |
| **11** | PMPS **10** | 30 | CuCl | bpy | 16 900 | 1.6 | 14 |
| **12** | PMPS **10** | 30 | CuCl | ethoxy | 21 000 | 2.1 | 21 |

**Table 8.5.** GPC determined molecular weight characteristics of POEGMA-PMPS-POEGMA copolymers (*theoretical/$^+$GPC determined degree of polymerisation) (bpy = 2,2,-bipyridine; ethoxy = 2-(2-pyridyl methanimine)aminoethoxyethanol)

### 8.3.3.2. NMR Analysis

$^1$H and $^{13}$C NMR analysis confirmed the structure of the copolymers (fig. **8.7**). $^1$H NMR integral data was used to determine the block lengths of the POEGMA segments and were compared to the block lengths determined via GPC (table **8.6**).

From the $^{1}H$ NMR data, it is evident that the relative units of POEGMA compared to PMPS are consistently higher than the number of units determined via SEC. This is expected in view of the fact that POEGMA has long side chains, and does not behave like either PMPS or PS in THF.

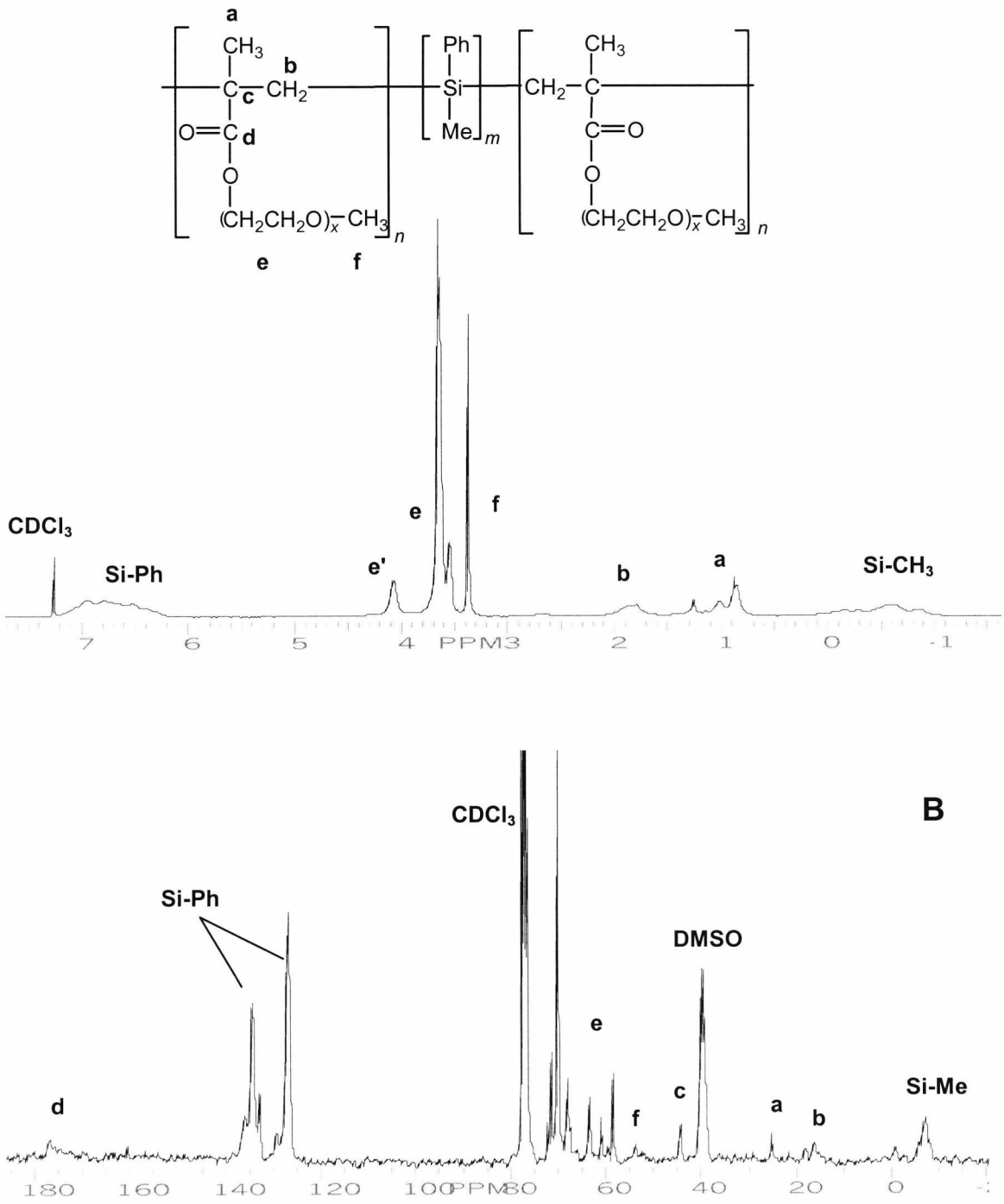


**Fig. 8.7.** (A) $^{1}H$ NMR and (B) $^{13}C$ NMR spectra of POEGMA-PMPS-POEGMA **10**. (e' is the $CH_2$ next to the ester group. DMSO was used as well as $CDCl_3$ in $^{13}C$ NMR spectrum).

| Copolymer | Hydrophilic block (GPC) | | | Block ($^1$H NMR) | |
|---|---|---|---|---|---|
| | $M_n$ | $M_w/M_n$ | $DP_n^+$ | $M_n$ | $DP_n$ |
| PMPS-POEGMA**7** | 3 650 | 1.95 | 12 | 4 200 | 14 |
| PMPS-POEGMA**8** | 4 400 | 1.85 | 15 | 6 900 | 23 |
| PMPS-POEGMA**9** | 3 550 | 1.4 | 12 | - | - |
| PMPS-POEGMA**10** | 5 850 | 1.7 | 19 | 7 800 | 26 |
| PMPS-POEGMA**11** | 4 250 | 1.3 | 14 | 5 400 | 18 |
| PMPS-POEGMA**12** | 6 300 | 2.3 | 21 | 8 700 | 29 |

**Table 8.6.** GPC determined molecular weight characteristics of the OEGMA blocks and comparison with $^1$H NMR values

### 8.3.3.3. Conclusions and Future work

A range of amphiphilic POEGMA-PMPS-POEGMA block copolymers were successfully synthesised for the first time using ATRP.

Future work might involve the use of different functional ligands in the synthesis of POEGMA-PMPS-POEGMA, while percentage conversion data and kinetic studies need to be investigated. Thermal analysis of these samples would also be of interest. In addition, the length of the OEGMA side chains could be varied (e.g. OEGMA with $M_n$ = 450 contains ethylene oxide side chains of 7-8 units long). Also, the POEGMA blocks involved here contain methoxy-capped ethylene glycol side chains; hydroxy-functionalised OEGMA could also be used.

## 8. References


[1] Muhlenbach, A.; Gaynor, S.G.; Matyjaszewski, K. *Macromolecules* **1998**, 31, 6046.

[2] a) Ma, Q.C.; Wooley, K.L. *J. Polym. Sci., Polym. Chem.* **2000**, 38, 4805.

b) Cheng, G.L.; Boker, A.A.; Zhang, M.F.; Krausch, G.; Muller, A.H.E. *Macromolecules* **2001**, 34, 6883.

c) Matyjaszewski, K.; Miller, P.J.; Shukla, N.; Immaraporn, B.; Gelman, A.; Luokala, B.B.; Sicloran, T.M.; Kickelbick, G.; Vallant, T.; Hoffman, H.; Pakula, T. *Macromolecules* **1999**, 32, 8716.

[3] a) Reining, B.; Keul, H.; Hocker, H. *Polymer* **1999**, 40, 3555.

b) Reining, B.; Keul, H.; Hocker, H. *Polymer* **2002**, 42, 7145.

[4] Zhang, L.; Yu, K.; Eisenberg, A. *Science* **1996**, 272, 1777.

[5] Wang, X.S.; Malet, F.L.G.; Armes, S.P.; Haddleton, D.M.; Perrier, S. *Macromolecules* **2001**, 34, 162.

[6] Haddleton, D.M.; Kukulj, D.; Duncalf, D.J.; Heming, A.M.; Shooter, A.J. *Macromolecules* **1998**, 31, 5201

[7] Robinson, K.L.; Khan, M.A.; de Paz-Banez, M.V.; Wang, X.S.; Armes, S.P. *Macromolecules* **2001**, 34, 3155.

# 9. Further investigations of amphiphilic block copolymers

## 9.1. Introduction

Recently, interest in amphiphilic block copolymers (ABCs) has intensified due to their aggregation behaviour in solution and corresponding potential applications in biochemistry [chapter 4]. Here, the properties and possible applications of the polysilane ABCs synthesised previously [chapter 8] are discussed. In particular, preliminary experiments were carried out to investigate the suitability of the block copolymers for applications in three areas of research – drug delivery systems, cell growth, and bioelectronics. Firstly, investigations into the behaviour of the block copolymers in water and the type of aggregates formed were observed. The photodegradation of the polysilane segments of the aggregates was also investigated, with a view to possible applications as chemical delivery vehicles. Secondly, thin films were prepared on gold and glass substrates for experiments involving cell growth on monolayers. Finally, conductivity measurements on thin films for possible applications in bioelectronics were investigated. A brief introduction for each application is given.

### 9.1.1. Amphiphilic block copolymers as drug delivery vehicles

Research into new drug delivery systems (DDS) is driven by the need to maximise the therapeutic activity of the drug, whilst also minimising any harmful side effects. Micelle-forming ABCs are an important class of compound in DDS and have recently been developed as long-circulating drug vehicles.[1] The block copolymers involved are of interest since hydrophobic drugs can be physically trapped inside the hydrophobic core of the micelle and then transported at concentrations higher than would be possible in an aqueous medium. In such cases, the hydrophilic segments form a tight shell around a central micellar core. ABCs are especially useful as in DDS because the size and the morphology of the micelles can be controlled by altering the chemical properties and compositions of the blocks involved.[2]

The hydrophilic section of ABCs used in DDS is most commonly made up of poly(ethylene oxide) (PEO), which is a non-toxic, highly hydrated polymer.[1] PEO is

often used in blood-contacting biomaterials and contact lenses, as well as chromatography. The PEO segment in copolymers can hydrogen bond with the aqueous solution forming the corona around the core. The corona of PEO aggregates are capable of avoiding being sequestered by the reticuloendothelial system (RES) and can deliver drugs more effectively to sites such as solid tumours.[3] PEO is effective because it prevents the binding of proteins, such as immunoglobins, that identify DDS's as foreign bodies. It also prevents the adhesion of drug vehicles onto the surface of phagocytes, cells that "digest" bacteria, foreign invaders, and dead cells. The reticuloendothelial system is a diffuse system of phagocytic cells derived from the bone marrow stem cells that are associated with the connective tissue framework of the liver, spleen, lymph nodes and other serious cavities.

PEO block copolymer micelles (such as those formed by combining PEO with a poly(amino acid)[1]), contain cores which can act as a reservoir for drugs that are stabilised against chemical modification. Both AB and ABA block copolymers (where A=PEO) can be used to form such micelles. The 'stealth' qualities of the PEO corona leads to an increase in blood circulation time and allows the drugs to be administered over a period of time. The effectiveness of systems in terms of drug delivery can be measured by the extent of temporal and distribution control.[4] Temporal control involves being able to adjust either the period of time over which the drug is released or to be able to trigger a release at a given time. Distribution control is the extent to which the DDS can be directed to the desired site of activity.[5]

### 9.1.2. Orientation and alignment of cells on substrates

Part of the research into cell culture technology is known as micro patterning and involves controlling the growth and alignment of cells on various topologies.[6] Usually, a monolayer of cells is cultured on a hydrophilic surface in order to study the effects of topology. Different cells will react differently to various topologies, which can be determined using micro- and nanotechnology. The majority of research currently undertaken is on groove-ridge topographies in order to reproduce the topology of the *in vivo* conditions. An area of debate within such micro patterning studies stems from whether or not the alignment of cells is due to the topographical or chemical properties of the substrate surface.[7]

### 9.1.3. Bioelectronics and bioelectronic sensors

Interest in bioelectronics has been progressing rapidly in recent years and is an area of research that combines chemistry, biochemistry and physics.[8] Interest in the electrochemistry of biomaterials at electrode surfaces has led to the development of bioelectronic devices. These devices involve the immobilisation of a biomaterial onto a (semi-)conducting support and the electronic transduction of biological processes involved with the biological matrices.[9] The combination of a redox enzyme immobilised onto an electrode support to form an electrical contact gives rise to a variety of applications in bioelectronics and opticobioelectronics.[10] These bioelectronic devices can be used in amperometric biosensors, sensoric arrays, logic gates, and optical memories. The biomaterials most commonly used include proteins such as enzymes, as well as lower molecular weight molecules that exhibit affinity with other biomaterials. The biological processes can be turned into a variety of electronic signals that are transferred to the electrode. The electronic transduction that occurs between the enzyme and the substrate provides a way of detecting the concentration of the substrate, leading to the development of enzyme-based biosensor devices. However, the enzyme is incompatible with the hard inorganic electrode, and so denaturation occurs.[11] Polymers have been used to immobilise enzymes onto electrode supports, although this has led to an ineffective transfer of electrons between the redox-active centre and the electrode surface. More recently, redox active polymers have been used to immobilise the enzyme using three different approaches: (a) entrapment of biomolecules during polymerisation;[12] (b) electrostatic interactions between the enzyme and the polymer matrix;[13] and (c) covalent coupling of the polymer and the enzyme via functional groups on the polymer.[14]

## 9.2. Experimental

### 9.2.1. Materials and Apparatus

*Materials*

ABCs (POEGMA-PMPS-POEGMA and PHEMA-PMPS-PHEMA) were synthesised as described previously [section 8.2]. Glucose, glucose oxidase (*Aspergillus niger*), uranyl acetate dihydrate (dye, Acros), and calceine (flourexon trisodium salt, indicator grade, Acros) were used as received. Dialysis was carried out against de-ionised water using dialysis membranes with an exclusion limit of approximately 10 000.

*Microscopy*

Transmission Electron Microscopy was carried out using a JEOL JEM (200-FX) operating at 120 kV. Scanning Electron Microscopy was carried out using a Cambridge Stereoscan S-200. Samples were deposited onto copper grids (200 mesh, C covered) prior to analysis.

*Optical and size measurements*

UV degradation was carried out using a Shimadzu Photodiode Array Spectrophotometer Multispec-1501 (Deuterium and Tungsten lamps).

Gel permeation chromatography (GPC) was carried out at room temperature using a 600 mm x 5 mm mixed D Plgel column with THF as eluent at a flow rate of 1 ml $min^{-1}$, and a Knauer variable wavelength UV detector in series with a refractive index detector. Aqueous GPC was performed on an uncalibrated Waters 590 GPC, with a UV detector set at 210 nm, 270 nm, and 334 nm.

*Electrochemical measurements*

Indium tin oxide (ITO) plates were prepared and cleaned previously by F. Brustolin at the Technical University of Eindhoven. ITO-coated glass plates were cleaned by sonication (10 min.) in acetone before spin coating. Cyclic voltammetry and amperometry experiments were carried out in a cell designed by F. Brustolin at the Technical University of Eindhoven. The cell consisted of a working electrode involving a Pt wire attached to an ITO plate, a Pt counter electrode plate, an Ag/AgCl reference electrode, and a phosphate buffer solution (0.1M, pH 7) as the electrolyte

solution (fig. **9.1**). The cell was wrapped in foil in order to protect the films from photochemical degradation. A similar cell with an electrolyte solution of dichloromethane and tetrabutylammoniumhexafluorophosphate ($TBAPF_6$) was also used.

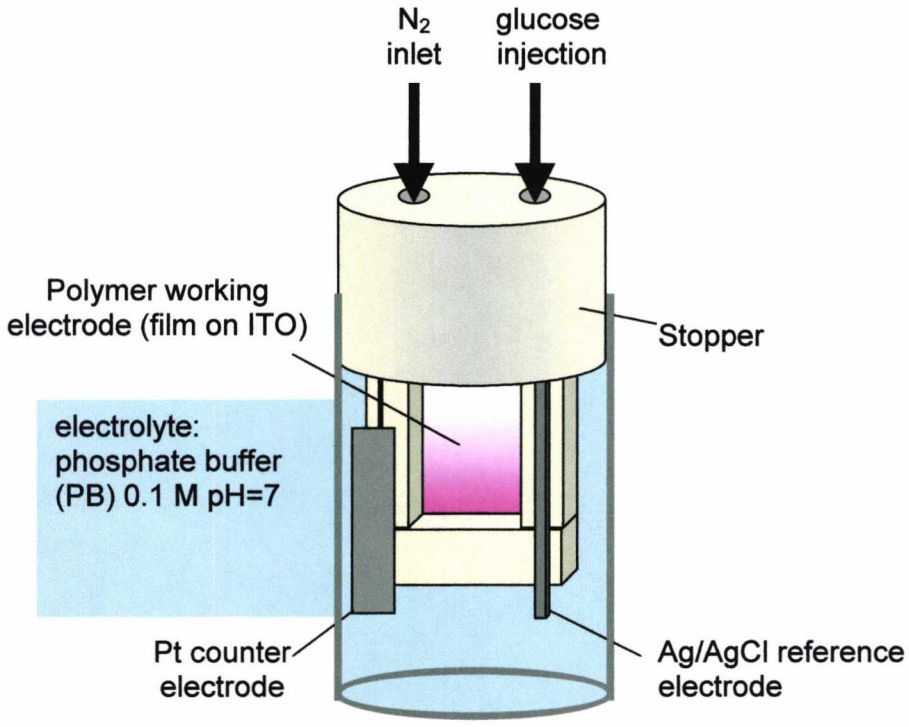


**Fig. 9.1.** Representation of the cell used for voltammetry and amperometry (Reprinted with permission from Fiorella Brustolin)

### 9.2.2. Aggregation of block copolymers in water

In total, six copolymer samples underwent dialysis and were analysed using TEM and SEM. These samples were PHEMA-PMPS-PHEMA copolymers **2** & **6**; POEGMA-PMPS-POEGMA copolymers **7**, **8**, **9**, & **12**).

#### 9.2.2.1. Dialysis

A sample of copolymer (20 mg) was dissolved in THF (2 ml) before water (8 ml) was added drop-wise over a one-hour period. The samples were transferred to dialysis 'bags' and dialysed against water for 24 hours, away from any sources of UV light.[15]

The water in the beaker (3 L) surrounding the bags was replaced three times. After dialysis, the samples were transferred to vials, sealed and stored in the dark.
A second set of experiments involved the incorporation of a dye into the procedure. A sample of copolymer (5.0 mg) was dissolved in THF (0.5 ml) prior to the drop-wise addition of an aqueous solution of calceine (1.5 ml, 0.200 mol $dm^{-3}$) and then water (1.5 ml). Dialysis was carried out as before. The water surrounding the dialysis bags was replaced several times over a 24 hour period.

#### 9.2.2.2. Transmission Electron Microscopy (TEM)

Small drops of the aqueous solutions of the block copolymers were deposited onto copper grids in order to view the samples using TEM. Two grids were prepared for each sample. The first grid was prepared by depositing a 20 μl drop on the grid, after which the drop was removed almost immediately using filter paper. The second grid was prepared in the same way, except that the droplet was allowed to remain on the grid for sixty seconds prior to its removal. The grids were then wrapped in foil and left overnight to dry under vacuum in a dessicator.
Further TEM experiments led to the grids (which had been prepared and analysed previously) being stained using uranyl acetate dihydrate ($C_4H_6U{\cdot}H_2O$) (1% w/v in water). This staining agent (20 μl) was dropped onto the each of the grids and left for 30 seconds. Excess stain which had not been soaked up by the grids was then removed using filter paper and the grids were dried overnight under vacuum in a dessicator at room temperature.

#### 9.2.2.3. Scanning Electron Microscopy (SEM)

The samples prepared for TEM were also used for SEM analysis.

### 9.2.3. UV degradation of aqueous solutions of the block copolymers

Solutions were taken from the dialysed samples prepared previously and diluted in water (10% v/v in water) to obtain an absorbance (at 334nm) of approx. 0.8. UV spectra were recorded over time as the UV lamp continuously irradiated the block

copolymer samples. A time scan was run for each of the samples for 2 - 4 h runs in order to monitor degradation at both 270 nm and 334 nm. Two methods were used to achieve irradiation. Firstly, the copolymers were degraded using a wavelength set at either 334 nm, 270 nm, or 210 nm. Secondly, using a wavelength range via a diode lamp, polymer degradation was also investigated. After degradation had occurred, the copolymers were analysed via aqueous GPC. Water from the irradiated POEGMA-PMPS-POEGMA **8** sample was removed under reduced pressure at 70°C, and dissolved in THF, and analysed via GPC using THF as the eluent.

### 9.2.4. Cell growth experiments

#### 9.2.4.1. Contact angle measurements

POEGMA-PMPS-POEGMA **8** was dissolved in THF and spun onto a substrate of gold, glass, or glass with lines of gold. A water droplet was deposited on to the film and after two seconds, a picture was taken of the droplet. The contact angle was measured from the inner angle between the droplet and the substrate surface. In the case of the thin film deposited on the substrate with lines of gold, two similar procedures were carried out. Pictures were taken as a water droplet was deposited onto the gold and glass areas of the substrate, with the lines of gold either parallel or perpendicular to the line of sight of the camera.

#### 9.2.4.2. Cell growth

Thin films were prepared for cell growth experiments using a solution of POEGMA-PMPS-POEGMA **8** (15.9 mg, $M_n$ = 12,600, $M_w/M_n$ = 1.8) in 3 ml of THF. The films were spun onto a number of substrates including glass, gold, and gold-patterned glass. The thin films were then immersed in a glucose solution and cell culture experiments were carried out (Appendix **9.1**).

### 9.2.5. Cyclic voltammetry and amperometry

#### 9.2.5.1. Preparation of thin films on ITO plates

Solutions of POEGMA-PMPS-POEGMA **8** were cast onto ITO plates in preparation for voltammetry and amperometry experiments. In some cases, an enzyme, glucose oxidase, was incorporated into the solutions. Films were cast from either pure THF, or from water/THF mixtures in ratios (v/v) of 90/10 or 70/30. A typical procedure is described here.

A solution of POEGMA-PMPS-POEGMA **8** (0.10 ml, 3.97 x $10^{-4}$ moldm$^{-3}$) in THF was added to an aqueous solution of glucose oxidase (0.90 ml, 6.25 x $10^{-6}$ moldm$^{-3}$). The solution was then used to spin coat the ITO plates, ensuring the film was spread uniformly to the edges of the plate. The films were aged for 3 h in the fridge (0°C).

#### 9.2.5.2. Cyclic Voltammetry

Preliminary cyclic voltammetry experiments were performed on POEGMA-PMPS-POEGMA films cast from pure THF onto ITO plate electrodes. Dichloromethane with $TBAPF_6$ was employed as the electrolyte solution. The sample was cycled several times at a scan rate of 100 mV/s, and a scan window for the solution of dichloromethane and ranged from -1.7 to 2.0 V. In experiments using thin films cast from glucose oxidase solutions, a buffer solution was used. The solution of the cell was degassed for more than one hour using nitrogen. Glucose was then injected into the cell. After several minutes the potential was measured at a scan rate of 100 mV/s within a scan window of –1 to 1 V. Cycling was repeated several times.

#### 9.2.5.3. Amperometry

A constant potential of 900 mV (first oxidation wave) was used for amperometry experiments. Once the solution had stabilised, i.e. no further change in current observed, glucose (2.0 mmol dm$^{-3}$) was injected into the buffer solution and the change in current measured. The procedure was repeated several times, with various concentrations of glucose injected each time (mmol dm$^{-3}$): 4.0, 6.0, 8.0, 16.0, & 24.0.

## 9.3. Results and Discussion

### 9.3.1. Aggregation Behaviour

A number of block copolymer samples (table **9.1**) were chosen to see whether or not they would form aggregates. After dialysing the samples, a slightly milky cloudiness, indicative of aggregation or precipitation of the copolymers, could be seen in each of the samples, with some containing crystal-like flakes.

#### 9.3.1.1. Transmission electron microscopy (TEM)

TEM was used to examine the size and types of aggregates formed by the various different samples (Appendix **9.2**). Some typical pictures are shown in fig. **9.2** and fig. **9.3**. Several different types of aggregation were observed, including micelles, vesicles and plate-like aggregates, which seemed to display crystalline character (table **9.1**). Negative staining of the grids was carried out to try to improve the visibility of aggregates such as vesicles and micelles, although improvement was negligible.

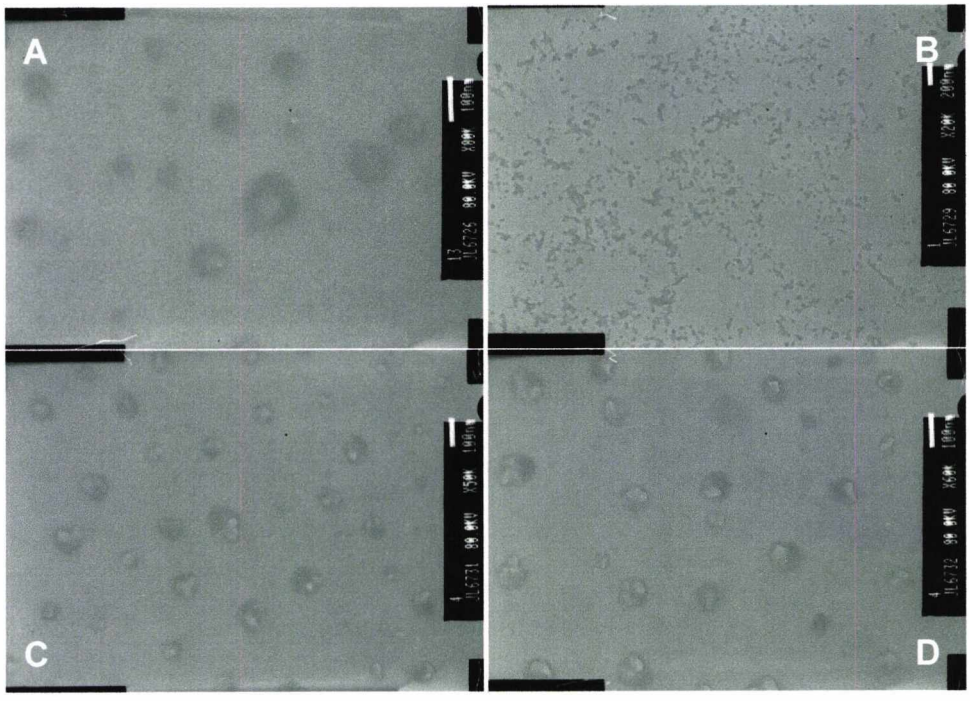


**Fig. 9.2.** TEM of samples of (**A**) POEGMA-PMPS-POEGMA **12**, (**B**) PHEMA-PMPS-PHEMA **2**, and (**C, D**) POEGMA-PMPS-POEGMA **8**.

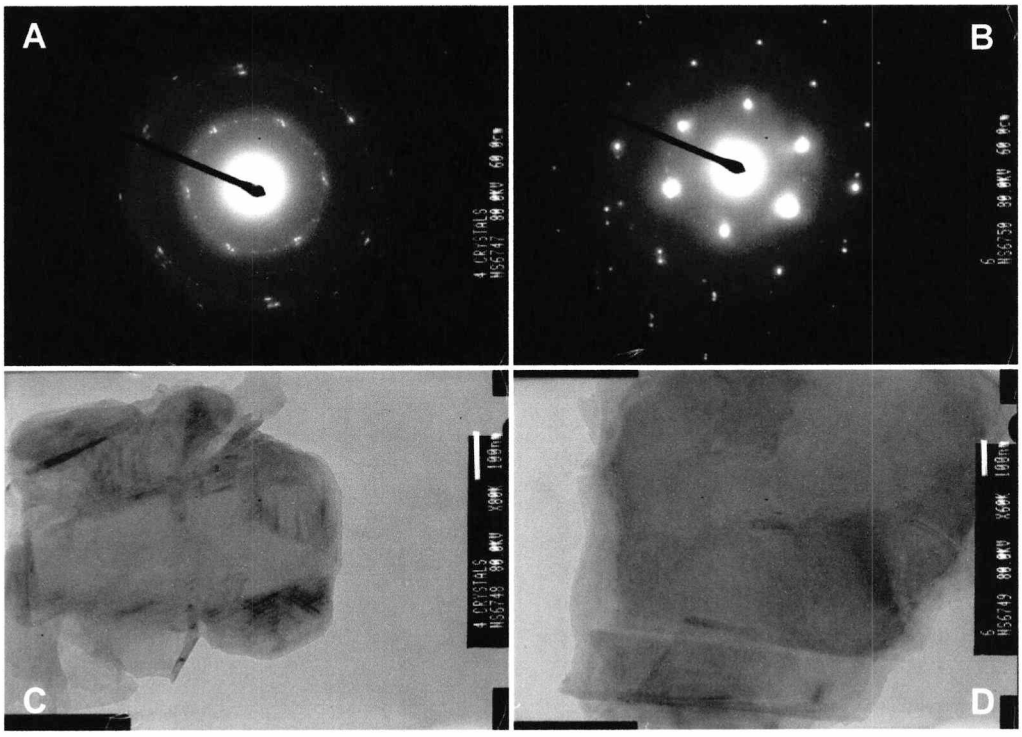


**Fig. 9.3.** TEM of (**A, C**) POEGMA-PMPS-POEGMA **8** and (**B, D**) POEGMA-PMPS-POEGMA **9** with corresponding electron diffraction patterns.

In a number of cases, both micellar and possibly vesicular-type aggregates were observed. The most common type of aggregation observed involved micelles, as shown in fig. 9.2.B. The contrast between a lighter central area, possibly corresponding to the core, and a darker outer area indicative of a corona suggests vesicular aggregates of approximately 100 nm in diameter were also observed. In fig. 9.2, pictures A (POEGMA-PMPS-POEGMA **12**), C and D (POEGMA-PMPS-POEGMA **8**) show this same kind of aggregation behaviour. Large plate-like crystals, possibly lamellae, were also observed in some cases. Representations of the expected micellar, vesicular, and lamellar structures are shown in fig. **9.4**. If the lengths of the Si-Si bonds are ~2.3 Å and the C-C bonds are ~1.5 Å, then the lengths of the copolymers should be of the order of 10-20 nm. Hence, the aggregates observed as being 10-20 nm in diameter are most probably micelles, while the aggregates with diameters greater than 100 nm could be vesicular.

Electron diffraction patterns were also measured, revealing hexagonal patterning throughout. Although usually described as amorphous, PMPS has been shown to have 10% crystallinity at room temperature, and to have diffraction patterns indicative

of a lattice of near-hexagonal symmetry.[16] However, a mesophase such as this is usually associated with the more crystalline alkyl-substituted polysilanes.[17] For example, poly(di-*n*-hexylsilane) undergoes transition from the crystalline to hcm phase as it is heated above 43°C.[18]

In addition, it was noted that, as the electron beam was directed towards the various aggregates, they became lighter. It appeared as if the aggregates were beginning to degrade.

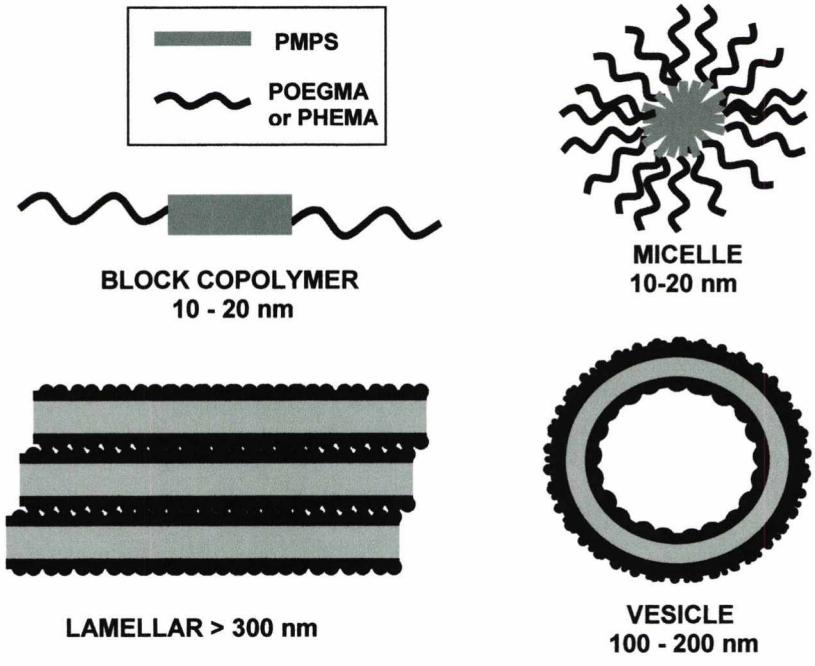


**Fig. 9.4.** Possible types and dimensions of aggregates observed via electron microscopy

Sommerdijk *et al.*[19] have already observed the formation of vesicles by a PMPS-poly(ethylene oxide) multi-block copolymer (diameter: 100-180 nm) [see section 5.1.5.1]. Sakurai and co-workers[20] have also described aggregates formed by amphiphilic poly(methyl-*n*-hexyl)silane (PHMS) di-block copolymers [see section 5.1.5.2]. Micelles of 50-60 nm in diameter (determined by AFM) were formed from methanol solutions of a di-block copolymer of PHMS and PHEMA ($M_n$ = 18,000, $M_w/M_n$ = 1.8). In addition, micelles with either hydrophilic or hydrophobic cores were formed, depending on the solvent to which the polymer was added.

| Copolymer | PMPS block ($M_n$)* | Hydrophilic block ($M_n$)* | TEM | SEM |
|---|---|---|---|---|
| PMPS-(PHEMA)$_2$ **2** | 3 800 | 1 400 | Aggregated clusters, some micelles ~10-20 nm | Micelles/vesicles 50-100(?) nm |
| PMPS-(PHEMA)$_2$ **6** | 8 400 | 2 050 | Not many aggregates except for a few micelles 10-20 nm | Crystals 20-50 μm, micelles 50-100 nm |
| PMPS-(POEGMA)$_2$ **7** | 3 800 | 3 650 | Mainly plate-like w/ vesicles, micelles 50-100 nm | - |
| PMPS-(POEGMA)$_2$ **8** | 3 800 | 4 400 | Plate-like 300-1000 nm. Possible micelles, vesicles | - |
| PMPS-(POEGMA)$_2$ **9** | 3 800 | 3 550 | Plate-likes ~ 600 nm. Clusters, ill-defined aggregates | micelles and vesicles 1-2 μm |
| PMPS-(POEGMA)$_2$ **12** | 8 400 | 6 300 | Possible vesicles 50-100 nm. Several micelles 10-20 mm | micelles 50-100 nm, crystals 5-10 μm |

**Table 9.1.** TEM analysis of aggregates of PMPS block copolymers (*$M_n$ determined via GPC analysis [section 8.3])

### 9.3.1.2. Scanning electron microscopy (SEM)

Representive SEM images are shown in fig. **9.5**, while a summary of observed aggregates are described in table 9.1. For the most part, SEM analysis revealed aggregates such as micelles (fig. 9.5.A, fig. 9.5.C) and crystalline material (fig. 9.5.B, fig. 9.5.D). The aggregates in pictures A and C are approximately 100 nm in diameter, and may be micellar. Although they may appear to be ellipsoidal, this is not the case and is instead due the particles being slightly out of focus. The discrepancy in the size of the micelles compared to TEM may be due to the fact that particles often appeared more blurred in the SEM. In addition, the resolution of the SEM was not as good as that of the TEM, and therefore it is possible that smaller particles may not have been observed.

The image shown in B was observed quite frequently in a number of samples, and resembles a burst vesicle. Large crystals were also observed, much like those observed using TEM.

The type of aggregates observed in both TEM and SEM are indicative of ABCs. It is possible that the formation of spherical aggregates demonstrates that organic molecules may be transported in their interior. However, since vesicles were not observed throughout, perhaps an alternative approach to the formation of aggregates in water is required.

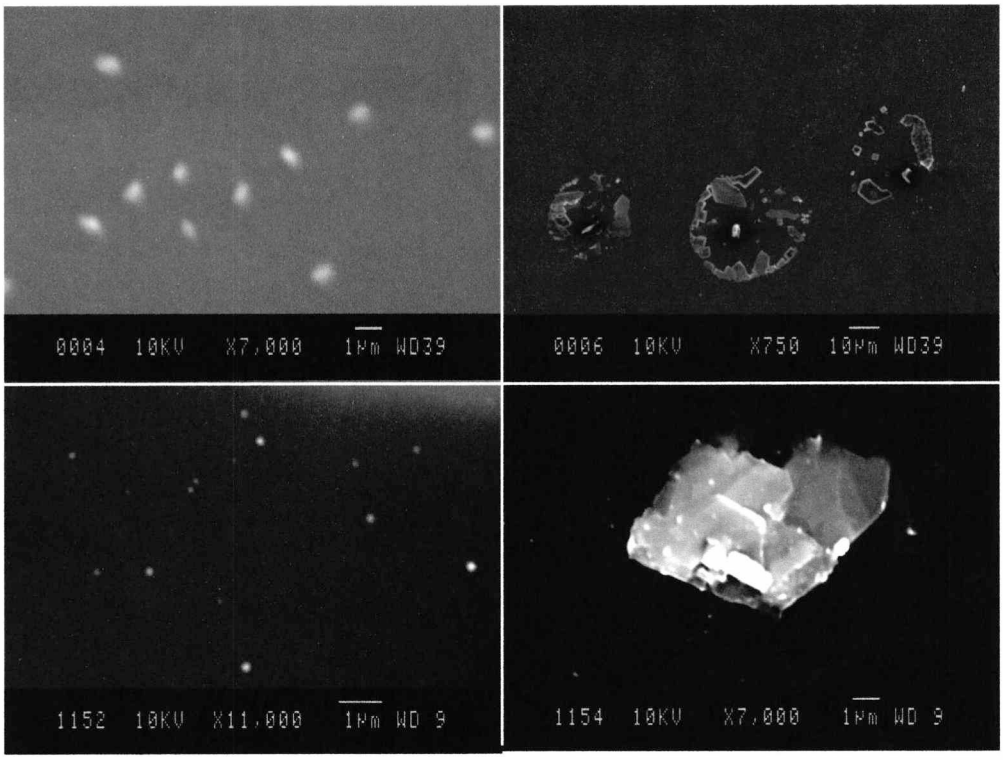


**Fig. 9.5.** SEM analysis of (**A**, **B**) PHEMA-PMPS-PHEMA **6** and (**C**, **D**) POEGMA-PMPS-POEGMA **12**.

### 9.3.2. Photodegradation of the aggregates in water

Polysilanes are photolabile and undergo photodegradation reactions primarily via photoscission in the presence of UV light [section 1.6]. In previous studies, the multi-block copolymer, $PMPS_m$-$PEO_n$, was UV irradiated at 360 nm.[21] Measurements

involving surface-pressure isotherms confirmed that the PMPS segments had been degraded. The products most likely to be formed upon photolysis of the PMPS block in aqueous media include a variety of hydrolysis products, including silanols and oligosilane fragments.[21] Sakurai and co-workers have formed shell cross-linked micelles involving polysilane (PHMS) cores [section 5.1.5.3].[22] A continuos blue-shift in the UV absorption spectra occurred as the shell cross-linked micelles were degraded using UV light (> 280 nm) to produce hollow micelles.

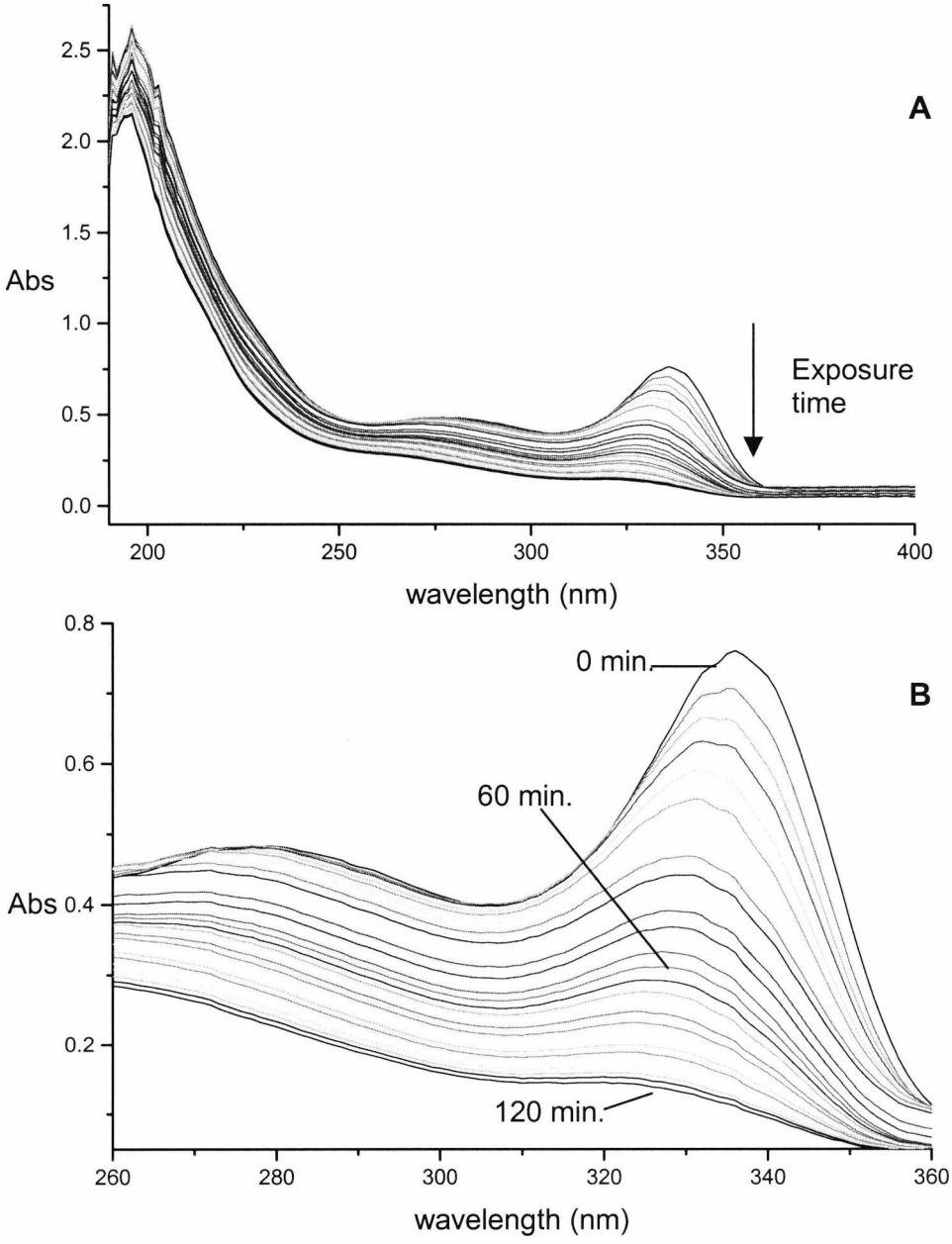


**Fig. 9.6.** UV spectra overlay (**A**) as POEGMA-PMPS-POEGMA **6** is irradiated for 2 hours and (**B**) a more detailed plot highlighting the relevant $\sigma-\sigma^*$ and $\sigma-\pi^*$ absorptions.

The aggregated samples of POEGMA-PMPS-POEGMA and PHEMA-PMPS-PHEMA were irradiated using a diode UV lamp (wavelength range of 180 nm to 450 nm). The effect of irradiation on the PMPS block copolymers was followed by measuring the absorptions at five minute intervals over a two hour period. By measuring the changes in the UV spectra of the block copolymers at five minute intervals it was possible to follow the effects of irradiation of the samples in water. An example of copolymer degradation followed by UV-vis spectroscopic analysis is shown in fig. **9.6**.

Each line represents the UV spectrum at five minute intervals. At 0 min., the UV spectrum showed an identical spectrum for a standard PMPS sample. After 2 hours, the characteristic peaks at 335 nm and 275 nm had practically disappeared. The peak originally observed at 335 nm is due to the $\sigma$–$\sigma^*$ transition of the Si-Si bonds in the backbone of the polymer. Hence, the polymer is degraded by the UV lamp since the intensity of the 335 nm peak decreases. Also, the wavelength of $\sigma$–$\sigma^*_{Si\text{-}Si}$ is dependent on the chain length. Therefore as the polymer is degraded, it is possible to view a decrease in wavelength of the $\sigma$–$\sigma^*$ peak. The $\sigma$–$\pi^*$ peak also disappears as interaction between the backbone and the phenyl ring decreases. Fig. **9.7** shows a plot of absorption vs. time for the $\sigma$–$\sigma^*$ peak. After 2 hours, the absorption of the peak decreased to about 20% of its original intensity. Virtually identical plots were observed for various block copolymer samples (Fig. **9.8**).

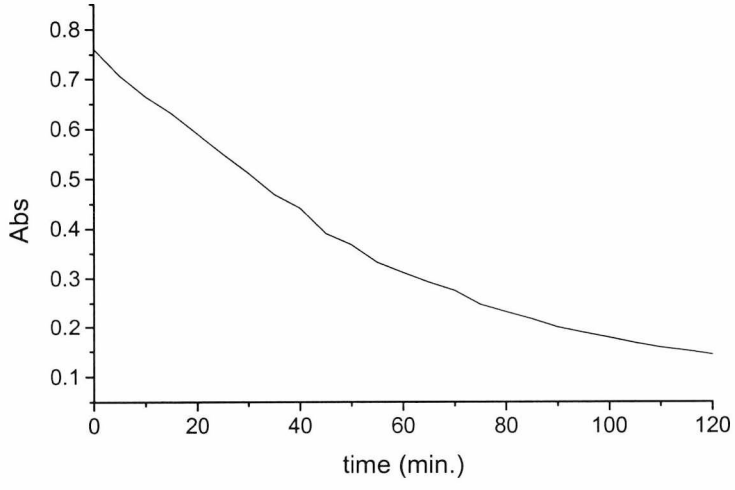


**Fig. 9.7.** Plot of UV absorption at 335 nm for POEGMA-PMPS-POEGMA **6** in water irradiated from 180-600 nm

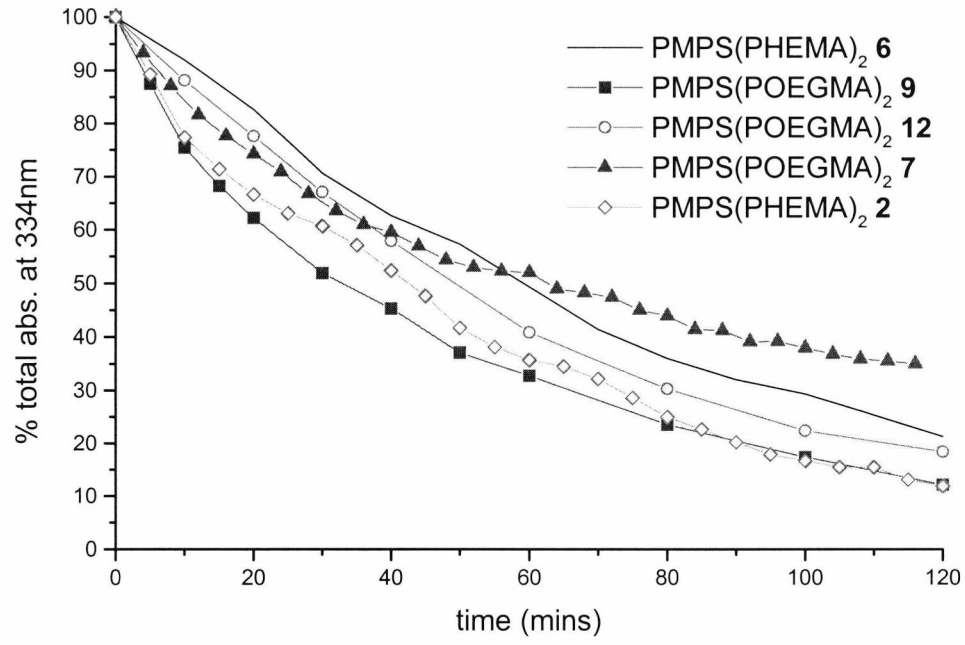


**Fig. 9.8.** Plot of UV absorption at 334 nm for samples in water as irradiation occurs.

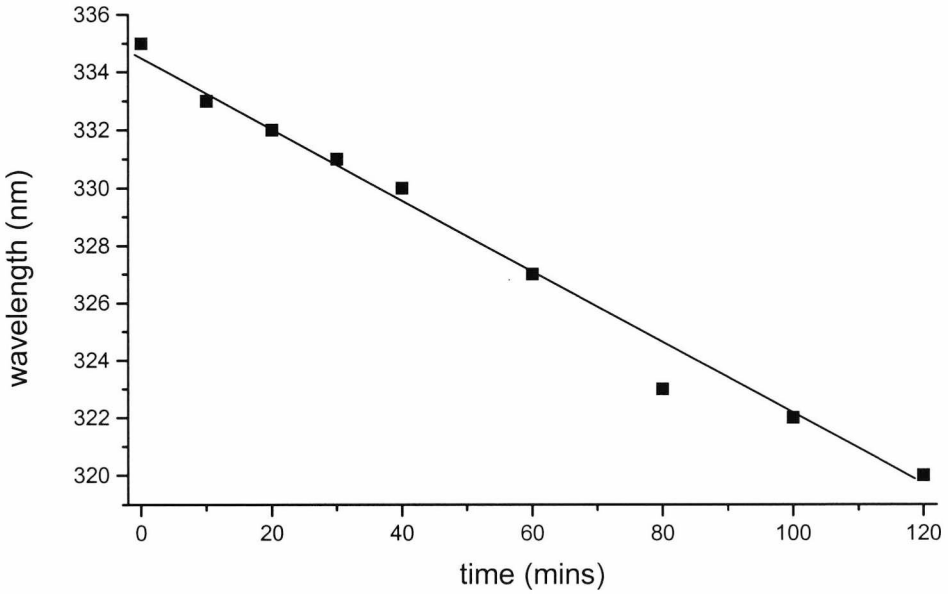


**Fig. 9.9.** Plot of wavelength of σ–σ* peak maximum against time (POEGMA-PMPS-POEGMA **6**)

A linear plot illustrating the blue-shift in the wavelength of the peak maximum from 335 to 320 nm is shown in fig. **9.9**. This is evidence that the number of conjugated silicon atoms in the polymer backbone is decreasing. Jones *et al.*[23] have studied the correlation between the number of repeat units in PMPS with the wavelength of the

peak due to σ–σ* absorption. It was observed that a maximum wavelength is reached as the length of the PMPS chain exceeds approx. 40 units (~340 nm). As the length of the chain decreased, so did the UV absorption, $\lambda_{max}$, of the peak; for example, a $\lambda_{max}$ of 332 nm corresponds to ~15 catenated silicon atoms. The UV absorptions for PMPS oligomers of 2 to 5 repeat units have been shown to range from 230 nm to 260 nm.[24]

### 9.3.2.1. Molecular Weight Analysis

The degradation of the samples was followed using an aqueous GPC set up with a molecular weight range of 100,000 to 1,000,000. Using aqueous GPC it was hoped that the size of the aggregates could be shown. However, the molecular weight limits of the column used for GPC analysis were too low, causing the aggregates to be eluted too quickly (after only 4.5 min.). An example of the GPC plots observed at 334 nm are shown in fig **9.10**. If the GPC column had had a larger molecular weight range, it might have been possible to observe a high molecular weight peak, due to the aggregates, and a second lower molecular weight peak, formed as a result of the subsequent degradation of the polysilane chains. No low molecular weight peaks were observed.

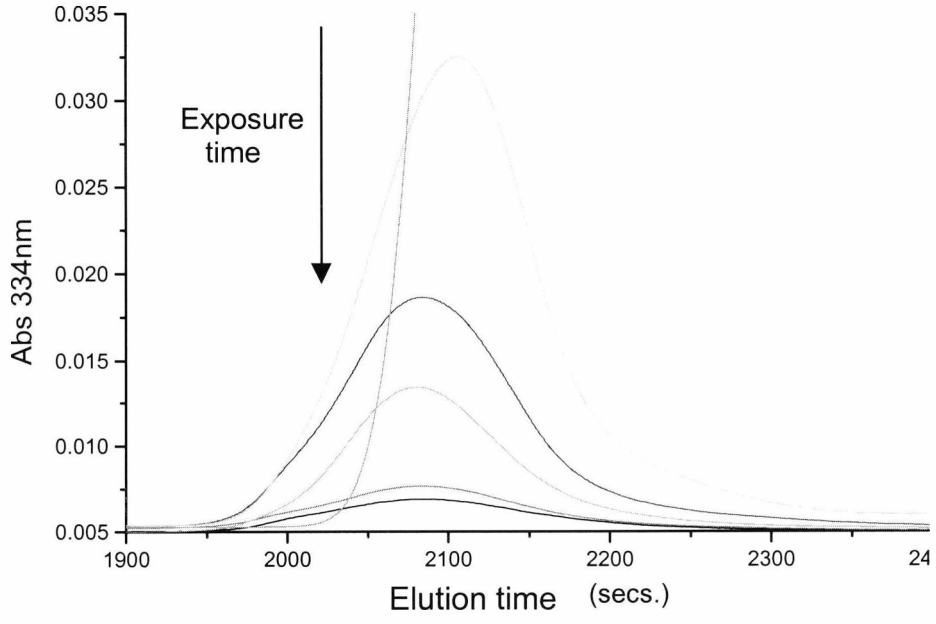


**Fig. 9.10.** GPC overlay ($\lambda_{max}$ 334 nm) of irradiated PHEMA-PMPS-PHEMA **2**. As the sample is irradiated, the amount of aggregated sample detected at ~2100 sec. decreases.

After the samples were degraded, the water was removed under reduced pressure. The samples were then analysed by GPC, with THF as the eluent (using a UV detector, $\lambda_{max}$ = 254 nm). It proved difficult to run GPCs since only a small amount of sample could be recovered after degradation and only a relatively small amount was degraded in the first place (a few milligrams). However, GPC overlays of POEGMA-PMPS-POEGMA **3** and PHEMA-PMPS-PHEMA **2** before and after degradation are shown in fig. **9.11**. In both cases, the molecular weight of the polymer decreased and its polydispersity increased.

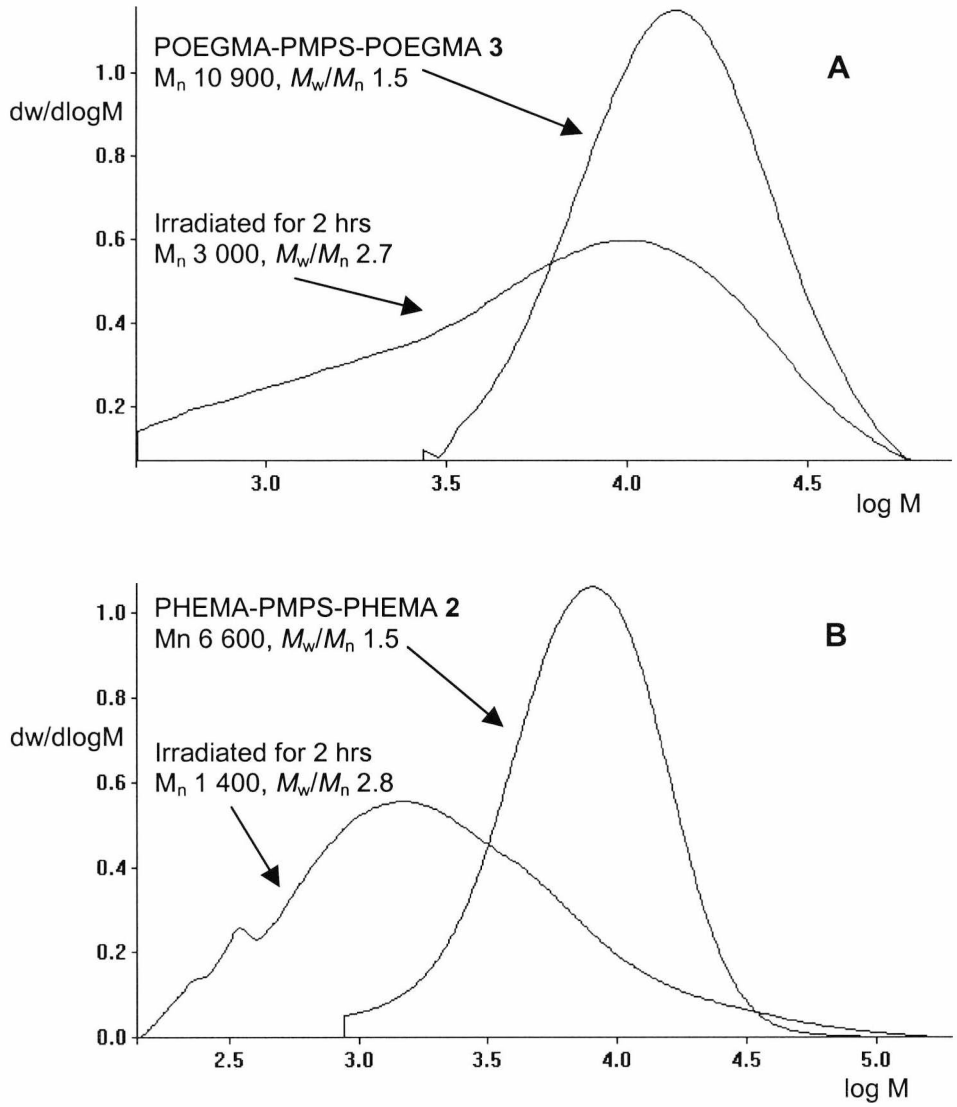


**Fig. 9.11.** GPC overlay ($\lambda_{max}$ = 254 nm) of (A) POEGMA-PMPS-POEGMA **3** and (B) PHEMA-PMPS-PHEMA **2** before and after irradiation.

If more degraded sample was available, it would have been interesting to analyse the samples via GPC using both RI and UV ($\lambda_{max}$ 254 nm and 334 nm). The RI determined GPC distributions are not shown since a more concentrated solution is required. It might have been possible to observe whether or not the OEGMA and HEMA segments remained intact, whilst the polysilane blocks had been degraded. In addition, the irradiated samples could have been analysed using techniques such as IR and NMR spectroscopy. Using these techniques it might have been possible to show the effect of degradation on the PMPS backbone, i.e. the formation of siloxane chains, silanols, or silane fragments.

### 9.3.2.2. Encapsulation of a dye

An attempt was made to encapsulate a dye (calceine) inside the aggregates, while the dye in the water was removed. The dye has an absorption of approx. 450 nm, and therefore if the dye is removed from water surrounding the aggregates, and an absorption at 450 nm remains, then the dye is encapsulated in the aggregates.

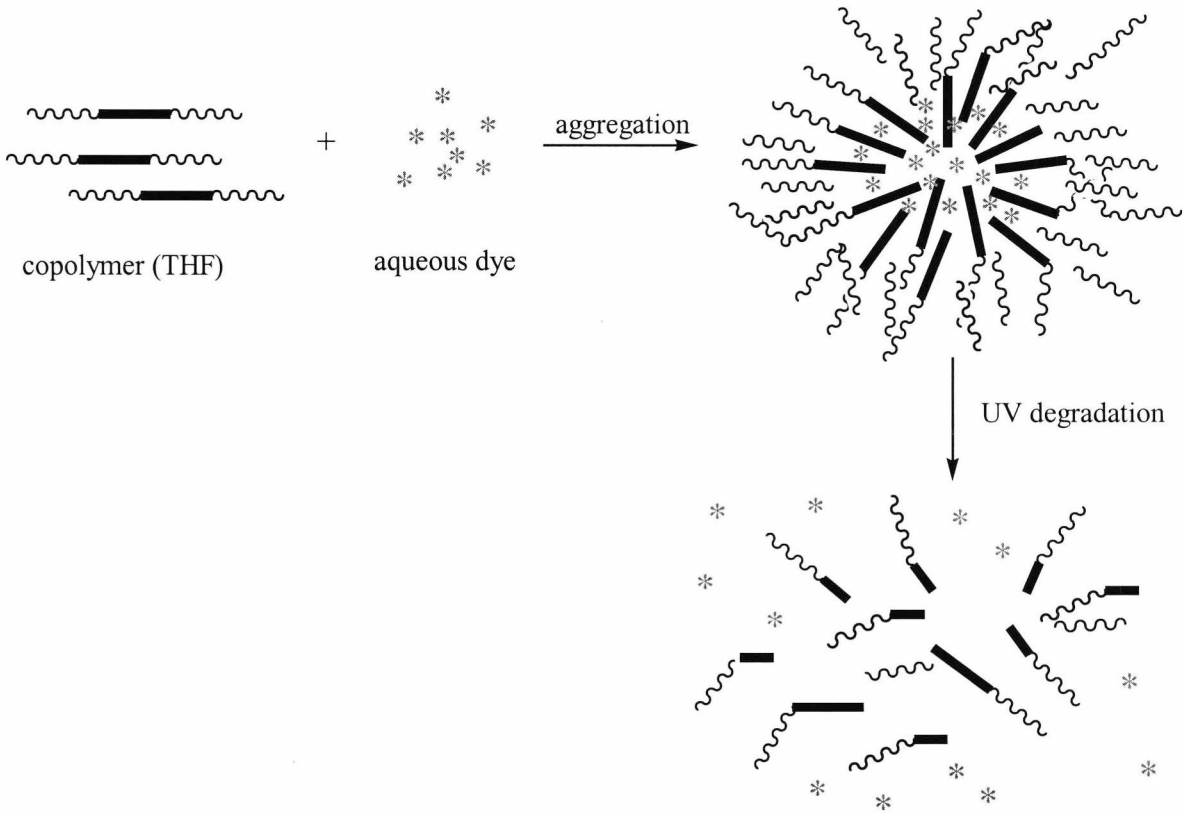


**Fig. 9.11.** Encapsulation of a dye (e.g. uranyl acetate) into the copolymer aggregate, followed by UV degradation and subsequent release of dye

As the sample is irradiated, the dye would be released into the aqueous medium (fig. **9.11**). This would demonstrate a potential application in the field of drug delivery systems, or other chemical delivery systems whereby the encapsulated solution inside the aggregates could be activated using UV light.

It proved too difficult to remove the dye in the surrounding aqueous medium around the dialysis bags. At first, the attempt involved the replacing and replenishing of the water around the dialysis bags. This took too long as the dye continued to spread into the water. Another attempt by filtering the dye-containing water from the aggregates proved unsuccessful. With more time, the procedure of separating the copolymer aggregates from the dye using a sephadex column could have proved more beneficial. This has been shown to be the case for the aqueous solution of the multi-block copolymer, $PMPS_m$-$PEO_n$, which was separated from a dye using a Sephadex column.[21] It is probable that the dye was leaching out from within the aggregates in the present study.

### 9.3.3. Cell growth on thin films

Research into the deformation of muscle tissue at a cellular level due to sustained mechanical loads is an area of cell growth technology currently being investigated at the Technical University of Eindhoven. Preliminary experiments involved measuring the contact angles of water droplets on the thin films of the PMPS block copolymers in order to determine the nature of the surface morphologies. Subsequently, cell growth experiments were carried out on a number of the thin films spun onto glass and gold substrates.

#### 9.3.3.1. Contact angle measurements on thin films

The contact angles of water droplets placed on the thin films of copolymers cast onto gold, gold-patterned and glass substrates was measured to determine whether the surface morphology of the thin films differed (fig. **9.12**). The thickness of the films were not measured here.

For a copolymer film deposited on gold substrate, the contact angle was 70°. For the same copolymer, the film on a glass substrate gave a contact angle of ~ 20° (fig. **9.13**). This suggests that the copolymer film is aligned differently when on gold

compared to glass. The increased contact angle suggests decreased hydrophilicity, meaning that either PMPS blocks or the methacrylic backbone of the POEGMA segments are present at the surface of the film. The contact angle on the glass film is low, which would suggest that ethylene glycol chains are more prominent at the surface of the film. In addition, subsequent investigations of cell growth onto the films showed that the film deposited on glass tended to peel off.

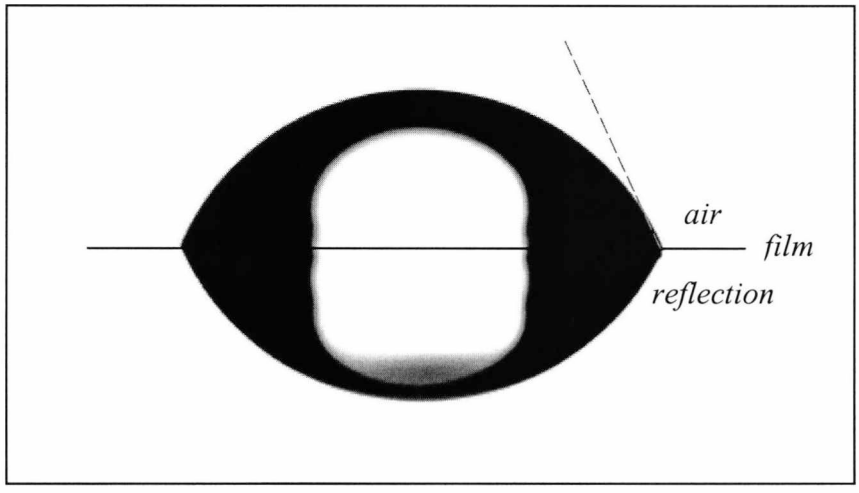


**Fig. 9.12.** Picture of a drop of water after 2 seconds on a thin film of POEGMA-PMPS-POEGMA **2** spun onto a gold substrate

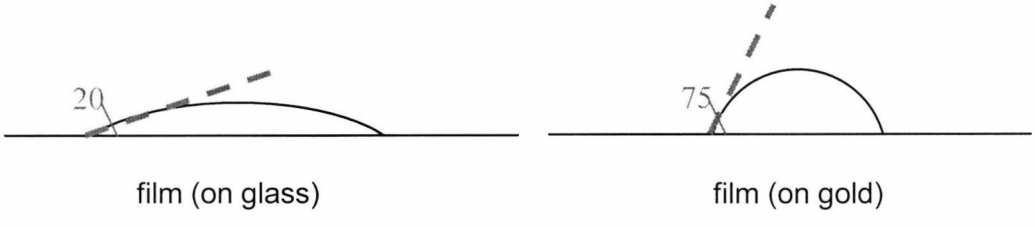


**Fig. 9.13.** Representation of droplet on glass compared to gold substrates

A drop of water was deposited onto films spun onto gold patterned substrates. Pictures showed how the water droplet has a relatively high contact angle on gold, but starts to flow when in contact with the glass sections of the substrate. Two different experiments showed how the droplet appeared after 2 seconds; the first with gold lines (~3 mm by ~10 mm) placed parallel to the line of sight of the camera (fig. **9.14**), while the other was turned 90°, with the gold lines perpendicularly placed (fig. **9.15**).

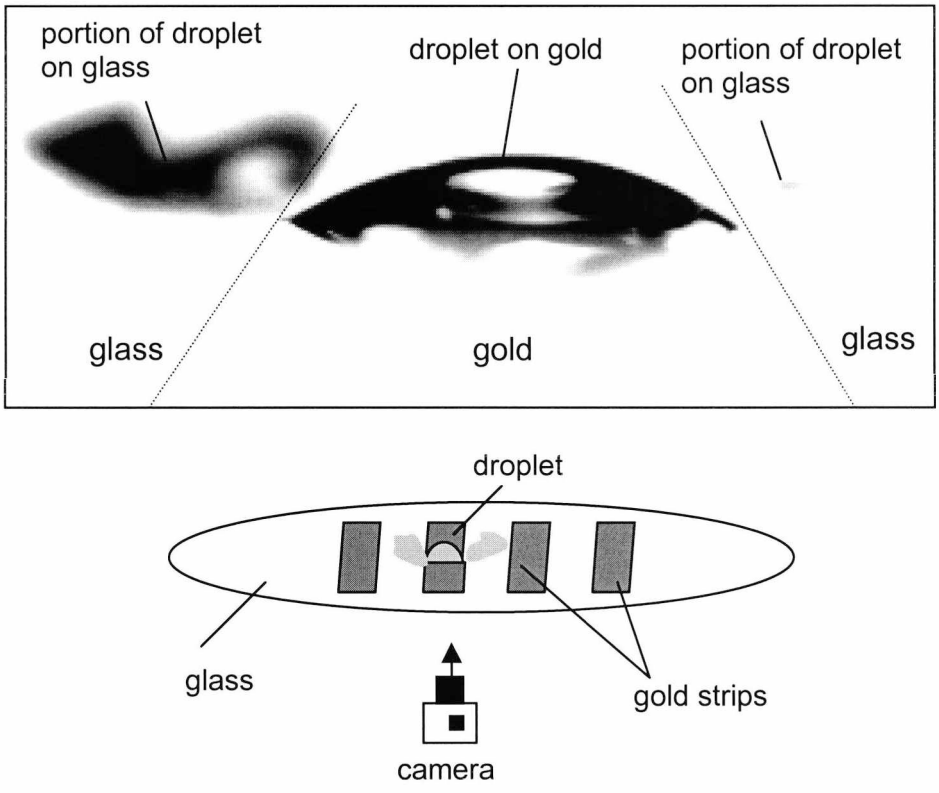


**Fig. 9.14.** Picture of droplet taken two seconds after deposition. Schematic of a water droplet on a gold patterned substrate. The droplet loses shape on glass (out of focus).

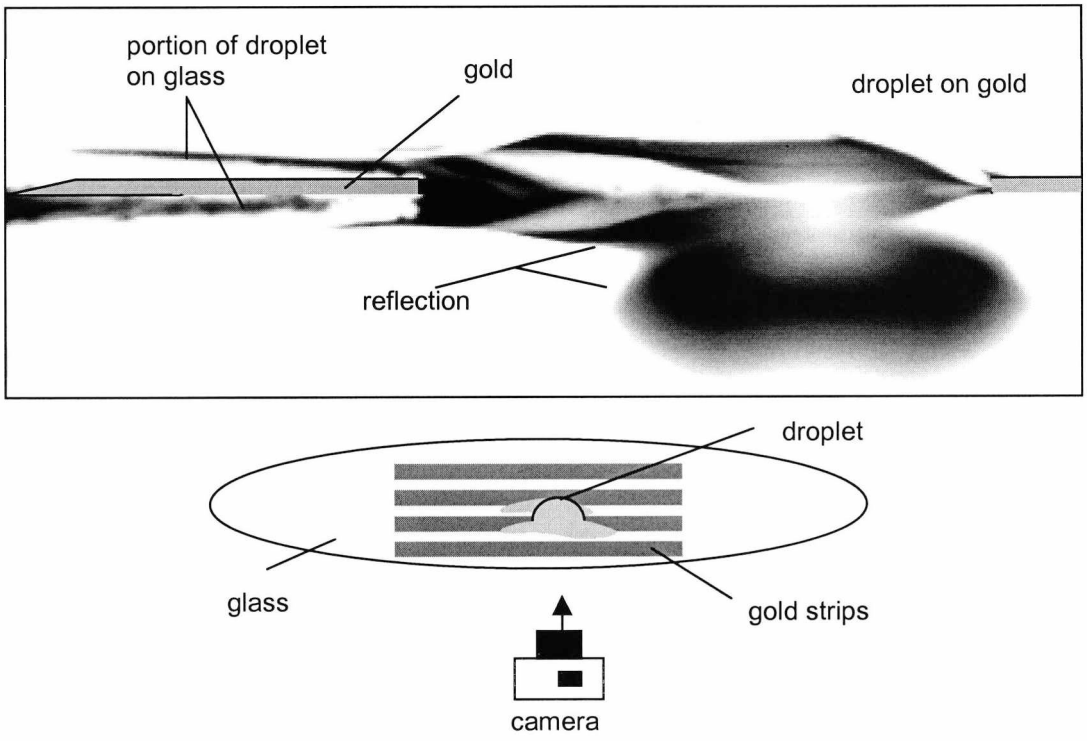


**Fig. 9.15.** Picture of droplet taken two seconds after deposition. Schematic of a water droplet on a gold patterned substrate, with gold strips placed perpendicularly to the line of sight of the camera. Deformation of droplet occurs on glass, and flows to left of picture.

### 9.3.3.2. Cell growth

In order to examine the effects of deformation on muscle tissue, it is necessary to have a suitable model on which experiments can be carried out. One such model involves the growth of a monolayer of muscle cells that can be used to analyse the response of cells to mechanical loading. An accurate model is required and therefore it is important that the cells are grown in an aligned manner so that *in vivo* cell growth conditions can be reproduced. Hence, the aim of the research was to control the growth, spreading, and alignment of muscle cells of mice by chemical induction. For this purpose, a polymer capable of binding to cells and the ability to form a self-assembled monolayer on gold is needed.

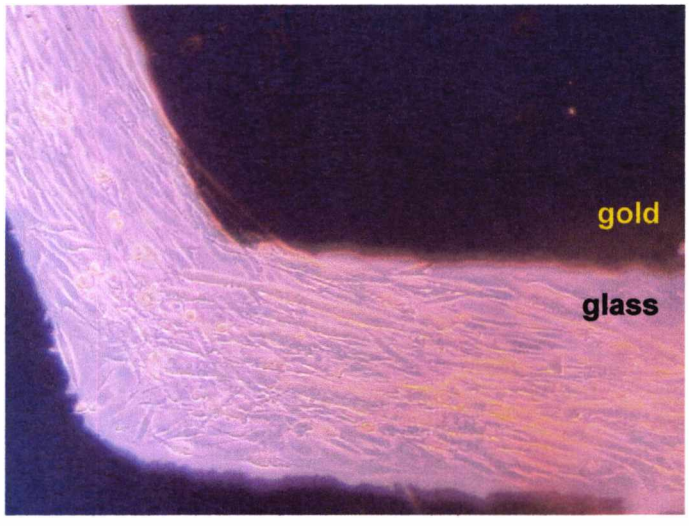


**Fig. 9.16.** Alignment of cells (myotubes) on a thin film of POEGMA-PMPS-POEGMA **2** deposited on a gold (dark areas) and glass (light area) patterned substrate.

It was hoped that cells could be grown onto the copolymer films in order to show biocompatibility. If a polymer is conducting, and is deposited on a metal, it may be possible to apply a current to influence cell adherence. Hence, thin films of POEGMA-PMPS-POEGMA **2** were prepared by spin-coating on gold, glass, and gold patterned glass substrates in order to observe how the cells would grow.[25] The substrates were then immersed in a serum, and cell growth was observed and recorded (appendix **9.3**). However, preliminary results found that the cells grew with a high

degree of ordering on the areas of the film deposited on the glass sections (fig. **9.16**), while hardly any growth occurred on the film deposited on the gold sections. The reasons for this could be either due to the topographical (physical) nature of the film, or the macroscopic ordering of the polymer within the film (chemical).

In conjunction with the contact angle measurements, there is some evidence that the morphology of the film on glass and gold differs, and therefore the reasons for aligned growth may be chemical. However, it was later realised that the film on glass tended to peel off and wash away, while the film on gold remained intact. Therefore, the cells grew on the clean glass surface, as opposed to the copolymer film. The alignment of cells is therefore believed to be due to the topography of the substrate, while the cells do not grow on the film because of the presence of ethylene oxide. Oligo- and poly(ethylene glycol) are known to be resistant to protein absorption, probably due to the adsorption of monolayers of water that act as a barrier.[26] In addition, the degree of resistance to protein absorption has also been determined to be proportional to the weight percentage and length of the glycol chains.[27]

#### 9.3.3.3. Further work

Further research[28] involving POEGMA-PMPS-POEGMA thin films and cell growth has confirmed that copolymer films on glass peel off and are washed away with water. X-ray photoelectron spectroscopy (XSP) and atomic force microscopy (AFM) studies have been used to investigate the surfaces of the copolymer films. Also, by irradiating sections of PHEMA-PMPS-PHEMA thin films using UV light, and subsequently removing the irradiated segments, patterned growth of cells has been achieved. It is hoped that by irradiating certain areas of the thin films, a two-dimensional biomaterial scaffold can be developed to control the alignment of myotubes.

### 9.3.4. Cyclic voltammetry and amperometry

Enzyme-based bioelectronics requires that electronic transduction occurs via either the depletion of the reaction or via the formation of a product (scheme **9.1**). So long as electron transfer between the electrode and redox enzyme is fast, the resulting current will correspond to the turnover rate of electron exchange between the

substrate and the biocatalyst. This in turn corresponds to the actual substrate concentration in the system.

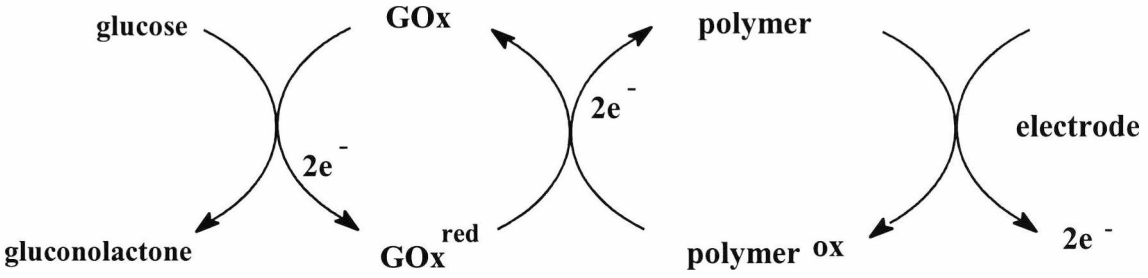


**Scheme 9.1.** Electronic transduction occurring via the oxidation of glucose to gluconolactone.

A difficulty arises from the fact that direct electrical communication between the redox proteins and the electrode is usually prohibited due to the size of the enzyme involved. Since the enzyme is very large, the donor-acceptor distance is too great and affects the electron-transfer rate. The redox centre for most redox proteins is imbedded deep inside the protein and is therefore effectively insulated, resulting in a lack of electrical contact with the electrode. Since the field of bioelectronics is dependent on the interaction between the biomaterials and the electrode surface, the assembly and immobilisation of the enzyme onto the electrode is of great importance. One route for overcoming this problem has been the use of redox or conducting polymers.[29]

Research in the area of enzyme-based bioelectronics has resulted in the quasi-reversible electrochemistry of glucose oxidase at carbon and gold surfaces. For biosensors, the possibilities of 'wiring' the proteins to electrodes means that there is no need for electron transfer mediators. The reversible direct chemistry of glucose oxidase attached at a self-assembled monolayer has been achieved, for example, using 3,3'-dithiobis-sulfosuccinimidyl proprionate (DTSSP) on a gold surface.[30]

It was believed that the combination of a biocompatible polymer (POEGMA), with a conducting polymer (PMPS) might find application in this particular field of bioelectronics. Hence, the incorporation of an enzyme into a POEGMA-PMPS-POEGMA film was investigated in order to detect the concentration of glucose in solution.

### 9.3.4.1. Cyclic voltammetry

The purpose of the voltammetry experiments was to determine whether the films of POEGMA-PMPS-POEGMA **2** were stable to cycling and whether it was possible to achieve electrical contact between the electroactive polymer and the ITO electrode. In order to determine the electrochemical features of the polymer, cyclic voltammetry was performed on films cast from pure THF, using $TBAPF_6$ in dichloromethane as the electrolyte solution. The organic electrolyte was chosen instead of water in order to have a wider voltage range (-1.7 to 2.0 V) without interference of other redox reactions (e.g. water is reduced at –0.83 V to form $H_2$). The sample was cycled several times, with no deviation occurring from the original curve, which is shown in fig. **9.18**. It follows from this reproducibility that there is no electrochemical degradation and that the film is not dissolved by the electrolyte solution. The voltammogram in fig. 9.18 shows oxidation waves at 1.03 and 1.42 V and overlapping multiple reduction peaks at –0.89, -1.25, and -1.43 V, respectively.

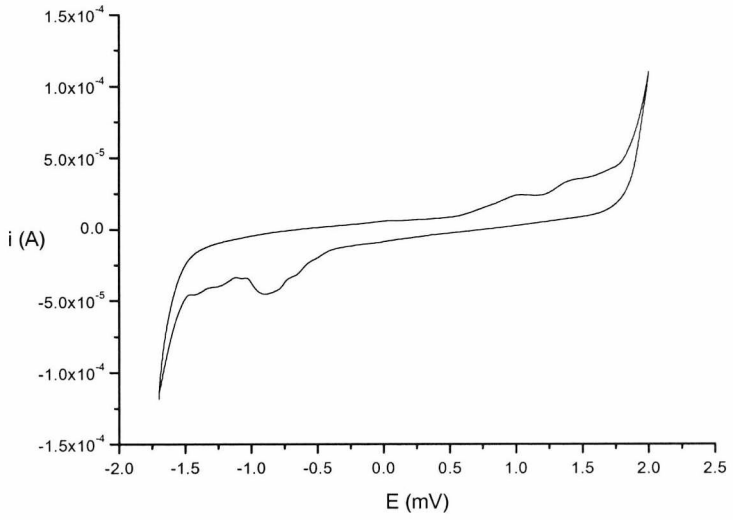


**Fig. 9.18.** Cyclic voltammogram of POEGMA-PMPS-POEGMA **2** in dichloromethane

It has been shown that dialkyl polysilanes undergo electro-oxidation between 1.4 and 1.6 V.[31] For polysilanes with electron-donating substituents, these values are substantially lower. For a thin film of PMPS homopolymer, the value of the peak potential is about 1.0 V.[31] However, polysilanes have previously been shown not to

be stable on cycling; they undergo irreversible degradation upon oxidation, leading to the formation of siloxanes. West and co-workers have described the oxidation of cyclic polysilanes (scheme **9.2**).[32]

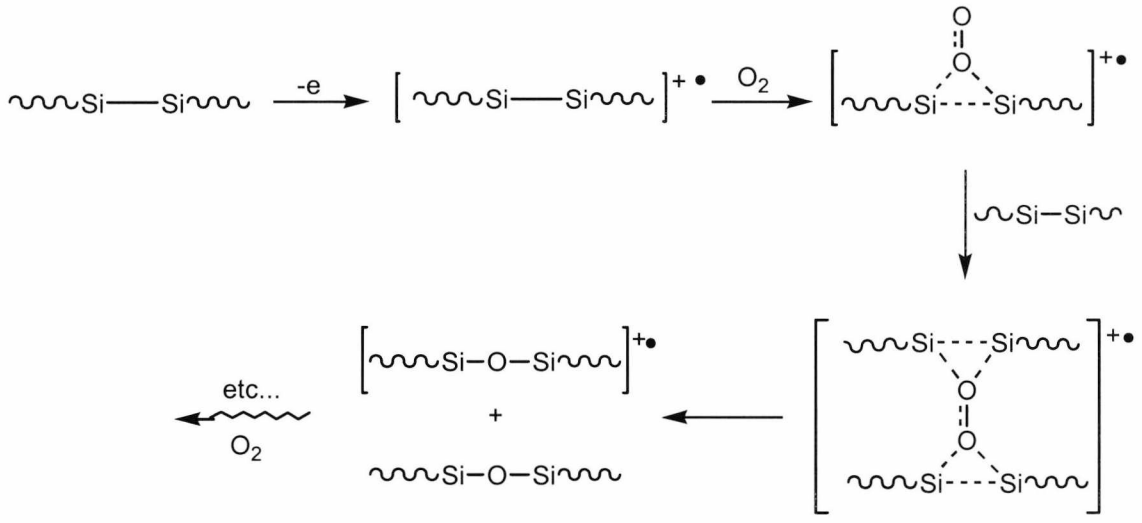


**Scheme 9.2.** Photochemical degradation of polysilanes in the presence of oxygen

However, it is important to note that the cyclic voltammetry experiments described here involved cells that have been deoxygenated using nitrogen. Hence it is proposed that the reversible nature of the PMPS copolymer films could be due to the lack of oxygen in the system. The oxidation waves are due to the formation of radical cation species which are not subsequently oxidised to form siloxanes. As the films are cycled, the silane chains are reduced once more, as the applied potential becomes negative. It is also possible that the presence of the POEGMA chains has, to an extent, protected the polysilane chains from any oxygen, water, and ions in the cell which would lead to irreversible oxidation.

Glucose oxidase was immobilised in a copolymer film by adding a THF solution of POEGMA-PMPS-POEGMA **2** to an aqueous solution of glucose oxidase. A minimal amount of THF (10%) was used to dissolve the copolymer since THF is harmful to enzymes such as glucose oxidase. The films cast from POEGMA-PMPS-POEGMA **2** were also shown to be stable upon cycling in the phosphate buffer solution (fig. **9.19**). The appearance of an unidentified feature at 0.05 V is observed for the sample containing the enzyme, and is consistent with other films containing the enzyme.[33]

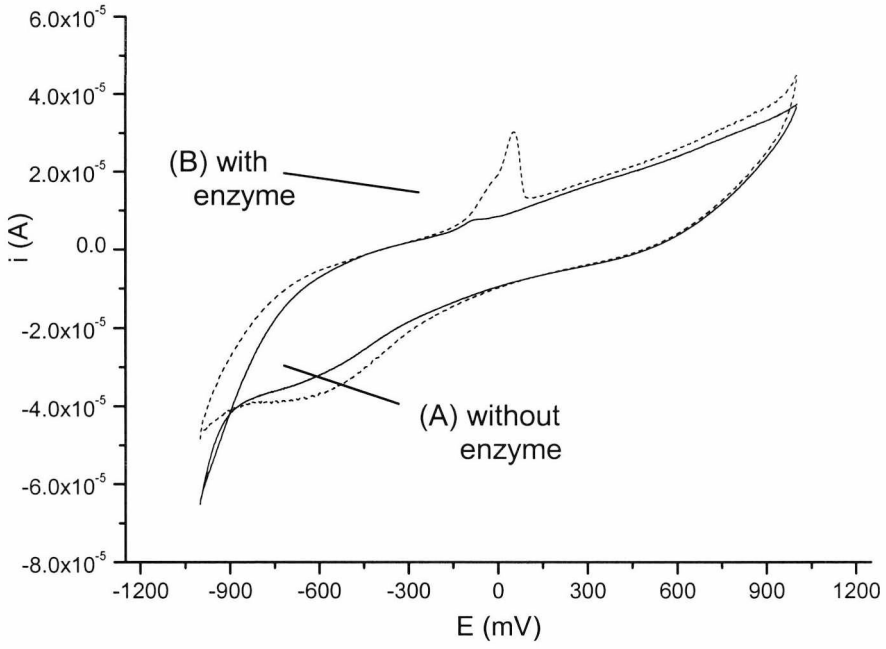


**Fig. 9.19.** Cyclic voltammograms of cast films: (**A**) POEGMA-PMPS-POEGMA **2** in THF, and (**B**) POEGMA-PMPS-POEGMA **2** with glucose oxidase from a solution containing 10% THF in water.

### 9.3.4.2. Amperometry

Amperometry of the PMPS was carried out at a constant potential corresponding to the first oxidation wave observed in the voltammogram in dichloromethane (0.9 V). At this fixed voltage, the current was initially quite high, and steadily decreased, until eventually becoming constant due to the stabilisation of the solution. Once the solution was stable, a known concentration of glucose was injected, and the corresponding change in potential measured (fig. **9.20**). The measurement was performed at the first oxidation wave since the polymer is partially oxidized, improving conductivity.

The injection of glucose was repeated several times using fresh thin films on ITO plates on each occasion. By adding various concentrations of glucose and measuring the current, it was possible to create a graph of current vs. glucose concentration (fig. **9.21**). From the points on this graph, a preliminary calibration curve was developed, with possibilities for detecting unknown concentrations of glucose in solution.

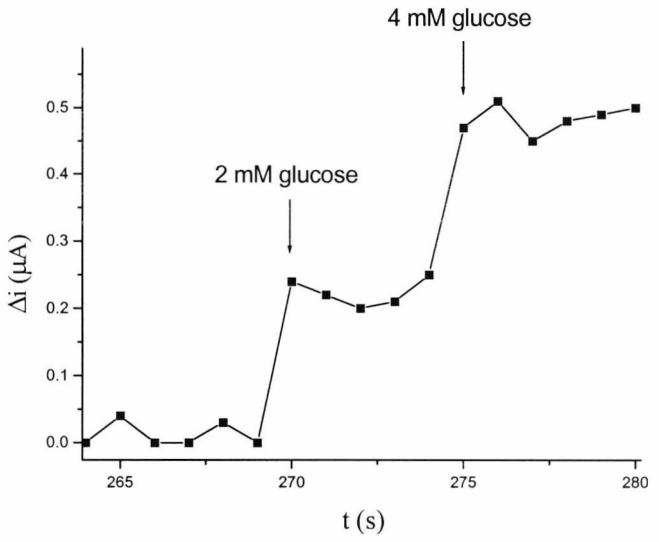


**Fig. 9.20.** Change in anodic current (μA) vs. time at a fixed voltage (0.9 V). At time $t_1$ (270 sec.), 2mM of glucose is injected into the solution, and again at $t_2$ (275 SCEs.).

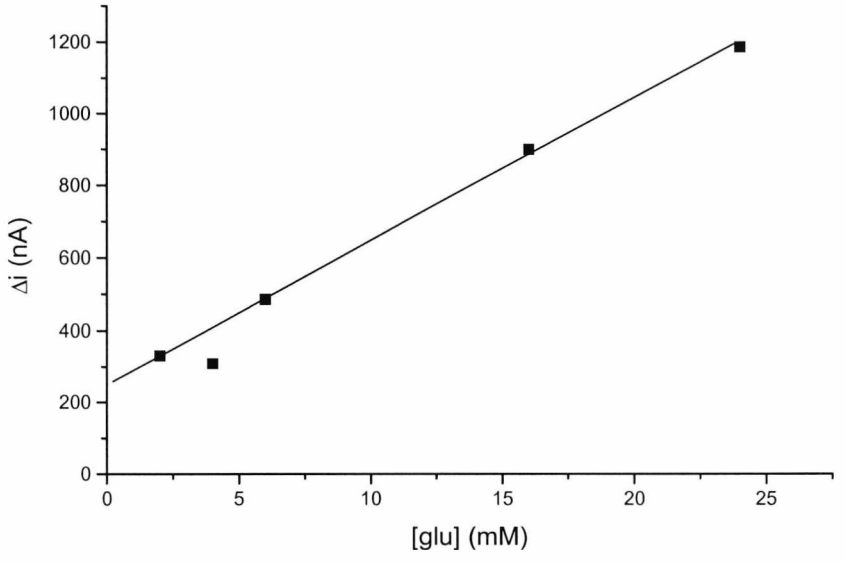


**Fig. 9.21.** Plot of the change in anodic current (Δi) vs. glucose concentration [glu] (mM)

### 9.3.4.3. Summary

Films of POEGMA-PMPS-POEGMA **2** were shown to be stable upon cyclic voltammetry in dichloromethane and in water (buffer solution). Amperometry experiments showed that a correlation between glucose concentration and potential was evident. A crude calibration curve for determining glucose concentration in

solution was demonstrated. Preliminary results suggest films of POEGMA-PMPS-POEGMA provided a suitable matrix of GOx, allowing for direct communication of the active site of the enzyme and the conjugated polymer segments.

### 9.3.5. Conclusions

The amphiphilic ABA block copolymers of PMPS have a number of promising properties which might lead to various applications. The ABCs formed aggregates such as plate-like crystals and micelles in water, while vesicles were also observed. Hexagonal patterning was observed upon electron diffraction of the samples, suggesting that a high degree of ordering of the polysilane blocks is occurring. The aggregated samples were also successfully irradiated and their degradation followed using UV spectroscopy, indicating that the ABCs may find applications in the area of chemical transport. Future work that would be of interest includes whether a dye can be contained within the aggregates.

In addition, cell growth experiments involving the muscle cells of mice were carried out on thin films of POEGMA-PMPS-POEGMA. Preliminary results observed that cells were growing in the same direction on the gold sections of the patterned substrates. Topographical data that might explain this result was collected from the contact angle measurements on glass and gold films. Further research into the UV degradation of portions of the films to achieve cell growth patterning is ongoing.

POEGMA-PMPS-POEGMA was also used to cast films on ITO plates. Within the films, an enzyme (glucose oxidase) was successfully immobilised. Cyclic voltammetry experiments showed that cycling of the applied voltage did not result in the degradation of the polysilane chain. At a constant voltage (0.9 V), amperometry experiments showed that by changing the concentration of glucose in the cell, the anodic current would also change. Therefore, preliminary results suggests that the immobilisation of an enzyme into a thin film of POEGMA-PMPS-POEGMA could allow a bioelectronic sensor to be constructed.

## 9. References


[1] a) Kwon, G.S.; Kataoka, K. *Adv. Drug Deliv. Rev.* **1995,** 16, 295.

b) Kwon, G.S.; Okano, T. *Adv. Drug Deliv. Rev.* **1996**, 21, 107.

[2] a) Allen, C.; Maysinger, D.; Eisenberg, A. *Colloids Surfaces B Physicochem. Eng. Aspects* **1999**, 3181.

b) Yang, L.; Alexandridis, P. *Curr. Opin. Colloid Interface Sci.* **2000**, 5, 132.

[3] a) Wu, N.M.; Da, D.; Rudoll, T.L.; Needham, D.; Whorton, A.R.; Dehirst, M.W. *Cancer Res.* **1993**, 53, 3765.

b) Gabizon, A.; Catane, R.; Uziely, R.; Kaufman, B.; Safra, T.; Cohen, R.; Martin, F.; Huang, A.; Barenholz, Y. *Cancer Res.* **1994**, 53, 987.

[4] Rosler, A.; Vandermeulen, G.W.M.; Klok, H.-A. *Adv. Drug Deliv. Rev.* **2001**, 53, 95.

[5] For a review of the applications of block copolymers in surface modification, drug targeting, etc. see: Kumar, N.; Ravikumar, M.N.V., Domb, A.J. *Adv. Drug Deliv. Rev.* **2001**, 53, 23.

[6] a) Folch, A.; Toner, M. *Annu. Rev. Biomed. Eng.* **2000**, 02, 227.

b) Holmes, T.C. *Trends Biotechnol.* **2002**, 20, 16.

c) Hynes, R.D. *Trends Cell Biol.* **1999**, 9, M33.

[7] Curtis, A.S.G.; Wilkinson, C.D.W. *J. Biomater. Sci. Polym. Edu.* **1998**, 9, 1313.

[8] a) Gopel, W.; Heiduschka, P. *Biosens. Bioelectron.* **1994**, 9, III-XIII.

b) Gopel, W. *Biosens. Bioelectron.* **1995**, 10, 35.

[9] For a review of redox enzymes and conductive supports for biolectronic applications and references therein see: Willner, I.; Katz, E. *Angew. Chem. Int. Ed.* **2000**, 39, 1180.

[10] D'Souza, S.F. *Current Science* **1999**, 77, 69.

[11] Xiao, Y.; Ju, H.-X.; Chen, H.-Y. *Anal. Chim. Acta* **1999**, 391, 73.

[12] Hiller, M.; Kranz, C.; Huber, J.; Bauerle, P.; Schuhumann, W. *Adv. Mater.* **1996**, 8, 219.

[13] a) Sadik, O.A. *Electroanalysis* 1999, 11, 839.

b) Koopal, C.G.J.; de Ruiter, B.; Nolte, R.J.M. *Chem. Commun.* **1991**, 1691.

[14] a) Yamauchi, T.; Kojima, K.; Oshima, K.; Shimomura, M.; Miyauchi, S. *Synth. Met.* **1999**, 102, 1320.

b) Yon-Hin, B.F.Y.; Smolander, M.; Crompton, T.; Lowe, C.R. *Anal. Chem.* **1993**, 65, 2067.

[15] Zhang, L.; Eisenberg, A. *J. Am. Chem. Soc.* **1996**, 118, 3168

[16] Demoustrier-Champagne, S.; Jonas, A.; Devaux, J. *J. Polym. Sci. Polym. Phys.* 1997, 35, 1727.

[17] a) Asuke, T.; West, R. *Macromolecules* **1991**, 24, 343.

b) Asuke, T.; West, R. *J. Inorg. Organomet. Polym.* **1994**, 4, 45.

c) Bukalov, S.S.; Leites, L.A.; West, R.; Asuke, T. *Macromolecules* **1996**, 29, 2907.

[18] Miller, R.D.; Hofer, D.; Rabolt, J.F.; Fickes, G.N. *J. Am. Chem. Soc.* **1985**, 107, 2172.

[19] Sommerdijk, N. A. J. M.; Holder S. J.; Hiorns, R. C.; Jones, R. G.; Nolte R. J. M. *Macromolecules* **2000**, *33*, 8289.

[20] Sanji, T.; Kitayama, F.; Sakurai, H. *Macromolecules* **1999**, 32, 5718.

[21] Kros, A.; Jansen, J.A.; Holder, S.J.; Nolte, R.J.M.; Sommerdijk, N.A.J.M. *J. Adhes. Sci. Technol.*

**2002**, 16, 143.

[22] a) Sanji, T.; Nakatsura, Y.; Kitayama, F.; Sakurai, H. *Chem. Comm.* **1999**, 2201.
b) Sanji, T.; Nakatsura, Y.; Ohnishi, S.; Sakurai, H. *Macromolecules* **2000**, 33, 8524.

[23] Jones, R.G.; Wong, W.K.C. *Organometallics* **1998**, 17, 59.

[24] Kimata, Y.; Suzuki, H.; Satoh, S.; Kuriyama, A. *Chem. Lett.* **1994**, 1163.

[25] All cell growth experiments were carried out by R. Lems and N. Sommerdijk at the Technical University of Eindhoven (TUE).

[26] Herbert, C.B.; McLernon, T.L.; Hypolite, C.L.; Adams, D.N.; Pikus, L. *Chem. Biol.* **1997**, 4, 731.

[27] Irvine, D.S.; Mayes, A.M. *Biomacromolecules* **2001**, 2, 85.

[28] Ongoing research into cell growth on thin films of PMPS block copolymers is being carried out by D.C. Popescu, R. Lems C.V.C. Bouten at the TUE under the supervision of N.A.J.M. Sommerdijk.

[29] Schuhumann, W. *Mikrochimica Acta* **1995**, 121, 1.

[30] Jiang, L.; McNeil, C.J.; Cooper, J.M. *J. Chem. Soc., Chem. Commun.* 1995, 1293.

[31] Diaz, A.; Miller, R.D. *J. Electrochem. Soc.* **1985**, 132, 834.

[32] a) Zhang, Z.-R.; Becker, J.Y.; West, R. *J. Appl. Electrochem.* **1998**, 28, 517.
b) Becker, J.Y.; Shakkour, E.; West, R. *Tetrahedron Lett.* **1992**, 33, 5633.

[33] Other films of polymers, such as polythiophenes, containing the enzyme glucose oxidase have been cycled in buffer solution by F. Brustolin at the TUE. The voltammograms also showed a peak at ~0.05V.

## Appendix 9.1. Cell growth – experimental details

### 1. Medium

Dulbecco's modified Eagle's medium (500 ml) (DMEM), high glucose (Biochrom FG 0435).

Fetal Bovine Serum (100 ml, 20 %) (Biochrom S0113), HEPES Buffer (1 M, 10 ml) (Biochrom L1613), non-essential amino acids (5 ml), gentamicine (2.5 ml).

### 2. Differentiation medium

500 ml DMEM

10 ml Horse Serum

5 ml non-essential amino acids

10 ml HEPES Buffer 1 M (Biochrom L1613)

2.5 ml gentamicine

### 3. Experimental for C2C12 cells

Solvent – Trypsine/EDTA

Sterile PBS

"Myoblasten" – growth medium for C2C12 cells

"Myotubuli" – differentiation medium for C2C12 cells

Cell growth was performed in an oven at 37 ºC with a $CO_2$ concentration of 5 % in the atmosphere:

1. After 70-80 % growth of the cells, the media is transferred every 3-4 days.
2. Media is then removed using a pipette on the end of a vacuum
3. Cells are rinsed twice with PBS
4. 3 ml of trypsine is then added and left for two minutes before being removed and left in the oven for 5 minutes.
5. Flask is tapped in order to knock cells loose, leaving just circular cells
6. Media is then added and differentiation takes place (i.e."divide")

Differentiation into myotubes:

1. Remove media after 70-80 % growth
2. Rinse twice with PBS
3. Refresh media every 3-4 days

## Appendix 9.2. Transmission electron microscopy – pictures

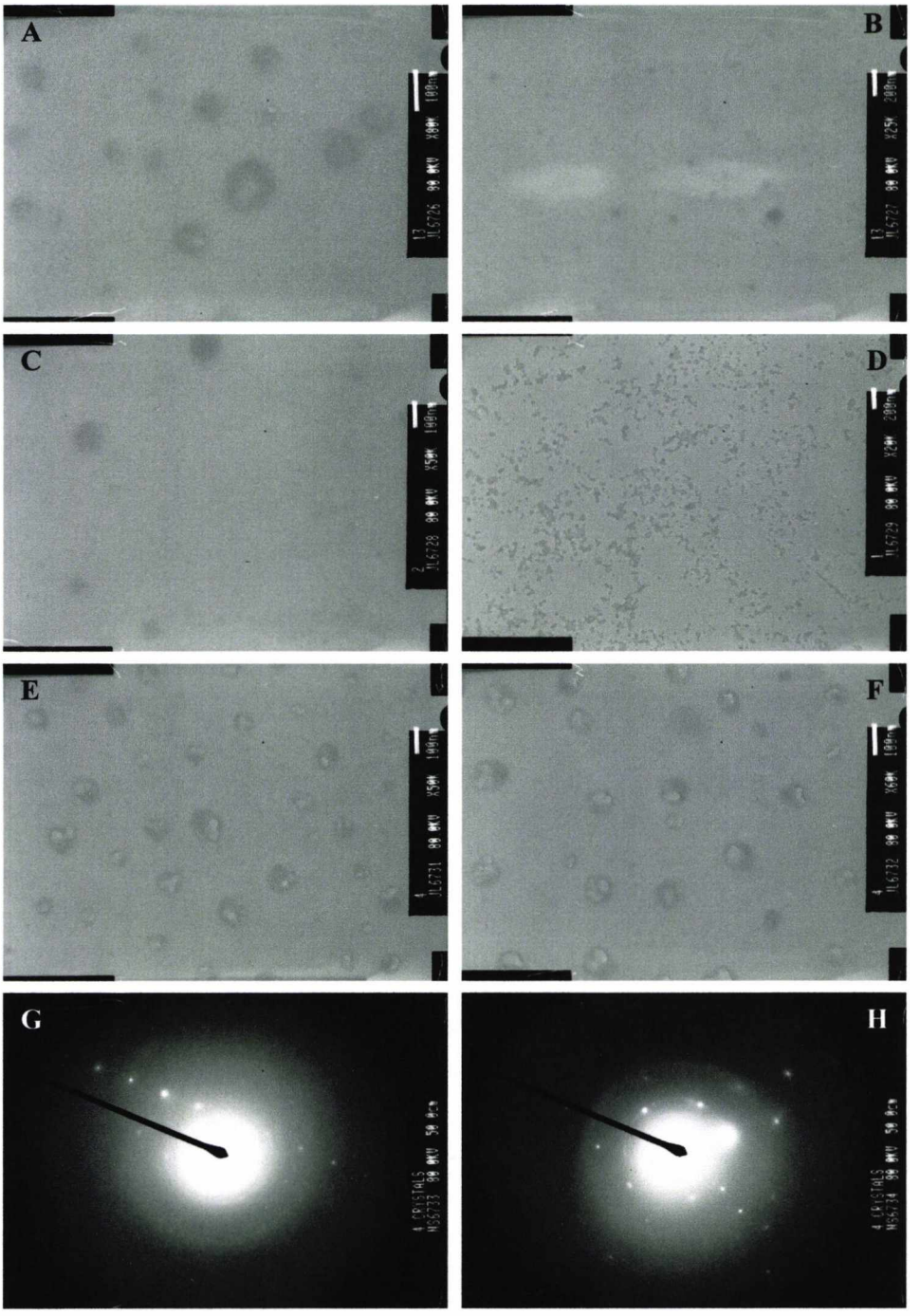


**Fig. 1.** TEM images of (A, B) POEGMA-PMPS-POEGMA **12**, (C) POEGMA-PMPS-POEGMA **7**, (D) PHEMA-PMPS-PHEMA 1, (E-H) POEGMA-PMPS-POEGMA **8**

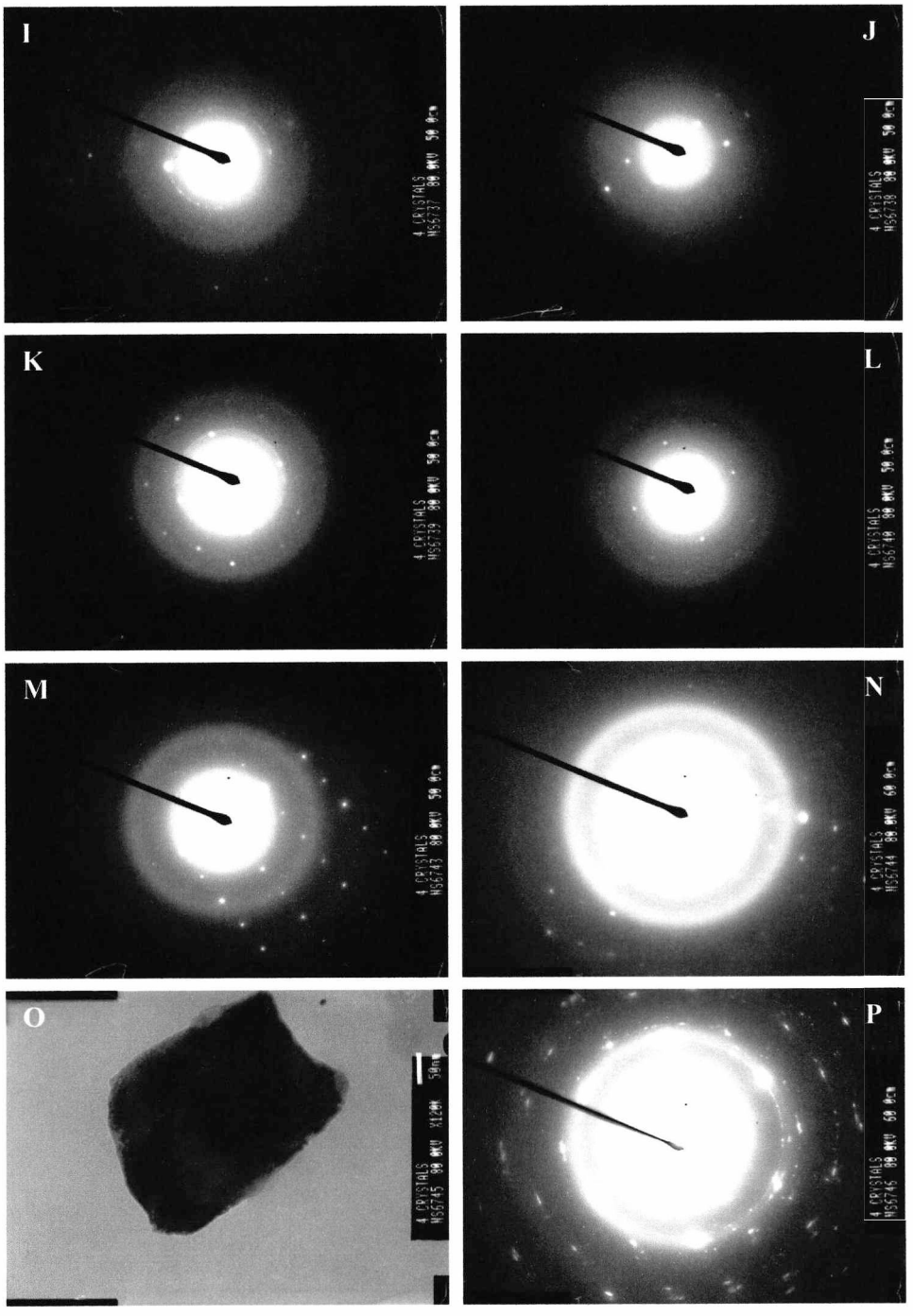


**Fig. 2.** Electron diffraction pattern images (I-N & P) of aggregates (O) of POEGMA-PMPS-POEGMA **8**

## Appendix 9.3. Cell growth pictures

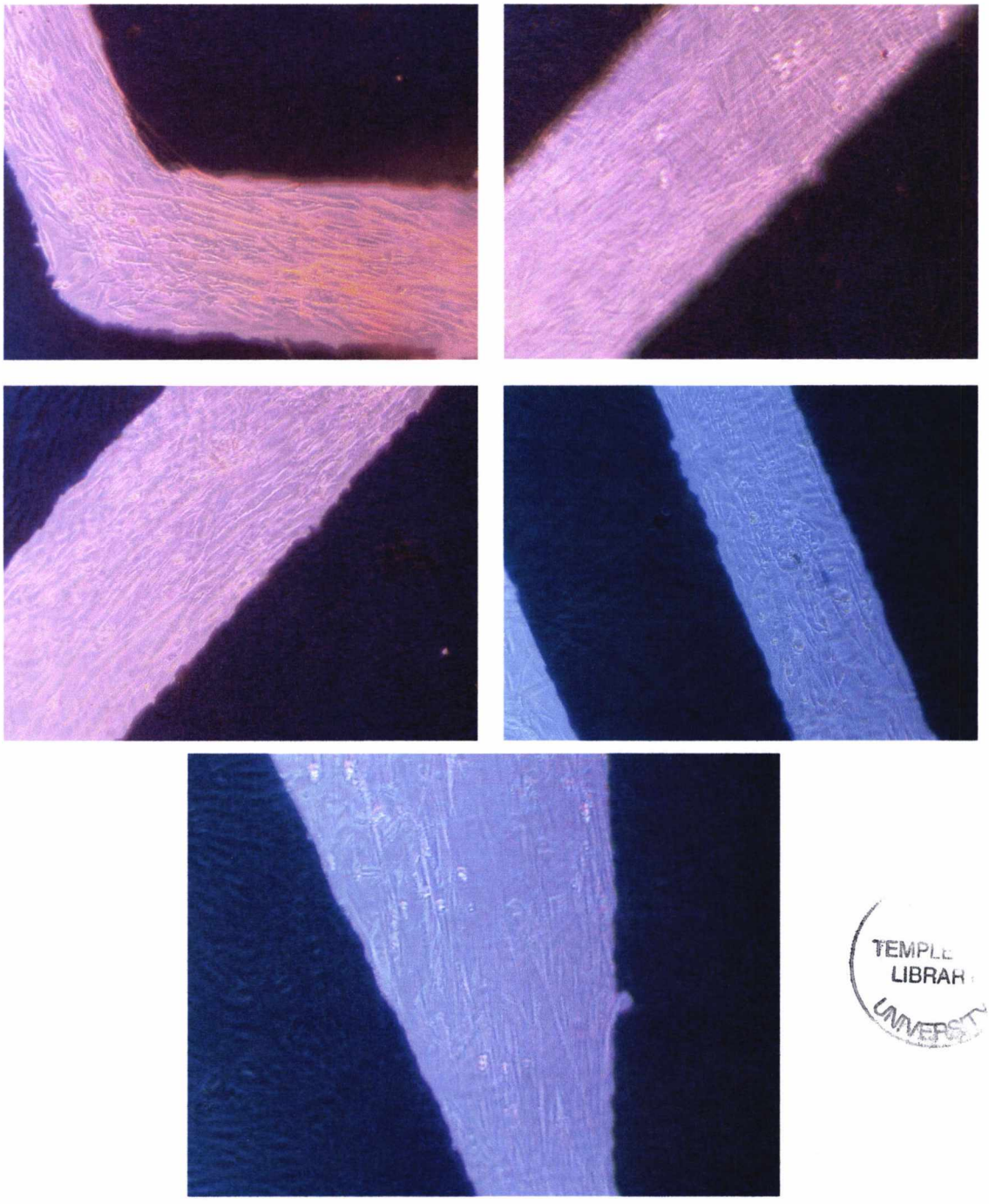



**Fig. 3.** Photographs of growth an alignment of cells on films of POEGMA-PMPS-POEGMA spun onto gold/glass substrates